# Physics-based algorithms and divergence free finite elements for coupled flow problems

A Dissertation
Presented to
the Graduate School of
Clemson University

In Partial Fulfillment
of the Requirements for the Degree
Doctor of Philosophy
Mathematical Science

by
Nicholas E. Wilson
August 2012

Accepted by:
Dr. Leo Rebholz, Committee Chair
Dr. Vincent Ervin
Dr. Eleanor Jenkins
Dr. Jeong-Rock Yoon

# Abstract

This thesis studies novel physics-based methods for simulating incompressible fluid flow described by the Navier-Stokes equations (NSE) and magnetohydrodynamics equations (MHD). It is widely accepted in computational fluid dynamics (CFD) that numerical schemes which are more physically accurate lead to more precise flow simulations especially over long time intervals. A prevalent theme throughout will be the inclusion of as much physical fidelity in numerical solutions as efficiently possible. In algorithm design, model selection/development, and element choice, subtle changes can provide better physical accuracy, which in turn provides better overall accuracy (in any measure). To this end we develop and study more physically accurate methods for approximating the NSE, MHD, and related systems.

Chapter 3 studies extensions of the energy and helicity preserving scheme for the 3D NSE developed in [64], to a more general class of problems. The scheme is studied together with stabilizations of grad-div type in order to mitigate the effect of the Bernoulli pressure error on the velocity error. We prove stability, convergence, discuss conservation properties, and present numerical experiments that demonstrate the advantages of the scheme.

In Chapter 4, we study a finite element scheme for the 3D NSE that globally conserves energy and helicity and, through the use of Scott-Vogelius elements, enforces pointwise the solenoidal constraints for velocity and vorticity. A complete numerical analysis is given, including proofs for conservation laws, unconditional stability and optimal convergence. We also show the method can be efficiently computed by exploiting a connection between this method, its associated penalty method, and the method arising from using grad-div stabilized Taylor-Hood elements. Finally, we give numerical examples which verify the theory and demonstrate the effectiveness of the scheme.

In Chapter 5, we extend the work done in [8] that proved, under mild restrictions, grad-div stabilized Taylor-Hood solutions of Navier-Stokes problems converge to the Scott-Vogelius solution of that same problem. In [8] even though the analytical convergence rate was only shown to be $\gamma^{-\frac{1}{2}}$ (where $\gamma$ is the stabilization parameter), the computational results suggest the rate may be

improvable $\gamma^{-1}$. We prove herein the analytical rate is indeed $\gamma^{-1}$, and extend the result to other incompressible flow problems including Leray-$\alpha$ and MHD. Numerical results are given that verify the theory.

Chapter 6 studies an efficient finite element method for the NS-$\omega$ model, that uses van Cittert approximate deconvolution to improve accuracy and Scott-Vogelius elements to provide pointwise mass conservative solutions and remove the dependence of the (often large) Bernoulli pressure error on the velocity error. We provide a complete numerical analysis of the method, including well-posedness, unconditional stability, and optimal convergence. Several numerical experiments are given that demonstrate the performance of the scheme, and how the use of Scott-Vogelius elements can dramatically improve solutions.

Chapter 7 extends Leray-$\alpha$-deconvolution modeling to the incompressible MHD. The resulting model is shown to be well-posed, and have attractive limiting behavior both in its filtering radius and order of deconvolution. Additionally, we present and study a numerical scheme for the model, based on an extrapolated Crank-Nicolson finite element method. We show the numerical scheme is unconditionally stable, preserves energy and cross-helicity, and optimally converges to the MHD solution. Numerical experiments are provided that verify convergence rates, and test the scheme on benchmark problems of channel flow over a step and the Orszag-Tang vortex problem.

# Acknowledgments

I would like to thank all of my family members, professors, and friends who helped me over the past four years. Your support and encouragement made this possible.

I especially want to thank my advisor Dr. Leo Rebholz. I owe much of my success to him and the knowledge he shared with me.

I am also thankful for my committee members Dr. Vincent Ervin, Dr. Eleanor Jenkins, and Dr. Jeong-Rock Yoon. I have learned a lot from their courses as well as our conversations.

I would like to thank the following people for collaborating with me on the contents of this dissertation: Dr. Michael Case, Benjamin Cousins, Dr. Vincent Ervin, Dr. Alexander Labovsky, Dr. Alexander Linke, Dr. Carolina Manica, Dr. Monica Neda, Dr. Maxim Olshanskii, and Dr. Leo Rebholz.

I am thankful to have a great family. My mother, father, and sister have supported my education and believed in my success even when I doubted it.

Lastly, I would like to thank my fiance Dr. Tara Steuber, who made the last four years seem to go by quickly.

# Table of Contents

# List of Tables

# List of Figures

# Chapter 1

# Introduction

The study of fluid flow is at the forefront of many scientific fields and engineering applications such as aerodynamics, weather predictions and modeling ocean currents. It is tempting to think that after centuries of study and great advances in computational power little, only little knowledge might remain undiscovered. However, even the most fundamental mathematical questions remains unanswered: the existence and uniqueness of solutions in $3d$ of the equations of fluid motion. Additionally, while the advances in computer technology have aided the scientific community's understanding of fluid flow, there are still many flows which we cannot hope to simulate with modern computational tools. In fact, the field of computational fluid dynamics (CFD) is and will continue to be stifled by current technologies for the foreseeable future.

This thesis is concerned with more accurately and efficiently predicting fluid flow in computational simulations. A prevalent theme throughout will be the inclusion of as much physical fidelity in numerical solutions as efficiently possible. In algorithm design, model selection/development, element choice, etc., subtle changes can provide better physical accuracy, which in turn provides better overall accuracy (in any measure). To this end, we develop and study more physically accurate methods for approximating the Navier-Stokes equations (NSE), magnetohydrodynamics (MHD), and related models.

The NSE are derived from conservation of momentum and mass, and describe the motion of incompressible viscous Newtonian fluid flows. The equations in dimensionless form are given by

$$u_t - \nu \Delta u + u \cdot \nabla u + \nabla p \quad = \quad f, \tag{1.0.1}$$

$$\nabla \cdot u \quad = \quad 0. \tag{1.0.2}$$

Here $u$ is the fluid velocity, $p$ is the pressure, $f$ is an external body force, and $\nu$ is the kinematic viscosity. The Reynolds number (Re=$\nu^{-1}$) is the only control parameter of the flow. For low Reynolds number, the viscous forces dominate, making the flow smooth and easily predictable. Flows characterized by these properties are referred to as laminar. Turbulent flows, in contrast, are unstable and chaotic. Such flows are a result of dominating inertial forces and correspond to high Reynolds numbers.

Coupling the NSE with Maxwell's equations gives the MHD system, which describe the motion of electrically conducting non-magnetic fluids, such as salt water, liquid metals (e.g. mercury and sodium) and plasmas. MHD in dimensionless form is given by

$$u_t + \nabla \cdot (uu^T) - \nu \Delta u + \frac{s}{2}\nabla(B \cdot B) - s\nabla \cdot BB^T + \nabla p \;=\; f, \tag{1.0.3}$$

$$\nabla \cdot u \;=\; 0, \tag{1.0.4}$$

$$B_t + \nu_m \nabla \times (\nabla \times B) + \nabla \times (B \times u) \;=\; \nabla \times g, \tag{1.0.5}$$

$$\nabla \cdot B \;=\; 0, \tag{1.0.6}$$

where $u$, $p$, $\nu$ and $f$ represent the same quantities as in (1.0.1)-(1.0.2), $\nabla \times g$ represents a forcing on the magnetic field $B$, $\nu_m(=\text{Re}_m^{-1})$ is the inverse of the magnetic Reynolds' number, and the coupling number $s = \frac{Ha^2}{ReRe_m}$, where $Ha$ is the Hartmann number (the ratio of Lorentz forces to shear forces).

In the absence of viscosity and external force the NSE conserves energy $(=\frac{1}{2}\int_\Omega |u|^2 dx)$. MHD also conserves energy $(= \frac{1}{2}\int_\Omega (|u|^2 + s|B|^2)dx)$ in the absence of external force, kinematic viscosity and magnetic diffusivity . In addition to energy, under the respective conditions the 3d NSE conserves helicity $(= \int_\Omega u \cdot (\nabla \times u))$ and the 3d MHD conserves cross helicity $(= \int_\Omega u \cdot B)$. More recently, scientists have come to better understand the importance of helicity and cross helicity. In 1992 a famous paper of Moffatt and Tsoniber found helicity to be of comparable importance to energy in the NSE [54]. Similarly, the importance of cross-helicity in MHD is also known to be of fundamental importance [49].

Most numerical schemes which simulate fluid flow conserve energy as this typically coincides with algorithm stability. However, numerical schemes often neglect other fundamental physical laws or only enforce the physical laws in a weak sense. This is, in part, due to a perceived increase in computational cost to conserve a second integral invariant. However, it is widely accepted in CFD that physical fidelity in a numerical scheme produces more accurate predictions, especially over longer time intervals. Thus, numerical schemes which correctly account for physical quantities in addition to energy can give solutions which are not only more accurate, but also more physically

relevant. Examples of such schemes include Arakawa's energy and enstrophy conserving scheme for the 2D NSE [1] and related extensions [22], energy and potential enstrophy schemes pioneered by Arakawa and Lamb, and Navon, [2, 55, 56], an energy and helicity conserving scheme for 3D axisymmetric flow by J.-G. Liu and W. Wang [49], and most recently a 3d scheme for the full NSE with periodic boundary conditions [64].

A physical law which is commonly enforced weakly in the NSE is conservation of mass. Physically, (1.0.2) is interpreted to mean mass is a pointwise conserved quantity in incompressible fluid flows. However, finite element numerical schemes often only impose global mass conservation weakly (e.g. $\int_{\Omega}(\nabla \cdot u_h)q_h = 0$, where $u_h$ is the discrete velocity solution, and for each $q_h$ in the approximating pressure space). Depending on the element choice, this can lead to mass conservation being very inaccurate [8]. Lack of physical fidelity in such a fundamental quantity challenges the physical relevance of a numerical solution.

One common element which can lead to poor mass conservation is the Taylor-Hood (TH) element. The TH element uses continuous polynomials of degree $k$ to approximate velocity and continuous polynomials of degree $(k-1)$ to approximate pressure. It was found in [42, 59, 62] that adding the identically zero term $-\gamma\nabla(\nabla \cdot u)$ at the continuous level could improve mass conservation when using TH elements. The technique is referred to as grad-div stabilization and owes its success to a sharp energy bound. By adding the zero term at the continuous level, the 'usual' [37] discrete model satisfies

$$\|u_h^M\|^2 + \nu\Delta t \sum_{n=0}^{M-1} \|\nabla u_h^{n+\frac{1}{2}}\|^2 + \gamma\Delta t \sum_{n=0}^{M-1} \|\nabla \cdot u_h^{n+\frac{1}{2}}\|^2 \le C(data).$$

Thus, as $\gamma$ increases, mass conservation will improve.

Similar to the TH element, the Scott-Vogelius (SV) element [68] uses continuous polynomials of degree $k$ to approximate velocity. Unlike the TH element the SV element uses discontinuous polynomials of degree $(k-1)$ to approximate the pressure. This modest change enforces pointwise mass conservation but slightly increases the number of degrees of freedom in the system. It is known that SV elements are LBB stable and admit optimal convergence properties under the mild restrictions that $k \ge d$, where $d$ is the dimension of $\Omega$, and solutions are computed on a barycenter refined mesh [76] (e.g. see Figure 1.1) .

A connection has been established between the SV element solutions and the grad-div stabilized TH element solutions to the NSE [8]. On a fixed mesh, as $\gamma \to \infty$ the TH solution tends to the SV solution; that is, $\|u_h^{TH} - u_h^{SV}\| \to 0$. The authors have shown an analytic convergence rate
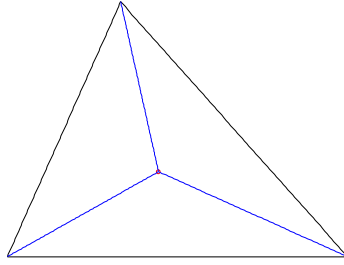
Figure 1.1: A barycenter refined triangle

of $\gamma^{\frac{-1}{2}}$. However, numerical experiments hint at a faster convergence rate of $\gamma^{-1}$. In Chapter 5 we extend the connection between the SV element solutions and the grad-div stabilized TH solutions and show an analytic convergence rate of $\gamma^{-1}$ for Stokes type problems.

The sacrifice of conserving physical properties is in part motivated by reducing the number of degrees of freedom required to simulate flow problems. Turbulent flows especially devour computational resources. According to the Kolmogorov estimate, to solve NSE accurately, a mesh must contain approximately $Re^{\frac{3}{2}}$ discretization points in 2d and $Re^{\frac{9}{4}}$ discretization points in 3d. Thus, direct numerical simulation of turbulent flows is expensive! Recent work on FEM for the '$\alpha$ models' [43, 44, 52, 6, 66, 50, 12, 11, 28] has shown their effectiveness at producing accurate solutions to the NSE and the MHD on significantly coarser meshes than direct simulations require. One of the '$\alpha$ models', called Navier-Stokes-$\overline{\omega}$ (NS-$\overline{\omega}$) appears particularly promising, and is given by

$$u_t + (\nabla \times D_N F u) \times u + \nabla q - \nu \Delta u \;\; = \;\; f, \qquad\qquad (1.0.7)$$

$$\nabla \cdot u \;\; = \;\; 0. \qquad\qquad (1.0.8)$$

Here $F$ denotes the Helmholtz filter: $F := (-\alpha^2 \Delta + I)^{-1}$ where $\alpha > 0$ is the filtering radius, and $D_N$ is the $N^{th}$ order van Cittert approximate deconvolution operator, $D_N := \sum_{n=0}^{N} (I - F)^n$. This model is of particular interest because, in addition to energy conservation, the model conserves a model helicity. Moreover, it is an analog of NS-$\alpha$, but can more efficiently be computed. Solving NS-$\overline{\omega}$ with SV elements enforces pointwise mass conservation in the scheme and gives more physical significance to our solutions (Chapter 4, [51]).

Simulations for MHD flows require the same number of mesh points as simulations for NSE flows to be successfully resolved. However, MHD flows contain an additional unknown, the magnetic field, making MHD flows more complex than NSE flows. Thus, modeling is imperative for MHD flows [10, 33, 35, 39, 75]. We extend the work done by Yu and Li on the MHD Leray-$\alpha$ model [75]

to the MHD Leray-deconvolution model which is given by

$$u_t - Re^{-1}\Delta u + D_N \overline{u} \cdot \nabla u - s D_N \overline{B} \cdot \nabla B + \nabla p = f,$$

$$B_t - Re_m^{-1}\Delta B + D_N \overline{u} \cdot \nabla B - D_N \overline{B} \cdot \nabla B = \nabla \times g,$$

$$\nabla \cdot u = 0,$$

$$\nabla \cdot B = 0.$$

We perform an analytic study of the continuous model, and the numerical scheme presented for the model, and provide numerical experiments which show its effectiveness on benchmark problems (Chapter 6). We remark that the discretized MHD equations are overdetermined and hence require a Lagrange multiplier, which leads to a second solenoidal constraint in the numerical scheme. Thus, the SV element is crucial in simulating MHD flows.

Despite enforcing solenoidal constraints pointwise the SV element presents obstacles. Specifically, the SV element has a larger pressure space than the TH element; in fact the SV pressure space can be comparable in size to the velocity space. Thus, efficiency is a concern when using the SV element. Efficiency may be improved using Temam's penalty method [69] as discussed in [65]. We study a finite element scheme for the 3D NSE that employs the SV element and Temam's penalty method that conserves energy and helicity (Chapter 7).

The body of this thesis is comprised of seven chapters. Chapter 2 presents mathematical preliminaries and notations which are used throughout the report, including the definitions of the TH and SV elements. Chapter 3 extends the work done in [64] to the more general homogenous boundary conditions. We study the scheme with two types of stabilization and show that the scheme is stable, conserves energy and under mild conditions conserves model helicity. Lastly, we give evidence of the advantages of the scheme by simulating a complex flow problem and comparing against the usual Crank-Nicolson scheme for NSE.

Chapter 4 presents a study of the NS-$\overline{\omega}$ turbulence model with SV elements. Channel flow around a cylinder and over a step are benchmark flow problems which we simulate to show improved mass conservation using SV rather than TH elements. Chapter 5 extends the work done in [8] to show analytically grad-div stabilized TH solutions to Stokes type problems converge to the SV solutions with rate $\gamma^{-1}$. Chapter 6 presents the MHD Leray-deconvolution model and provides analysis of the continuous model, the numerical scheme presented for the model, and solutions to the benchmark problems of channel flow over a step and the Orszag-Tang vortex problem. Chapter 7 presents a numerical scheme for NSE and an analytic study of the scheme which is based on Temam's penalty

method and leads to increased efficiency in 3D computations of the benchmark problem of channel flow over a step.

# Chapter 2

# Preliminaries

For the analysis in this thesis we consider either periodic or no slip boundary conditions. For periodic boundary conditions we assume the domain $\Omega$ is the L-periodic box $(0, L)^d$, and for no slip boundary conditions we assume $\Omega$ denotes a bounded, polyhedral domain in $\mathbb{R}^d$ (d=2, or 3). The $L^2(\Omega)$ norm and inner product will be denoted by $\|\cdot\|$ and $(\cdot, \cdot)$. Likewise, the $L^p(\Omega)$ norms and the Sobolev $W_p^k(\Omega)$ norms are denoted by $\|\cdot\|_{L^p}$ and $\|\cdot\|_{W_p^k}$, respectively. For the semi-norm in $W_p^k(\Omega)$ we use $|\cdot|_{W_p^k}$. $H^k$ is used to represent the Sobolev space $W_2^k(\Omega)$, and $\|\cdot\|_k$ denotes the norm in $H^k$. For functions $v(x, t)$ defined on the entire time interval $(0, T)$, we define $(1 \leq m < \infty)$

$$\|v\|_{\infty, k} := \operatorname*{ess\,sup}_{0 < t < T} \|v(t, \cdot)\|_k, \qquad \text{and} \qquad \|v\|_{m, k} := \left( \int_0^T \|v(t, \cdot)\|_k^m \, dt \right)^{1/m}.$$

In the discrete case we use the analogous norms:

$$\|\|v\|\|_{\infty, k} := \max_{0 \leq n \leq M} \|v_n\|_k, \qquad \|\|v_{1/2}\|\|_{\infty, k} := \max_{0 \leq n \leq M-1} \|v_{n+1/2}\|_k,$$

$$\|\|v\|\|_{m, k} := \left( \triangle t \sum_{n=0}^{M} \|v_n\|_k^m \right)^{1/m}, \qquad \|\|v_{1/2}\|\|_{m, k} := \left( \triangle t \sum_{n=0}^{M-1} \|v_{n+1/2}\|_k^m \right)^{1/m}.$$

For $s \in \mathbb{R}$ we recall the spaces $H_0^s$ and $H_p^s$

$$H_0^s(\Omega) := \{ w \in H^s(\Omega), \, w = 0 \text{ on } \partial\Omega \}, \text{ and}$$

$$H_p^s(\Omega) := \{ w \in H_{loc}^s(\mathbb{R}^d), \, \text{L-periodic}, \, \nabla \cdot w = 0, \, \int_\Omega w = 0 \}.$$

The space $X$ is $H_p^1(\Omega)$ in the periodic boundary case and $(H_0^1)^d$ for Dirichlet boundary conditions. We use as the norm on $X$ the $H^1$ seminorm which, because of the boundary condition, is equivalent to the $H^1$ norm; for $v \in X$, $\|v\|_X := \|\nabla v\|$. We denote the dual space of $X$ by $X'$, with

the norm $\|\cdot\|_*$. We denote the pressure space by $Q = L^2_0(\Omega) := \{q \in L^2(\Omega) : \int_\Omega q = 0\}$ corresponding to Dirichlet boundary conditions and in the periodic case $Q = L^2_{0,p}(\Omega) := \{q \in L^2_p : \int_\Omega q = 0\}$. The space of weakly divergent free functions, $V := \{v \in X : (\nabla \cdot v, q) = 0, \forall q \in Q\}$, and the dual space of $V$ will be denoted by $V'$.

For TH elements, $(X_h, Q_h)$ is made of $((P_k)^d, P_{k-1})$, $k \geq 2$ velocity/pressure elements. Thus we have, for a given regular mesh $\mathcal{T}_h$, and homogenous Dirichlet boundary conditions,

$$X_h := \left\{ v_h : v_h|_e \in P_k(e), \forall e \in \mathcal{T}_h, v_h \in [C^0(\overline{\Omega})]^d, v_h|_{\partial\Omega} = 0 \right\},$$

$$Q_h := \left\{ q_h : q_h|_e \in P_{k-1}(e), \forall e \in \mathcal{T}_h, q_h \in C^0(\overline{\Omega}), q_h \in L^2_0(\Omega) \right\}.$$

For periodic boundary conditions the spaces are defined by

$$X_h := \left\{ v_h : v_h|_e \in P_k(e), \forall e \in \mathcal{T}_h, v_h \in [C^0(\overline{\Omega})]^d, v_h|_{\partial\Omega} = \text{periodic} \right\},$$

$$Q_h := \left\{ q_h : q_h|_e \in P_{k-1}(e), \forall e \in \mathcal{T}_h, q_h \in C^0(\overline{\Omega}), q_h \in L^2_p(\Omega) \right\}.$$

In addition to the TH approximation spaces we define the SV velocity and pressure approximation spaces. Let $\mathcal{T}_h$ denote the mesh that ensures the SV pair is LBB stable, for example:

(A1) in $2d$, $k \geq 4$ and the mesh has no singular vertices [63],

(A2) in $3d$, $k \geq 6$ [77],

(A3) when $k \geq d$ and the mesh is a barycenter refinement of a regular mesh [76, 63], or

(A4) on Powell-Sabin meshes when $k = 1$ and $d = 2$ or when $k = 2$ and $d = 3$ [78].

We note that the SV velocity approximation space is the same as the TH velocity approximation space and define the SV pressure space to be

$$Q_h^{SV} := \{q_h \in L^2_0(\Omega) : q_{h|T} \in P_{k-1} \forall T \in \mathcal{T}_h\}, \text{ or}$$

$$Q_h^{SV} := \{q_h \in L^2_p(\Omega) : q_{h|T} \in P_{k-1} \forall T \in \mathcal{T}_h\}.$$

Since it is discontinuous, the dimension of the pressure space for SV elements is significantly larger than for TH elements. This creates a greater total number of degrees of freedom needed for linear solves using SV elements. Although the velocity spaces of the TH and SV elements are the same, the spaces of discretely divergence free subspaces are different, and thus we denote the TH and SV

discretely divergence free subspaces respectively as

$$
\begin{aligned}
V_h &:= \{v_h \in X_h : (\nabla \cdot v_h, q_h) = 0 \;\; \forall q_h \in Q_h\}, \\
V_h^{SV} &:= \{v_h \in X_h^{SV} : (\nabla \cdot v_h, q_h) = 0 \;\; \forall q_h \in Q_h^{SV}\}.
\end{aligned}
$$

The SV elements are very attractive from the mass conservation point of view since their discrete velocity space and discrete pressure space fulfill an important property, namely

$$
\nabla \cdot \; X_h^{SV} \subset Q_h^{SV}.
$$

Thus, using SV elements, weak mass conservation via $(\nabla \cdot v_h, q_h) = 0, \;\; \forall q_h \in Q_h^{SV}$ implies strong (pointwise) mass conservation, since $||\nabla \cdot v_h|| = 0$ by choosing $q_h = \nabla \cdot v_h$. Such a result, or choice of test function, is not possible with many element choices, including TH.

Chapter 3 and Chapter 4 make use of the curl of the velocity, which is known as vorticity. These chapters prescribe homogenous Dirichlet boundary conditions for the velocity, and so we do not define a discrete vorticity space in the context of periodic boundary conditions. However, we use a more general space for the discrete vorticity space when velocity is prescribed no slip boundary conditions. Even though the velocity satisfies homogeneous Dirichlet boundary conditions, it is believed to be inappropriate to enforce homogeneous Dirichlet boundary conditions for the vorticity. We choose the boundary condition to be a no-slip boundary condition *along* the boundary, and hence we define the space

$$
W_h := \left\{ v_h : v_h \in [C^0(\Omega)]^3, \forall_{e \in \mathcal{T}_h} (v_h)_{|e} \in P_k(e), v_h \times n|_{\partial \Omega} = 0 \right\} \supset X_h.
$$

We use $t^n := n\Delta t$, and for both continuous and discrete functions of time

$$
v^{n+\frac{1}{2}} := \frac{v((n+1)\Delta t) + v(n\Delta t)}{2}.
$$

For the convergence studies, we make use of the following approximation properties:

$$
\begin{aligned}
\inf_{v_h \in V_h^{SV}} \|u - v_h\| &\leq C(\beta) \\
\inf_{v \in X_h^{SV}} \|u - v\| &\leq Ch^{k+1}|u|_{k+1}, \quad u \in (H^{k+1}(\Omega))^d, \\
\inf_{v \in X_h^{SV}} \|u - v\|_1 &\leq Ch^k|u|_{k+1}, \quad u \in (H^{k+1}(\Omega))^d, \\
\inf_{r \in Q_h^{SV}} \|p - r\| &\leq Ch^{s+1}|p|_{s+1}, \quad p \in H^{s+1}(\Omega)
\end{aligned}
$$

For the analysis in this thesis we use three trilinear operators which are defined below along with their respective bounds. The first trilinear operator is used when the nonlinear term in the NSE is in rotational form and is given by

**Definition 2.0.1.** *Define* $b_1 :\ X \times\ X \times\ X \to \mathbb{R}$ *, by*

$$
b_1(u, v, w) := ((\nabla \times u) \times v, w).
$$

The following bounds will be used often in our analysis

**Lemma 2.0.1.** *For* $u, v, w \in\ X$*, or* $L^\infty(\Omega)$ *and* $\nabla \times u \in L^\infty(\Omega)$*, when indicated, the trilinear term* $b(u, v, w)$ *satisfies*

$$
\begin{aligned}
|b_1(u, v, w)| &\leq\ \|\nabla \times u\|\|v\|_\infty\|w\|, &\text{(2.0.1)} \\
|b_1(u, v, w)| &\leq\ \|\nabla \times u\|_\infty\|v\|\|w\|\,, &\text{(2.0.2)} \\
|b_1(u, v, w)| &\leq\ C_0(\Omega)\|\nabla \times u\|\|\nabla v\|\|\nabla w\|\,, &\text{(2.0.3)} \\
|b_1(u, v, w)| &\leq\ C_0(\Omega)\|v\|^{1/2}\|\nabla v\|^{1/2}\|\nabla \times u\|\|\nabla w\|\,, &\text{(2.0.4)}
\end{aligned}
$$

*and if* $u,\ v,\ w \in V$ *and* $w \in (H^2(\Omega))^d$*, then*

$$
|b_1(u, v, w)| \leq C\|w\|_2\|\nabla v\|\|u\| \tag{2.0.5}
$$

*Proof.* The first two estimates follow immediately from the definition of $b_1$. The proof of the next two bounds are easily adapted from the usual bounds of the nonlinearity in non-rotational form. The last bound takes more work. Begin with a simple vector identity and that the curl is self adjoint

with $u$, $v$, $w \in X$:

$$|((\nabla \times u) \times v, w)| = |(w \times v, \nabla \times u)| = |(\nabla \times (w \times v), u)| \qquad (2.0.6)$$

Continuing with another vector identity for the curl of the cross product of two vectors,

$$\nabla \times (w \times v) = v \cdot \nabla w - w \cdot \nabla v + (\nabla \cdot v)w - (\nabla \cdot w)v, \qquad (2.0.7)$$

which reduces, since $v$, $w \in V$, to

$$\nabla \times (w \times v) = v \cdot \nabla w - w \cdot \nabla v. \qquad (2.0.8)$$

Combining this with (2.0.6), we have by Holder and Poincare's inequalities,

$$
\begin{aligned}
|((\nabla \times u) \times v, w)| &\leq |(v \cdot \nabla w, u)| + |(w \cdot \nabla v, u)| \\
&\leq C\|w\|_2\|\nabla v\|\|u\|. \qquad (2.0.9)
\end{aligned}
$$

$\square$

The second trilinear operator is the skew-symmetric operator $b^* : X \times X \times X \to \mathbb{R}$ is defined by

$$b^*(u, v, w) := \frac{1}{2}(u \cdot \nabla v, w) - \frac{1}{2}(u \cdot \nabla w, v).$$

The following bounds on $b^*$ will be used.

**Lemma 2.0.2.** *There exists a constant $C_s$ dependent only on the size of $\Omega$ such that $\forall u, v, w \in X_h$,*

$$
\begin{aligned}
b^*(u, v, w) &\leq C_s\|\nabla u\|\|\nabla v\|\|\nabla w\| \\
b^*(u, v, w) &\leq C_s\|\nabla u\|\|\nabla v\|\|w\|^{1/2}\|\nabla w\|^{1/2}
\end{aligned}
$$

*Proof.* This well known lemma is proven, e.g., in [37]. $\square$

We define the final trilinear operator, $b_3(\cdot, \cdot, \cdot)$, which will be used in Chapter 7.

**Definition 2.0.2.** *Define the trilinear operator $b_3 : L^1(\Omega) \times W_1^1(\Omega) \times L^1(\Omega) \to \mathbb{R}$ as*

$$b_3(u, v, w) = (u \cdot \nabla v, w),$$

*whenever the integral exists finitely.*

**Lemma 2.0.3.** *Let $n$ denote the dimension of $\Omega$. Then the form $b_3(\cdot, \cdot, \cdot)$ is trilinear continuous on $H^{m_1}(\Omega) \times H^{m_2+1}(\Omega) \times H^{m_3}(\Omega)$ where $m_i \geq 0 \ \forall i$ and*

$$m_1 + m_2 + m_3 \geq \tfrac{n}{2} \ \text{if} \ m_i \neq \tfrac{n}{2}, \ \text{or}$$
$$m_1 + m_2 + m_3 > \tfrac{n}{2} \ \text{if} \ m_i = \tfrac{n}{2} \ \text{for some} \ i.$$

*Proof.* This operator has been studied extensively and is well known in the theory of the NSE. The interested reader is referred to [70]. □

**Corollary 2.0.1.** *The following inequalities will be utilized throughout Chapter 7*

1. *For every $u, v, w \in H^1_p(\Omega)$*

$$b_3(u, v, w) \leq C\|u\|_1\|v\|_1\|w\|_1. \tag{2.0.10}$$

2. *For all $u, v, w \in H^1_p(\Omega)$*

$$b_3(u, v, w) \quad = \quad -b_3(u, w, v), \tag{2.0.11}$$

   *which implies that*

$$b_3(u, v, v) \quad = \quad 0. \tag{2.0.12}$$

3. *For all $u \in H^1_p(\Omega)$, $v \in H^2_p(\Omega)$ and $w \in H^0_p(\Omega)$,*

$$b_3(u, v, w) \leq \|u\|_1\|v\|_2\|w\|. \tag{2.0.13}$$

*Proof.* These are well known identities follow immediately from Lemma 2.0.3. □

The following two lemmas are also employed in the studies of the finite element analysis.

**Lemma 2.0.4.** *Assume $u \in C^0(t_n, t_{n+1}; L^2(\Omega))$. If $u$ is twice differentiable in time and $u_{tt} \in L^2((t_n, t_{n+1}) \times \Omega)$ then*

$$\|u_{n+1/2} - u(t_{n+1/2})\|^2 \quad \leq \quad \frac{1}{48}(\Delta t)^3 \int_{t_n}^{t_{n+1}} \|u_{tt}\|^2 \, dt. \tag{2.0.14}$$

12

*If $u_t \in C^0(t_n, t_{n+1}; L^2(\Omega))$ and $u_{ttt} \in L^2((t_n, t_{n+1}) \times \Omega)$ then*

$$\|\frac{u_{n+1} - u_n}{\Delta t} - u_t(t_{n+1/2})\|^2 \leq \frac{1}{1280}(\Delta t)^3 \int_{t_n}^{t_{n+1}} \|u_{ttt}\|^2 \, dt \quad and \tag{2.0.15}$$

*if $\nabla u \in C^0(t_n, t_{n+1}; L^2(\Omega))$ and $\nabla u_{tt} \in L^2((t_n, t_{n+1}) \times \Omega)$ then*

$$\|\nabla(u_{n+1/2} - u(t_{n+1/2}))\|^2 \leq \frac{(\Delta t)^3}{48} \int_{t_n}^{t_{n+1}} \|\nabla u_{tt}\|^2 \, dt. \tag{2.0.16}$$

The proof of Lemma 2.0.4 is based on the Taylor expansion with remainder. It is more of technical nature and therefore omitted herein.

The analysis in this thesis uses two discrete Gronwall inequalities, recalled from [37], for example, and a continuous Gronwall inequality. These are given below.

**Lemma 2.0.5** (Discrete Gronwall Lemma (version 1)). *Let $\Delta t$, $H$, and $a_n, b_n, c_n, d_n$ (for integers $n \geq 0$) be finite nonnegative numbers such that*

$$a_l + \Delta t \sum_{n=0}^{l} b_n \leq \Delta t \sum_{n=0}^{l-1} d_n a_n + \Delta t \sum_{n=0}^{l} c_n + H \quad for \ l \geq 1. \tag{2.0.17}$$

*Then for $\Delta t > 0$*

$$a_l + \Delta t \sum_{n=0}^{l} b_n \leq \exp\left(\Delta t \sum_{n=0}^{l-1} d_n\right)\left(\Delta t \sum_{n=0}^{l} c_n + H\right) \quad for \ l \geq 1. \tag{2.0.18}$$

**Lemma 2.0.6** (Discrete Gronwall Lemma (version2)). *Let $\Delta t$, $H$, and $a_n, b_n, c_n, d_n$ (for integers $n \geq 0$) be finite nonnegative numbers such that*

$$a_l + \Delta t \sum_{n=0}^{l} b_n \leq \Delta t \sum_{n=0}^{l} d_n a_n + \Delta t \sum_{n=0}^{l} c_n + H \quad for \ l \geq 0. \tag{2.0.19}$$

*Suppose that $\Delta t d_n < 1 \ \forall n$. Then, for $\Delta t > 0$*

$$a_l + \Delta t \sum_{n=0}^{l} b_n \leq \exp\left(\Delta t \sum_{n=0}^{l} \frac{d_n}{1 - \Delta t d_n}\right)\left(\Delta t \sum_{n=0}^{l} c_n + H\right) \quad for \ l \geq 0. \tag{2.0.20}$$

**Lemma 2.0.7.** *(Continuous Gronwall inequality) Let $f(x)$ and $B(x)$ be functions which are piecewise continuous on the interval $[a, b]$ and let $K$ be a nonnegative scalar. Further, assume that $f(x)$*

and $B(x)$ satisfy $\forall t \in [a, b]$

$$\int_a^t g(s)ds + f(t) \leq K + \int_a^t B(s)f(s)ds. \tag{2.0.21}$$

Then, $\forall t \in [a, b]$ we have the following upper bound

$$\int_a^s g(s)ds + f(t) \leq K e^{\int_a^t B(s)ds}. \tag{2.0.22}$$

**Lemma 2.0.8.** *(Aubin-Lions Lemma). Let $X_0, X$, and $X_1$ be Banach spaces such that $X_0 \subset X \subset X_1$. Suppose that $X_0$ is compactly embedded in $X$ and that $X$ is continuously embedded in $X_1$. Additionally, assume that $X_0$ and $X_1$ are reflexive spaces. For $1 < p, q < \infty$, let*

$$W := \{u \in L^p([0, T]; X_0) | \partial_t u \in L^q([0, T]; X_1)\}.$$

*Then the embedding of $W$ into $L^p([0, T]; X)$ is also compact.*

Define $R_h$ to be the orthogonal complement of $V_h^{SV}$ in $V_h$ with respect to the $(\nabla \cdot, \nabla \cdot)$ inner product. That is

$$V_h =: V_h^{SV} \oplus R_h,$$

**Lemma 2.0.9.** *There exists a constant $M < \infty$ satisfying $\forall r_h \in R_h$,*

$$\|\nabla r_h\| \leq M \|\nabla \cdot r_h\|.$$

*Proof.* Define

$$M := \max_{v_h \in R_h, \|\nabla v_h\|=1} \frac{1}{\|\nabla \cdot v_h\|}$$

Observe $M < \infty$ since $v_h \in R_h$, $\|\nabla \cdot v_h\| > 0$, and the max is taken over a compact set of $\mathbf{R^n}$. For any $r_h \in R_h$, there is an $e_h \in R_h$ satisfying $\|\nabla e_h\| = 1$ and

$$r_h = \|\nabla r_h\| e_h.$$

Taking divergence of both sides, then $L^2$ norms gives

$$\|\nabla \cdot r_h\| = \|\nabla r_h\| \|\nabla \cdot e_h\|.$$

Rearranging and using the definition of $M$ finishes the proof. $\qquad \square$

Since we study discretizations of a fluid model, we must deal with discrete differential filters. Continuous differential filters were introduced into turbulence modeling by Germano [24] and used for various models and regularizations [13, 5, 28]. They can arise, for example, as approximations to Gaussian filters of high qualitative and quantitative accuracy [21].

**Definition 2.0.3** (Continuous Helmholtz-filter). *For $v \in (L^2(\Omega))^d$ and $\alpha > 0$ fixed, denote the filtering operation on $v$ by $\overline{v}$, where $\overline{v}$ is the unique solution in $X$ to*

$$-\alpha^2 \Delta \overline{v} + \overline{v} = v. \tag{2.0.23}$$

We denote by $F := (-\alpha^2 \Delta + I)^{-1}$, so $Fv = \overline{v}$. We define next the discrete differential filter following Manica and Kaya-Merdan [53], but also enforcing incompressibility:

**Definition 2.0.4** (Discrete Helmholtz filter). *Given $v \in (L^2(\Omega))^d$, for a given filtering radius $\alpha > 0$, $\overline{v}^h = F_h v$ is the unique solution in $X_h^{SV}$ of: Find $(\overline{v}^h, \lambda_h) \in (X_h^{SV}, Q_h^{SV})$ satisfying*

$$\alpha^2 (\nabla \overline{v}^h, \nabla \chi_h) + (\overline{v}^h, \chi_h) - (\lambda_h, \nabla \cdot \chi_h) + (\nabla \cdot \overline{v}^h, r_h) = (v, \chi_h) \quad \forall (\chi_h, r_h) \in (X_h^{SV}, Q_h^{SV}). \tag{2.0.24}$$

**Remark 2.0.1.** *The definition of the discrete Helmholtz filter is defined using SV elements. The definition of the discrete filter using TH elements is a straight forward extension and so we omit it.*

We next introduce the following lemma which bounds the solution to the filtered problem by data.

**Lemma 2.0.10.** *For $v \in X$, we have the following bounds*

$$\|\overline{v}^h\| \leq \|v\|, \quad \|\nabla \overline{v}^h\| \leq \|\nabla v\| \ and \ \|\nabla \times \overline{v}^h\| \leq \|\nabla v\|. \tag{2.0.25}$$

*Proof.* The proof can be found in [44]. $\qquad \square$

We now define the van Cittert approximate deconvolution operators.

**Definition 2.0.5.** *The continuous and discrete van Cittert deconvolution operators $D_N$ and $D_N^h$ are*

$$D_N v := \sum_{n=0}^{N} (I - F)^n v, \qquad D_N^h v := \sum_{n=0}^{N} (\Pi_h - F_h)^n v. \tag{2.0.26}$$

*where $\Pi_h$ denotes the $L^2$ projection $\Pi^h : (L^2(\Omega))^d \to X_h$.*

For order of deconvolution $N = 0, 1, 2, 3$ and $v \in X_h$ we have

$$
\begin{aligned}
D_0^h v &= v, \\
D_1^h v &= 2v - \overline{v}^h, \\
D_2^h v &= 3v - 3\overline{v}^h + \overline{\overline{v}^h}^h, \\
D_3^h v &= 4v - 6\overline{v}^h + 4\overline{\overline{v}^h}^h - \overline{\overline{\overline{v}^h}^h}^h.
\end{aligned}
$$

$D_N$ was shown to be an $O(\alpha^{2N+2})$ approximate inverse to the filter operator $F$ in Lemma 2.1 of [16]. The proof is an algebraic identity and holds in the discrete case as well, giving the following.

**Lemma 2.0.11.** $D_N$ and $D_N^h$ are bounded, self-adjoint positive operators. For $v \in (L^2(\Omega))^d$,

$$
v = D_N \overline{v} + (-1)^{(N+1)} \alpha^{2N+2} \Delta^{N+1} F^{(N+1)} v
$$

and

$$
v = D_N^h \overline{v}^h + (-1)^{(N+1)} \alpha^{2N+2} \Delta_h^{N+1} F_h^{(N+1)} v
$$

**Lemma 2.0.12.** For $v \in X$, we have the following bounds

$$
\|\nabla \times D_N^h \overline{v}^h\| \le C(N)\|\nabla v\|. \tag{2.0.27}
$$

*Proof.* The proof follows from an inductive argument based on the definition of the deconvolution operator $D_N^h$ and Lemma 2.0.10. $\qquad \square$

**Lemma 2.0.13.** For smooth $\phi$ the discrete approximate deconvolution operator satisfies

$$
\|v - D_N^h \overline{v}^h\| \le C\alpha^{2N+2}\|\Delta^{N+1} F^{N+1} v\| + C(\alpha h^k + h^{k+1})\left( \sum_{n=1}^{N+1} |F^n v|_{k+1} \right). \tag{2.0.28}
$$

This is proven in [43].

The dependence of the $|F^n(v)|_{k+1}$ terms in (2.0.28) upon the *filter radius* $\alpha$, for a general smooth function $\phi$, is not fully understood for deconvolution order $N \ge 2$ (i.e. for $n \ge 2$)[17, 36]. In the case of $v$ periodic $|F^n(v)|_{k+1}$ is independent of $\alpha$. Also, for $v$ satisfying homogeneous Dirichlet boundary conditions, with the additional property that $\Delta^j v = 0$ on $\partial\Omega$ for $0 \le j \le \left[\frac{k+1}{2}\right] - 1$, the $|F^n(v)|_{k+1}$ are independent of $\alpha$. Our analysis of the method is for general $N$, and thus for $N \ge 2$, we make this assumption of independence. However, our computations are for $N = 1$, and our experience has shown there is typically little or no gain for larger N with polynomials approximating

16

velocities with degree three or less. For elements with higher order polynomials, we would expect a difference.

The Leray-deconvolution model first filters the velocity and then approximately unfilters it. Hence we are interested in properties of the operator $(D_N \circ F)$, which is denoted by $H_N$ by Layton and Lewandowski [41], and we continue this notation.

**Definition 2.0.6.** *The operator* $H_N : H_p^0(\Omega) \to H_p^0(\Omega)$ *is defined by*

$$H_N w := (D_N \circ F)w.$$

Next we list some properties of the operator $H_N$ proved in [41], which will be used in our analysis.

**Lemma 2.0.14.** *Let* $s \in \mathbb{R}$ *be nonnegative. Then*

1. *For* $s \geq 0$ $H_N$ *maps* $H_p^s$ *into itself compactly.*

2. *If* $w \in H_p^s(\Omega)$ *then* $H_N(w) \in H_p^{s+2}(\Omega)$. *That is* $\|H_N w\|_{s+2} \leq C(\alpha, N)\|w\|_s$.

3. $H_N$ *commutes with the gradient operator, i.e.* $H_N \circ \nabla(\cdot) = \nabla \circ H_N(\cdot)$.

4. *If* $w \in H_p^s(\Omega)$ *then* $H_N(w) \to w$ *strongly in* $H_p^s(\Omega)$ *when* $\alpha$ *is fixed and* $N \to \infty$.

**Remark 2.0.2.** *The constant,* $C(\alpha, N)$, *in 2 can go to infinity as* $\alpha \to 0$ *or as* $N \to \infty$.

# Chapter 3

# Stable Computing with an Enhanced Physics Based Scheme for the 3D Navier-Stokes Equations

In this chapter we extend the enhanced-physics based helicity scheme of [64] to homogeneous Dirichlet boundary conditions for the velocity with appropriate stabilizations. We propose three numerical schemes that are extensions of the helicity conserving scheme studied by Rebholz. The first scheme we propose is a direct extension of the enhanced physics based scheme to homogenous Dirichlet boundary conditions (i.e. we do not stabilize the scheme). The other two schemes are stabilized. The first scheme is stabilized using the usual grad-div stabilization [62], and the second is stabilized using a modified grad-div stabilization term.

The usual grad-div stabilization term in our numerical scheme is derived by adding the identically 0 term $-\gamma\nabla(\nabla \cdot u)$ to the continuous NSE. In the numerical scheme the term penalizes for lack of discrete mass conservation, and nullifies the effect of the pressure error on the velocity error [42, 52, 62]. The model we study uses the rotational form of the NSE nonlinearity and so the pressure used is the more complex Bernoulli pressure, which can adversely effect the velocity error. Tthe modified grad-div stabilization term is derived similarly by adding the identically 0 term $-\gamma\nabla(\nabla \cdot u_t)$ to the continuous NSE. The modified grad-div stabilization also penalizes for lack of discrete mass conservation, and nullifies the effect of the pressure error on the velocity error.

The use of stabilization is not without potential drawbacks. Adding the stabilization terms to the numerical scheme changes the energy balance, which is not ideal but often advantageous

in practice. We show that the modified grad-div stabilization terms alters the energy balance less than the typical grad-div stabilization term, and provide a numerical experiments that shows the improvement when the stabilization terms are used.

## 3.1  Algorithms

**Algorithm 3.1.1** (Enhanced-physics based helicity schemes for homogeneous Dirichlet boundary conditions). *Given a time step $\Delta t > 0$, finite end time $T := M\Delta t$, and initial velocity $u_h^0 \in V_h$, find $w_h^0 \in W_h$ and $\lambda_h^0 \in Q_h$ satisfying $\forall (\chi_h, r_h) \in (W_h, Q_h)$*

$$(w_h^0, \chi_h) + (\lambda_h^0, \nabla \cdot \chi_h) = (\nabla \times u_h^0, \chi_h), \tag{3.1.1}$$

$$(\nabla \cdot w_h^0, r_h) = 0. \tag{3.1.2}$$

*Then for $n = 0, 2, ..., M - 1$, find $(u_h^{n+1}, w_h^{n+1}, p_h^{n+1}, \lambda_h^{n+1}) \in (X_h, W_h, Q_h, Q_h)$ satisfying $\forall (v_h, \chi_h, q_h, r_h) \in (X_h, W_h, Q_h, Q_h)$*

$$(\frac{u_h^{n+1} - u_h^n}{\Delta t}, v_h) + STAB - (p_h^{n+1}, \nabla \cdot v_h)$$
$$+ (w_h^{n+\frac{1}{2}} \times u_h^{n+\frac{1}{2}}, v_h) + \nu(\nabla u_h^{n+\frac{1}{2}}, \nabla v_h) = (f(t^{n+\frac{1}{2}}), v_h) \tag{3.1.3}$$

$$(\nabla \cdot u_h^{n+1}, q_h) = 0 \tag{3.1.4}$$

$$(w_h^{n+\frac{1}{2}}, \chi_h) + (\lambda_h^{n+1}, \nabla \cdot \chi_h) = (\nabla \times u_h^{n+\frac{1}{2}}, \chi_h) \tag{3.1.5}$$

$$(\nabla \cdot w_h^{n+\frac{1}{2}}, r_h) = 0. \tag{3.1.6}$$

*where*

$$STAB = \begin{cases} 0 & \textit{helicity scheme 1} \\ \gamma(\nabla \cdot u_h^{n+\frac{1}{2}}, \nabla \cdot v_h) & \textit{helicity scheme 2} \\ \frac{\gamma}{\Delta t}(\nabla \cdot (u_h^{n+1} - u_h^n), \nabla \cdot v_h) & \textit{helicity scheme 3} \end{cases}$$

**Remark 3.1.1.** *We have found it computationally advantageous to decouple the 4 equation system (3.1.3)-(3.1.6) into a velocity-pressure system (3.1.3)-(3.1.4) and a projection system (3.1.5)-(3.1.6), then solve (3.1.3)-(3.1.6) by iterating between the two sub-systems. This typically requires more iterations and linear solves to converge than solving the fully-coupled system using a Newton method. However the linear solves are much easier in the decoupled system. Note also that for the decoupled system the work required is only slightly more than a usual implicit Crank-Nicolson method (i.e. without vorticity projection) since the extra work is (relatively inexpensive) projection solves. Moreover,*

*for nonhomogeneous boundary conditions, this decoupling leads to a simplified boundary condition for the vorticity: $w_h = I_h(\nabla \times u_h)$ on the boundary, where $I_h$ is an appropriate interpolation operator.*

## 3.2 Stability, conservation laws, and existence of solutions

In this section we prove fundamental mathematical and physical properties of the 3 helicity schemes: unconditional stability, solution existence and conservation laws. We begin with stability.

### 3.2.1 Stability

**Lemma 3.2.1.** *Solutions to Algorithm 3.1.1 are nonlinearly stable. That is, they satisfy:*

*helicity scheme 1:*

$$\left\|u_h^M\right\|^2 + \nu\Delta t \sum_{n=0}^{M-1} \left\|\nabla u_h^{n+\frac{1}{2}}\right\|^2 \leq \frac{\Delta t}{\nu} \sum_{n=0}^{M-1} \|f\|_*^2 + \left\|u_h^0\right\|^2 = C(data). \tag{3.2.1}$$

*helicity scheme 2:*

$$\left\|u_h^M\right\|^2 + \Delta t \sum_{n=0}^{M-1} \left(2\gamma \left\|\nabla \cdot u_h^{n+\frac{1}{2}}\right\|^2 + \nu \left\|\nabla u_h^{n+\frac{1}{2}}\right\|^2\right) \leq \frac{\Delta t}{\nu} \sum_{n=0}^{M-1} \|f\|_*^2 + \left\|u_h^0\right\|^2 = C(data). \tag{3.2.2}$$

*helicity scheme 3:*

$$\left\|u_h^M\right\|^2 + \gamma \left\|\nabla \cdot u_h^M\right\|^2 + \nu\Delta t \sum_{n=0}^{M-1} \left\|\nabla u_h^{n+\frac{1}{2}}\right\|^2$$
$$\leq \frac{\Delta t}{\nu} \sum_{n=0}^{M-1} \|f\|_*^2 + \left\|u_h^0\right\|^2 + \gamma \left\|\nabla \cdot u_h^0\right\| = C(data). \tag{3.2.3}$$

*helicity schemes 1,2,3:*

$$\Delta t \sum_{n=0}^{M-1} \left\|w_h^{n+\frac{1}{2}}\right\|^2 \leq \Delta t \sum_{n=0}^{M-1} \left\|\nabla u_h^{n+\frac{1}{2}}\right\|^2 = C(data). \tag{3.2.4}$$

*helicity schemes 1,2,3:*

$$\Delta t \sum_{n=1}^{M} \left(\|p_h^n\|^2 + \|\lambda_h^n\|^2\right) \leq C(data). \tag{3.2.5}$$

*$C(data)$ is a constant dependent on $T, \nu, \gamma, f, u_h^0$ and $\Omega$.*

*Proof.* To prove the bounds on velocity for each of the helicity schemes, choose $v_h = u_h^{n+\frac{1}{2}}$ in (3.1.3). The nonlinear and pressure terms are then zero. The triangle inequality and summing over time steps then completes the proofs of (3.2.1),(3.2.2),(3.2.3).

20

To prove (3.2.4) choose $\chi_h = w_h^{n+\frac{1}{2}}$ in (3.1.5) and $r_h = \lambda_h^{n+1}$ in (3.1.6). After combining the equations we obtain

$$\left\|w_h^{n+\frac{1}{2}}\right\|^2 = (\nabla \times u_h^{n+\frac{1}{2}}, w_h^{n+\frac{1}{2}}) \leq \left\|\nabla \times u_h^{n+\frac{1}{2}}\right\| \left\|w_h^{n+\frac{1}{2}}\right\|$$

$$\leq \frac{1}{2}\left\|\nabla \times u_h^{n+\frac{1}{2}}\right\|^2 + \frac{1}{2}\left\|w_h^{n+\frac{1}{2}}\right\|^2 \leq \left\|\nabla u_h^{n+\frac{1}{2}}\right\|^2 + \frac{1}{2}\left\|w_h^{n+\frac{1}{2}}\right\|^2.$$

Rearranging, and summing over time steps we obtain (3.2.4).

To obtain the stated bound for $\lambda_h^n$, we begin with the inf-sup condition satisfied by $X_h$ ($\subset W_h$) and $Q_h$ and use (3.1.5) to obtain

$$\|\lambda_h^n\| \leq \frac{1}{\beta} \sup_{\chi_h \in X_h} \frac{(\lambda_h^n, \nabla \cdot \chi_h)}{\|\chi_h\|_X} \leq \frac{1}{\beta} \sup_{\chi_h \in X_h} \frac{(\nabla \times u_h^{n-\frac{1}{2}}, \chi_h) - (w_h^{n-\frac{1}{2}}, \chi_h)}{\|\chi_h\|_X}$$

$$\leq \frac{1}{\beta}\left(\|\nabla \times u_h^{n-\frac{1}{2}}\| + \|w_h^{n-\frac{1}{2}}\|\right) \leq \frac{2}{\beta}\left(\|\nabla u_h^{n-\frac{1}{2}}\| + \|w_h^{n-\frac{1}{2}}\|\right).$$

Using the bounds for $\nabla u_h^{n+\frac{1}{2}}$ (see (3.2.1)-(3.2.3)) and $w_h^{n+\frac{1}{2}}$ (see (3.2.4)) we obtain the bound for $\lambda_h^n$. The bound for the pressure is established in an analogous manner. $\qquad\square$

### 3.2.2 Existence

**Lemma 3.2.2.** *Solutions exist to each of the three helicity schemes presented in Algorithm 3.1.1.*

*Proof.* For each of the helicity schemes, this is a straight-forward extension of the existence proof given for the periodic case in [64]. The result is a consequence of the Leray-Schauder fixed point theorem and the stability bounds of Lemma 3.2.1. $\qquad\square$

We now study the conservation laws for energy and helicity in the helicity schemes. It is shown in [64] that, when restricted to the periodic case, the non-stabilized helicity scheme of Algorithm 3.1.1 (helicity scheme 1) conserves energy and helicity. In the case of homogeneous boundary conditions for velocity, this physically important feature for energy is still preserved. However, as one might expect, the stabilization term in helicity schemes 2 and 3 alters the energy balance. Lemma 3.2.3 shows these energy balances.

The energy balance of helicity scheme 1, the unstabilized helicity scheme, is analogous to that for the continuous NSE. However, for helicity scheme 2, we see the effect of the stabilization on the energy balance in the term $\gamma \Delta t \sum_{n=0}^{M-1} \left\|\nabla \cdot u_h^{n+\frac{1}{2}}\right\|^2$ on the left hand side of (3.2.7). For most choices of elements, one may have that each term in this sum is small, but over a long time interval this sum can grow to significantly (and non-physically) alter the balance. The energy balance for

helicity scheme 3 differs from helicity scheme 1's energy balance in the addition of only two small terms, instead of a sum. Hence this indicates that the modified grad-div stabilization, for problems over a long time interval, offers a more physically relevant energy balance than the usual grad-div stabilization (helicity scheme 2).

### 3.2.3 Conservation Laws

**Lemma 3.2.3.** *The helicity schemes of Algorithm 3.1.1 admit the following energy conservation laws:*

*helicity scheme 1:*

$$\frac{1}{2}\left\|u_h^M\right\|^2 + \nu\Delta t \sum_{n=0}^{M-1}\left\|\nabla u_h^{n+\frac{1}{2}}\right\|^2 = \Delta t \sum_{n=0}^{M-1}(f(t^{n+\frac{1}{2}}), u_h^{n+\frac{1}{2}}) + \frac{1}{2}\left\|u_h^0\right\|^2 . \quad (3.2.6)$$

*helicity scheme 2:*

$$\frac{1}{2}\left\|u_h^M\right\|^2 + \nu\Delta t \sum_{n=0}^{M-1}\left\|\nabla u_h^{n+\frac{1}{2}}\right\|^2 + \gamma\Delta t \sum_{n=0}^{M-1}\left\|\nabla\cdot u_h^{n+\frac{1}{2}}\right\|^2 = \Delta t \sum_{n=0}^{M-1}(f(t^{n+\frac{1}{2}}), u_h^{n+\frac{1}{2}}) + \frac{1}{2}\left\|u_h^0\right\|^2 .$$

$$(3.2.7)$$

*helicity scheme 3:*

$$\frac{1}{2}(\left\|u_h^M\right\|^2 + \gamma\left\|\nabla\cdot u_h^M\right\|^2) + \nu\Delta t \sum_{n=0}^{M-1}\left\|\nabla u_h^{n+\frac{1}{2}}\right\|^2 = \Delta t \sum_{n=0}^{M-1}(f(t^{n+\frac{1}{2}}), u_h^{n+\frac{1}{2}})$$

$$+ \frac{1}{2}(\left\|u_h^0\right\|^2 + \gamma\left\|\nabla\cdot u_h^0\right\|^2) . \quad (3.2.8)$$

*Proof.* The proofs of these results follow from choosing $v_h = u_h^{n+\frac{1}{2}}$ in Algorithm 3.1.1 for each of the helicity schemes. The key point is that the nonlinear term vanishes with this choice of test function, and thus does not contribute to the energy balance equations. $\square$

We now consider the discrete helicity conservation in Algorithm 3.1.1. We begin with the case of imposing Dirichlet boundary conditions on the projected vorticity, i.e. $W_h = X_h$. Although this case is nonphysical, analysis of it is the first step in understanding more complex boundary conditions.

In this case, the helicity schemes' discrete nonlinearity preserves helicity, however the sta-

bilization terms do not. We state the precise results in the next lemma. Denote the discrete helicity at time level $n$ by $H_h^n := (u_h^n, \nabla \times u_h^n)$. Note that from (3.1.4),(3.1.5), $H_h^n := (u_h^n, w_h^n)$.

**Lemma 3.2.4.** *If $W_h := X_h$, the helicity schemes of Algorithm 3.1.1 admit the following helicity conservation laws.*

*helicity scheme 1:*

$$H_h^M + 2\nu\Delta t \sum_{n=0}^{M-1} (\nabla u_h^{n+\frac{1}{2}}, \nabla w_h^{n+\frac{1}{2}}) = 2\nu\Delta t \sum_{n=0}^{M-1} (f(t^{n+\frac{1}{2}}), \nabla w_h^{n+\frac{1}{2}}) + H_h^0. \quad (3.2.9)$$

*helicity scheme 2:*

$$H_h^M + 2\nu\Delta t \sum_{n=0}^{M-1} (\nabla u_h^{n+\frac{1}{2}}, \nabla w_h^{n+\frac{1}{2}}) + 2\gamma\Delta t \sum_{n=0}^{M-1} (\nabla \cdot u_h^{n+\frac{1}{2}}, \nabla \cdot w_h^{n+\frac{1}{2}})$$
$$= 2\Delta t \sum_{n=0}^{M-1} (f(t^{n+\frac{1}{2}}), \nabla w_h^{n+\frac{1}{2}}) + H_h^0. \quad (3.2.10)$$

*helicity scheme 3:*

$$H_h^M + 2\nu\Delta t \sum_{n=0}^{M-1} (\nabla u_h^{n+\frac{1}{2}}, \nabla w_h^{n+\frac{1}{2}}) + 2\gamma \sum_{n=0}^{M-1} (\nabla \cdot (u_h^{n+1} - u_h^n), \nabla \cdot w_h^{n+\frac{1}{2}})$$
$$= 2\Delta t \sum_{n=0}^{M-1} (f(t^{n+\frac{1}{2}}), \nabla w_h^{n+\frac{1}{2}}) + H_h^0. \quad (3.2.11)$$

*Proof.* Choosing $v_h = w_h^{n+\frac{1}{2}}$ elimates the nonlinear term and the pressure term from (3.1.3) for each of the 3 helicity schemes, and reduces the time difference term to

$$\frac{1}{\Delta t}(u_h^{n+1} - u_h^n, w_h^{n+\frac{1}{2}}) = \frac{1}{\Delta t}(u_h^{n+1} - u_h^n, \nabla \times u_h^{n+\frac{1}{2}})$$
$$= \frac{1}{2\Delta t}\left((u_h^{n+1}, \nabla \times u_h^{n+1}) + (u_h^{n+1}, \nabla \times u_h^n) - (u_h^n, \nabla \times u_h^{n+1}) - (u_h^n, \nabla \times u_h^n)\right)$$
$$= \frac{1}{2\Delta t}\left(H_h^{n+1} - H_h^n\right), \quad (3.2.12)$$

as, for $v, w \in H_0^1(\Omega)$, $(v, \nabla \times w) = (w, \nabla \times v)$.

Using (3.2.12) helicity scheme 1 becomes

$$\frac{1}{2\Delta t}\left(H_h^{n+1} - H_h^n\right) + \nu(\nabla u_h^{n+\frac{1}{2}}, \nabla w_h^{n+\frac{1}{2}}) = (f(t^{n+\frac{1}{2}}), w_h^{n+\frac{1}{2}}) \quad (3.2.13)$$

23

Multiplying by $2\Delta t$ and summing over time steps completes the proof of (3.2.9).

The proofs of (3.2.10) and (3.2.11) follow the same way, except they will contain their respective stabilization terms. □

Lemma 3.2.4 shows that if we impose Dirichlet boundary conditions on the vorticity, then the nonlinearity is able to preserve helicity. Hence for helicity scheme 1, we see a helicity balance analogous to that of the true physics. However, the stabilization terms do not preserve helicity, and thus appear in the helicity balances for helicity schemes 2 and 3.

Interestingly, if the term $\gamma(\nabla \cdot w_h^{n+1}, \nabla \cdot \chi_h)$ is added to the left hand side of the vorticity projection equation (3.1.5), one can show that helicity scheme 3 conserves both helicity and energy. This results from the cancellation of the stabilization term in helicity scheme 3's momentum equation when $v_h$ is chosen to be $w_h^{n+\frac{1}{2}}$ and $\chi_h$ is chosen as $u_h^{n+1}$ and $u_h^n$ respectively. However, computations using this additional term with helicity scheme 3 were inferior to those of helicity scheme 3 defined above.

Similar conservation laws for helicity, even for helicity scheme 1, do not appear to hold for the nonhomogeneous boundary condition for vorticity, i.e. $X_h \neq W_h$. Due to the definitions of these spaces, extra terms arise in the balance that correspond to the difference between the projection of the curl into discretely divergence-free subspaces of $W_h$ and $X_h$. These extra terms will be small except at strips along the boundary, but nonetheless global helicity conservation will fail to hold. However, more typical helicity schemes, e.g. usual trapezoidal convective form or rotational form [37], introduce nonphysical helicity over the entire domain and thus the helicity schemes of Algorithm 2.1 still provide a better treatment of helicity than such helicity schemes.

## 3.3 Convergence

Three numerical helicity schemes are described in Algorithm 2.1. We prove in detail convergence of solutions of helicity scheme 3 to an NSE solution. Convergence results for helicity schemes 1 and 2 can be established in an analogous manner.

Let $P_{V_h} : L^2 \to V_h$ denote the projection of $L^2$ onto $V_h$, i.e. $P_{V_h}(w) := s_h$ where

$$(s_h, v_h) = (w, v_h), \forall v_h \in V_h.$$

For simplicity in stating the a priori theorem we summarize here the regularity assumptions for the solution $u(x, t)$ to the NSE.

$$u \in L^2(0,T;H^{k+2}(\Omega)) \cap L^\infty(0,T;H^1(\Omega)), \tag{3.3.1}$$

$$u(\cdot,t) \in H_0^1(\Omega), \tag{3.3.2}$$

$$u_t \in L^2(0,T;H^{k+1}(\Omega)) \cap L^\infty(0,T;H^{k+1}(\Omega)), \tag{3.3.3}$$

$$u_{tt} \in L^2(0,T;H^{k+1}(\Omega)), \tag{3.3.4}$$

$$u_{ttt} \in L^2(0,T;L^2(\Omega)) \tag{3.3.5}$$

$$(u \times (\nabla \times u))_{tt} \in L^2(0,T;L^2(\Omega)). \tag{3.3.6}$$

**Theorem 3.3.1.** *For $u,p$ solutions of the NSE with $p \in L^2(0,T;H^k(\Omega))$, $u$ satisfying (3.3.1)-(3.3.6), $f \in L^2(0,T;X^*(\Omega))$, and $u_0 \in V_h$, $(u_h^n, w_h^n)$ given by helicity scheme 3 of Algorithm 2.1 for $n = 1, ..., M$ and $\Delta t$ sufficiently small, we have that*

$$\left\| u(T) - u_h^M \right\| + \left\| \nabla \cdot (u(T) - u_h^M) \right\| + \left( \nu \Delta t \sum_{n=0}^{M-1} \left\| \nabla (u^{n+\frac{1}{2}} - u_h^{n+\frac{1}{2}}) \right\|^2 \right)^{1/2} \leq$$

$$C(\gamma, T, \nu^{-3}, u) \left( h^k \|u(T)\|_{k+1} + h^k \|\|u\|\|_{2,k+1} + h^k \|\|p\|\|_{2,k} + h^k \|\|u_t\|\|_{2,k+1} \right.$$

$$+ h^k \|\|u_t\|\|_{\infty,k+1} + h^k \|\|u_t\|\|_{\infty,1} \|\|u\|\|_{2,k+1} + (\Delta t)^{1/2} h^k \|u_{tt}\|_{2,k+1} + (\Delta t)^2 \|u_{ttt}\|_{2,0}$$

$$+ (\Delta t)^2 \|u_{tt}\|_{2,1} + (\Delta t)^2 \|(u \times (\nabla \times u))_{tt}\|_{2,0} + h^{k+1} \|\|u\|\|_{\infty,1} \|\|\nabla \times u\|\|_{2,k+1} \right). \tag{3.3.7}$$

*Proof of Theorem.* Since $(u,p)$ solves the NSE, we have $\forall v_h \in X_h$ that

$$(u_t(t^{n+\frac{1}{2}}), v_h) - (u(t^{n+\frac{1}{2}}) \times (\nabla \times u(t^{n+\frac{1}{2}})), v_h) - (p(t^{n+\frac{1}{2}}), \nabla \cdot v_h)$$

$$+ \nu(\nabla u(t^{n+\frac{1}{2}}), \nabla v_h) = (f(t^{n+\frac{1}{2}}), v_h). \tag{3.3.8}$$

Adding $(\frac{u^{n+1}-u^n}{\Delta t}, v_h)$ and $\nu(\nabla u^{n+\frac{1}{2}}, \nabla v_h)$ to both sides of (3.3.8) we obtain

$$\frac{1}{\Delta t}(u^{n+1} - u^n, v_h) + \left( (\nabla \times u(t^{n+\frac{1}{2}}) \times u(t^{n+\frac{1}{2}})), v_h \right) - (p(t^{n+\frac{1}{2}}), \nabla \cdot v_h) + \nu(\nabla u^{n+\frac{1}{2}}, \nabla v_h)$$

$$= (f(t^{n+\frac{1}{2}}), v_h) + \left( \frac{u^{n+1}-u^n}{\Delta t} - u_t(t^{n+\frac{1}{2}}), v_h \right) + \nu(\nabla u^{n+\frac{1}{2}} - \nabla u(t^{n+\frac{1}{2}}), \nabla v_h). \tag{3.3.9}$$

Next, subtracting (3.1.3) from (3.3.9), label $e^n := u^n - u_h^n$, and adding the identically zero term

25

$\frac{\gamma}{\Delta t}(\nabla \cdot (\frac{u^{n+1} - u^n}{\Delta t}), \nabla \cdot v_h)$ to the LHS gives

$$\frac{1}{\Delta t}(e^{n+1} - e^n, v_h) + \nu(\nabla e^{n+\frac{1}{2}}, \nabla v_h) + \frac{\gamma}{\Delta t}(\nabla \cdot (e^{n+1} - e^n, \nabla \cdot v_h))$$
$$= -\left(\nabla \times u(t^{n+\frac{1}{2}}) \times u(t^{n+\frac{1}{2}}), v_h\right) + \left(w_h^{n+\frac{1}{2}} \times u_h^{n+\frac{1}{2}}, v_h\right) + \left(p(t^{n+\frac{1}{2}}) - p_h^{n+1}, \nabla \cdot v_h\right)$$
$$+ \left(\frac{u^{n+1} - u^n}{\Delta t} - u_t(t^{n+\frac{1}{2}}), v_h\right) + \nu\left(\nabla u^{n+\frac{1}{2}} - \nabla u(t^{n+\frac{1}{2}}), \nabla v_h\right). \quad (3.3.10)$$

We split the error into two pieces $\Phi_h$ and $\eta$: $e^n = u^n - u_h^n = (u^n - U^n) + (U^n - u_h^n) := \eta^n + \Phi_h^n$, where $U^n$ denotes the interpolant of $u^n$ in $V_h$, yielding

$$\frac{1}{\Delta t}(\Phi_h^{n+1} - \Phi_h^n, v_h) + \nu(\nabla \Phi_h^{n+\frac{1}{2}}, \nabla v_h) + \frac{\gamma}{\Delta t}(\nabla \cdot (\Phi_h^{n+1} - \Phi_h^n), \nabla \cdot v_h) = -\frac{1}{\Delta t}(\eta^{n+1} - \eta^n, v_h)$$
$$- \nu(\nabla \eta^{n+\frac{1}{2}}, \nabla v_h) - \frac{\gamma}{\Delta t}(\nabla \cdot (\eta^{n+1} - \eta^n), \nabla \cdot v_h) - \left((\nabla \times u(t^{n+\frac{1}{2}})) \times u(t^{n+\frac{1}{2}}), v_h\right)$$
$$+ (w_h^{n+\frac{1}{2}} \times u_h^{n+\frac{1}{2}}, v_h) + (p(t^{n+\frac{1}{2}}) - p_h^{n+1}, \nabla \cdot v_h) + \left(\frac{u^{n+1} - u^n}{\Delta t} - u_t(t^{n+\frac{1}{2}}), v_h\right)$$
$$+ \nu(\nabla u^{n+\frac{1}{2}} - \nabla u(t^{n+\frac{1}{2}}), \nabla v_h). \quad (3.3.11)$$

Choosing $v_h = \Phi_h^{n+\frac{1}{2}}$ yields

$$\frac{1}{2\Delta t}\left(\|\Phi_h^{n+1}\|^2 - \|\Phi_h^n\|^2\right) + \nu\left\|\nabla \Phi_h^{n+\frac{1}{2}}\right\|^2 + \frac{\gamma}{2\Delta t}\left(\|\nabla \cdot \Phi_h^{n+1}\|^2 - \|\nabla \cdot \Phi_h^n\|^2\right)$$
$$= -\frac{1}{\Delta t}(\eta^{n+1} - \eta^n, \Phi_h^{n+\frac{1}{2}}) - \nu(\nabla \eta^{n+\frac{1}{2}}, \nabla \Phi_h^{n+\frac{1}{2}}) - \frac{\gamma}{\Delta t}\left(\nabla \cdot (\eta^{n+1} - \eta^n), \nabla \cdot \Phi_h^{n+\frac{1}{2}}\right)$$
$$- \left(\nabla \times u(t^{n+\frac{1}{2}}) \times u(t^{n+\frac{1}{2}}), \Phi_h^{n+\frac{1}{2}}\right) + (w_h^{n+\frac{1}{2}} \times u_h^{n+\frac{1}{2}}, \Phi_h^{n+\frac{1}{2}}) + (p(t^{n+\frac{1}{2}}) - p_h^{n+1}, \nabla \cdot \Phi_h^{n+\frac{1}{2}})$$
$$+ \left(\frac{u^{n+1} - u^n}{\Delta t} - u_t(t^{n+\frac{1}{2}}), \Phi_h^{n+\frac{1}{2}}\right) + \nu(\nabla u^{n+\frac{1}{2}} - \nabla u(t^{n+\frac{1}{2}}), \nabla \Phi_h^{n+\frac{1}{2}}). \quad (3.3.12)$$

We have the following bounds for the terms on the RHS (see [18]).

$$-\nu(\nabla \eta^{n+\frac{1}{2}}, \nabla \Phi_h^{n+\frac{1}{2}}) \leq \frac{\nu}{12}\left\|\nabla \Phi_h^{n+\frac{1}{2}}\right\|^2 + 3\nu\left\|\nabla \eta^{n+\frac{1}{2}}\right\|^2 \quad (3.3.13)$$

$$\frac{1}{\Delta t}(\eta^{n+1} - \eta^n, \Phi_h^{n+\frac{1}{2}}) \le \frac{1}{2} \left\| \frac{\eta^{n+1} - \eta^n}{\Delta t} \right\|^2 + \frac{1}{2} \left\| \Phi_h^{n+\frac{1}{2}} \right\|^2$$

$$= \frac{1}{2} \int_\Omega \left( \frac{1}{\Delta t} \int_{t^n}^{t^{n+1}} \eta_t \, dt \right)^2 d\Omega + \frac{1}{2} \left\| \Phi_h^{n+\frac{1}{2}} \right\|^2$$

$$\le \frac{1}{2} \int_\Omega \left( 2|\eta_t(t^{n+1})|^2 + 2 \int_{t^n}^{t^{n+1}} |\eta_{tt}|^2 \, dt \right) d\Omega + \frac{1}{2} \left\| \Phi_h^{n+\frac{1}{2}} \right\|^2$$

$$= \left\| \eta_t(t^{n+1}) \right\|^2 + \int_{t^n}^{t^{n+1}} \left\| \eta_{tt} \right\|^2 \, dt + \frac{1}{2} \left\| \Phi_h^{n+\frac{1}{2}} \right\|^2. \qquad (3.3.14)$$

Similarly,

$$\frac{\gamma}{\Delta t} \left( \nabla \cdot (\eta^{n+1} - \eta^n), \nabla \cdot \Phi_h^{n+\frac{1}{2}} \right) \le \gamma \left\| \nabla \cdot \eta_t(t^{n+1}) \right\|^2 + \gamma \int_{t^n}^{t^{n+1}} \left\| \nabla \cdot \eta_{tt} \right\|^2 \, dt + \frac{\gamma}{2} \left\| \nabla \cdot \Phi_h^{n+\frac{1}{2}} \right\|^2.$$
$$(3.3.15)$$

$$\left( \frac{u^{n+1} - u^n}{\Delta t} - u_t(t^{n+\frac{1}{2}}), \Phi_h^{n+\frac{1}{2}} \right) \le \frac{1}{2} \left\| \frac{u^{n+1} - u^n}{\Delta t} - u_t(t^{n+\frac{1}{2}}) \right\|^2 + \frac{1}{2} \left\| \Phi_h^{n+\frac{1}{2}} \right\|^2$$

$$= \frac{(\Delta t)^3}{2560} \int_{t^n}^{t^{n+1}} \left\| u_{ttt} \right\|^2 \, dt + \frac{1}{2} \left\| \Phi_h^{n+\frac{1}{2}} \right\|^2 \qquad (3.3.16)$$

$$\nu(\nabla u^{n+\frac{1}{2}} - \nabla u(t^{n+\frac{1}{2}}), \nabla \Phi_h^{n+\frac{1}{2}}) \le 3\nu \left\| \nabla u^{n+\frac{\nu}{12}} - \nabla u(t^{n+\frac{1}{2}}) \right\|^2 + \frac{\nu^2}{2} \left\| \Phi_h^{n+\frac{1}{2}} \right\|^2 \qquad (3.3.17)$$

$$= \frac{\nu(\Delta t)^3}{16} \int_{t^n}^{t^{n+1}} \left\| \nabla u_{tt} \right\|^2 \, dt + \frac{\nu}{12} \left\| \Phi_h^{n+\frac{1}{2}} \right\|^2 \qquad (3.3.18)$$

For the pressure term, since $\Phi_h^{n+\frac{1}{2}} \in V_h$, for any $q_h \in Q_h$,

$$(p(t^{n+\frac{1}{2}}) - p_h^{n+1}, \nabla \cdot \Phi_h^{n+\frac{1}{2}}) = (p(t^{n+\frac{1}{2}}) - q_h, \nabla \cdot \Phi_h^{n+\frac{1}{2}}), \qquad (3.3.19)$$

which implies

$$(p(t^{n+\frac{1}{2}}) - p_h^{n+1}, \nabla \cdot \Phi_h^{n+\frac{1}{2}}) \le \frac{1}{2\gamma} \inf_{q_h \in Q_h} \left\| p(t^{n+\frac{1}{2}}) - q_h \right\|^2 + \frac{\gamma}{2} \left\| \nabla \cdot \Phi_h^{n+\frac{1}{2}} \right\|^2. \qquad (3.3.20)$$

Utilizing (3.3.13)-(3.3.20) we now have

$$\frac{1}{2\Delta t}\left(\left\|\Phi_h^{n+1}\right\|^2 - \left\|\Phi_h^n\right\|^2\right) + \frac{\gamma}{2\Delta t}\left(\left\|\nabla\cdot\Phi_h^{n+1}\right\|^2 - \left\|\nabla\cdot\Phi_h^n\right\|^2\right) + \frac{5\nu}{6}\left\|\nabla\Phi_h^{n+\frac{1}{2}}\right\|^2$$

$$\leq 3\nu\left\|\nabla\eta^{n+\frac{1}{2}}\right\|^2 + \frac{\gamma}{\Delta t}\left\|\nabla\cdot\eta_t(t^{n+1})\right\|^2 + \frac{\gamma}{\Delta t}\int_{t^n}^{t^{n+1}}\left\|\nabla\cdot\eta_{tt}\right\|^2\,dt + \frac{1}{2\gamma}\inf_{q_h\in Q_h}\left\|p(t^{n+\frac{1}{2}}) - q_h\right\|^2$$

$$+ C(1+\nu)\Delta t^3\left(\int_{t^n}^{t^{n+1}}\left\|u_{ttt}\right\|^2\,dt + \int_{t^n}^{t^{n+1}}\left\|\nabla u_{tt}\right\|^2\,dt\right) + \frac{\nu^2+1}{2}\left\|\Phi_h^{n+\frac{1}{2}}\right\|^2 + \gamma\left\|\nabla\cdot\Phi_h^{n+\frac{1}{2}}\right\|^2$$

$$+ (w_h^{n+\frac{1}{2}}\times u_h^{n+\frac{1}{2}}, \Phi_h^{n+\frac{1}{2}}) - \left((\nabla\times u(t^{n+\frac{1}{2}}))\times u(t^{n+\frac{1}{2}}), \Phi_h^{n+\frac{1}{2}}\right)$$

$$\left\|\eta_t(t^{n+1})\right\|^2 + \int_{t^n}^{t^{n+1}}\left\|\eta_{tt}\right\|^2\,dt. \quad (3.3.21)$$

For the nonlinear terms we have

$$(w_h^{n+\frac{1}{2}}\times u_h^{n+\frac{1}{2}}, \Phi_h^{n+\frac{1}{2}}) - \left((\nabla\times u(t^{n+\frac{1}{2}}))\times u(t^{n+\frac{1}{2}}), \Phi_h^{n+\frac{1}{2}}\right) + \left((\nabla\times u^{n+\frac{1}{2}})\times u^{n+\frac{1}{2}}, \Phi_h^{n+\frac{1}{2}}\right)$$

$$- \left((\nabla\times u^{n+\frac{1}{2}})\times u^{n+\frac{1}{2}}, \Phi_h^{n+\frac{1}{2}}\right)$$

$$= \left((w_h^{n+\frac{1}{2}} - \nabla\times u^{n+\frac{1}{2}})\times u^{n+\frac{1}{2}}, \Phi_h^{n+\frac{1}{2}}\right) + \left(w_h^{n+\frac{1}{2}}\times(u_h^{n+\frac{1}{2}} - u^{n+\frac{1}{2}}), \Phi_h^{n+\frac{1}{2}}\right)$$

$$+ \left((\nabla\times u^{n+\frac{1}{2}})\times u^{n+\frac{1}{2}} - (\nabla\times u(t^{n+\frac{1}{2}}))\times u(t^{n+\frac{1}{2}}), \Phi_h^{n+\frac{1}{2}}\right)$$

$$= \left((w_h^{n+\frac{1}{2}} - \nabla\times u^{n+\frac{1}{2}})\times u^{n+\frac{1}{2}}, \Phi_h^{n+\frac{1}{2}}\right) - \left(w_h^{n+\frac{1}{2}}\times\eta^{n+\frac{1}{2}}, \Phi_h^{n+\frac{1}{2}}\right)$$

$$+ \left((\nabla\times u^{n+\frac{1}{2}})\times u^{n+\frac{1}{2}} - (\nabla\times u(t^{n+\frac{1}{2}}))\times u(t^{n+\frac{1}{2}}), \Phi_h^{n+\frac{1}{2}}\right) \quad (3.3.22)$$

We bound the second to last and last terms in (3.3.22) by

$$(w_h^{n+\frac{1}{2}}\times\eta^{n+\frac{1}{2}}, \Phi_h^{n+\frac{1}{2}}) \leq C\left\|w_h^{n+\frac{1}{2}}\right\|\left\|\nabla\eta^{n+\frac{1}{2}}\right\|\left\|\nabla\Phi_h^{n+\frac{1}{2}}\right\|$$

$$\leq \frac{\nu}{12}\left\|\nabla\Phi_h^{n+\frac{1}{2}}\right\|^2 + 3\nu^{-1}\left\|w_h^{n+\frac{1}{2}}\right\|^2\left\|\nabla\eta^{n+\frac{1}{2}}\right\|^2 \quad (3.3.23)$$

$$(u(t^{n+\frac{1}{2}})\times(\nabla\times u(t^{n+\frac{1}{2}})) - u^{n+\frac{1}{2}}\times(\nabla\times u^{n+\frac{1}{2}}), \Phi_h^{n+\frac{1}{2}})$$

$$\leq \frac{\nu}{12}\left\|\nabla\Phi_h^{n+\frac{1}{2}}\right\|^2 + 3\nu^{-1}\left\|u(t^{n+\frac{1}{2}})\times(\nabla\times u(t^{n+\frac{1}{2}})) - u^{n+\frac{1}{2}}\times(\nabla\times u^{n+\frac{1}{2}})\right\|^2$$

$$\leq \frac{\nu}{12}\left\|\nabla\Phi_h^{n+\frac{1}{2}}\right\|^2 + \frac{3}{48}\nu^{-1}(\Delta t)^3\int_{t^n}^{t^{n+1}}\left\|(u\times(\nabla\times u))_{tt}\right\|^2\,dt. \quad (3.3.24)$$

For the first term in (3.3.22), we need a bound on $\left\|\nabla\times u^{n+\frac{1}{2}} - w_h^{n+\frac{1}{2}}\right\|$. This is obtained by restricting $\chi_h$ to $V_h$ in (3.1.5) and then subtracting $(\nabla\times u^{n+\frac{1}{2}}, \chi_h)$ from both sides of (3.1.5), which

gives us

$$(\nabla \times u^{n+\frac{1}{2}} - w_h^{n+\frac{1}{2}}, \chi_h) = (\nabla \times (u^{n+\frac{1}{2}} - u_h^{n+\frac{1}{2}}), \chi_h)$$

$$= (\nabla \times \eta^{n+\frac{1}{2}}, \chi_h) + (\nabla \times \Phi_h^{n+\frac{1}{2}}, \chi_h).$$

By the definition of $P_{V_h}$,

$$(P_{V_h}(\nabla \times u^{n+\frac{1}{2}}) - w_h^{n+\frac{1}{2}}, \chi_h) = (\nabla \times u^{n+\frac{1}{2}} - w_h^{n+\frac{1}{2}}, \chi_h)$$

$$= (\nabla \times (u^{n+\frac{1}{2}} - u_h^{n+\frac{1}{2}}), \chi_h)$$

$$= (\nabla \times \eta^{n+\frac{1}{2}}, \chi_h) + (\nabla \times \Phi_h^{n+\frac{1}{2}}, \chi_h)$$

Choosing $\chi_h = P_{V_h}(\nabla \times u^{n+\frac{1}{2}}) - w_h^{n+\frac{1}{2}}$ we obtain

$$\left\| P_{V_h}(\nabla \times u^{n+\frac{1}{2}}) - w_h^{n+\frac{1}{2}} \right\|^2 \le 2 \left( \left\| \nabla \eta^{n+\frac{1}{2}} \right\|^2 + \left\| \nabla \Phi_h^{n+\frac{1}{2}} \right\|^2 \right). \tag{3.3.25}$$

Now using (3.3.25) and, from Poincare's inequality, $\left\| \Phi_h^{n+\frac{1}{2}} \right\| \le C \left\| \nabla \Phi_h^{n+\frac{1}{2}} \right\|$ we obtain

$$\left( (P_{V_h}(\nabla \times u^{n+\frac{1}{2}}) - w_h^{n+\frac{1}{2}}) \times u^{n+\frac{1}{2}}, \Phi_h^{n+\frac{1}{2}} \right)$$

$$\le C \left\| \nabla u^{n+\frac{1}{2}} \right\| \left\| P_{V_h}(\nabla \times u^{n+\frac{1}{2}}) - w_h^{n+\frac{1}{2}} \right\| \left\| \Phi_h^{n+\frac{1}{2}} \right\|^{\frac{1}{2}} \left\| \nabla \Phi_h^{n+\frac{1}{2}} \right\|^{\frac{1}{2}}$$

$$\le C \left\| \nabla u^{n+\frac{1}{2}} \right\| \left( \left\| \nabla \eta^{n+\frac{1}{2}} \right\| \left\| \nabla \Phi_h^{n+\frac{1}{2}} \right\| + \left\| \Phi_h^{n+\frac{1}{2}} \right\|^{\frac{1}{2}} \left\| \nabla \Phi_h^{n+\frac{1}{2}} \right\|^{\frac{3}{2}} \right)$$

$$\le \frac{\nu}{12} \left\| \nabla \Phi_h^{n+\frac{1}{2}} \right\|^2 + C\nu^{-1} \left\| \nabla u^{n+\frac{1}{2}} \right\|^2 \left\| \nabla \eta^{n+\frac{1}{2}} \right\|^2 + \frac{\nu}{12} \left\| \nabla \Phi_h^{n+\frac{1}{2}} \right\|^2 + C\nu^{-3} \left\| \nabla u^{n+\frac{1}{2}} \right\|^4 \left\| \Phi_h^{n+\frac{1}{2}} \right\|^2.$$

$$\tag{3.3.26}$$

Also, we have that

$$\left( (\nabla \times u^{n+\frac{1}{2}} - P_{V_h}(\nabla \times u^{n+\frac{1}{2}})) \times u^{n+\frac{1}{2}}, \Phi_h^{n+\frac{1}{2}} \right)$$

$$\le C \left\| \nabla \times u^{n+\frac{1}{2}} - P_{V_h}(\nabla \times u^{n+\frac{1}{2}}) \right\| \left\| \nabla u^{n+\frac{1}{2}} \right\| \left\| \nabla \Phi_h^{n+\frac{1}{2}} \right\|$$

$$\le \frac{\nu}{12} \left\| \nabla \Phi_h^{n+\frac{1}{2}} \right\|^2 + C \left\| \nabla u^{n+\frac{1}{2}} \right\|^2 \left\| \nabla \times u^{n+\frac{1}{2}} - P_{V_h}(\nabla \times u^{n+\frac{1}{2}}) \right\|^2 \tag{3.3.27}$$

Combining (3.3.27) and (3.3.26) we obtain the required bound for $\left( (w_h^{n+\frac{1}{2}} - \nabla \times u^{n+\frac{1}{2}}) \times u^{n+\frac{1}{2}}, \Phi_h^{n+\frac{1}{2}} \right)$.
Noting that $\left\| \nabla \cdot \Phi_h^{n+\frac{1}{2}} \right\|^2 \le 1/2 \left( \left\| \nabla \cdot \Phi_h^{n+1} \right\|^2 + \left\| \nabla \cdot \Phi_h^n \right\|^2 \right)$, substituting the bounds derived in

(3.3.23), (3.3.24), (3.3.26), and (3.3.27) into (3.3.21) yields

$$
\frac{1}{2\Delta t}\left(\left\|\Phi_h^{n+1}\right\|^2 - \left\|\Phi_h^n\right\|^2\right) + \frac{\gamma}{2\Delta t}\left(\left\|\nabla\cdot\Phi_h^{n+1}\right\|^2 - \left\|\nabla\cdot\Phi_h^n\right\|^2\right) + \frac{\nu}{2}\left\|\nabla\Phi_h^{n+\frac{1}{2}}\right\|^2
$$

$$
\leq \left(\frac{\nu^2+4}{2} + C\nu^{-3}\left\|\nabla u^{n+\frac{1}{2}}\right\|^4\right)\left\|\Phi_h^{n+\frac{1}{2}}\right\|^2 + \frac{\gamma}{2}\left(\left\|\nabla\cdot\Phi_h^{n+1}\right\|^2 + \left\|\nabla\cdot\Phi_h^n\right\|^2\right)
$$

$$
+ \frac{1}{2\gamma}\inf_{q_h\in Q_h}\left\|p(t^{n+1}) - q_h\right\|^2 + C\nu\left\|\nabla\eta^{n+\frac{1}{2}}\right\|^2 + \left\|\eta_t(t^{n+1})\right\|^2 + \gamma\left\|\nabla\cdot\eta_t(t^{n+1})\right\|^2
$$

$$
+ C\nu^{-1}\left\|w_h^{n+\frac{1}{2}}\right\|^2\left\|\nabla\eta^{n+\frac{1}{2}}\right\|^2 + \nu^{-1}\left\|\nabla u^{n+\frac{1}{2}}\right\|^2\left\|\nabla\eta^{n+\frac{1}{2}}\right\|^2 + \int_{t^n}^{t^{n+1}}\left\|\eta_{tt}\right\|^2\,dt
$$

$$
+ \gamma\int_{t^n}^{t^{n+1}}\left\|\nabla\cdot\eta_{tt}\right\|^2\,dt + C\Delta t^3\left(\int_{t^n}^{t^{n+1}}\left\|u_{ttt}\right\|^2\,dt + \int_{t^n}^{t^{n+1}}\left\|\nabla u_{tt}\right\|^2\,dt\right)
$$

$$
+ C\nu^{-1}(\Delta t)^3\int_{t^n}^{t^{n+1}}\left\|(u\times(\nabla\times u))_{tt}\right\|^2\,dt + C\left\|\nabla u^{n+\frac{1}{2}}\right\|^2\left\|\nabla\times u^{n+\frac{1}{2}} - P_{V_h}(\nabla\times u^{n+\frac{1}{2}})\right\|^2
$$

$$
\tag{3.3.28}
$$

Next multiply by $2\Delta t$, sum over time steps, and use the Gronwall inequality Lemma **??** to yield

$$
\left\|\Phi_h^M\right\|^2 + \gamma\left\|\nabla\cdot\Phi_h^M\right\|^2 + \nu\Delta t\sum_{n=0}^{M-1}\left\|\nabla\Phi_h^{n+\frac{1}{2}}\right\|^2
$$

$$
\leq C\exp\left(2\Delta t\sum_{n=0}^{M-1}\gamma + \frac{\nu^2+4}{2} + C\nu^{-3}\left\|\nabla u^{n+\frac{1}{2}}\right\|^4\right)\left(\Delta t\sum_{n=1}^{M}\frac{1}{2\gamma}\inf_{q_h\in Q_h}\left\|p(t^n) - q_h\right\|^2\right.
$$

$$
+ \Delta t\sum_{n=0}^{M}\nu\left\|\nabla\eta^n\right\|^2 + \Delta t\sum_{n=1}^{M}\left\|\eta_t(t^n)\right\|^2 + \Delta t\sum_{n=1}^{M}\gamma\left\|\nabla\eta_t(t^n)\right\|^2 + \Delta t\sum_{n=0}^{M-1}\nu^{-1}\left\|w_h^{n+\frac{1}{2}}\right\|^2\left\|\nabla\eta^{n+\frac{1}{2}}\right\|^2
$$

$$
+ \Delta t\sum_{n=0}^{M-1}\nu^{-1}\left\|\nabla u^{n+\frac{1}{2}}\right\|^2\left\|\nabla\eta^{n+\frac{1}{2}}\right\|^2 + \Delta t\sum_{n=0}^{M-1}\int_{t^n}^{t^{n+1}}\left\|\eta_{tt}\right\|^2\,dt
$$

$$
+ \Delta t\sum_{n=0}^{M-1}\gamma\int_{t^n}^{t^{n+1}}\left\|\nabla\cdot\eta_{tt}\right\|^2\,dt + (\Delta t)^4\left\|u_{ttt}\right\|_{2,0}^2 + (\Delta t)^4\left\|\nabla u_{tt}\right\|_{2,0}^2 + (\Delta t)^4\left\|(u\times(\nabla\times u))_{tt}\right\|_{2,0}^2
$$

$$
\left. + \Delta t\sum_{n=0}^{M-1}\left\|\nabla u^{n+\frac{1}{2}}\right\|^2\left\|\nabla\times u^{n+\frac{1}{2}} - P_{V_h}(\nabla\times u^{n+\frac{1}{2}})\right\|^2\right) \tag{3.3.29}
$$

Recall the approximation properties of $U^n\in V_h$, $q_h\in Q_h$, and $P_{V_h}$ [37]:

$$
\left\|\eta(t^n)\right\|_s \leq Ch^{k+1-s}\left\|u(t^n)\right\|_{k+1},\quad s=0,1,\quad\text{and}
$$

$$
\inf_{q_h\in Q_h}\left\|p(t^n) - q_h\right\| \leq Ch^k\left\|p(t^n)\right\|_k
$$

$$
\left\|w^n - P_{V_h}(w^n)\right\| \leq Ch^{k+1}\left\|w^n\right\|_{k+1}.
$$

Estimate (3.3.29) then becomes

$$
\left\| \Phi_h^M \right\|^2 + \gamma \left\| \nabla \cdot \Phi_h^M \right\|^2 + \nu \Delta t \sum_{n=0}^{M-1} \left\| \nabla \Phi_h^{n+\frac{1}{2}} \right\|^2
$$

$$
\leq C \exp \left( 2\Delta t \sum_{n=0}^{M-1} \gamma + \frac{\nu^2 + 4}{2} + C\nu^{-3} \left\| \nabla u^{n+\frac{1}{2}} \right\|^4 \right) \left( \frac{1}{2\gamma} h^{2k} \|\|p\|\|_{2,k}^2 \right.
$$

$$
+ \nu\, h^{2k} \|\|u\|\|_{2,k+1}^2 + h^{2k+2} \|\|u_t\|\|_{2,k+1}^2 + \gamma\, h^{2k} \|\|u_t\|\|_{2,k+1}^2
$$

$$
+ \nu^{-1} h^{2k} \|\|u_t\|\|_{\infty,1}^2 \|\|u\|\|_{2,k+1}^2 + \Delta t\, \gamma\, h^{2k} \|u_{tt}\|_{2,k+1}^2 + \Delta t\, h^{2k+2} \|u_{tt}\|_{2,k+1}^2
$$

$$
+ (\Delta t)^4 \|u_{ttt}\|_{2,0}^2 + (\Delta t)^4 \|\nabla u_{tt}\|_{2,0}^2 + (\Delta t)^4 \|(u \times (\nabla \times u))_{tt}\|_{2,0}^2
$$

$$
+ \left( \nu \Delta t \sum_{n=0}^{M-1} \left\| w_h^{n+\frac{1}{2}} \right\|^2 \right) \nu^{-2} h^{2k} \|\|u_t\|\|_{\infty,k+1}^2 + h^{2k+2} \|\|u\|\|_{\infty,1}^2 \|\|\nabla \times u\|\|_{2,k+1}^2 \bigg). \quad (3.3.30)
$$

Finally, using the stability estimate for $\nu \Delta t \sum_{n=0}^{M-1} \left\| w_h^{n+\frac{1}{2}} \right\|^2$ from (3.2.4), and an application of the triangle inequality, we obtain (3.3.7).

$\square$

**Remark 3.3.1.** *As expected, if $(X_h, Q_h)$ is chosen to be the inf-sup stable pair $(P_k, P_{k-1})$, $k \geq 2$, then with the smoothness assumptions (3.3.1)-(3.3.6) and $p \in L^2(0, T; H^k(\Omega))$ the $H^1$ convergence for the velocity is*

$$
\|\|u - u_h\|\|_{2,1} \leq C(\Delta t^2 + h^k) \tag{3.3.31}
$$

**Remark 3.3.2.** *The significant computational improvement of helicity schemes 2 and 3 over helicity scheme 1 is somewhat masked in the statement of the a priori error bound for the velocity (for helicity scheme 3) given in (3.3.7). For helicity scheme 1 the pressure contribution to the bound is $\frac{C}{\nu} \|p - q_h\|$, whereas for helicity schemes 2 and 3 the pressure contribution is given by $C \|p - q_h\|$, see (3.3.20). The presence of $\nu$ in the denominator for helicity scheme 1 suggests a superior numerical performance of helicity schemes 2 and 3 if a large pressure error is present.*

## 3.4 Numerical Experiments

This section presents two numerical experiments, the first to confirm convergence rates and the second to compare the helicity schemes' accuracies over a longer time interval, against each other and a commonly used helicity scheme. For both experiments, we will compute approximations to the Ethier-Steinman exact Navier-Stokes solution on $[-1, 1]^3$ [19], although we choose different parameters and viscosities for the two tests. We find in the first numerical experiment, computed
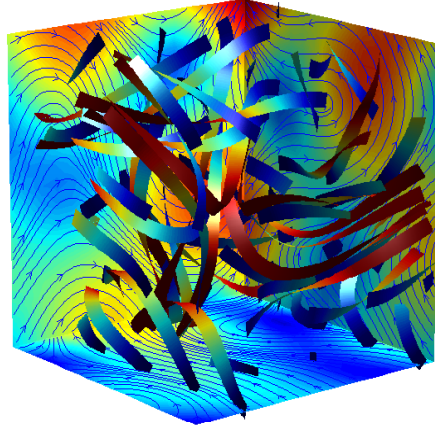
Figure 3.1: The velocity solution to the Ethier-Steinman problem with $a = 1.25$, $d = 1$ at $t = 0$ on the $(-1, 1)^3$ domain. The complex flow structure is seen in the stream ribbons in the box and the velocity streamlines and speed contours on the sides.

convergence rates from successive mesh and time-step refinements indeed match the predicted rates from section 4. For the second experiment, the advantage of using the stabilized enhanced physics based helicity scheme is demonstrated.

For chosen parameters $a, d$ and viscosity $\nu$, the exact Ethier-Steinman NSE solution is given by

$$u_1 = -a\left(e^{ax}\sin(ay + dz) + e^{az}\cos(ax + dy)\right)e^{-\nu d^2 t} \tag{3.4.1}$$

$$u_2 = -a\left(e^{ay}\sin(az + dx) + e^{ax}\cos(ay + dz)\right)e^{-\nu d^2 t} \tag{3.4.2}$$

$$u_3 = -a\left(e^{az}\sin(ax + dy) + e^{ay}\cos(az + dx)\right)e^{-\nu d^2 t} \tag{3.4.3}$$

$$\begin{aligned} p = {} & -\frac{a^2}{2}(e^{2ax} + e^{2ay} + e^{2az} + 2\sin(ax + dy)\cos(az + dx)e^{a(y+z)} \\ & + 2\sin(ay + dz)\cos(ax + dy)e^{a(z+x)} \\ & + 2\sin(az + dx)\cos(ay + dz)e^{a(x+y)})e^{-2\nu d^2 t} \end{aligned} \tag{3.4.4}$$

We give the pressure in its usual form, although our helicity scheme approximates instead the Bernoulli pressure $P = p + \frac{1}{2}|u|^2$. This problem was developed as a 3d analogue to the Taylor vortex problem, for the purpose of benchmarking. Although unlikely to be physically realized, it is a good test problem because it is not only an exact NSE solution, but also it has non-trivial helicity which implies the existence of complex structure [54] in the velocity field. The $t = 0$ solution for $a = 1.25$ and $d = 1$ is illustrated in Figure 3.1. For both experiments below, we use

32

$u^0 = (u_1(0), u_2(0), u_3(0))^T$ as the initial condition and enforce Dirichlet boundary conditions for velocity to be the interpolant of $u(t)$ on the boundary, while a do-nothing boundary condition is used for the vorticity projection. All computations with helicity schemes 2 and 3 use stabilization parameter $\gamma = 1$.

### 3.4.1   Numerical Test 1: Convergence rate verification

| $h$ | $\Delta t$ | $\lvert\lvert\lvert u - u_{\mathrm{S1}} \rvert\rvert\rvert_{2,1}$ | rate | $\lvert\lvert\lvert u - u_{\mathrm{S2}} \rvert\rvert\rvert_{2,1}$ | rate | $\lvert\lvert\lvert u - u_{\mathrm{S3}} \rvert\rvert\rvert_{2,1}$ | rate |
|---|---|---|---|---|---|---|---|
| 1 | 0.001 | 0.01560 | - | 0.01556 | - | 0.01579 | - |
| 0.5 | 0.0005 | 0.00390 | 2.00 | 0.00391 | 1.99 | 0.00395 | 2.00 |
| 0.25 | 0.00025 | 0.000979 | 1.99 | 0.000979 | 2.00 | 0.000984 | 2.01 |
| 0.125 | 0.000125 | 0.000245 | 2.00 | 0.000245 | 2.00 | 0.000246 | 2.00 |

Table 3.1: The $\lvert\lvert\lvert u_{NSE} - u_h \rvert\rvert\rvert_{2,1}$ errors and convergence rates for each of the three helicity scheme of algorithm 3.1.1.

To verify convergence rates predicted in section 4, we compute approximations to (3.4.1)-(3.4.4) with parameters $a = d = \pi/4$, viscosity $\nu = 1$, and end-time $T = 0.001$. Since $(P_2, P_1)$ elements are being used, we expect $O(h^2 + \Delta t^2)$ convergence of $\lvert\lvert\lvert u_{NSE} - u_h \rvert\rvert\rvert_{2,1}$ for each of the three helicity schemes of Algorithm 3.1.1. Errors and rates in this norm are shown in table 3.1, and we find they match those predicted by the theory. Note the finest mesh provides 112,454 total degrees of freedom.

### 3.4.2   Numerical Test 2: Comparison of the helicity schemes

For our second test, we compute approximations to (3.4.1)-(3.4.4) with $a = 1.25$, $d = 1$, kinematic viscosity $\nu = 0.002$, end time $T = 0.5$, using all 3 helicity schemes from Algorithm 3.1.1. We use 3,072 tetrahedral elements, which provides 41,472 velocity degrees of freedom, and 46,875 degrees of freedom for the projected vorticity since here there are degrees of freedom on the boundary. It is important to note that due to the splitting of the projection equations from the NSE system in the solver and since the projection equation is well-conditioned, the time spent for assembling and solving the projection equations is negligible.

In addition to the 3 helicity schemes of Algorithm 3.1.1, for comparison, we also compute approximations using the well-known convective form Crank-Nicolson (CCN) FEM for the Navier-Stokes equations [37, 25, 29]. We run the simulations with time-step $\Delta t = 0.005$. Results of the simulations are shown in Figures 3.2 and 3.3, where the $L^2(\Omega)$ error and the helicity error are plotted against time. It is clear from the pictures that the enhanced physics based helicity scheme is
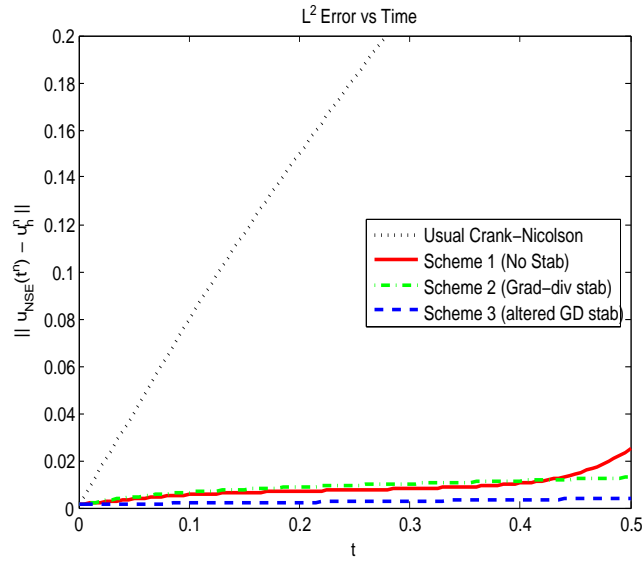
Figure 3.2: The plot above shows $L_2$ error of the velocity vs time for the four helicity schemes of Test 2. We see in the plot that the stabilizations add accuracy to the enhanced-physics helicity scheme, and that the altered grad-div stabilization gives slightly better results than the usual grad-div stabilization. It can also be seen that the enhanced-physics helicity scheme is far more accurate in this metric than the usual Crank-Nicolson helicity scheme.

superior to the usual Crank-Nicolson helicity scheme, and its advantage becomes more pronounced with larger time. Also it is seen that the stabilizations of the enhanced-physics helicity scheme improve accuracy.
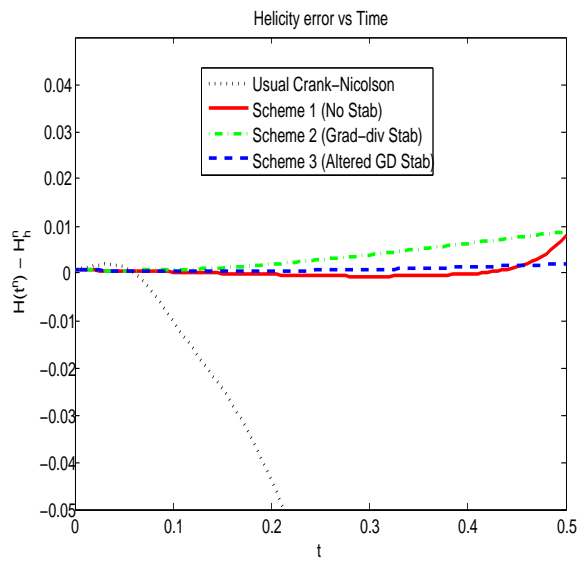
Figure 3.3: The plot above shows helicity error vs time for the four helicity schemes of Test 2. We see in the plot that helicity is far more accurate in the enhanced-physics helicity scheme, and even better with stabilizations, than the usual Crank-Nicolson helicity scheme.

# Chapter 4

# Large scale NSE computations without a pressure space

We study a finite element scheme for the 3d NSE that globally conserves energy and helicity and, through the use of SV elements, enforces pointwise the solenoidal constraints for velocity and vorticity. A complete numerical analysis is given, including proofs for conservation laws, unconditional stability and optimal convergence. We also show the method can be efficiently computed by exploiting a connection between this method, its associated penalty method, and the method arising from use of grad-div stabilized TH elements. Finally, we give numerical examples which verify the theory and demonstrate the effectiveness of the scheme.

## 4.1 The Algorithm

**Algorithm 4.1.1.** *Given a time step $\Delta t > 0$, finite end time $T := M\Delta t$, and initial velocity $u_h^0 \in V_h$, find $w_h^0 \in W_h$ and $\lambda_h^0 \in Q_h$ satisfying $\forall (\chi_h, r_h) \in (W_h, Q_h)$*

$$
\begin{aligned}
(w_h^0, \chi_h) + (\lambda_h^0, \nabla \cdot \chi_h) &= (\nabla \times u_h^0, \chi_h), & (4.1.1) \\
(\nabla \cdot w_h^0, r_h) &= 0. & (4.1.2)
\end{aligned}
$$

*Then for $n = 01, , 2, ..., M - 1$, find $(u_h^{n+1}, w_h^{n+1}, p_h^{n+1}, \lambda_h^{n+1}) \in (X_h, W_h, Q_h, Q_h)$ satisfying*
*$\forall (v_h, \chi_h, q_h, r_h) \in (X_h, W_h, Q_h, Q_h)$*

$$(\frac{u_h^{n+1} - u_h^n}{\Delta t}, v_h) - (P_h^{n+1}, \nabla \cdot v_h)$$

$$+(w_h^{n+\frac{1}{2}} \times u_h^{n+\frac{1}{2}}, v_h) + \nu(\nabla u_h^{n+\frac{1}{2}}, \nabla v_h) = (f(t^{n+\frac{1}{2}}), v_h) \tag{4.1.3}$$

$$(\nabla \cdot u_h^{n+1}, q_h) = 0 \tag{4.1.4}$$

$$(w_h^{n+1}, \chi_h) + (\lambda_h^{n+1}, \nabla \cdot \chi_h) = (\nabla \times u_h^{n+1}, \chi_h) \tag{4.1.5}$$

$$(\nabla \cdot w_h^{n+\frac{1}{2}}, r_h) = 0. \tag{4.1.6}$$

## 4.2 Numerical analysis of the scheme

In this section we provide a complete numerical analysis of the scheme. We prove unconditional stability, solution existence, conservation laws, and optimal convergence.

### 4.2.1 Stability and solution existence

**Lemma 4.2.1.** *Solutions to Algorithm 4.1.1 are unconditionally stable. That is, they satisfy:*

$$\left\| u_h^M \right\|^2 + \nu \Delta t \sum_{n=0}^{M-1} \left\| \nabla u_h^{n+\frac{1}{2}} \right\|^2 \leq \frac{\Delta t}{\nu} \sum_{n=0}^{M-1} \left\| f(t^{n+\frac{1}{2}}) \right\|_*^2 + \left\| u_h^0 \right\|^2 = C(data). \tag{4.2.1}$$

$$\Delta t \sum_{n=0}^{M-1} \left\| w_h^{n+\frac{1}{2}} \right\|^2 \leq \tilde{C} \Delta t \sum_{n=0}^{M-1} \left\| \nabla u_h^{n+\frac{1}{2}} \right\|^2 = C(data). \tag{4.2.2}$$

$$\Delta t \sum_{n=1}^{M} \left( \| P_h^n \|^2 + \| \lambda_h^n \|^2 \right) \leq C(data). \tag{4.2.3}$$

$C(data)$ *is a constant dependent on* $T, \nu, \gamma, f, u_h^0$ *and* $\Omega$*, but independent of* $h$ *and* $\Delta t$*.*

*Proof.* To prove the bound on the velocity choose $v_h = u_h^{n+\frac{1}{2}}$ in (4.1.3). The nonlinear and pressure terms are then zero. The triangle inequality, and summing over time steps then completes the proof of (4.2.1).

To prove (4.2.2) choose $\chi_h = w_h^{n+\frac{1}{2}}$ in (4.1.5) and $r_h = \lambda_h^{n+1}$ in (4.1.6). After combining

the equations we obtain

$$\left\|w_h^{n+\frac{1}{2}}\right\|^2 = (\nabla \times u_h^{n+\frac{1}{2}}, w_h^{n+\frac{1}{2}}) \leq \left\|\nabla \times u_h^{n+\frac{1}{2}}\right\| \left\|w_h^{n+\frac{1}{2}}\right\|$$

$$\leq \frac{1}{2}\left\|\nabla \times u_h^{n+\frac{1}{2}}\right\|^2 + \frac{1}{2}\left\|w_h^{n+\frac{1}{2}}\right\|^2$$

$$\leq \left\|\nabla u_h^{n+\frac{1}{2}}\right\|^2 + \frac{1}{2}\left\|w_h^{n+\frac{1}{2}}\right\|^2.$$

Rearranging, and summing over time steps we obtain (4.2.2).

To obtain the stated bound for $\lambda_h^n$, we begin with the inf-sup condition satisfied by $X_h$ ($\subset W_h$) and $Q_h$ and use (4.1.5) to obtain

$$\|\lambda_h^n\| \leq \frac{1}{\beta} \sup_{\chi_h \in X_h} \frac{(\lambda_h^n, \nabla \cdot \chi_h)}{\|\chi_h\|_X} \leq \frac{1}{\beta} \sup_{\chi_h \in X_h} \frac{(\nabla \times u_h^{n-\frac{1}{2}}, \chi_h) - (w_h^{n-\frac{1}{2}}, \chi_h)}{\|\chi_h\|_X}$$

$$\leq \frac{1}{\beta}\left(\|\nabla \times u_h^{n-\frac{1}{2}}\| + \|w_h^{n-\frac{1}{2}}\|\right) \leq \frac{2}{\beta}\left(\|\nabla u_h^{n-\frac{1}{2}}\| + \|w_h^{n-\frac{1}{2}}\|\right).$$

Using the bounds for $\nabla u_h^{n+\frac{1}{2}}$ in (4.2.1) and $w_h^{n+\frac{1}{2}}$ in (4.2.2) we obtain the bound for $\lambda_h^n$. The bound for the pressure is established in an analogous manner. $\qquad\square$

We show existence for the equivalent nonlinear problem: Given, $\nu, \Delta t > 0$, $f^{n+\frac{1}{2}} \in V_h'$, and $u_h^n \in V_h$, find $(u_h, w_h) \in V_h \times V_h$ satisfying

$$\frac{2}{\Delta t}(u_h, v_h) + (u_h \times w_h, v_h) + \frac{\nu}{2}(\nabla u_h, \nabla v_h)$$

$$+\frac{\nu}{2}(w_h, \nabla \times v_h) = (f^{n+\frac{1}{2}}, v_h) \ \forall v_h \in V_h, \tag{4.2.4}$$

$$(w_h - \nabla \times u_h, \chi_h) = 0 \ \forall \chi_h \in V_h. \tag{4.2.5}$$

Restricting the test functions to $V_h$ ensures equations (4.2.4)-(4.2.5) are equivalent to (**??**)-(**??**). We now formulate (4.2.4)-(4.2.5) as a fixed point problem, $y = F(y)$, and use the Leray-Schauder fixed point theorem. We first prove several preliminary lemmas, followed by a theorem which proves that a solution to (4.2.4)-(4.2.5) exists.

**Lemma 4.2.2.** *For $\nu, \Delta t > 0$, there exists a unique solution $(u_h, w_h)$ to the following: Given $g \in V_h'$, find $(u_h, w_h) \in V_h \times V_h$ satisfying*

$$\frac{2}{\Delta t}(u_h, v_h) + \frac{\nu}{2}(\nabla u_h, \nabla v_h) + \frac{\nu}{2}(w_h, \nabla \times v_h) = (g, v_h) \ \forall v_h \in V_h, \tag{4.2.6}$$

$$(w_h - \nabla \times u_h, \chi_h) = 0 \ \forall \chi_h \in V_h. \tag{4.2.7}$$

38

*Proof.* We will prove uniqueness of solutions to (4.2.6)-(4.2.7) by showing only the trivial solutions solves the homogeneous problem, which will also imply the existence of solutions to the finite-dimensional problem. Since the space $V_h$ includes only zero-mean functions, functions and operators are uniquely solvable, and thus we need not consider the adjoint problem. Choose $v_h = u_h$ in (4.2.6), $\chi_h = w_h$ in (4.2.7), and substitute (4.2.7) into (4.2.6). This gives

$$\frac{2}{\Delta t}\|u_h\|^2 + \frac{\nu}{2}\|\nabla u_h\|^2 + \frac{\nu}{2}\|w_h\|^2 = 0,$$

which implies $u_h = w_h = 0$. $\qquad\qquad\square$

This lemma allows us to define a solution operator to (4.2.6)- (4.2.7).

**Definition 4.2.1.** *We define the solution operator $T : V_h' \to (V_h \times V_h)$ to be the solution operator of (4.2.6)- (4.2.7): if $g \in V_h'$, then $T(g) = (u_h, w_h)$ solves (4.2.6)- (4.2.7).*

We have that $T$ is well defined by the previous lemma, and we now prove it is bounded and linear.

**Lemma 4.2.3.** *The solution operator $T$ is linear, bounded, and continuous.*

*Proof.* The linearity of $T$ follows from the fact that $T$ is a solution operator to a linear problem. To see that $T$ is bounded (and thus continuous since it is linear), we let $v_h = u_h, \chi_h = w_h$ in (4.2.6)-(4.2.7), multiply (4.2.7) by $\frac{\nu}{2}$, and add the equations. This gives

$$\frac{2\|u_h\|^2}{\Delta t} + \frac{\nu}{4}\|\nabla u_h\|^2 + \frac{\nu}{2}\|w_h\|^2 \leq \frac{1}{\nu}\|g\|_{V'}^2. \tag{4.2.8}$$

Then since $u_h, w_h$ are finite-dimensional, $\|u_h, w_h\|_{V_h \times V_h} \leq C\|g\|_{V'}$. Hence,

$$\|T\| = \sup_{g \in V_h'} \frac{\|T(g)\|}{\|g\|_{V_h'}} = \sup_{g \in V_h'} \frac{\|u_h, w_h\|_{V_h \times V_h}}{\|g\|_{V_h'}} \leq C. \tag{4.2.9}$$

$\qquad\qquad\square$

We next define the operator $N$. The function $F$ that will be used in the formulation of the fixed point problem will be a composition of $T$ and $N$.

**Definition 4.2.2.** *We define the operator $N$ on $(V_h \times V_h)$ by*

$$N(u_h, w_h) := f^{n+\frac{1}{2}} + \frac{2}{\Delta t}u_h^n + u_h \times w_h. \tag{4.2.10}$$

We now prove properties for $N$ necessary for use in Leray-Schauder.

**Lemma 4.2.4.** *For the nonlinear operator $N$, we have that $N : V_h \times V_h \to V_h'$, $N$ is bounded, and $N$ is continuous.*

*Proof.* To show $N$ maps as stated, we let $(u_h, w_h) \in V_h \times V_h$ and write

$$\|N(u_h, w_h)\|_{V_h'} = \sup_{v_h \in V_h} \frac{(N(u_h, w_h), v_h)}{\|v_h\|_1}.$$

From the definition of $N$, we have that $\frac{(f^{n+\frac{1}{2}}, v_h) + (2(\Delta t)^{-1} u_h^n, v_h)}{\|v_h\|_1} \leq \|f\|_{V_h'} + C_1\|u_h^n\| \leq C_2$, and that

$$\frac{(u_h \times w_h, v_h)}{\|v_h\|_1} \leq \|u_h\|_\infty \|w_h\| \leq C_3 \tag{4.2.11}$$

since $u_h$ and $w_h$ are given to be in $V_h$, and all norms are equivalent in finite dimension. Hence $\|N(u_h, w_h)\|_{V_h'} < C$, and so $N$ maps as stated. Note we have also proven $N$ is bounded.

The equivalence of norms in finite dimension is also key in showing that $N$ is continuous, as

$$\|N(u, w) - N(u_k, w_k)\|_{V_h'} \leq \|u \times (w - w_k)\|_{V_h'} + \|(u - u_k) \times w_k\|_{V_h'}$$

$$\leq \|u\|_\infty \|w - w_k\| + \|w_k\|_\infty \|u - u_k\| \tag{4.2.12}$$

and thus $\to 0$ as $\|(u, w) - (u_k, w_k)\| \to 0$. $\qquad\square$

We now define the operator $F : (V_h \times V_h) \to (V_h \times V_h)$ to be the composition of $T$ and $N$: $F(y) = T(N(Y))$.

**Lemma 4.2.5.** *$F$ is well defined and compact, and a solution to $y = F(y)$ solves (4.2.4)-(4.2.5).*

*Proof.* $F$ is well defined because $N$ and $T$ are. The fact that $F$ is compact follows from the fact that both $N$ and $T$ are continuous and bounded. It can easily be seen that a fixed point of $F$ solves (4.2.4)-(4.2.5) by expanding $F$. $\qquad\square$

We are now ready to prove existence to (4.2.4)-(4.2.5) .

**Theorem 4.2.1.** *Let $y_\lambda = (u_\lambda, w_\lambda) \in V_h \times V_h$ and consider the family of fixed point problems $y_\lambda = \lambda F(y_\lambda)$, $0 \leq \lambda \leq 1$. A solution $y_\lambda$ to any of these fixed point problems satisfies $\|y_\lambda\| < K$, independent of $\lambda$. Since $F$ is compact, and fixed points of $F$ solve (4.2.4)-(4.2.5), by the Leray-Schauder theorem there exist solutions to (4.2.4)-(4.2.5) .*

*Proof.* All we have to show to prove this theorem is that solutions to $y_\lambda = \lambda F(y_\lambda)$ are bounded independent of $\lambda$. Using the definition of $F$ and the linearity of $T$ we have that

$$y_\lambda = \lambda F(y_\lambda) = \lambda T(N(y_\lambda)) = T(\lambda N(y_\lambda)) = T(\lambda(f^{n+\frac{1}{2}} + \frac{2}{\Delta t} u_h^n + u_\lambda \times w_\lambda), \quad (4.2.13)$$

which implies that

$$\frac{2}{\Delta t}(u_\lambda, v) - \lambda(u_\lambda \times w_\lambda, v) + \frac{\nu}{2}(\nabla u_\lambda, \nabla v_h)$$
$$+ \frac{\nu}{2}(w_\lambda, \nabla \times v_h) = (\lambda f^{n+\frac{1}{2}}, v_h) + \frac{2\lambda}{\Delta t}(u_h^n, v_h) \; \forall v_h \in V_h, (4.2.14)$$
$$(w_\lambda - \nabla \times u_\lambda, \chi_h) = 0 \; \forall \chi_h \in V_h. \quad (4.2.15)$$

Multiply (4.2.15) by $\frac{\nu}{2}$, let $\chi_h = w_\lambda$ in (4.2.15), $v_h = u_\lambda$ in (4.2.14), and add the equations. Similarly to the stability estimate, this gives

$$\frac{1}{\Delta t}\|u_\lambda\|^2 + \frac{\nu}{4}\|\nabla u_\lambda\|^2 + \frac{\nu}{2}\|w_\lambda\|^2 \leq$$
$$\lambda^2(\frac{1}{\nu}\|f^{n+\frac{1}{2}}\|^2 + \frac{1}{\Delta t}\|u_h^n\|^2) \leq (\frac{1}{\nu}\|f^{n+\frac{1}{2}}\|^2 + \frac{1}{\Delta t}\|u_h^n\|^2) \leq C, \quad (4.2.16)$$

which is a bound independent of $\lambda$. Thus the theorem is proven. $\qquad \square$

### 4.2.2 Conservation laws for discrete solutions

In this section we study the discrete conservation laws of Algorithm 4.1.1. Specifically, we show the incompressibility constraints are satisfied pointwise and that the scheme admits an energy and helicity balance which is analogous to these balances for the continuous NSE.

**Lemma 4.2.6.** *Assuming $(X_h, Q_h) = (P_k, P_{k-1}^{disc})$ with $k \geq d$ and periodic boundary conditions, we have the discrete velocity and vorticity are divergence free at every timestep, that is*

$$\|\nabla \cdot u_h^{n+1}\| = 0, \quad (4.2.17)$$

$$\|\nabla \cdot w_h^{n+1}\| = 0. \quad (4.2.18)$$

*Proof.* Note that the SV pair satisfies $\nabla \cdot X_h \subset Q_h$ and therefore we can choose $q_h = \nabla \cdot u_h^{n+\frac{1}{2}}$ in (4.1.5). This gives

$$\|\nabla \cdot u_h^{n+\frac{1}{2}}\|^2 = 0. \quad (4.2.19)$$

Identity (4.2.17) follows from taking the square root of both sides of (4.2.19).

To derive (4.2.18) note that the use of periodic boundary conditions guarantees that $W_h \subset X_h$ and thus $\nabla \cdot W_h \subset Q_h$. Now choosing $r_h = \nabla \cdot w_h^{n+\frac{1}{2}}$ and proceeding as before gives (4.2.18). $\quad\square$

We now study the energy and helicity conservation of the scheme. Denote the discrete energy and helicity at time level $n$ by $E_h^n := \frac{1}{2}\|u_h^n\|^2$ and $H_h^n := (u_h^n, \nabla \times u_h^n)$ respectively. Notice that from (4.1.4) and (4.1.5), $H_h^n := (u_h^n, w_h^n)$.

**Lemma 4.2.7.** *Algorithm 4.1.1 admits the following energy and helicity conservation laws.*

$$\frac{1}{2}\|E_h^M\|^2 + \nu\Delta t \sum_{n=0}^{M-1} \|\nabla u_h^{n+\frac{1}{2}}\|^2 \;=\; \Delta t \sum_{n=0}^{M-1} (f(t^{n+\frac{1}{2}}), u_h^{n+\frac{1}{2}}) + \frac{1}{2}\left\|E_h^0\right\|^2 . \qquad (4.2.20)$$

$$H_h^M + 2\Delta t\nu \sum_{n=0}^{M-1} (\nabla u_h^{n+\frac{1}{2}}, \nabla w_h^{n+\frac{1}{2}}) \;=\; H_h^0 + 2\Delta t\nu \sum_{n=0}^{M-1} (f(t^{n+\frac{1}{2}}), u_h^{n+\frac{1}{2}}) \qquad (4.2.21)$$

*Proof.* To prove (4.2.20) and (4.2.21) we choose $v_h = u_h^{n+\frac{1}{2}}$ and $v_h = w_h^{n+\frac{1}{2}}$ in (4.1.3). The key point is that the nonlinear term vanishes with these choices of test functions, and thus does not contribute to the energy and helicity balance equations. $\quad\square$

### 4.2.3 Convergence

We now prove optimal convergence of solutions to Algorithm 4.1.1 to an NSE solution. Let $P_{V_h} : L^2 \to V_h$ denote the projection of $L^2$ onto $V_h$, i.e. $P_{V_h}(w) := s_h$ where

$$(s_h, v_h) \;=\; (w, v_h), \forall v_h \in V_h .$$

For simplicity in stating the a priori theorem we summarize here the regularity assumptions for the solution $u(x,t)$ to the NSE.

$$u \in L^2(0,T; H^{k+1}(\Omega)) \cap L^\infty(0,T; H^1(\Omega)), \qquad (4.2.22)$$

$$u(\cdot,t) \in H_0^1(\Omega), \quad \nabla \times u \in L^2(0,T; H^{k+1}(\Omega)), \qquad (4.2.23)$$

$$u_t \in L^2(0,T; H^{k+1}(\Omega)) \cap L^\infty(0,T; H^{k+1}(\Omega)), \qquad (4.2.24)$$

$$u_{tt} \in L^2(0,T; H^{k+1}(\Omega)), \qquad (4.2.25)$$

$$u_{ttt} \in L^2(0,T; L^2(\Omega)) \qquad (4.2.26)$$

$$(u \times (\nabla \times u))_{tt} \in L^2(0,T; L^2(\Omega)). \qquad (4.2.27)$$

**Theorem 4.2.2.** *For $u$, $p$ solutions of the NSE with $p \in L^2(0, T; H^k(\Omega))$, $u$ satisfying (4.2.22)-(4.2.27), $f \in L^2(0, T; X^*(\Omega))$, and $u_0 \in V_h$, $(u_h^n, w_h^n)$ given by Algorithm 4.1.1 for $n = 1, ..., M$ and $\Delta t$ sufficiently small, we have that*

$$\left\| u(T) - u_h^M \right\| + \left( \nu \Delta t \sum_{n=0}^{M-1} \left\| \nabla(u^{n+\frac{1}{2}} - u_h^{n+\frac{1}{2}}) \right\|^2 + \left\| \nabla \times u^{n+1/2} - w_h^{n+1/2} \right\|^2 \right)^{1/2} \leq$$

$$C(T, \nu^{-3}, u) \left( h^k \|u(T)\|_{k+1} + h^k \|\|u\|\|_{2,k+1} + h^k \|\|u_t\|\|_{2,k+1} \right.$$

$$+ h^k \|\|u_t\|\|_{\infty,k+1} + h^k \|\|u_t\|\|_{\infty,1} \|\|u\|\|_{2,k+1} + (\Delta t)^{1/2} h^k \|u_{tt}\|_{2,k+1} + (\Delta t)^2 \|u_{ttt}\|_{2,0}$$

$$+ (\Delta t)^2 \|u_{tt}\|_{2,1} + (\Delta t)^2 \|(u \times (\nabla \times u))_{tt}\|_{2,0} + \left. h^{k+1} \|\|u\|\|_{\infty,1} \|\|\nabla \times u\|\|_{2,k+1} . \right) \quad (4.2.28)$$

**Remark 4.2.1.** *This proof is similar to the convergence proof in Chapter 3. The fundamental difference in the proofs is that now we are assuming the use of the SV element, which while maintaing optimal approximation properties removes the adverse (often large) effect of the Bernoulli pressure occurring when computing a scheme in rotational form of the NSE.*

*Proof of Theorem.* Since $(u, p)$ solves the NSE, we have $\forall v_h \in X_h$ that

$$(u_t(t^{n+\frac{1}{2}}), v_h) + (u(t^{n+\frac{1}{2}}) \times (\nabla \times u(t^{n+\frac{1}{2}})), v_h) - (p(t^{n+\frac{1}{2}}), \nabla \cdot v_h)$$

$$+ \nu(\nabla u(t^{n+\frac{1}{2}}), \nabla v_h) = (f(t^{n+\frac{1}{2}}), v_h). \quad (4.2.29)$$

Adding $(\frac{u^{n+1} - u^n}{\Delta t}, v_h)$ and $\nu(\nabla u^{n+\frac{1}{2}}, \nabla v_h)$ to both sides of (4.2.29) we obtain

$$\frac{1}{\Delta t}(u^{n+1} - u^n, v_h) + \left( (\nabla \times u(t^{n+\frac{1}{2}}) \times u(t^{n+\frac{1}{2}})), v_h \right) - (p(t^{n+\frac{1}{2}}), \nabla \cdot v_h)$$

$$+ \nu(\nabla u^{n+\frac{1}{2}}, \nabla v_h) = (f(t^{n+\frac{1}{2}}), v_h) + \left( \frac{u^{n+1} - u^n}{\Delta t} - u_t(t^{n+\frac{1}{2}}), v_h \right)$$

$$+ \nu(\nabla u^{n+\frac{1}{2}} - \nabla u(t^{n+\frac{1}{2}}), \nabla v_h). \quad (4.2.30)$$

Next, subtracting (4.1.3) from (4.2.30) and labelling $e^n := u^n - u_h^n$ gives

$$\frac{1}{\Delta t}(e^{n+1} - e^n, v_h) + \nu(\nabla e^{n+\frac{1}{2}}, \nabla v_h) = \left( (\nabla \times u(t^{n+\frac{1}{2}}) \times u(t^{n+\frac{1}{2}})), v_h \right) + \left( w_h^{n+\frac{1}{2}} \times u_h^{n+\frac{1}{2}}, v_h \right)$$

$$+ \left( p(t^{n+\frac{1}{2}}) - p_h^{n+1}, \nabla \cdot v_h \right) + \left( \frac{u^{n+1} - u^n}{\Delta t} - u_t(t^{n+\frac{1}{2}}), v_h \right) + \nu \left( \nabla u^{n+\frac{1}{2}} - \nabla u(t^{n+\frac{1}{2}}), \nabla v_h \right).$$

We split the error into two pieces $\Phi_h$ and $\eta$: $e^n = u^n - u_h^n = (u^n - U^n) + (U^n - u_h^n) := \eta^n + \Phi_h^n,$

where $U^n$ denotes the interpolant of $u^n$ in $V_h$, yielding

$$\frac{1}{\Delta t}(\Phi_h^{n+1} - \Phi_h^n, v_h) + \nu(\nabla\Phi_h^{n+\frac{1}{2}}, \nabla v_h) = -\frac{1}{\Delta t}(\eta^{n+1} - \eta^n, v_h) - \nu(\nabla\eta^{n+\frac{1}{2}}, \nabla v_h)$$

$$\left((\nabla \times u(t^{n+\frac{1}{2}}) \times u(t^{n+\frac{1}{2}})), v_h\right) + (w_h^{n+\frac{1}{2}} \times u_h^{n+\frac{1}{2}}, v_h) + (p(t^{n+\frac{1}{2}}) - p_h^{n+1}, \nabla \cdot v_h)$$

$$+ \left(\frac{u^{n+1} - u^n}{\Delta t} - u_t(t^{n+\frac{1}{2}}), v_h\right) + \nu(\nabla u^{n+\frac{1}{2}} - \nabla u(t^{n+\frac{1}{2}}), \nabla v_h). \quad (4.2.31)$$

Choosing $v_h = \Phi_h^{n+\frac{1}{2}}$ vanishes the pressure term and yields

$$\frac{1}{2\Delta t}\left(\|\Phi_h^{n+1}\|^2 - \|\Phi_h^n\|^2\right) + \nu\left\|\nabla\Phi_h^{n+\frac{1}{2}}\right\|^2 = -\frac{1}{\Delta t}(\eta^{n+1} - \eta^n, \Phi_h^{n+\frac{1}{2}}) - \nu(\nabla\eta^{n+\frac{1}{2}}, \nabla\Phi_h^{n+\frac{1}{2}})$$

$$- \left(\nabla \times u(t^{n+\frac{1}{2}}) \times u(t^{n+\frac{1}{2}}), \Phi_h^{n+\frac{1}{2}}\right) + (w_h^{n+\frac{1}{2}} \times u_h^{n+\frac{1}{2}}, \Phi_h^{n+\frac{1}{2}})$$

$$+ \left(\frac{u^{n+1} - u^n}{\Delta t} - u_t(t^{n+\frac{1}{2}}), \Phi_h^{n+\frac{1}{2}}\right) + \nu(\nabla u^{n+\frac{1}{2}} - \nabla u(t^{n+\frac{1}{2}}), \nabla\Phi_h^{n+\frac{1}{2}}). \quad (4.2.32)$$

We have the following bounds for the terms on the RHS (see [18]).

$$-\nu(\nabla\eta^{n+\frac{1}{2}}, \nabla\Phi_h^{n+\frac{1}{2}}) \leq \frac{\nu}{12}\left\|\nabla\Phi_h^{n+\frac{1}{2}}\right\|^2 + 3\nu\left\|\nabla\eta^{n+\frac{1}{2}}\right\|^2 \quad (4.2.33)$$

$$\frac{1}{\Delta t}(\eta^{n+1} - \eta^n, \Phi_h^{n+\frac{1}{2}}) \leq \frac{1}{2}\left\|\frac{\eta^{n+1} - \eta^n}{\Delta t}\right\|^2 + \frac{1}{2}\left\|\Phi_h^{n+\frac{1}{2}}\right\|^2$$

$$= \frac{1}{2}\int_\Omega\left(\frac{1}{\Delta t}\int_{t^n}^{t^{n+1}} \eta_t\, dt\right)^2 d\Omega + \frac{1}{2}\left\|\Phi_h^{n+\frac{1}{2}}\right\|^2$$

$$\leq \frac{1}{2}\int_\Omega\left(2|\eta_t(t^{n+1})|^2 + 2\int_{t^n}^{t^{n+1}} |\eta_{tt}|^2\, dt\right) d\Omega + \frac{1}{2}\left\|\Phi_h^{n+\frac{1}{2}}\right\|^2$$

$$= \left\|\eta_t(t^{n+1})\right\|^2 + \int_{t^n}^{t^{n+1}} \|\eta_{tt}\|^2\, dt + \frac{1}{2}\left\|\Phi_h^{n+\frac{1}{2}}\right\|^2. \quad (4.2.34)$$

Similarly,

$$\left(\frac{u^{n+1} - u^n}{\Delta t} - u_t(t^{n+\frac{1}{2}}), \Phi_h^{n+\frac{1}{2}}\right) \leq \frac{1}{2}\left\|\frac{u^{n+1} - u^n}{\Delta t} - u_t(t^{n+\frac{1}{2}})\right\|^2 + \frac{1}{2}\left\|\Phi_h^{n+\frac{1}{2}}\right\|^2$$

$$= \frac{(\Delta t)^3}{2560}\int_{t^n}^{t^{n+1}} \|u_{ttt}\|^2\, dt + \frac{1}{2}\left\|\Phi_h^{n+\frac{1}{2}}\right\|^2, \quad (4.2.35)$$

$$\nu(\nabla u^{n+\frac{1}{2}} - \nabla u(t^{n+\frac{1}{2}}), \nabla\Phi_h^{n+\frac{1}{2}}) \leq 3\nu\left\|\nabla u^{n+\frac{\nu}{12}} - \nabla u(t^{n+\frac{1}{2}})\right\|^2 + \frac{\nu^2}{2}\left\|\Phi_h^{n+\frac{1}{2}}\right\|^2$$

$$= \frac{\nu(\Delta t)^3}{16}\int_{t^n}^{t^{n+1}} \|\nabla u_{tt}\|^2\, dt + \frac{\nu}{12}\left\|\Phi_h^{n+\frac{1}{2}}\right\|^2. \quad (4.2.36)$$

44

Utilizing (4.2.33)-(4.2.36) we now have

$$
\frac{1}{2\Delta t}\left(\left\|\Phi_h^{n+1}\right\|^2 - \left\|\Phi_h^n\right\|^2\right) + \frac{5\nu}{6}\left\|\nabla\Phi_h^{n+\frac{1}{2}}\right\|^2 \leq 3\nu\left\|\nabla\eta^{n+\frac{1}{2}}\right\|^2 + \int_{t^n}^{t^{n+1}}\left\|\eta_{tt}\right\|^2\,dt
$$
$$
+ C(1+\nu)\Delta t^3\left(\int_{t^n}^{t^{n+1}}\left\|u_{ttt}\right\|^2\,dt + \int_{t^n}^{t^{n+1}}\left\|\nabla u_{tt}\right\|^2\,dt\right) + \frac{\nu^2+1}{2}\left\|\Phi_h^{n+\frac{1}{2}}\right\|^2
$$
$$
+ \left\|\eta_t(t^{n+1})\right\|^2 + (w_h^{n+\frac{1}{2}}\times u_h^{n+\frac{1}{2}}, \Phi_h^{n+\frac{1}{2}}) - \left((\nabla\times u(t^{n+\frac{1}{2}}))\times u(t^{n+\frac{1}{2}}), \Phi_h^{n+\frac{1}{2}}\right). \quad (4.2.37)
$$

Treatment of the nonlinear terms is the same as in [9] which gives.

$$
\frac{1}{2\Delta t}\left(\left\|\Phi_h^{n+1}\right\|^2 - \left\|\Phi_h^n\right\|^2\right) + \frac{\nu}{2}\left\|\nabla\Phi_h^{n+\frac{1}{2}}\right\|^2 \leq \left(\frac{\nu^2+4}{2} + C\nu^{-3}\left\|\nabla u^{n+\frac{1}{2}}\right\|^4\right)\left\|\Phi_h^{n+\frac{1}{2}}\right\|^2
$$
$$
+ C\nu\left\|\nabla\eta^{n+\frac{1}{2}}\right\|^2 + \left\|\eta_t(t^{n+1})\right\|^2 + C\nu^{-1}\left\|w_h^{n+\frac{1}{2}}\right\|^2\left\|\nabla\eta^{n+\frac{1}{2}}\right\|^2 + \nu^{-1}\left\|\nabla u^{n+\frac{1}{2}}\right\|^2\left\|\nabla\eta^{n+\frac{1}{2}}\right\|^2
$$
$$
+ \int_{t^n}^{t^{n+1}}\left\|\eta_{tt}\right\|^2\,dt + C\Delta t^3\left(\int_{t^n}^{t^{n+1}}\left\|u_{ttt}\right\|^2\,dt + \int_{t^n}^{t^{n+1}}\left\|\nabla u_{tt}\right\|^2\,dt\right)
$$
$$
+ C\nu^{-1}(\Delta t)^3\int_{t^n}^{t^{n+1}}\left\|(u\times(\nabla\times u))_{tt}\right\|^2\,dt + C\left\|\nabla u^{n+\frac{1}{2}}\right\|^2\left\|\nabla\times u^{n+\frac{1}{2}} - P_{V_h}(\nabla\times u^{n+\frac{1}{2}})\right\|^2
$$
$$
(4.2.38)
$$

Next multiplying by $2\Delta t$, summing over time steps, and using Lemma **??** yields

$$
\left\|\Phi_h^M\right\|^2 + \nu\Delta t\sum_{n=0}^{M-1}\left\|\nabla\Phi_h^{n+\frac{1}{2}}\right\|^2
$$
$$
\leq C exp\left(2\Delta t\sum_{n=0}^{M-1}\frac{\nu^2+4}{2} + C\nu^{-3}\left\|\nabla u^{n+\frac{1}{2}}\right\|^4\right)\left(\Delta t\sum_{n=0}^{M}\nu\left\|\nabla\eta^n\right\|^2 + \Delta t\sum_{n=1}^{M}\left\|\eta_t(t^n)\right\|^2\right.
$$
$$
+ \Delta t\sum_{n=0}^{M-1}\nu^{-1}\left\|w_h^{n+\frac{1}{2}}\right\|^2\left\|\nabla\eta^{n+\frac{1}{2}}\right\|^2 + \Delta t\sum_{n=0}^{M-1}\nu^{-1}\left\|\nabla u^{n+\frac{1}{2}}\right\|^2\left\|\nabla\eta^{n+\frac{1}{2}}\right\|^2
$$
$$
+ \Delta t\sum_{n=0}^{M-1}\int_{t^n}^{t^{n+1}}\left\|\eta_{tt}\right\|^2\,dt + (\Delta t)^4\left\|u_{ttt}\right\|_{2,0}^2 + (\Delta t)^4\left\|\nabla u_{tt}\right\|_{2,0}^2
$$
$$
+ (\Delta t)^4\left\|(u\times(\nabla\times u))_{tt}\right\|_{2,0}^2 + \Delta t\sum_{n=0}^{M-1}\left\|\nabla u^{n+\frac{1}{2}}\right\|^2\left\|\nabla\times u^{n+\frac{1}{2}} - P_{V_h}(\nabla\times u^{n+\frac{1}{2}})\right\|^2\right) \quad (4.2.39)
$$

Recall the approximation properties of $U^n \in V_h$, $q_h \in Q_h$, and $P_{V_h}$ [37]

$$
\left\|\eta(t^n)\right\|_s \leq Ch^{k+1-s}\left\|u(t^n)\right\|_{k+1}, \quad s = 0, 1, \quad \text{and}
$$
$$
\left\|w^n - P_{V_h}(w^n)\right\| \leq Ch^{k+1}\left\|w^n\right\|_{k+1}.
$$

Estimate (4.2.39) then becomes

$$\left\|\Phi_h^M\right\|^2 + \nu\Delta t \sum_{n=0}^{M-1} \left\|\nabla\Phi_h^{n+\frac{1}{2}}\right\|^2$$

$$\leq C\exp\left(2\Delta t \sum_{n=0}^{M-1} \frac{\nu^2+4}{2} + C\nu^{-3}\left\|\nabla u^{n+\frac{1}{2}}\right\|^4\right) \left(\nu\, h^{2k}\|\|u\|\|_{2,k+1}^2\right.$$

$$+\ h^{2k+2}\|\|u_t\|\|_{2,k+1}^2 + \nu^{-1}h^{2k}\|\|u_t\|\|_{\infty,1}^2\|\|u\|\|_{2,k+1}^2 + \Delta t\, h^{2k+2}\|u_{tt}\|_{2,k+1}^2$$

$$+\ (\Delta t)^4\|u_{ttt}\|_{2,0}^2 + (\Delta t)^4\|\nabla u_{tt}\|_{2,0}^2 + (\Delta t)^4\|(u\times(\nabla\times u))_{tt}\|_{2,0}^2$$

$$+\ \left(\nu\Delta t\sum_{n=0}^{M-1}\left\|w_h^{n+\frac{1}{2}}\right\|^2\right)\nu^{-2}h^{2k}\|\|u_t\|\|_{\infty,k+1}^2 + \left. h^{2k+2}\|\|u\|\|_{\infty,1}^2\|\|\nabla\times u\|\|_{2,k+1}^2 \,.\right) \quad (4.2.40)$$

Finally, from the boundness estimate for $\nu\Delta t\sum_{n=0}^{M-1}\left\|w_h^{n+\frac{1}{2}}\right\|^2$ from (4.2.2), and an application of the triangle inequality we obtain (4.2.28).

$\square$

## 4.3 Improved efficiency through decoupling

Algorithm 4.1.1 can be twice decoupled to allow for more efficient solves of the nonlinear system. First, the nonlinear system should be decoupled into velocity-pressure and vorticity projection pieces. Once this is done, one is left to solve several saddle point systems at each timestep. Due to the use of SV elements, we are able to use the classical penalty method to obtain optimally accurate solutions while eliminating the saddle point structure of the linear systems. The key point here is that the pointwise div-free subspace of the velocity space is guaranteed to have optimal approximation properties in the setting where SV elements are LBB stable [65]. We prove now a connection between the $(P_k, P_{k-1}^{disc})$ SV solution and $(P_k, Q_h)$ element solutions, where $Q_h$ can be chosen from $\{P_{k-1},\ P_{k-2},\ ...,\ P_1,\ P_0,\{0\}\}$, the last of which leads directly to the penalty method for both the reduced velocity and vorticity systems.

**Theorem 4.3.1.** *Let $Q_h$ be specified so that the $(P_k, Q_h)$ pair is LBB stable. Then on a fixed mesh, the $(P_k, Q_h)$ velocity solutions to (4.1.1)-(4.1.6) converge to the SV solution with convergence order $\gamma^{-1}$ in the energy norm, as $\gamma \to \infty$; that is, if $u_h$ is the TH velocity solution and $u_h^0$ is the SV velocity solution, then*

$$\|u_h - u_h^0\|_{l^2(0,T;H^1(\Omega))} \leq \frac{C}{\gamma} \qquad (4.3.1)$$

**Remark 4.3.1.** *The pair $(P_k, Q_h)$ is LBB stable when $Q_h$ is chosen to be $P_r$ (for $0 \le r < k$). Of particular interest is the case when $Q_h = \{0\}$ which is equivalent to a dual-penalty method, similar to that of Temam's in [69].*

*Proof.* Let $(u_h^{n+1}, w_h^{n+1}, p_h^{n+1}, l_h^{n+1})$ and $(u_h^{0,n+1}, w_h^{0,n+1}, p_h^{0,n+1}, \lambda_h^{0,n+1})$ denote the SV and $(P_k, Q_h)$ solutions to (4.1.3)-(4.1.6) respectively. Additionally, denote the velocity and vorticity differences of the solutions as $r^{n+\frac{1}{2}}$ and $s^{n+\frac{1}{2}}$ so that

$$r^{n+\frac{1}{2}} := u_h^{n+\frac{1}{2}} - u_h^{0,n+\frac{1}{2}}, \tag{4.3.2}$$

$$s^{n+\frac{1}{2}} := w_h^{n+\frac{1}{2}} - w_h^{0,n+\frac{1}{2}}. \tag{4.3.3}$$

Orthogonally decompose $r^{n+\frac{1}{2}} = \mathring{r}^{n+\frac{1}{2}} + r^{n+\frac{1}{2}}$ and $s^{n+\frac{1}{2}} = \mathring{s}^{n+\frac{1}{2}} + s^{n+\frac{1}{2}}$ so that $r^{n+\frac{1}{2}}, s^{n+\frac{1}{2}} \in V_h^0$ and $\mathring{r}^{n+\frac{1}{2}}, \mathring{s}^{n+\frac{1}{2}} \in R_h$. Note it follows from (4.1.4) and the above decomposition that $(\nabla \cdot \mathring{r}^{n+1}, q_h) = 0$ $\forall q_h \in Q_h$.

Pick $v_h = \mathring{r}^{n+\frac{1}{2}}$ in (4.1.3), then the $(P_k, Q_h)$ and SV solutions satisfy respectively

$$(\frac{u_h^{n+1} - u_h^n}{\Delta t}, \mathring{r}^{n+\frac{1}{2}}) + \gamma(\nabla \cdot u_h^{n+\frac{1}{2}}, \nabla \cdot \mathring{r}^{n+\frac{1}{2}}) + (w_h^{n+\frac{1}{2}} \times u_h^{n+\frac{1}{2}}, \mathring{r}^{n+\frac{1}{2}})$$
$$+ \nu(\nabla u_h^{n+\frac{1}{2}}, \nabla \mathring{r}^{n+\frac{1}{2}}) = (f(t^{n+\frac{1}{2}}), \mathring{r}^{n+\frac{1}{2}}) \tag{4.3.4}$$

$$(\frac{u_h^{0,n+1} - u_h^{0,n}}{\Delta t}, \mathring{r}^{n+\frac{1}{2}}) + (p_h^{0,n+\frac{1}{2}}, \nabla \cdot \mathring{r}^{n+\frac{1}{2}}) + (w_h^{0,n+\frac{1}{2}} \times u_h^{0,n+\frac{1}{2}}, \mathring{r}^{n+\frac{1}{2}})$$
$$+ \nu(\nabla u_h^{0,n+\frac{1}{2}}, \nabla \mathring{r}^{n+\frac{1}{2}}) = (f(t^{n+\frac{1}{2}}), \mathring{r}^{n+\frac{1}{2}}) \tag{4.3.5}$$

Subtracting (4.3.5) from (4.3.4), rearranging and reducing with the following identities

$$\nabla \cdot u_h^{n+\frac{1}{2}} = \nabla \cdot r^{n+\frac{1}{2}} = \nabla \cdot \mathring{r}^{n+\frac{1}{2}} \tag{4.3.6}$$

$$(\nabla r^{n+\frac{1}{2}}, \nabla \mathring{r}^{n+\frac{1}{2}}) = \nu \|\nabla \mathring{r}^{n+\frac{1}{2}}\|^2 \tag{4.3.7}$$

gives

$$\frac{1}{\Delta t}(r^{n+1}, \mathring{r}^{n+\frac{1}{2}}) - \frac{1}{\Delta t}(r^n, \mathring{r}^{n+\frac{1}{2}}) + \nu \|\mathring{r}^{n+\frac{1}{2}}\|^2 + \gamma \|\nabla \cdot \mathring{r}^{n+\frac{1}{2}}\|^2$$
$$= (w_h^{n+\frac{1}{2}} \times u_h^{n+\frac{1}{2}}, \mathring{r}^{n+\frac{1}{2}}) - (w_h^{0,n+\frac{1}{2}} \times u_h^{0,n+\frac{1}{2}}, \mathring{r}^{n+\frac{1}{2}}) - (p_h^{0,n+\frac{1}{2}}, \mathring{r}^{n+\frac{1}{2}}). \tag{4.3.8}$$

Standard inequalities, bounds on solutions and Lemma 2.0.1 yields

$$\frac{1}{\Delta t}(r^{n+1}, \mathring{r}^{n+\frac{1}{2}}) - \frac{1}{\Delta t}(r^n, \mathring{r}^{n+\frac{1}{2}}) + \nu \|\mathring{r}^{n+\frac{1}{2}}\|^2 + \gamma \|\nabla \cdot \mathring{r}^{n+\frac{1}{2}}\|^2 \le C \|\nabla \mathring{r}^{n+\frac{1}{2}}\|. \tag{4.3.9}$$

Similarly, if $\chi_h = \mathring{s}^{n+\frac{1}{2}}$ in (4.1.5), the $(P_k, Q_h)$ and SV solutions respectively satisfy

$$(w_h^{n+\frac{1}{2}}, \mathring{s}^{n+\frac{1}{2}}) + \gamma(\nabla \cdot w_h^{n+\frac{1}{2}}, \nabla \cdot \mathring{s}^{n+\frac{1}{2}}) + (\lambda_h^{n+\frac{1}{2}}, \mathring{s}^{n+\frac{1}{2}}) = (\nabla \times u_h^{n+\frac{1}{2}}, \mathring{s}^{n+\frac{1}{2}}), \quad (4.3.10)$$

$$(w_h^{0,n+\frac{1}{2}}, \mathring{s}^{n+\frac{1}{2}}) + (l_h^{0,n+\frac{1}{2}}, \mathring{s}^{n+\frac{1}{2}}) = (\nabla \times u_h^{0,n+\frac{1}{2}}, \mathring{s}^{n+\frac{1}{2}}). \quad (4.3.11)$$

Subtracting (4.3.11) from (4.3.10) and rearranging gives

$$\|\mathring{s}^{n+\frac{1}{2}}\|^2 + \gamma(\nabla \cdot w_h^{n+\frac{1}{2}}, \nabla \cdot \mathring{s}^{n+\frac{1}{2}}) = -(s^{n+\frac{1}{2}}, \mathring{s}^{n+\frac{1}{2}}) - (\lambda_h^{n+\frac{1}{2}}, \mathring{s}^{n+\frac{1}{2}}) + (\nabla \times u_h^{n+\frac{1}{2}}, \mathring{s}^{n+\frac{1}{2}})$$

$$+ (l_h^{0,n+\frac{1}{2}}, \mathring{s}^{n+\frac{1}{2}}) - (\nabla \times u_h^{0,n+\frac{1}{2}}, \mathring{s}^{n+\frac{1}{2}}). \ (4.3.12)$$

Reducing with standard inequalities, bounds on solutions, lemma and the following identity

$$\nabla \cdot w_h^{n+\frac{1}{2}} = \nabla \cdot s^{n+\frac{1}{2}} = \nabla \cdot \mathring{s}^{n+\frac{1}{2}} \qquad (4.3.13)$$

gives

$$\|\nabla \cdot \mathring{s}^{n+\frac{1}{2}}\| \le \frac{C}{\gamma}. \qquad (4.3.14)$$

Next for $\chi_h = s^{n+\frac{1}{2}}$ in (4.1.5) the $(P_k, Q_h)$ and SV solutions then satisfy the following equalities

$$(w_h^{n+\frac{1}{2}}, s^{n+\frac{1}{2}}) = (\nabla \times u_h^{n+\frac{1}{2}}, s^{n+\frac{1}{2}}), \qquad (4.3.15)$$

$$(w_h^{0,n+\frac{1}{2}}, s^{n+\frac{1}{2}}) = (\nabla \times u_h^{0,n+\frac{1}{2}}, s^{n+\frac{1}{2}}). \qquad (4.3.16)$$

Subtracting (4.3.16) from (4.3.15),rearranging and using standard inequalities gives

$$\|s^{n+\frac{1}{2}}\|^2 \le \|\mathring{s}^{n+\frac{1}{2}}\| \|s^{n+\frac{1}{2}}\| + \|\nabla \times r^{n+\frac{1}{2}}\| \|s^{n+\frac{1}{2}}\|. \qquad (4.3.17)$$

Reducing gives

$$\|\nabla s^{n+\frac{1}{2}}\| \le C(\|\mathring{s}^{n+\frac{1}{2}}\| + \|\nabla r^{n+\frac{1}{2}}\|). \qquad (4.3.18)$$

Choosing $v_h = r^{n+\frac{1}{2}}$ in (4.1.3) admits the following equalities for the $(P_k, Q_h)$ and SV

solution, respectively:

$$\frac{1}{\Delta t}(u_h^{n+1} - u_h^n, r^{n+\frac{1}{2}}) + (w_h^{n+\frac{1}{2}} \times u_h^{n+\frac{1}{2}}, r^{n+\frac{1}{2}}) + \nu(\nabla u_h^{n+\frac{1}{2}}, r^{n+\frac{1}{2}}) = (f(t^{n+\frac{1}{2}}), r^{n+\frac{1}{2}}) \quad (4.3.19)$$

$$\frac{1}{\Delta t}(u_h^{0,n+1} - u_h^{0,n}, r^{n+\frac{1}{2}}) + (w_h^{0,n+\frac{1}{2}} \times u_h^{0,n+\frac{1}{2}}, r^{n+\frac{1}{2}}) + \nu(\nabla u_h^{0,n+\frac{1}{2}}, r^{n+\frac{1}{2}}) = (f(t^{n+\frac{1}{2}}), r^{n+\frac{1}{2}}) \quad (4.3.20)$$

Subtracting (4.3.20) from (4.3.19) and rearranging gives

$$\frac{1}{\Delta t}(r^{n+1}, r^{n+\frac{1}{2}}) - \frac{1}{\Delta t}(r^n, r^{n+\frac{1}{2}}) + \nu\|\nabla r^{n+\frac{1}{2}}\|^2 \quad (4.3.21)$$

$$= (w_h^{n+\frac{1}{2}} \times u_h^{n+\frac{1}{2}}, r^{n+\frac{1}{2}}) \quad - \quad (w_h^{0,n+\frac{1}{2}} \times u_h^{0,n+\frac{1}{2}}, r^{n+\frac{1}{2}}). \quad (4.3.22)$$

We majorize the left hand side by rewriting the nonlinear terms using a standard identity which yields

$$\frac{1}{\Delta t}(r^{n+1}, r^{n+\frac{1}{2}}) - \frac{1}{\Delta t}(r^n, r^{n+\frac{1}{2}}) + \nu\|\nabla r^{n+\frac{1}{2}}\|^2 \quad (4.3.23)$$

$$\leq |(w_h^{n+\frac{1}{2}} \times r^{n+\frac{1}{2}}, r^{n+\frac{1}{2}})| \quad + \quad |(s^{n+\frac{1}{2}} \times u_h^{0,n+\frac{1}{2}}, r^{n+\frac{1}{2}})|. \quad (4.3.24)$$

The first nonlinear term reduces using orthogonality and bounds on solutions. We bound the second nonlinear term by splitting $s^{n+\frac{1}{2}}$ into its orthogonal components which gives

$$\frac{1}{\Delta t}(r^{n+1}, r^{n+\frac{1}{2}}) - \frac{1}{\Delta t}(r^n, r^{n+\frac{1}{2}}) + \nu\|\nabla r^{n+\frac{1}{2}}\|^2 \leq C\|r^{n+\frac{1}{2}}\|^2 \quad (4.3.25)$$

$$+ C_1\|\nabla \mathring{s}^{n+\frac{1}{2}}\|\|r^{n+\frac{1}{2}}\| + C_2\|\nabla s^{n+\frac{1}{2}}\|\|\nabla r^{n+\frac{1}{2}}\|. \quad (4.3.26)$$

To the right hand side we add $C_1\|\nabla \mathring{s}^{n+\frac{1}{2}}\|\|\nabla \mathring{r}^{n+\frac{1}{2}}\|$ and $C_2\|\nabla s^{n+\frac{1}{2}}\|\|\nabla \mathring{r}^{n+\frac{1}{2}}\|$. Then reducing with (4.3.14), (4.3.18) and standard inequalities gives

$$\frac{1}{\Delta t}(r^{n+1}, r^{n+\frac{1}{2}}) - \frac{1}{\Delta t}(r^n, r^{n+\frac{1}{2}}) + \nu\|\nabla r^{n+\frac{1}{2}}\|^2 \leq \frac{C}{\gamma} + Ch^{-1}\|r^{n+\frac{1}{2}}\|^2. \quad (4.3.27)$$

Adding (4.3.9) and (4.3.27), dropping the stiffness term and reducing gives

$$\frac{1}{2\Delta t}\|r^{n+1}\|^2 - \frac{1}{2\Delta t}\|r^n\|^2 + \gamma\|\nabla \cdot \mathring{r}^{n+\frac{1}{2}}\|^2 \leq \frac{C}{\gamma} + Ch^{-1}\|r^{n+\frac{1}{2}}\|^2 + C\|\nabla \cdot \mathring{r}^{n+\frac{1}{2}}\|. \quad (4.3.28)$$

Using standard inequalities, multiplying by $2\Delta t$ and summing over time steps yields

$$\|r^M\|^2 + \gamma\Delta t \sum_{n=0}^{M-1}\|\nabla \cdot \mathring{r}^{n+\frac{1}{2}}\|^2 \leq \|r^0\|^2 + C\Delta t \sum_{n=0}^{M-1}\|r_h^{n+\frac{1}{2}}\|^2 + \frac{\tilde{C}T}{\gamma}. \quad (4.3.29)$$

49

The discrete Gronwall inequality finishes the proof. □

### 4.3.1 Penalty Method Formulation

We now show that Algorithm 4.1.1 using the SV elements is equivalent to a dual penalty method with the TH elements $(P_k, \{0\})$. The penalty method is

**Algorithm 4.3.1.** *Given a time step $\Delta t > 0$, finite end time $T := M\Delta t$, and initial velocity $u_h^0 \in V_h$, find $w_h^0 \in W_h$ and $\lambda_h^0 \in Q_h$ satisfying $\forall (\chi_h, r_h) \in (W_h, Q_h)$*

$$
\begin{align}
(w_h^0, \chi_h) + (\lambda_h^0, \nabla \cdot \chi_h) &= (\nabla \times u_h^0, \chi_h), \tag{4.3.30}\\
(\nabla \cdot w_h^0, r_h) &= 0. \tag{4.3.31}
\end{align}
$$

*Then for $n = 0, 1, 2, ..., M-1$, find $(u_h^{n+1}, w_h^{n+1}, P_h^{n+1}, \lambda_h^{n+1}) \in (X_h, W_h, Q_h, Q_h)$ satisfying $\forall (v_h, \chi_h, q_h, r_h) \in (X_h, W_h, Q_h, Q_h)$*

$$
\begin{align}
(\frac{u_h^{n+1} - u_h^n}{\Delta t}, v_h) - (P_h^{n+1}, \nabla \cdot v_h) & \notag \\
+ (w_h^{n+\frac{1}{2}} \times u_h^{n+\frac{1}{2}}, v_h) + \nu(\nabla u_h^{n+\frac{1}{2}}, \nabla v_h) &= (f(t^{n+\frac{1}{2}}), v_h) \tag{4.3.32}\\
(\nabla \cdot u_h^{n+\frac{1}{2}}, q_h) + \varepsilon(P_h^{n+1}, q_h) &= 0 \tag{4.3.33}\\
(w_h^{n+\frac{1}{2}}, \chi_h) - (\lambda_h^{n+1}, \nabla \cdot \chi_h) &= (\nabla \times u_h^{n+1}, \chi_h) \tag{4.3.34}\\
(\nabla \cdot w_h^{n+\frac{1}{2}}, r_h) + \varepsilon(\lambda_h^{n+1}, r_h) &= 0. \tag{4.3.35}
\end{align}
$$

Now choosing $q_h = \nabla \cdot v_h$ and $r_h = \nabla \cdot \chi_h$ in (4.3.33) and (4.3.35) respectively then rearranging gives

$$
\begin{align}
\varepsilon^{-1}(\nabla \cdot u_h^{n+\frac{1}{2}}, \nabla \cdot v_h) &= -(P_h^{n+1}, \nabla \cdot v_h) \tag{4.3.36}\\
\varepsilon^{-1}(\nabla \cdot w_h^{n+\frac{1}{2}}, \nabla \cdot \chi_h) &= -(\lambda_h^{n+1}, \nabla \cdot \chi_h) \tag{4.3.37}
\end{align}
$$

Substituting (4.3.35) and (4.3.37) into (4.1.3) and (4.1.5) respectively gives

$$
\begin{align}
(\frac{u_h^{n+1} - u_h^n}{\Delta t}, v_h) + \varepsilon^{-1}(\nabla \cdot u_h^{n+1}, \nabla \cdot v_h) & \notag \\
+ (w_h^{n+\frac{1}{2}} \times u_h^{n+\frac{1}{2}}, v_h) + \nu(\nabla u_h^{n+\frac{1}{2}}, \nabla v_h) &= (f(t^{n+\frac{1}{2}}), v_h) \tag{4.3.38}\\
(w_h^{n+\frac{1}{2}}, \chi_h) + \varepsilon^{-1}(\nabla \cdot w_h^{n+\frac{1}{2}}, \nabla \cdot \chi_h) &= (\nabla \times u_h^{n+\frac{1}{2}}, \chi_h); \tag{4.3.39}
\end{align}
$$

$$
\tag{4.3.40}
$$

50

which is identical to the scheme for the stabilized $(P_k, \{0\})$ element pair, with the identification of $\gamma = \epsilon^{-1}$.

## 4.4    Numerical Experiments

In this section we present two numerical experiments. This first is a verification of predicted convergence rates, and the second is a simulation of channel flow over a 3d forward-backward step. All computations were performed in MATLAB. Linear solves were performed using 'backslash', which is very efficient when using the penalty method formulation of the discrete problem.

### 4.4.1    Numerical Test 1: Convergence rate verification

To verify convergence rates predicted in Section 3, we compute approximations to to the model problem with solution

$$
\begin{align}
u_1 &= \cos(2\pi z)(1 + 0.01t) \tag{4.4.1}\\
u_2 &= \sin(2\pi z)(1 + 0.01t) \tag{4.4.2}\\
u_3 &= \sin(2\pi z)(1 + 0.01t) \tag{4.4.3}\\
p &= \sin(2\pi(x + y + z)). \tag{4.4.4}
\end{align}
$$

from $t = 0$ to $T = 1$, with $\nu = 1$. We use the penalty method with grad-div parameter $\gamma = 10,000$, and compute with $X_h = P_3$, on barycenter refinements of uniform meshes.

Errors and rates are shown in Tables 4.1 and 4.2, for successively finer meshes and reduced timesteps. Optimal rates are observed for velocity and vorticity in the indicated norms, verifying the results of Section 3. We note that on the finest mesh, (decoupled) linear solves averaged 66 seconds on a 2 x 2.66 GHz Quad-Core Intel Xeon processor with 12 GB 1066 MhZ DDR3 memory, and 21 seconds on the second finest mesh, and 60 seconds on the finest one. Each nonlinear solve required between 3 and 4 iterations, and thus between 6 and 8 (reduced) linear solves for each of velocity and vorticity.

### 4.4.2    3 dimensional channel flow over a forward-backward step

We now present results for time dependent 3d channel flow over a forward-backward facing step with $Re = 200$. A diagram of the flow domain is given in Figure 4.1. The flow we study is an altered version of the flow studied in [32], but with a different treatment of boundary conditions.

| $h$ | $\Delta t$ | $\dim(X_h)$ | Total dof | $\|\|u - u_h\|\|_{L^\infty(L^2)}$ | rate | $\|\|u - u_h\|\|_{L^2(H^1)}$ | rate |
|------|------|------|------|------|------|------|------|
| 1/2 | T | 3,189 | 10,218 | 4.134e-2 | | 9.025e-1 | |
| 1/4 | T/3 | 23,871 | 78,462 | 2.761e-3 | 3.90 | 1.041e-1 | 3.12 |
| 1/6 | T/6 | 78,987 | 261,654 | 5.6274e-4 | 3.92 | 3.013e-2 | 3.00 |
| 1/8 | T/9 | 185,115 | 615,990 | 1.794e-4 | 3.97 | 1.298e-2 | 3.01 |
| 1/10 | T/18 | 359,373 | 1,198,746 | 7.374e-5 | 3.98 | 6.593e-3 | 3.04 |

Table 4.1: The errors and rates for the velocity solution in numerical experiment 1. Rates appear optimal. The 'Total dof' column shows the total degrees of freedom required if SV elements were used.

| $h$ | $\Delta t$ | $\|\|w - w_h\|\|_{L^2(L^2)}$ | rate | $\|\|\nabla \cdot u_h\|\|_{L^\infty(L^2)}$ | $\|\|\nabla \cdot w_h\|\|_{L^\infty(L^2)}$ |
|------|------|------|------|------|------|
| 1/2 | T | 5.445e-1 | | 1.8631e-4 | 3.778e-6 |
| 1/4 | T/3 | 6.186e-2 | 3.14 | 2.283e-5 | 1.687e-7 |
| 1/6 | T/6 | 1.675e-2 | 3.22 | 2.121e-5 | 2.797e-8 |
| 1/8 | T/9 | 7.085e-3 | 2.99 | 4.226e-5 | 8.077e-9 |
| 1/10 | T/18 | 3.453e-3 | 3.22 | 4.214e-5 | 3.235e-9 |

Table 4.2: The errors and rates for the vorticity in numerical experiment 1, as well as the errors in the velocity and vorticity divergences.

First, we choose no-slip boundaries for the channel walls. For the inflow conditions, [32] uses the constant inflow profile $u_{in} =< 0, 1, 0 >$, which is both nonphysical and not appropriate for a velocity-vorticity method since vorticity at the inflow edges will approach infinity as the meshwidth decreases. Thus, instead, we treat the problem as an infinite channel and enforce $u_{in} = u_{out}$, and taking the initial condition to be the steady $Re = 50$ solution.

We use $X_h = P_3$, and compute on a barycenter refined tetrahedral mesh, which provides 1,282,920 total degrees of freedom for the full SV discretization, 398,001 of which form the velocity space. The system is solved with the penalty method described above with $\gamma = 10,000$. A timestep of $\Delta t = 0.025$ is used, and we compute to $T = 10$. Visualizations of the solution are shown in Figures 4.2 and 4.3, and the correct physical behavior is realized - an eddy detaches from the step and moves down the channel, and a new eddy forms.
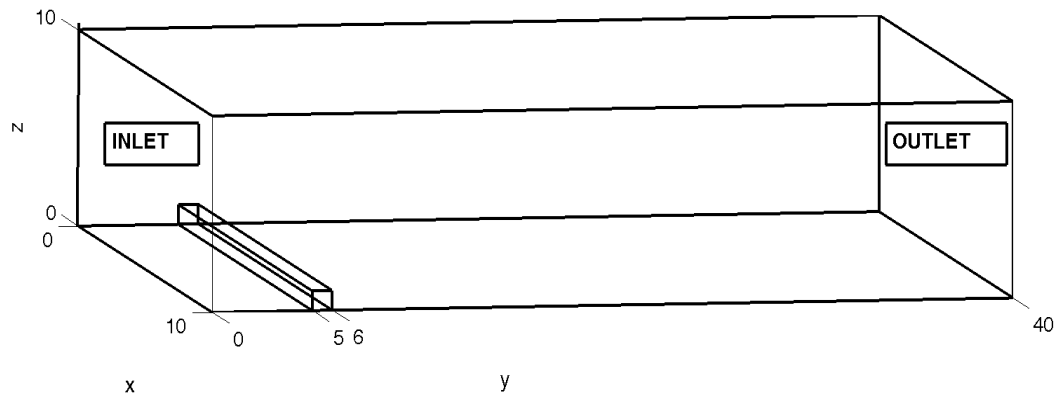
Figure 4.1: Shown above is domain for the 3d channel flow over a step problem.



Figure 4.2: Shown above is the $x = 5$ sliceplane of speed contours and velocity streamlines at $T = 10$. An eddy can be observed to have moved down the channel, and a second eddy has formed behind the step.

Figure 4.3: Shown above is a plot of the same velocity field as in Figure 4.2, but zoomed in near the step. Streamribbons are used to visualize the flow, and more clearly show the eddies.

# Chapter 5

# Convergence Rate of Grad-div Stabilized TH solutions to SV solutions

## 5.1 Order of convergence for NSE approximations

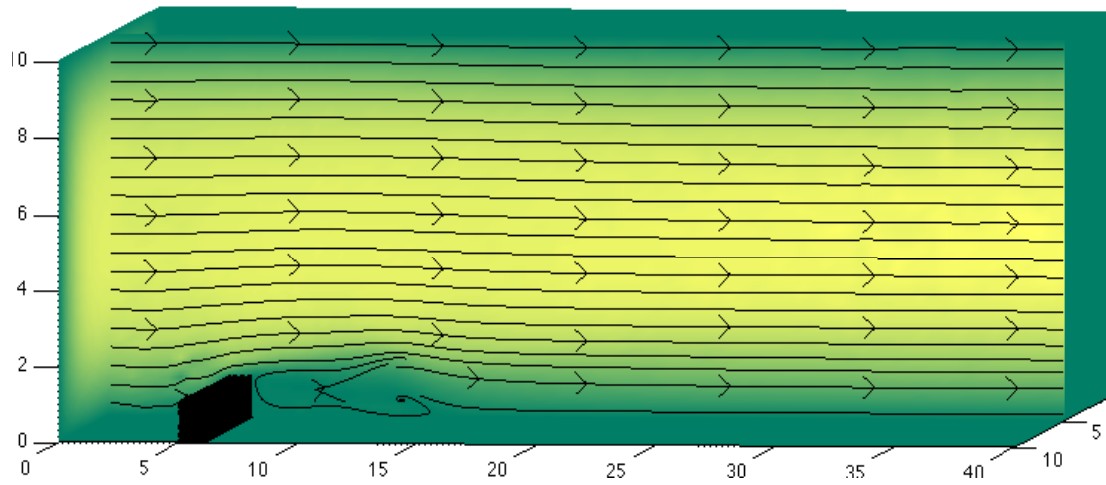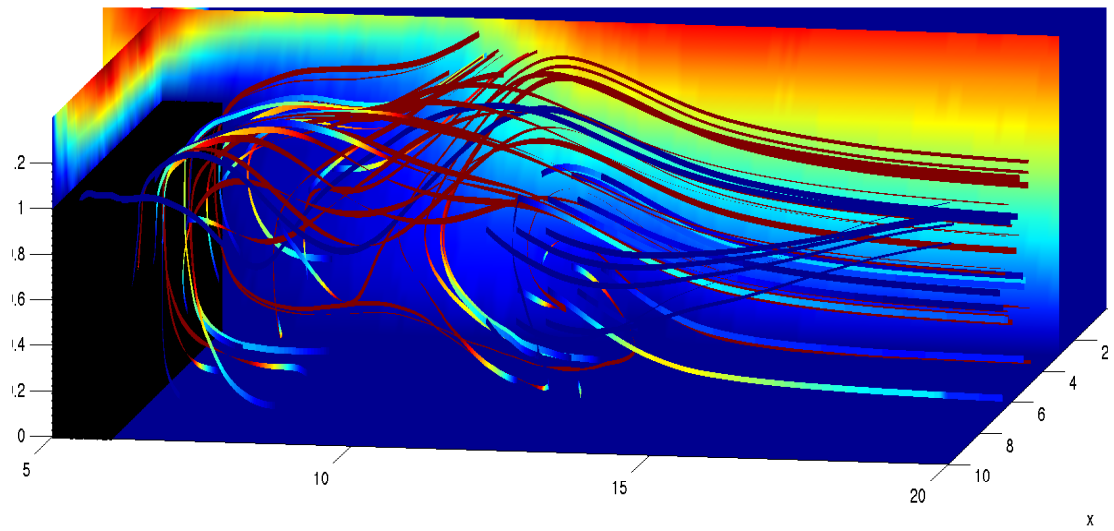We consider the rate of convergence of finite element approximations of the NSE using grad-div stabilized TH formulations to the solution of SV elements, as the grad-div stabilization parameter $\gamma$ tends to zero. We show first for the steady case, then for the time-dependent case, that the rate is $O(\gamma^{-1})$.

### 5.1.1 The steady NSE case

Consider the discrete steady convective NSE formulation: Find $(u_h, p_h) \in (X_h, P_h)$ such that $\forall (v_h, q_h) \in (X_h, P_h)$, where $P_h = Q_h$ (TH) or $\widetilde{Q_h}$ (SV),

$$b^*(u_h, u_h, v_h) - (p_h, \nabla \cdot v_h) + \nu(\nabla u_h, \nabla v_h) + \gamma(\nabla \cdot u_h, \nabla \cdot v_h) = (f, v_h) \qquad (5.1.1)$$

$$(\nabla \cdot u_h, q_h) = 0. \qquad (5.1.2)$$

We note that for the case of SV elements, the grad-div term trivially vanishes.

Define $\alpha := 1 - C_s \nu^{-2} \|f\|_{-1}$. The formulation (5.1.1)-(5.1.2) is known to be well-posed under the small data condition $\alpha > 0$ [37], for either element choice, due to assumptions on the

mesh and polynomial degree.

**Lemma 5.1.1.** *Solutions to* (5.1.1)-(5.1.2) *exist and satisfy*

$$\nu\|\nabla u_h\|^2 + 2\gamma\|\nabla \cdot u_h\|^2 \quad \leq \quad \nu^{-1}\|f\|_{-1}^2 \tag{5.1.3}$$

$$\text{If } P_h = Q_h\text{: } \|p_h - \gamma(\nabla \cdot u_h)\| \quad \leq \quad \|f\|_{-1}\left(1 + C_s\nu^{-2}\|f\| + \nu^{-1}\right) \tag{5.1.4}$$

$$\text{If } P_h = \widetilde{Q_h}\text{: } \|p_h\| \quad \leq \quad \|f\|_{-1}\left(1 + C_s\nu^{-2}\|f\| + \nu^{-1}\right) \tag{5.1.5}$$

*If $\alpha > 0$, then solutions are unique.*

*Proof.* Taking $v_h = u_h$ in (5.1.1) and using Cauchy-Schwarz and Young's inequalities gives (5.1.3). The pressure bounds follow directly from the discrete LBB condition and the bound (5.1.3). The SV pressure bound does not include the term with $\gamma$ since the grad-div term is trivially zero in this case. $\qquad \square$

**Remark 5.1.1.** *We consider limiting behavior as $\gamma \to \infty$, and thus the bound* (5.1.4) *seems insufficient to guarantee stability of the pressure in the limit. However, the following theorem implies that $\|\nabla \cdot u_h\| \leq \frac{C}{\gamma}$, and the TH pressure solution is indeed bounded by a data-dependent constant, independent of $\gamma$.*

**Theorem 5.1.1.** *On a fixed mesh and with data satisfying $\alpha > 0$, the TH velocity solutions to* (5.1.1)-(5.1.2) *converge to the SV velocity solution with convergence order $\gamma^{-1}$ in the energy norm, as $\gamma \to \infty$; that is, if $u_h$ is the TH solution and $u_h^0$ is the SV solution, then*

$$\|\nabla(u_h - u_h^0)\| \leq \frac{C}{\gamma}.$$

*Proof.* Let $(u_h^0, p_h^0) \in (V_h^0, \widetilde{Q_h})$ denote the solution of (5.1.1)-(5.1.2) using SV elements, $(u_h, p_h) \in (V_h, Q_h)$ for the TH solution, and the difference between them to be $r_h \in V_h$, so that

$$u_h = u_h^0 + r_h.$$

For the TH solution $u_h$, setting $v_h = w_h^0 \in V_h^0$ and $s_h \in R_h$, respectively, in (5.1.1) gives the equations

$$b^*(u_h, u_h, w_h^0) + \nu(\nabla u_h, \nabla w_h^0) \quad = \quad (f, w_h^0), \tag{5.1.6}$$

$$b^*(u_h, u_h, s_h) + \nu(\nabla u_h, \nabla s_h) + \gamma(\nabla \cdot u_h, \nabla \cdot s_h) \quad = \quad (f, s_h). \tag{5.1.7}$$

56

Similarly, the SV solution $u_h^0 \in V_h^0$ satisfies

$$b^*(u_h^0, u_h^0, w_h^0) + \nu(\nabla u_h^0, \nabla w_h^0) = (f, w_h^0), \tag{5.1.8}$$

$$b^*(u_h^0, u_h^0, s_h) - (p_h^0, \nabla \cdot s_h) = (f, s_h). \tag{5.1.9}$$

From (5.1.7) and (5.1.9), we have

$$b^*(u_h, u_h, s_h) + \nu(\nabla u_h, \nabla s_h) + \gamma(\nabla \cdot u_h, \nabla \cdot s_h) = b^*(u_h^0, u_h^0, s_h) - (p_h^0, \nabla \cdot s_h), \tag{5.1.10}$$

and since $(\nabla u_h, \nabla s_h) = (\nabla r_h, \nabla s_h)$ and $\nabla \cdot u_h = \nabla \cdot r_h$,

$$\nu(\nabla r_h, \nabla s_h) + \gamma(\nabla \cdot r_h, \nabla \cdot s_h) = b^*(u_h^0, u_h^0, s_h) - b^*(u_h, u_h, s_h) - (p_h^0, \nabla \cdot s_h)$$

$$= -b^*(r_h, u_h^0, s_h) - b^*(u_h, r_h, s_h) - (p_h^0, \nabla \cdot s_h). \tag{5.1.11}$$

Orthogonally decompose $r_h =: r_h^0 + r_h'$, where $r_h^0 \in V_h^0$ and $r_h' \in r_h$. Now setting $v_h = r_h'$ in (5.1.11) gives, after reducing with orthogonality properties and using Lemma 2.0.9,

$$\nu\|\nabla r_h'\|^2 + \gamma\|\nabla \cdot r_h'\|^2 = -b^*(r_h, u_h, r_h') - b^*(u_h^0, r_h, r_h') - (p_h^0, \nabla \cdot r_h')$$

$$\leq C\left(M\|\nabla r_h\|\|\nabla u_h^0\| + M\|\nabla r_h\|\|\nabla u_h\| + \|p_h^0\|\right)\|\nabla \cdot r_h'\| \tag{5.1.12}$$

Since $u_h$, $u_h^0$ are uniformly bounded by the data by (5.1.3), independent of $\gamma$, $r_h$ is also. Using this and (5.1.5) provides

$$\nu\|\nabla r_h'\|^2 + \gamma\|\nabla \cdot r_h'\|^2 \leq C\|\nabla \cdot r_h'\|. \tag{5.1.13}$$

Dropping the first term on the left and dividing by $\|\nabla \cdot r_h'\|$ gives

$$\|\nabla \cdot r_h'\| \leq \frac{C}{\gamma}, \tag{5.1.14}$$

which implies from Lemma 2.0.9 that

$$\|\nabla r_h'\| \leq \frac{C}{\gamma}. \tag{5.1.15}$$

It remains to bound $\|\nabla r_h^0\|$. From (5.1.6), (5.1.8), and taking $w_h^0 = r_h^0$, we get

$$b^*(u_h, u_h, r_h^0) + \nu(\nabla u_h, \nabla r_h^0) = b^*(u_h^0, u_h^0, r_h^0) + \nu(\nabla u_h^0, \nabla r_h^0), \qquad (5.1.16)$$

which reduces to

$$\begin{aligned}
\nu(\nabla r_h, \nabla r_h^0) &= b^*(u_h^0, u_h^0, r_h^0) - b^*(u_h, u_h, r_h^0), \\
&= -b^*(u_h, r_h, r_h^0) - b^*(r_h, u_h^0, r_h^0). \qquad (5.1.17)
\end{aligned}$$

Skew symmetry properties and decomposing $r_h$ gives

$$\nu\|\nabla r_h^0\|^2 = -b^*(u_h, r_h', r_h^0) - b^*(r_h^0, u_h^0, r_h^0) - b^*(r_h', u_h^0, r_h^0). \qquad (5.1.18)$$

Standard inequalities and (5.1.3) now provides

$$\nu\|\nabla r_h^0\|^2 \leq C\|\nabla r_h'\|\|\nabla r_h^0\| + C_s\nu^{-1}\|f\|_{-1}\|\nabla r_h^0\|^2. \qquad (5.1.19)$$

Using the small data condition, then dividing through by $\|\nabla r_h^0\|$ gives

$$\|\nabla r_h^0\| \leq C\|\nabla r_h'\| \leq \frac{C}{\gamma}. \qquad (5.1.20)$$

The triangle inequality completes the proof, as

$$\|\nabla(u_h - u_h^0)\| = \|\nabla r_h\| \leq \|\nabla r_h^0\| + \|\nabla r_h'\| \leq \frac{C}{\gamma}. \qquad (5.1.21)$$

$$\square$$

**Lemma 5.1.2.** *If $p_h$ is the TH pressure and $p_h^0$ is the SV pressure then*

$$\|p_h^0 - (p_h - \gamma\nabla \cdot u_h)\| \leq \tfrac{C}{\gamma}.$$

*Proof.* The TH and SV solutions to (5.1.1)-(5.1.2) satisfy respectively

$$\begin{aligned}
b^*(u_h, u_h, v_h) - (p_h, \nabla \cdot v_h) + \nu(\nabla u_h, \nabla v_h) + \gamma(\nabla \cdot u_h, \nabla \cdot v_h) &= (f, v_h), \qquad (5.1.22) \\
b^*(u_h^0, u_h^0, v_h) - (p_h^0, \nabla \cdot v_h) + \nu(\nabla u_h^0, \nabla v_h) &= (f, v_h). \qquad (5.1.23)
\end{aligned}$$

58

Subtracting (5.1.23) from (5.1.22) and rearranging gives

$$(p_h^0 - (p_h - \gamma \nabla \cdot u_h), \nabla \cdot v_h) = b^*(u_h^0, u_h^0 - u_h, v_h) \quad + \quad b^*(u_h^0 - u_h, u_h, v_h)$$
$$+ \quad \nu(\nabla(u_h^0 - u_h), v_h). \qquad (5.1.24)$$

From Lemma 2.0.2, Theorem 5.1.1 and bounds on solutions it follows that

$$(p_h^0 - (p_h - \gamma \nabla \cdot u_h), \nabla \cdot v_h) \leq \frac{C}{\gamma} \|\nabla v_h\|. \qquad (5.1.25)$$

Dividing (5.1.25) by $\|\nabla v_h\|$ and the LBB condition (of the SV element) finishes the proof. □

## 5.1.2 The time-dependent case for the NSE

For the time-dependent case, we find an analogous result to the steady case. We consider the semi-discrete formulation, and extension to the usual temporal discretizations such as backward Euler and Crank-Nicolson is straight-forward, although technical. Thus we proceed to study the following problems: Given $u_h(0) \in V_h^0$, find $(u_h(t), p_h(t)) \in (X_h, P_h) \times (0, T]$ such that $\forall (v_h, q_h) \in (X_h, P_h)$, where $P_h = Q_h$ (TH) or $\widetilde{Q_h}$ (SV),

$$((u_h)_t, v_h) + b^*(u_h, u_h, v_h) - (p_h, \nabla \cdot v_h) + \nu(\nabla u_h, \nabla v_h)$$
$$+\gamma(\nabla \cdot u_h, \nabla \cdot v_h) \quad = \quad (f, v_h) \qquad (5.1.26)$$
$$(\nabla \cdot u_h, q_h) \quad = \quad 0. \qquad (5.1.27)$$

It is straight-forward to show (e.g. [37]) that this formulation admits unique solutions satisfying for $0 \leq t \leq T$,

$$\|u_h(t)\|^2 + \nu \int_0^t \|\nabla u_h(s)\|^2 \, ds + \gamma \int_0^t \|\nabla \cdot u_h(s)\|^2 \, ds \quad \leq \quad C(data), \qquad (5.1.28)$$
$$\text{If } P_h = Q_h \colon \|p_h\| \quad \leq \quad (1+\gamma) \cdot C(data), \qquad (5.1.29)$$
$$\text{If } P_h = \widetilde{Q_h} \colon \|p_h\| \quad \leq \quad C(data). \qquad (5.1.30)$$

**Remark 5.1.2.** *For the fully discrete case, there is a restriction that the time-step be small enough to get uniqueness; otherwise an analogous result holds.*

**Remark 5.1.3.** *With the following theorem, the bound (5.1.29) can be improved to be independent of $\gamma$.*

**Theorem 5.1.2.** *On a fixed mesh, the TH velocity solutions to* (5.1.26)-(5.1.27) *converge to the SV solution with convergence order* $\gamma^{-1}$ *in the energy norm, as* $\gamma \to \infty$. *That is, if* $u_h$ *is the TH solution and* $u_h^0$ *is the SV solution, then*

$$\|u_h - u_h^0\|_{L^2(0,T;H^1(\Omega))} \leq \frac{C}{\gamma}.$$

**Remark 5.1.4.** *The stability estimate* (5.1.28) *suggests the rate may be only* $\gamma^{-1/2}$ *since the SV solution is pointwise divergence-free, but the theorem proves it is indeed faster.*

*Proof.* Our strategy for this proof is similar to that of the steady case. Let $(u_h^0, p_h^0) \in (V_h^0, \widetilde{Q_h}) \times [0, T]$ denote the solution of (5.1.26)-(5.1.27) using SV elements, $(u_h, p_h) \in (V_h, Q_h) \times [0, T]$ for the TH solution, and the difference between them to be $r_h \in V_h \times [0, T]$, so that

$$u_h(t) = u_h^0(t) + r_h(t).$$

Again we orthogonally decompose $r_h(t) = r_h'(t) + r_h^0(t)$, where $r_h'(t) \in r_h$ and $r_h^0(t) \in V_h^0$; recall $V_h = V_h^0 \oplus R_h$ in the $X_h$ inner product.

Consider (5.1.26) with an arbitrary test function $s_h \in R_h \subset V_h$. The TH and SV solutions satisfy, respectively,

$$((u_h)_t, s_h) + b^*(u_h, u_h, s_h) + \nu(\nabla u_h, \nabla s_h) + \gamma(\nabla \cdot u_h, \nabla \cdot s_h) = (f, s_h), \quad (5.1.31)$$

$$((u_h^0)_t, s_h) + b^*(u_h^0, u_h^0, s_h) - (p_h^0, \nabla \cdot s_h) + \nu(\nabla u_h^0, \nabla s_h) = (f, s_h). \quad (5.1.32)$$

Subtracting and utilizing the following identities

$$\nabla \cdot u_h = \nabla \cdot r_h = \nabla \cdot r_h' \quad (5.1.33)$$

$$(\nabla r_h, \nabla s_h) = (\nabla r_h', \nabla s_h). \quad (5.1.34)$$

provides the equation

$$((r_h)_t, s_h) + \nu(\nabla r_h', \nabla s_h) + \gamma(\nabla \cdot r_h', \nabla \cdot s_h) = -b^*(r_h, u_h^0, s_h) - b^*(u_h, r_h, s_h) - (p_h^0, \nabla \cdot s_h).$$

Taking $s_h = r_h'$, then reducing with Lemmas 2.0.2 and 2.0.9, and (5.1.28) and (5.1.30) yields

$$
\begin{aligned}
((r_h)_t, r_h') &+ \nu\|\nabla r_h'\|^2 + \gamma\|\nabla \cdot r_h'\|^2 \\
&= -b^*(r_h, u_h^0, r_h') - b^*(u_h, r_h^0, r_h') - (p_h^0, \nabla \cdot r_h') \\
&\leq C_s\|\nabla r_h\|\|\nabla u_h^0\|\|\nabla r_h'\| + C_s\|\nabla u_h\|\|\nabla r_h^0\|\|\nabla r_h'\| + \|p_h^0\|\|\nabla \cdot r_h'\| \\
&\leq C_s\|\nabla r_h\|\|\nabla u_h^0\|M\|\nabla \cdot r_h'\| + C_s\|\nabla u_h\|\|\nabla r_h^0\|M\|\nabla \cdot r_h'\| + \|p_h^0\|\|\nabla \cdot r_h'\| \\
&\leq \left(C_s M\|\nabla r_h\|\|\nabla u_h^0\| + C_s M\|\nabla u_h\|\|\nabla r_h^0\| + \|p_h^0\|\right)\|\nabla \cdot r_h'\| \\
&\leq C\|\nabla \cdot r_h'\|. &\text{(5.1.35)}
\end{aligned}
$$

We now bound $r_h^0$. Consider (5.1.26) with an arbitrary test function $w_h^0 \in V_h^0$. The TH and SV solutions satisfy, respectively,

$$
((u_h)_t, w_h^0) + b^*(u_h, u_h, w_h^0) + \nu(\nabla u_h, \nabla w_h^0) = (f, w_h^0), \tag{5.1.36}
$$

$$
((u_h^0)_t, w_h^0) + b^*(u_h^0, u_h^0, w_h^0) + \nu(\nabla u_h^0, \nabla w_h^0) = (f, w_h^0). \tag{5.1.37}
$$

Subtracting gives

$$
((r_h)_t, w_h^0) + \nu(\nabla r_h, \nabla w_h^0) = -b^*(u_h, u_h, w_h^0) + b^*(u_h^0, u_h^0, w_h^0), \tag{5.1.38}
$$

which reduces to

$$
((r_h)_t, w_h^0) + \nu(\nabla r_h^0, \nabla w_h^0) = -b^*(r_h, u_h, w_h^0) - b^*(u_h^0, r_h, w_h^0). \tag{5.1.39}
$$

Taking $w_h^0 = r_h^0$ gives

$$
((r_h)_t, r_h^0) + \nu\|\nabla r_h^0\|^2 = -b^*(r_h, u_h, r_h^0) - b^*(u_h^0, r_h, r_h^0) \tag{5.1.40}
$$

$$
= -b^*(r_h^0, u_h, r_h^0) - b^*(r_h', u_h, r_h^0) - b^*(u_h^0, r_h', r_h^0) \tag{5.1.41}
$$

Using lemmas 2.0.2 and 2.0.9, and the uniform bound on solutions yields

$$
\begin{aligned}
((r_h)_t, r_h^0) &+ \nu\|\nabla r_h^0\|^2 \\
&\leq C_s\|\nabla r_h^0\|^{3/2}\|\nabla u_h\|\|r_h^0\|^{1/2} + C_s\|\nabla r_h'\|\|\nabla u_h\|\|\nabla r_h^0\| + C_s\|\nabla r_h'\|\|\nabla u_h^0\|\|\nabla r_h^0\| \\
&\leq C_s\|\nabla r_h^0\|^{3/2}\|\nabla u_h\|\|r_h^0\|^{1/2} + C\|\nabla \cdot r_h'\|. &\text{(5.1.42)}
\end{aligned}
$$

Adding (5.1.35) to (5.1.42) gives

$$((r_h)_t, r_h^0) + ((r_h)_t, r_h') + \nu\|\nabla r_h^0\|^2 + \nu\|\nabla r_h'\|^2 + \gamma\|\nabla \cdot r_h'\|^2$$
$$\leq C_s\|\nabla r_h^0\|^{3/2}\|\nabla u_h\|\|r_h^0\|^{1/2} + (C + \|p_h^0\|)\|\nabla \cdot r_h'\|, \quad (5.1.43)$$

which reduces with orthogonality properties, the uniform bounds on solutions, then standard inequalities to

$$\frac{1}{2}\frac{d}{dt}\|r_h\|^2 + \nu\|\nabla r_h\|^2 + \gamma\|\nabla \cdot r_h'\|^2$$
$$\leq \quad C_s\|\nabla r_h^0\|^{3/2}\|\nabla u_h\|\|r_h^0\|^{1/2} + C\|\nabla \cdot r_h'\|$$
$$\leq \quad C\|r_h\|^2 + \nu\|\nabla r_h\|^2 + \frac{C}{2\gamma} + \frac{\gamma}{2}\|\nabla \cdot r_h'\|^2. \quad (5.1.44)$$

This leaves

$$\frac{d}{dt}\|r_h\|^2 + \gamma\|\nabla \cdot r_h'\|^2 \leq C\|r_h\|^2 + \frac{C}{\gamma}. \quad (5.1.45)$$

The Gronwall inequality, $u_h(0) = u_h^0(0)$, and reducing gives us

$$\int_0^t \|\nabla \cdot r_h'\|^2 \, dt \leq \frac{C}{\gamma^2}, \quad (5.1.46)$$

which proves the theorem. $\qquad\square$

## 5.2 Extension to turbulence models

Recent work on finite element methods for the '$\alpha$ models' of fluid flow has proven their effectiveness at finding accurate solutions to flow problems on coarser spatial and temporal discretizations than are necessary for successful simulations of the NSE [43, 44, 52, 6, 66, 50, 12, 11, 28]. We prove the convergence result for grad-div stabilized TH solutions to SV solutions of the Leray-$\alpha$ model; analogous results / proofs for the other $\alpha$ models follow similarly. Since a goal of the $\alpha$-models is to find solutions on coarser meshes than would be used for the NSE, mass conservation of solutions can be very poor and thus large grad-div stabilization that preserves overall accuracy and improves the mass conservation will help to provide more physically relevant solutions.

The continuous Leray-$\alpha$ model formulation is: find $(u_h, p_h, w_h, \lambda_h) \in (X_h, P_h, X_h, P_h)$ such

that $\forall (v_h, q_h, \chi_h, \psi_h) \in (X_h, P_h, X_h, P_h)$, where $P_h = Q_h$ (TH) or $Q_h^{SV}$ (SV),

$$
\begin{aligned}
((u_h)_t, v_h) + b^*(w_h, u_h, v_h) - (p_h, \nabla \cdot v_h) + \nu(\nabla u_h, \nabla v_h) \qquad\qquad\qquad & \\
+\gamma(\nabla \cdot u_h, \nabla \cdot v_h) &= (f, v_h), & \text{(5.2.1)} \\
(\nabla \cdot u_h, q_h) &= 0, & \text{(5.2.2)} \\
(w_h, \chi_h) + \alpha^2(\nabla w_h, \nabla \chi_h) + (\lambda_h, \nabla \cdot \chi_h) + \gamma(\nabla \cdot w_h, \nabla \cdot \chi_h) &= (u_h, \chi_h), & \text{(5.2.3)} \\
(\nabla \cdot w_h, \psi_h) &= 0. & \text{(5.2.4)}
\end{aligned}
$$

The equations (5.2.3)-(5.2.4) are the discretization of the $\alpha$-filter, with discrete incompressiblity enforced. Advantages of using this discretization for the filter instead of the usual one are discussed in [6].

The following lemma will be useful for the analysis in this section.

**Lemma 5.2.1.** *If $(u_h, p_h, w_h, \lambda_h)$ solves (5.2.1)-(5.2.4) then $\|w_h\| \leq \|u_h\|$.*

*Proof.* The lemma can be verified quickly by choosing $\chi_h = w_h$ in (5.2.3) and using the Cauchy-Schwarz inequality. $\qquad\square$

**Theorem 5.2.1.** *On a fixed mesh the grad-div stabilized TH velocity solutions to (5.2.1)-(5.2.4) converge to the SV velocity solution with convergence order $\gamma^{-1}$ in the energy norm, as $\gamma \to \infty$. That is, if we denote the SV velocity solutions as $u_h^0$ and grad-div stabilized TH solution as $u_h$ then*

$$
\|u_h - u_h^0\|_{L^2(0,T;H^1(\Omega))} \leq \frac{C}{\gamma}.
$$

*Proof.* Let $(u_h^0, w_h^0, p_h^0, \lambda_h^0) \in (X_h, X_h, \tilde{Q}_h, \tilde{Q}_h) \times [0,T]$ denote the solution of (5.2.1)-(5.2.4) using SV elements, $(u_h, w_h, p_h, \lambda_h) \in (X_h, X_h, Q_h, Q_h) \times [0,T]$ for the TH solution. Let the difference between $u_h$ and $u_h^0$ be denoted by $r_u$ and the difference between $w_h$ and $w_h^0$ be denoted by $r_w$ so that

$$
\begin{aligned}
u_h(t) &= u_h^0(t) + r_u(t), \text{ and} \\
w_h(t) &= w_h^0(t) + r_w(t).
\end{aligned}
$$

Orthogonally decompose $r_u(t) = r_u'(t) + r_u^0(t)$, where $r_u'(t) \in R_h$ and $r_u^0(t) \in V_h^{SV}$. Similarly, orthogonally decompose $r_w(t) = r_w'(t) + r_w^0(t)$ so that $r_w'(t) \in R_h$ and $r_w^0(t) \in V_h^{SV}$.

Consider (5.2.1) and (5.2.3) with an arbitrary test function $s_h \in R_h \subset V_h$. The TH and SV

solutions satisfy, respectively,

$$((u_h)_t, s_h) + b^*(w_h, u_h, s_h) + \nu(\nabla u_h, \nabla s_h) + \gamma(\nabla \cdot u_h, \nabla \cdot s_h) = (f, s_h) \qquad (5.2.5)$$

$$((u_h^0)_t, s_h) + b^*(w_h^0, u_h^0, s_h) - (p^0, \nabla \cdot s_h) + \nu(\nabla u_h^0, \nabla s_h) = (f, s_h). \qquad (5.2.6)$$

Subtracting using previous identities gives

$$((r_u)_t, s_h) + \nu(\nabla r_u', \nabla s_h) + \gamma(\nabla \cdot r_u', \nabla \cdot s_h) = b^*(w_h^0, u_h^0, s_h) - b^*(w_h, u_h, s_h) - (p_h^0, s_h).$$

Taking $s_h = r_u'$, and reducing with Lemmas 2.0.2, 2.0.9 and 5.2.1, and uniqueness of solutions yields

$$\begin{aligned}
&((r_u)_t, r_u') + \nu\|\nabla r_u'\|^2 + \gamma\|\nabla \cdot r_u'\|^2 \\
&= b^*(w_h^0, u_h^0, r_u') - b^*(w_h, u_h, r_u') - (p_h^0, r_u') \\
&\leq C_s(\|\nabla w_h^0\|\|\nabla u_h^0\|\|\nabla r_u'\| + \|\nabla w_h\|\|\nabla u_h\|\|\nabla r_u'\|) + \|p_h^0\|\|\nabla \cdot r_u'\| \\
&\leq C\|\nabla \cdot r_u'\|. \qquad (5.2.7)
\end{aligned}$$

We now derive a similar bound for $r_w'$. Consider that the TH and SV solutions satisfy the following equations from (5.2.3):

$$(w_h, \chi_h) + \alpha^2(\nabla w_h, \nabla \chi_h) + (\lambda_h, \nabla \cdot \chi_h) + \gamma(\nabla \cdot w_h, \nabla \cdot \chi_h) = (u_h, \chi_h), \qquad (5.2.8)$$

$$(w_h^0, \chi_h) + \alpha^2(\nabla w_h^0, \nabla \chi_h) + (\lambda_h^0, \nabla \cdot \chi_h) = (u_h^0, \chi_h). \qquad (5.2.9)$$

Subtracting, choosing $\chi_h = r_w$, and rearranging gives

$$\|r_w\|^2 + \alpha^2\|\nabla r_w\|^2 + \gamma\|\nabla \cdot r_w'\|^2 = (r_u, r_w) - (\lambda_h^0, \nabla \cdot r_w'). \qquad (5.2.10)$$

The Cauchy-Schwarz inequality and Lemma 2.2 yields

$$\|\nabla \cdot r_w'\| \leq \frac{C}{\gamma}. \qquad (5.2.11)$$

Next we derive a bound for $r_w^0$. To do this we subtract (5.2.9) from (5.2.8) and choose $\chi_h = r_w^0$ which gives

$$(r_w, r_w^0) + \alpha^2\|\nabla r_w^0\|^2 = (r_u, r_w^0). \qquad (5.2.12)$$

64

From here we rearrange using Cauchy-Schwarz and equivalence of norms over finite dimensional Hilbert spaces which gives

$$\|\nabla r_w^0\| \leq C \left( \|\nabla r_u\| + \|\nabla r_w'\| \right). \tag{5.2.13}$$

We proceed similar to the time-dependent NSE case and bound $r_u^0$. Consider (5.2.1) with an arbitrary test function $v_h^{SV} \in V_h^{SV}$. The TH and SV solutions satisfy

$$((u_h)_t, v_h^{SV}) + b^*(w_h, u_h, v_h^{SV}) + \nu(\nabla u_h, \nabla v_h^{SV}) = (f, v_h^{SV}), \tag{5.2.14}$$

$$((u_h^0)_t, v_h^{SV}) + b^*(w_h^0, u_h^0, v_h^{SV}) + \nu(\nabla u_h^0, \nabla v_h^{SV}) = (f, V_h^{SV}). \tag{5.2.15}$$

Subtracting (5.2.15) from (5.2.14) rearranging and choosing $v_h = r_u^0$ gives

$$((r_u)_t, r_u^0) + \nu\|\nabla r_u^0\|^2 \leq |b^*(w_h^0, r_u, r_u^0)| + |b^*(r_w, u_h, r_u^0)|. \tag{5.2.16}$$

To majorize the first trilinear term in (5.2.16) use Lemmas 2.1 and 4.1, bounds on solutions and note that for orthogonal decompositions the triangle inequality is an equality. Lastly, using equivalence of norms gives

$$
\begin{aligned}
|b^*(w_h^0, r_u, r_u^0)| \leq C\|\nabla r_u\|\|\nabla r_u^0\| &\leq C\|\nabla r_u\|\|\nabla r_u^0\| + C\|\nabla r_u\|\|\nabla r_u'\| \\
&\leq C\|\nabla r_u\|^2 \\
&\leq C\|r_u\|^2.
\end{aligned} \tag{5.2.17}
$$

We bound the second trilinear using Lemma 2.1 and uniform bound on solutions. Then we split the $r_w$ term using the triangle inequality and use (5.2.13), which yields

$$
\begin{aligned}
|b^*(r_w, u_h, r_u^0)| &\leq C\|\nabla r_w\|\|\nabla r_u^0\| \\
&\leq C\|\nabla r_w'\|\|\nabla r_u^0\| + C\|\nabla r_w^0\|\|\nabla r_u^0\|.
\end{aligned} \tag{5.2.18}
$$

Adding $C\|\nabla r_w'\|\|\nabla r_u'\|$ and $C\|\nabla r_w^0\|\|\nabla r_u'\|$ to the right hand side of (5.2.18) and using orthogonality gives

$$|b^*(r_w, u_h, r_u^0)| \leq C\|\nabla r_w'\|\|\nabla r_u\| + C\|\nabla r_w^0\|\|\nabla r_u\|. \tag{5.2.19}$$

We majorize the first right hand side term using Lemma 2.2, bounds on solutions and (5.2.11). Additionally, we majorize the second right hand side term using (5.2.13). After we combine like terms we are left with

$$|b^*(r_w, u_h, r_u^0)| \leq \frac{C}{\gamma} + C\|\nabla r_u\|^2. \tag{5.2.20}$$

From equivalence of norms we have that $\|\nabla r_u\| \leq C\|r_u\|$. Therefore,

$$((r_u)_t, r_u^0) + \nu\|\nabla r_u^0\|^2 \quad \leq \quad \frac{C}{\gamma} + C\|r_u\|^2. \tag{5.2.21}$$

Adding (5.2.21) and (5.2.7) gives

$$\frac{d}{dt}\|r_u\|^2 + 2\gamma\|\nabla \cdot r_u'\|^2 \leq C\|r_u\|^2 + \frac{C}{\gamma}. \tag{5.2.22}$$

Analogous to the time-dependent NSE proof using the Gronwall inequality, $u_h(0) = u_h^0(0)$ and reducing finishes the proof. □

## 5.2.1 Numerical Verification for the Leray-$\alpha$ model

To numerically verify the velocity convergence rate shown above we consider the benchmark 2d problem of channel flow over a forward-backward step. The domain $\Omega$ is a 40×10 rectangle with a 1×1 step 5 units into the channel at the bottom. The top and bottom of the channel as well as the step are prescribed with no-slip boundary conditions, and the sides are given the parabolic profile $(y(10 - y)/25, 0)^T$. We use the initial condition $u_0 = (y(10 - y)/25, 0)^T$ inside $\Omega$, choose the viscosity $\nu = 1/600$ and run the test to T=10. The correct physical behavior is for an eddy to form behind the step (at larger $T$, the eddy will move down the channel and a new eddy will form).

A barycenter-refinement of a Delauney triangulation of $\Omega$ is used, which yields a total of 14,467 degrees of freedom for the $(P_2, P_1^{disc})$ SV computations and 9,427 for $(P_2, P_1)$ TH. A Crank-Nicolson time discretization is used with a timestep of $\Delta t = 0.01$. For the TH computations, we use grad-div stabilization parameters $\gamma = \{0, 1, 10, 100, 1,000, 10,000\}$.

Plots of the SV and TH solutions are shown in Figure 5.1, and the correct physical behavior is observed in both; in fact, these solutions are nearly indistinguishable. Plots of the TH solutions with $\gamma > 0$ are also nearly identical and so are omitted. Differences between the TH solutions with varying $\gamma$, and the SV solution are computed in the $H^1$ norm, and are shown (with rates) in Table 5.1; first order convergence is observed, in accordance with our theory. The divergence errors of the

TH solutions are given in Table 5.1, which also display first order convergence. Also of particular interest is that the TH solution with $\gamma = 0$ has very poor mass conservation, even though its plot appears correct.

| $\gamma$ | $\|u_{TH}^\gamma - u_{SV}\|_{H^1}$ | rate | $\|\nabla \cdot u_{TH}^\gamma\|$ |
|---|---|---|---|
| 0 | 2.0360 | - | 1.2466 |
| 1 | 0.1473 | 1.14 | 0.0085 |
| 10 | 0.0311 | 0.68 | 9.836E-4 |
| $10^2$ | 0.0035 | 0.94 | 8.774E-5 |
| $10^3$ | 3.616E-4 | 0.99 | 8.667E-6 |
| $10^4$ | 3.622E-5 | 1.00 | 8.948E-7 |

Table 5.1: Convergence of the grad-div stabilized TH Leray-$\alpha$ solutions toward the SV Leray-$\alpha$ solution, first order as $\gamma \to \infty$.
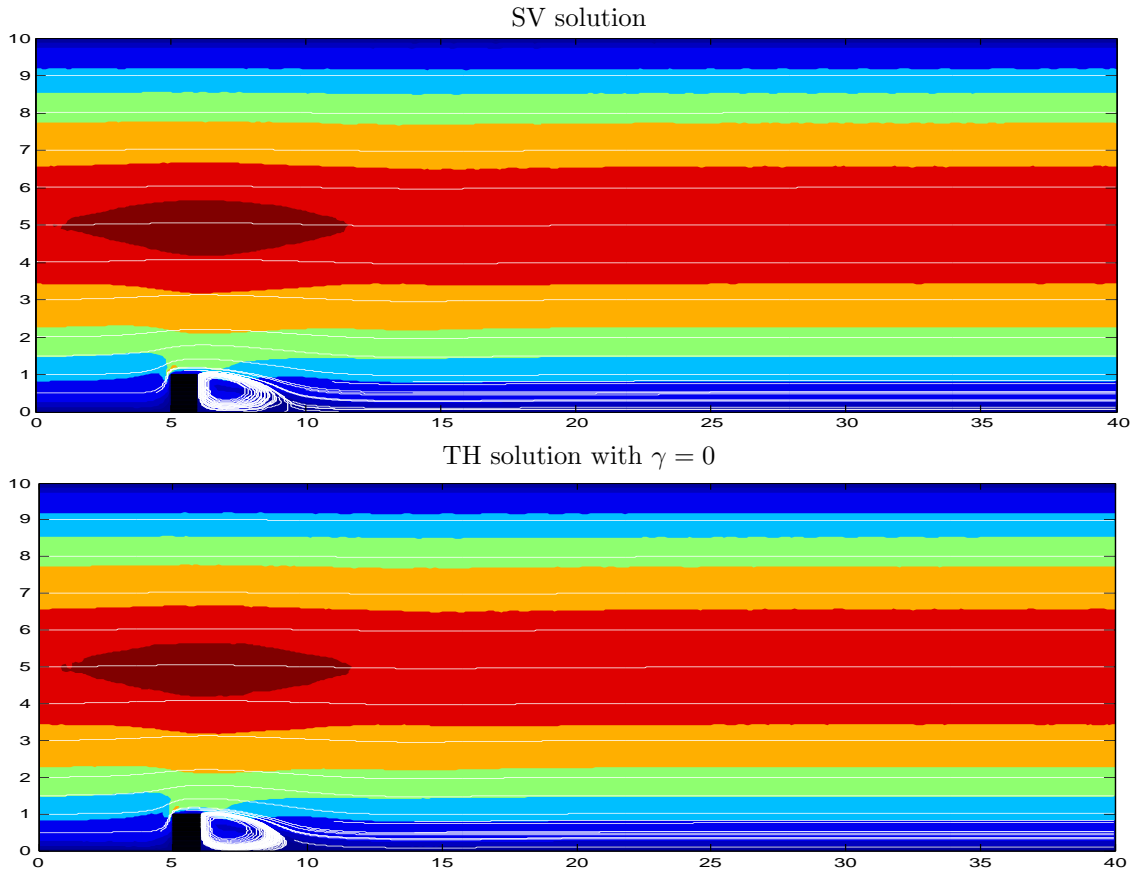


Figure 5.1: SV and TH solutions of the Leray-$\alpha$ model at $t = 10$.

## 5.3 Extension to magnetohydrodynamic flows

To understand a fluid flow which is influenced by a magnetic field one must understand the mutual interaction of a magnetic field and a velocity field. The system of differential equations which describe the flow of an electrically conductive and nonmagnetic incompressible fluid (e.g. liquid sodium) are called magnetohydrodynamics (MHD). These equations are commonly used in metallurgical industries to heat, pump, stir and levitate liquid metals [15].

We consider the steady MHD in the form studied in, e.g., [26, 27], which is the NSE coupled to the pre-Maxwell equations. For simplicity of the analysis, we restrict to homogeneous Dirichlet boundary conditions (or periodic) for both velocity and the magnetic field and consider a convex domain. The Galerkin finite element method that explicitly enforces incompressibility of both the velocity and magnetic fields and with grad-div stabilization of both velocity and magnetic fields is, $\forall (v_h, \chi_h, q_h, \psi_h) \in (X_h, X_h, Q_h, Q_h)$,

$$b^*(u_h, u_h, v_h) + \nu(\nabla u_h, \nabla v_h) - sb^*(B_h, B_h, v_h)$$
$$-(P_h, \nabla \cdot v_h) + \gamma(\nabla \cdot u_h, \nabla \cdot v_h) = (f, v_h) \tag{5.3.1}$$
$$(\nabla \cdot u_h, q_h) = 0 \tag{5.3.2}$$
$$\nu_m(\nabla B_h, \nabla \chi_h) - b^*(B_h, u_h, \chi_h) + b^*(u_h, B_h, \chi_h)$$
$$+(\lambda_h, \nabla \cdot \chi_h) + \gamma(\nabla \cdot B_h, \nabla \cdot \chi_h) = (\nabla \times G, \chi_h) \tag{5.3.3}$$
$$(\nabla \cdot B_h, \psi_h) = 0. \tag{5.3.4}$$

The Lagrange multiplier is added in (5.3.3) so that the divergence of the magnetic field can be explicitly enforced via (5.3.4) without overdetermining the discrete system.

For the choice of $(X_h, Q_h)$ to be Taylor Hood elements, both $\nabla \cdot u_h = 0$ and $\nabla \cdot B_h = 0$ are enforced weakly in (5.3.1)-(5.3.4), but if instead SV elements are chosen then pointwise enforcement is recovered (choose $q_h = \nabla \cdot u_h$ and $\psi_h = \nabla \cdot B_h$). Similar to the NSE case, there is a 'middle ground' of improved mass conservation while using TH elements, if $\gamma$ is chosen "large". Note we consider the stabilization parameters to be equal only for simplicity since we consider their limiting behavior; in practice it may be necessary to choose them differently for optimal accuracy.

**Lemma 5.3.1.** *Solutions to* (5.3.1) - (5.3.4) *exist and satisfy*

$$\|\nabla u_h\| \leq \nu^{-1}\|f\|_{-1} + s^{\frac{-1}{2}} \nu^{\frac{-1}{2}} \nu_m^{\frac{-1}{2}} \|G\| (=: M_1), \tag{5.3.5}$$
$$\|\nabla B_h\| \leq \nu^{\frac{-1}{2}} \nu_m^{\frac{-1}{2}} s^{\frac{-1}{2}} \|f\| + \nu_m^{-1}\|G\| (=: M_2). \tag{5.3.6}$$

If

$$\nu - C_s M_1 - 2s C_s M_2 \quad > \quad 0, \text{ and} \tag{5.3.7}$$

$$\nu_m - C_s M_1 - 2 C_s M_2 \quad > \quad 0 \tag{5.3.8}$$

then solutions are unique.

*Proof.* Existence of solutions is a straight forward application of the Leray-Schauder Theorem. To derive (5.3.5) and (5.3.6) we multiply (5.3.3) by $s$ and add it to (5.3.1). Next we choose $v_h = u_h$ and $\chi_h = B_h$. Noting that $b^*(B_h, B_h, u_h) = -b^*(B_h, u_h, B_h)$ leaves

$$\nu \|\nabla u_h\|^2 + s\nu_m \|\nabla B_h\|^2 \leq (f, u_h) + s(\nabla \times G, B_h). \tag{5.3.9}$$

The bounds can be derived from (5.3.9) by using Young's inequality.

To derive sufficient conditions for uniqueness assume (to get a contradiction) that there are two solutions to (5.3.1)-(5.3.4), $(u_h^1, B_h^1, p_h^1, \lambda_h^1)$ and $(u_h^2, B_h^2, p_h^2, \lambda_h^2)$. Now let $D_u := u_h^1 - u_h^2$ and $D_B := B_h^1 - B_h^2$. Substituting $u_h^1, u_h^2$ into (5.3.1), choosing $v_h = D_u$, subtracting and rearranging gives

$$\begin{aligned}
\nu \|\nabla D_u\|^2 + \gamma \|\nabla \cdot D_u\|^2 \quad &= \quad b^*(u_h^2, u_h^2, D_u) - b^*(u_h^1, u_h^1, D_u) \\
&+ \quad s b^*(B_h^1, B_h^1, D_u) - s b^*(B_h^2, B_h^2, D_u).
\end{aligned} \tag{5.3.10}$$

Using standard inequalities and noting that $b^*(v, u, u) = 0$ we can rewrite (5.3.10) as

$$\begin{aligned}
\nu \|\nabla D_u\|^2 + \gamma \|\nabla \cdot D_u\|^2 \quad &= \quad s b^*(B_h^1, D_B, D_u) + s b^*(D_B, B_h^2, D_u) \\
&- \quad b^*(D_u, u_h^1, D_u).
\end{aligned} \tag{5.3.11}$$

Scaling (5.3.3) by $s$ and similar treatment gives

$$\begin{aligned}
s\nu_m \|D_B\|^2 + s\gamma \|\nabla \cdot D_B\|^2 \quad &= \quad s b^*(B_h^1, D_u, D_B) + s b^*(D_B, u_h^2, D_B) \\
&- \quad s b^*(D_u, B_h^1, D_B).
\end{aligned} \tag{5.3.12}$$

Adding (5.3.11) and (5.3.12) and noting that $b^*(B_h^1, D_u, D_B) = -b^*(B_h^1, D_B, D_u)$, yields

$$
\begin{aligned}
\nu\|D_u\|^2 + s\nu_m\|D_B\|^2 \quad \leq \quad & sb^*(D_B, u_h^2, D_B) - sb^*(D_u, B_h^1, D_B) \\
+ \quad & sb^*(D_B, B_h^2, D_u) - b^*(D_u, u_h^1, D_u). \qquad (5.3.13)
\end{aligned}
$$

Utilizing Lemma 2.1 and Young's inequality we can now rewrite this as

$$
\|\nabla D_u\|^2(\nu - C_s M_1 - 2s C_s M_2) + \|\nabla D_B\|^2 s(\nu_m - C_s M_1 - 2C_s M_2) \leq 0. \qquad (5.3.14)
$$

Uniqueness then follows from (5.3.7) and (5.3.8). $\qquad\qquad\qquad\qquad\qquad\qquad\qquad\square$

### 5.3.1 Convergence of velocity and magnetic field TH solutions to the SV solution for steady MHD

We now extend the results above to the case of steady MHD, formulated by (5.3.1)-(5.3.4). Here there are two grad-div stabilization terms that arise in the analysis, but the main ideas of the proofs for the NSE carry through to this problem as well, although more technical details arise. An extension to time dependent MHD can be performed analogously to how the NSE was extended in Section 3.

**Theorem 5.3.1.** *On a fixed mesh the grad-div stabilized TH velocity and magnetic field solutions to (5.3.1)-(5.3.4) converge to the SV velocity and magnetic field solutions with convergence order $\gamma^{-1}$ in the energy norm, as $\gamma \to \infty$; if $(u_h, B_h)$ is the TH solution and $(u_h^0, B_h^0)$ is the SV solution, then*

$$
\|\nabla(u_h - u_h^0) + \|\nabla(B_h - B_h^0)\| \quad \leq \quad \frac{C}{\gamma}.
$$

*Proof.* Let $(u_h^0, p_h^0, B_h^0, \lambda_h^0) \in (V_h^{SV}, \tilde{Q}_h, V_h^{SV}, \tilde{Q}_h)$ denote the solution of (5.3.1)-(5.3.4) using SV elements, $(u_h, p_h, B_h, \lambda_h) \in (V_h, Q_h, V_h, Q_h)$ for the TH solution. Additionally, denote the difference between the velocity solutions and the magnetic field solutions by $r_u \in V_h$ and $r_B \in V_h$, so that

$$
\begin{aligned}
u_h &= u_h^0 + r_u, \\
B_h &= B_h^0 + r_B.
\end{aligned}
$$

Plugging in the TH and SV solutions into (5.3.1) gives the following equations: $\forall v_h \in V_h$,

$$b^*(u_h, u_h, v_h) + \nu(\nabla u_h, \nabla v_h) - sb^*(B_h, B_h, v_h) + \gamma(\nabla \cdot u_h, \nabla \cdot v_h) = (f, v_h), \quad (5.3.15)$$

$$b^*(u_h^0, u_h^0, v_h) + \nu(\nabla u_h^0, \nabla v_h) - sb^*(B_h^0, B_h^0, v_h) - (p_h^0, \nabla \cdot v_h) = (f, v_h). \quad (5.3.16)$$

Subtracting (5.3.16) from (5.3.15) gives

$$\nu(\nabla r_u, \nabla v_h) + \gamma(\nabla \cdot u_h, v_h) = -b^*(u_h^0, r_u, v_h) - b^*(r_u, u_h, v_h)$$

$$+ sb^*(B_h, r_B, v_h) + sb^*(r_b, B_h^0, v_h) - (p_h^0, \nabla \cdot v_h). \quad (5.3.17)$$

Similarly, plugging in the TH and SV solutions into (5.3.3) gives the following two equations: $\forall \chi_h \in V_h$,

$$\nu_m(\nabla B_h, \nabla \chi_h) - b^*(B_h, u_h, \chi_h) + b^*(u_h, B_h, \chi_h)$$

$$+ \gamma(\nabla \cdot B_h, \nabla \cdot \chi_h) = (\nabla \times G, \chi_h), \quad (5.3.18)$$

$$\nu_m(\nabla B_h^0, \nabla \chi_h) - b^*(B_h^0, u_h^0, \chi_h) + b^*(u_h^0, B_h^0, \chi_h)$$

$$+ (\lambda_h^0, \nabla \cdot \chi_h) = (\nabla \times G, \chi_h). \quad (5.3.19)$$

Subtracting (5.3.19) from (5.3.18) results in the following equality,

$$\nu_m(\nabla r_B, \nabla \chi_h) + \gamma(\nabla \cdot B_h, \nabla \cdot \chi_h) = b^*(B_h, r_u, \chi_h) + b^*(r_B, u_h^0, \chi_h)$$

$$- b^*(u_h^0, r_B, \chi_h) - b^*(r_u, B_h, \chi_h) + (\lambda_h^0, \nabla \cdot \chi_h). \quad (5.3.20)$$

Orthogonally decompose $r_u =: r_u^0 + r_u'$ and $r_B =: r_B^0 + r_B'$ where $r_u^0, r_B^0 \in V_h^{SV}$ and $r_u', r_B' \in R_h$. Choosing $v_h = r_u'$ in (5.3.17), $\chi_h = r_B'$ in (5.3.20) and adding the two resulting equations yields

$$\nu \|\nabla r_u'\|^2 + \gamma \|\nabla \cdot r_u'\|^2 + \nu_m \|\nabla r_B'\|^2 + \gamma \|\nabla \cdot r_B'^2\|^2 = -b^*(u_h^0, r_u^0, r_u')$$

$$- b^*(r_u, u_h, r_u') + sb^*(B_h, r_B, r_u') + sb^*(r_b, B_h^0, r_u') - (p_h^0, \nabla \cdot r_u')$$

$$+ b^*(B_h, r_u, r_B') + b^*(r_B, u_h^0, r_B') - b^*(u_h^0, r_B', r_B')$$

$$- b^*(r_u, B_h, r_B') + (\lambda_h^0, \nabla \cdot r_B') \quad (5.3.21)$$

71

From (5.3.5), (5.3.6) and Lemmas 2.1 and 2.0.9, we can transform (5.3.21) to

$$
\gamma \frac{\|\nabla \cdot r_u'\|^2 + \|\nabla \cdot r_B'\|^2}{\|\nabla \cdot r_u\| + \|\nabla \cdot r_B\|} \leq C_s M_1 M \|\nabla r_u^0\| + C_s M_1 M \|\nabla r_u\|
$$
$$
+ s C_s M_2 M \|\nabla r_B\| + s C_s M_2 M \|\nabla r_B\| + \|p^0\| + C_s M_2 M \|\nabla r_u\|
$$
$$
+ C_s M_1 M \|\nabla r_B\| + C_s M_1 M \|\nabla r_B^0\| + C_s M_2 M \|\nabla r_B\| + M \|\lambda_h^0\|. \tag{5.3.22}
$$

Since $u_h, u_h^0, B_h$ and $B_h^0$ are all bounded by data, $r_u, r_u^0, r_B$ and $r_B^0$ are as well. Therefore,

$$
\|\nabla \cdot r_u'\| + \|\nabla \cdot r_B'\| \leq \frac{C}{\gamma}. \tag{5.3.23}
$$

It remains to bound $\|r_u^0\|$ and $\|r_B^0\|$. We will majorize the terms individually and then combine the results. First, setting $v_h = r_u^0$ in (5.3.15) and (5.3.16), and rearranging gives the following

$$
\nu(\nabla u_h, \nabla r_u^0) = -b^*(u_h, u_h, r_u^0) + s b^*(B_h, B_h, r_u^0) + (f, r_u^0), \tag{5.3.24}
$$
$$
\nu(\nabla u_h^0, \nabla r_u^0) = -b^*(u_h^0, u_h^0, r_u^0) + s b^*(B_h^0, B_h^0, r_u^0) + (f, r_u^0). \tag{5.3.25}
$$

Subtracting (5.3.25) from (5.3.24), rewriting the nonlinear terms with standard identities and reducing with orthogonality properties gives

$$
\nu \|\nabla r_u^0\|^2 \leq |b^*(u_h^0, r_u', r_u^0)| + |b^*(r_u, u_h, r_u^0)|
$$
$$
+ |s b^*(B_h, r_B, r_u^0)| + |s b^*(r_B, B_h^0, r_u^0)|. \tag{5.3.26}
$$

Choosing $\chi_h = r_B^0$ in (5.3.18) and (5.3.19), and rearranging gives the following equalities

$$
\nu_m(\nabla B_h, \nabla r_B^0) = b^*(B_h, u_h, r_B^0) - b^*(u_h, B_h, r_B^0) + (\nabla \times G, r_B^0), \tag{5.3.27}
$$
$$
\nu_m(\nabla B_h^0, \nabla r_B^0) = b^*(B_h^0, u_h^0, r_B^0) - b^*(u_h^0, B_h^0, r_B^0) + (\nabla \times G, r_B^0). \tag{5.3.28}
$$

Subtracting (5.3.28) from (5.3.27), rewriting the nonlinear terms and reducing with orthogonality properties gives

$$
\nu_m \|\nabla r_B^0\|^2 \leq |b^*(B_h, r_u, r_B^0)| + |b^*(r_B, u_h^0, r_B^0)|
$$
$$
+ |b^*(u_h^0, r_B', r_B^0)| + |b^*(r_u, B_h, r_B^0)|. \tag{5.3.29}
$$

Adding (5.3.26) and (5.3.29) gives the following upper bound

$$
\begin{aligned}
\nu\|\nabla r_u^0\|^2 + \nu_m\|\nabla r_B^0\|^2 \quad \leq \quad & |b^*(u_h^0, r_u', r_u^0)| + |b^*(r_u, u_h, r_u^0)| + |sb^*(B_h, r_B, r_u^0)| \\
+ \quad & |sb^*(r_B, B_h^0, r_u^0)| + |b^*(B_h, r_u, r_B^0)| + |b^*(r_B, u_h^0, r_B^0)| \\
+ \quad & |b^*(u_h^0, r_B', r_B^0)| + |b^*(r_u, B_h, r_B^0)|.
\end{aligned}
\tag{5.3.30}
$$

Now using Lemma 2.1, (5.3.5), (5.3.6) and the triangle inequality yields

$$
\begin{aligned}
\nu\|\nabla r_u^0\|^2 + \nu_m\|\nabla r_B^0\|^2 \quad \leq \quad & C_s(M_1\|\nabla r_u^0\|^2 + M_1\|\nabla r_B^0\|^2 \\
+ \quad & 2sM_2\|\nabla r_B'\|\|\nabla r_u^0\| + 2M_1\|\nabla r_u'\|\|\nabla r_u^0\| \\
+ \quad & 2M_2\|\nabla r_u'\|\|\nabla r_B^0\| + +2M_1\|\nabla r_B'\|\|\nabla r_B^0\| \\
+ \quad & 2sM_2\|\nabla r_B^0\|\|\nabla r_u^0\| + 2M_2\|\nabla r_u^0\|\|\nabla r_B^0\|).
\end{aligned}
\tag{5.3.31}
$$

The first 2 terms may be subtracted from both sides of (5.3.31) immediately. The subsequent terms may be handled using Young's inequality to yield

$$
\begin{aligned}
(\frac{\nu}{2} - C_sM_1 - 2sC_sM_2 - 2C_sM_2)\|\nabla r_u^0\|^2 + (\frac{\nu_m}{2} - C_sM_1 - 2sC_sM_2 - 2C_sM_2)\|\nabla r_B^0\|^2 \\
\leq 16\nu^{-1}s^2C_s^2M_2^2\|\nabla r_B'\|^2 + 16\nu^{-1}C_2^2M_1^2\|\nabla r_u'\|^2 \\
+ 16\nu_m^{-1}C_s^2M_2^2\|\nabla r_u'\|^2 + 16\nu_m^{-1}C_s^2M_1^2\|\nabla r_B'\|^2.
\end{aligned}
$$

Provided that

$$
\begin{aligned}
\frac{\nu}{2} \quad & -C_sM_1 - 2sC_sM_2 - 2C_sM_2 > 0, \; and \\
\frac{\nu_m}{2} \quad & -C_sM_1 - 2sC_sM_2 - 2C_sM_2 > 0,
\end{aligned}
\tag{5.3.32}
$$

it follows from the triangle inequality that

$$
\|\nabla(u_h - u_h^0)\| + \|\nabla(B_h - B_h^0)\| \leq \frac{C}{\gamma}.
\tag{5.3.33}
$$

$\square$

### 5.3.2 Numerical verification for steady MHD

To numerically verify the MHD convergence theory, we select the test problem with solution

$$
u = \begin{bmatrix} \cos(y) \\ \sin(x) \end{bmatrix} ,\ B = \begin{bmatrix} x \\ -y \end{bmatrix} ,\ P = \sin(x+y), \tag{5.3.34}
$$

on the unit square with $\nu = \nu_m = 1$, $s = 1$ and $f$ and $g$ calculated from this information.

The mesh used was a barycenter-refined uniform triangulation of $\Omega$, which provided a total of $4{,}324$ degrees of freedom for the $(P_2, P_1)$ TH computations and $6{,}600$ for $(P_2, P_1^{disc})$ SV. The results are shown in Table 5.2, and first order convergence in the $H^1$ norm is observed for both velocity and the magnetic field.

| $\gamma$ | $\|u_{TH}^\gamma - u_{SV}\|_{H^1}$ | rate | $\|\nabla \cdot u_{TH}^\gamma\|$ | $\|B_{TH}^\gamma - B_{SV}\|_{H^1}$ | rate | $\|\nabla \cdot B_{TH}^\gamma\|$ |
|---|---|---|---|---|---|---|
| 0 | 7.052E-4 | - | 5.45E-4 | 4.293E-6 | - | 1.74E-6 |
| 1 | 4.740E-4 | - | 3.19E-4 | 2.923E-6 | - | 8.93E-7 |
| 10 | 1.729E-4 | 0.41 | 8.44E-5 | 1.138E-6 | 0.41 | 2.96E-7 |
| $10^2$ | 2.688E-5 | 0.81 | 1.16E-5 | 1.813E-7 | 0.80 | 4.66E-8 |
| $10^3$ | 2.860E-6 | 0.97 | 1.22E-6 | 1.936E-8 | 0.97 | 4.97E-9 |
| $10^4$ | 2.879E-7 | 1.00 | 1.23E-7 | 1.947E-9 | 1.00 | 5.00E-10 |

Table 5.2: Convergence of the grad-div stabilized TH steady MHD solutions toward the SV steady MHD solution, first order as $\gamma \to \infty$.

## 5.4 Extrapolating to approximate the $\gamma = \infty$ solution

The previous sections verified that, provided the SV element is stable, the grad-div stabilized TH solutions to Stokes type problems converge to the SV solution as $\gamma \to \infty$. However, in practice there are limitations on how large $\gamma$ may be chosen, because as $\gamma$ increases the resulting linear system becomes ill-conditioned. In this section we consider linearly and quadratically extrapolating from grad-div stabilized TH velocity solutions found with smaller $\gamma$ to approximate the SV solution in an effort to improve mass conservation.

Let the true solutions to $(5.1.1) - (5.1.2)$ be given by

$$
u = \begin{bmatrix} (x^4 - 2x^3 + x^2)(4y^3 - 6y^2 + 2y) \\ -(y^4 - 2y^3 + y^2)(4x^3 - 6x^2 + 2x) \end{bmatrix} , \tag{5.4.1}
$$

$$
P = x + y + \frac{1}{2}(\cos(y)^2 + \sin(x)^2), \tag{5.4.2}
$$

on the unit square with $\nu = \frac{1}{100}$.

Let $\gamma_k$ $(k = 1, 2$ or $3)$ denote a distinct stabilization parameter and let $(u_h^{\gamma_k}, p_h^{\gamma_k})$ denote Taylor-Hood solutions of (5.1.1)-(5.1.2) with stabilization parameters $\gamma_k$. Additionally, let $(u_{Ex}, p_{Ex})$ denote the extrapolated solution and $(u_h^0, p_h^0)$ denote the Scott-Vogelius solution to (5.1.1)-(5.1.2).

Computations were done on a barycenter-refined uniform triangulation of $\Omega$, which provided 2162 degrees of freedom for the $(P_2, P_1)$ TH elements and 3300 degrees of freedom for the $(P_2, P_1^{disc})$ SV element.

The results in Table 5.3 are for linear extrapolated solutions, and and Table 5.4 summarizes the results for quadratic extrapolated solutions. Little improvement is seen in linear extrapolation, but a dramatic improvement is observed for quadratic.

| $\gamma_1$ | $\gamma_2$ | $\|\nabla \cdot u_h^{\gamma_1}\|$ | $\|\nabla \cdot u_h^{\gamma_2}\|$ | $\|\nabla \cdot u_{Ex}\|$ | $\|u_{Ex} - u_h^0\|_{H^1}$ |
|---|---|---|---|---|---|
| 1 | 10 | 2.1946e-4 | 2.2585e-5 | 2.9595e-6 | 6.3507e-6 |
| 1 | 100 | 2.1964e-4 | 2.2653e-6 | 1.1318e-7 | 2.9811e-7 |
| 10 | 50 | 2.2585e-5 | 4.5292e-6 | 4.1681e-6 | 7.6739e-6 |
| 10 | 100 | 2.2585e-5 | 2.2653e-6 | 2.0621e-6 | 3.7978e-6 |
| 50 | 100 | 4.5292e-6 | 2.2653e-6 | 2.2427e-6 | 4.1293e-6 |

Table 5.3: Improved mass conservation using linear extrapolation.

| $\gamma_1$ | $\gamma_2$ | $\gamma_3$ | $\|\nabla \cdot u_{Ex}\|_{H^1}$ | $\|u_{EX} - u_h^0\|_{H^1}$ |
|---|---|---|---|---|
| 1 | 10 | 100 | 7.30832e-10 | 2.070203e-9 |
| 1 | 50 | 100 | 1.47103e-10 | 4.167215e-10 |

Table 5.4: Improved mass conservation using quadratic extrapolation

# Chapter 6

# NS-Omega

This chapter studies a finite element method for an 'α-model' known as the NS-$\overline{\omega}$ model. Successful DNS of fluid flows described by the incompressible NSE, if possible, is expensive for complex flows. Recently it has been found that 'α-models' are able to more accurately predict fluid flows on coarser spatial and temporal discretizations than DNS [43, 44, 52, 6, 66, 50, 12, 11, 28]. The NS-$\overline{\omega}$ model is particularly attractive because the model is well-posed, conserves energy, conserves a model helicity [46, 38], and it can be computed efficiently with unconditionally stable algorithms [44].

The continuous model is given by

$$u_t + (\nabla \times D_N F u) \times u + \nabla q - \nu \Delta u \;\; = \;\; f, \qquad\qquad (6.0.1)$$

$$\nabla \cdot u \;\; = \;\; 0, \qquad\qquad (6.0.2)$$

where $u$ and $f$ represent the same entities as they do for the NSE. The operators $F$ and $D_N$ are the Helmholtz filter and van Cittert approximate deconvolution operator respectively. The use of van Cittert approximate deconvolution increases the spatial accuracy of the model. We note that the model uses the rotational form of the NSE nonlinearity and so its Bernoulli pressure $(q = p + \frac{1}{2}|u|^2)$ is more complex than the usual pressure if the convective form of the nonlinearity is used for the NSE. Specifically, Bernoulli pressure contains a velocity component which can lead to large pressure approximation errors in finite element discretizations, and this can in turn adversely effect the velocity error. Using SV elements decouples the velocity and pressure error, and provides pointwise divergence free velocity approximations.

In addition to using SV elements the finite element discretization we use for the model

(6.0.1)-(6.0.2) also linearizes the regularized terms via Baker's method [3]. This decouples the momentum-mass system from the filtering and deconvolution, which makes the cost of filtering and higher orders of deconvolution negligible in comparison to the momentum-mass solve.

## 6.1 A numerical scheme for NS-$\overline{\omega}$

We now are ready to present the NS-$\overline{\omega}$ algorithm we study herein. The scheme uses a trapezoidal temporal discretization, and uses a Baker-type [3] extrapolation to linearize and maintain unconditional stability.

**Algorithm 6.1.1.** *Given kinematic viscosity $\nu > 0$, end-time $T > 0$, the time step is chosen $\Delta t < T = M\Delta t$, $f \in L^\infty(0, T; (H^{-1}(\Omega))^d$, the initial condition $u_0 \in V$, the filtering radius $\alpha > 0$, deconvolution order $N \geq 0$, first find $u_h^0 \in X_h^{SV}$ satisfying*

$$(u_h^0, v_h) - (\lambda_h, \nabla \cdot v_h) = (u_0, v_h), \quad \forall v_h \in X_h^{SV} \tag{6.1.1}$$

$$(\nabla \cdot u_h^0, r_h) = 0 \quad \forall r_h \in Q_h^{SV}, \tag{6.1.2}$$

*then set $u_h^{-1} := u_h^0$, and find $(u_h^{n+1}, q_h^{n+\frac{1}{2}}) \in (X_h^{SV}, Q_h^{SV})$ for $n = 0, 1, ..., M - 1$ satisfying*

$$\frac{1}{\Delta t}(u_h^{n+1} - u_h^n, v_h) + ((\nabla \times D_N^h F_h(\frac{3}{2}u_h^n - \frac{1}{2}u_h^{n-1}) \times u_h^{n+\frac{1}{2}}, v_h)$$
$$- (q_h^{n+\frac{1}{2}}, \nabla \cdot v_h) + \nu(\nabla u_h^{n+\frac{1}{2}}, \nabla v_h) = (f^{n+\frac{1}{2}}, v_h) \quad \forall v_h \in X_h^{SV}, \tag{6.1.3}$$

$$(\nabla \cdot u_h^{n+1}, r_h) = 0 \quad \forall r_h \in Q_h^{SV}. \tag{6.1.4}$$

### 6.1.1 Unconditional stability and well-posedness

**Lemma 6.1.1.** *Consider the NS-$\overline{\omega}$ algorithm 6.1.1. A solution $u_h^l$, $l = 1, \ldots M$, exists at each time-step and is unique. The algorithm is also unconditionally stable: the solutions satisfy the á priori bound:*

$$\|u_h^M\|^2 + \nu\Delta t \sum_{n=0}^{M-1} \|\nabla u_h^{n+1/2}\|^2 \leq \|u_h^0\|^2 + \frac{\Delta t}{\nu} \sum_{n=0}^{M-1} \|f^{n+1/2}\|_*^2. \tag{6.1.5}$$

*Proof.* The existence of a solution $u_h^n$ to the scheme in Algorithm 6.1.1 follows from the Leray-Schauder Principle [37]. The main step is deriving an á priori estimate, which can be obtained by setting $v_h = u_h^{n+1/2}$ in (6.1.3). The nonlinear term in the scheme vanishes with this choice. Thus,

for every $n$

$$\frac{1}{2\triangle t}(\|u_h^{n+1}\|^2 - \|u_h^n\|^2) + \nu\|\nabla u_h^{n+1/2}\|^2 \leq \frac{1}{2\nu}\|f^{n+1/2}\|_*^2 + \frac{\nu}{2}\|\nabla u_h^{n+1/2}\|^2,$$

i.e.,

$$\frac{1}{\triangle t}(\|u_h^{n+1}\|^2 - \|u_h^n\|^2) + \nu\|\nabla u_h^{n+1/2}\|^2 \leq \frac{1}{\nu}\|f^{n+1/2}\|_*^2.$$

Summing from $n = 0\ldots M-1$ gives the desired result. $\qquad\square$

Each time step in the scheme of Algorithm 6.1.1 only requires the solution of a linear system. Thus, the above stability estimate also implies that solutions at each time level exist uniquely.

**Remark 6.1.1.** *Since the kinetic energy $KE(u_h^n) := \frac{1}{2}\|u_h^n\|^2$ and energy dissipation $\varepsilon(u_h^n) := \nu\|\nabla u_h^n\|^2$ of NS-$\overline{\omega}$ , take the usual form, Lemma 6.1.1 implies*

$$KE(u_M^h) + \frac{\triangle t}{2}\sum_{n=0}^{M-1}\varepsilon(u_{n+1/2}^h) \leq KE(u_0^h) + \frac{\triangle t}{2\nu}\sum_{n=0}^{M-1}\|f^{n+1/2}\|_*^2. \tag{6.1.6}$$

*Thus, if $\nu = 0$ and $f = 0$, $KE(u_M^h) = KE(u_0^h)$. Hence Algorithm 6.1.1 is energy conserving.*

## 6.1.2 Convergence Analysis

Our main convergence result for the discrete NS-$\overline{\omega}$ model described in Algorithm 6.1.1 is given next.

**Theorem 6.1.1** (Convergence for discrete NS-$\overline{\omega}$ )**.** *Consider the discrete NS-$\overline{\omega}$ model. Let $(w(t), p(t))$ be a smooth, strong solution of the NSE such that the norms on the right hand side of (6.1.7)-(6.1.8) are finite. Suppose $(u_h^0, p_h^0)$ are the $V_h^{SV}$ and $Q_h^{SV}$ interpolants of $(w(0), p(0))$, respectively. Suppose $(u_h, q_h)$ satisfies the scheme (6.1.3)-(6.1.4). Then there is a constant $C = C(w, p)$ such that*

$$\|\|w - u_h\|\|_{\infty,0} \leq F(\triangle t, h, \alpha) + Ch^{k+1}\|\|w\|\|_{\infty,k+1}, \tag{6.1.7}$$

$$\left(\nu\triangle t\sum_{n=0}^{M-1}\|\nabla(w^{n+1/2} - (u_h^{n+1} + u_h^n)/2)\|^2\right)^{1/2} \leq F(\triangle t, h, \alpha) + C\nu^{1/2}(\triangle t)^2\|\nabla w_{tt}\|_{2,0}$$
$$+ C\nu^{1/2}h^k\|\|w\|\|_{2,k+1}, \tag{6.1.8}$$

*where*

$$
\begin{aligned}
F(\triangle t, h, \alpha) \quad &:= C^*\{(\nu + \nu^{-1})^{1/2} h^k \|\|w\|\|_{2,k+1} \\
&+ \nu^{-1/2} h^k \left( \|\|w\|\|_{4,k+1}^2 + \|\|\nabla w_{1/2}\|\|_{4,0}^2 \right) \\
&+ C(N)(\Delta t)^2 \left( \|w_{ttt}\|_{2,0} + \|f_{tt}\|_{2,0} + (\nu + \nu^{-1})^{1/2} \|\nabla w_{tt}\|_{2,0} \right) \\
&+ \nu^{-1/2}(\triangle t^2 + \alpha^{2N+2} + \alpha h^k + h^{k+1}) \|\|\nabla w_{1/2}\|\|_{2,0}\}.
\end{aligned} \tag{6.1.9}
$$

**Remark 6.1.1.** *There are two important points to note from theorem. First, the velocity error does not depend at all on the pressure error. Second, optimal accuracy can be achieved if $\alpha \leq O(h)$, and $2N + 2 \geq k$, which provides a guide for parameter selection.*

*Proof of Theorem 6.1.1.* Let

$$
b_\omega(u_h^{n+1/2}, v_h^{n+1/2}, \chi_h^{n+1/2}) := ((\nabla \times D_N^h F_h(\frac{3}{2} u_h^n - \frac{1}{2} u_h^{n-1})) \times v_h^{n+1/2}, \chi_h^{n+1/2}),
$$

and, then by adding and subtracting terms, we can write

$$
b_\omega(u_h^{n+1/2}, v_h^{n+1/2}, \chi_h^{n+1/2}) = b(u_h^{n+1/2}, v_h^{n+1/2}, \chi_h^{n+1/2}) - FE(u_h^{n+1/2}, v_h^{n+1/2}, \chi_h^{n+1/2}),
$$

where the linear extrapolated deconvolved filtering error FE is given by

$$
FE(u_h^{n+1/2}, v_h^{n+1/2}, \chi_h^{n+1/2}) := ((\nabla \times u_h^{n+1/2} - \nabla \times D_N^h F_h(\frac{3}{2} u_h^n - \frac{1}{2} u_h^{n-1})) \times v_h^{n+1/2}, \chi_h^{n+1/2}).
$$

At time $t_{n+1/2}$, the solution of the NSE $(w, p)$ satisfies

$$
\begin{aligned}
\left( \frac{w^{n+1} - w^n}{\Delta t}, v_h \right) \quad &+ \quad b_\omega(w^{n+1/2}, w^{n+1/2}, v_h) + \nu(\nabla w^{n+1/2}, \nabla v_h) \\
&= \quad (f^{n+1/2}, v_h) + Intp(w^n, v_h), \quad \forall v_h \in V_h^{SV}
\end{aligned} \tag{6.1.10}
$$

where the pressure term disappears since $V_h^{SV}$ is now pointwise div-free, as stated in Chapter 2. The term $Intp(w^n, v_h)$ collects the interpolation error, the above linear extrapolated deconvolved

filtering error and the consistency error. It is given by

$$
\begin{aligned}
Intp(w^n, v_h) \;=\; & \left( \frac{w^{n+1} - w^n}{\Delta t} - w_t(t_{n+1/2}), v_h \right) + \nu(\nabla w^{n+1/2} - \nabla w(t_{n+1/2}), \nabla v_h) \\
& + b_\omega(w^{n+1/2}, w^{n+1/2}, v_h) - b_\omega(w(t_{n+1/2}), w(t_{n+1/2}), v_h) \\
& - FE(w(t_{n+1/2}), w(t_{n+1/2}), v_h) \\
& + (f(t_{n+1/2}) - f_{n+1/2}, v_h).
\end{aligned}
\tag{6.1.11}
$$

Subtracting (6.1.10) from (6.1.3) and letting $e^n = w^n - u_h^n$ we have

$$
\begin{aligned}
\frac{1}{\Delta t}(e^{n+1} - e^n, v_h) + b_\omega(w^{n+1/2}, w^{n+1/2}, v_h) - b_\omega(u_h^{n+1/2}, u_h^{n+1/2}, v_h) & \\
+ \nu(\nabla e^{n+1/2}, \nabla v_h) = Intp(w^n, v_h) \quad, \quad \forall v^h \in V_h^{SV},
\end{aligned}
\tag{6.1.12}
$$

where the pressure term of NS-$\overline{\omega}$ disappears since $V_h^{SV}$ is now pointwise div-free. Decompose the error as $e^n = (w^n - U^n) - (u_h^n - U^n) := \eta^n - \phi_h^n$ where $\phi_h^n \in V_h^{SV}$, and $U$ is the $L^2$ projection of $w$ in $V_h^{SV}$. Setting $v_h = \phi_h^{n+1/2}$ in (6.1.12) we obtain

$$
\begin{aligned}
(\phi_h^{n+1} - \phi_h^n, \phi_h^{n+1/2}) + \nu\triangle t\|\nabla\phi_h^{n+1/2}\| - \triangle t\, b_\omega(u_h^{n+1/2}, e^{n+1/2}, \phi_h^{n+1/2}) & \\
- \triangle t\, b_\omega(e^{n+1/2}, w^{n+1/2}, \phi_h^{n+1/2}) = (\eta^{n+1} - \eta^n, \phi_h^{n+1/2}) + \triangle t\nu(\nabla\eta^{n+1/2}, \nabla\phi_h^{n+1/2}) & \\
+ \triangle t\, Intp(w^n, \phi_h),
\end{aligned}
$$

i.e.

$$
\begin{aligned}
\frac{1}{2}(\|\phi_h^{n+1}\|^2 - \|\phi_h^n\|^2) + \nu\triangle t\|\nabla\phi_h^{n+1/2}\|^2 = (\eta^{n+1} - \eta^n, \phi_h^{n+1/2}) + \triangle t\nu(\nabla\eta^{n+1/2}, \nabla\phi_h^{n+1/2}) & \\
+ \triangle t\, b_\omega(\eta^{n+1/2}, w^{n+1/2}, \phi_h^{n+1/2}) - \triangle t\, b_\omega(\phi_h^{n+1/2}, w^{n+1/2}, \phi_h^{n+1/2}) & \\
+ \triangle t\, b_\omega(u_h^{n+1/2}, \eta^{n+1/2}, \phi_h^{n+1/2}) + \triangle t\, Intp(w^n, \phi_h^{n+1/2}).
\end{aligned}
\tag{6.1.13}
$$

We now bound the terms in the RHS of (6.1.13) individually. According to the choice of $U$, $(\eta^{n+1} - \eta^n, \phi_h^{n+1/2}) = 0$. The Cauchy-Schwarz and Young's inequalities give

$$
\begin{aligned}
\nu\triangle t(\nabla\eta^{n+1/2}, \nabla\phi_h^{n+1/2}) \;\leq\; & \nu\triangle t\|\nabla\eta^{n+1/2}\|\,\|\nabla\phi_h^{n+1/2}\| \\
\leq\; & \frac{\nu\Delta t}{12}\|\nabla\phi_h^{n+1/2}\|^2 + C\nu\triangle t\|\nabla\eta^{n+1/2}\|^2.
\end{aligned}
\tag{6.1.14}
$$

80

Lemmas 2.0.1, 2.0.10 and 2.0.12 and standard inequalities give

$$\triangle t\, b_\omega(\eta^{n+1/2}, w^{n+1/2}, \phi_h^{n+1/2}) = \triangle t(\nabla \times D_N^h F_h(\frac{3}{2}\eta^n - \frac{1}{2}\eta^{n-1}) \times w^{n+1/2}, \phi_h^{n+1/2})$$

$$\leq C\triangle t\|\nabla \times D_N^h F_h(\frac{3}{2}\eta^n - \frac{1}{2}\eta^{n-1})\|\,\|\nabla w^{n+1/2}\|\,\|\nabla \phi_h^{n+1/2}\|$$

$$\leq C(N)\triangle t\|\nabla(\frac{3}{2}\eta^n - \frac{1}{2}\eta^{n-1})\|\,\|\nabla w^{n+1/2}\|\,\|\nabla \phi_h^{n+1/2}\|$$

$$\leq C(N)\triangle t(\|\nabla \eta^n\| + \|\nabla \eta^{n-1}\|)\,\|\nabla w^{n+1/2}\|\,\|\nabla \phi_h^{n+1/2}\|$$

$$\leq \frac{\nu\triangle t}{12}\|\nabla \phi_h^{n+1/2}\|^2 + C(N)\triangle t\,\nu^{-1}\,(\|\nabla \eta^n\|^2 + \|\nabla \eta^{n-1}\|^2)\|\nabla w^{n+1/2}\|^2, \qquad (6.1.15)$$

Using (2.0.5), we get

$$\triangle t\, b_\omega(\phi_h^{n+1/2}, w^{n+1/2}, \phi_h^{n+1/2}) = \triangle t\,(\nabla \times D_N^h F_h(\frac{3}{2}\phi_h^n - \frac{1}{2}\phi_h^{n-1}) \times w^{n+1/2}, \phi_h^{n+1/2})$$

$$\leq C\triangle t\,\left\|w^{n+1/2}\right\|_2 \left\|\nabla \phi_h^{n+1/2}\right\| \left\|D_N^h F_h(\frac{3}{2}\phi_h^n - \frac{1}{2}\phi_h^{n-1})\right\|$$

$$\leq C(N)\triangle t\,\left\|w^{n+1/2}\right\|_2 \left\|\nabla \phi_h^{n+1/2}\right\| (\|\phi_h^n\| + \|\phi_h^{n-1}\|)$$

$$\leq \frac{\nu\triangle t}{12}\|\nabla \phi_h^{n+1/2}\|^2 + C(N)\triangle t\,\nu^{-1}\,(\|\phi_h^n\|^2 + \|\phi_h^{n-1}\|^2)\|w^{n+1/2}\|_2^2. \qquad (6.1.16)$$

The final trilinear term requires a bit more effort. Begin by splitting the first entry of this term by adding and subtracting $w_{n+1/2}$, followed by rewriting the resulting error term as pieces inside and outside of the finite element space.

$$\triangle t b_\omega(u_h^{n+1/2}, \eta^{n+1/2}, \phi_h^{n+1/2}) = \triangle t b_\omega(\eta^{n+1/2}, \eta^{n+1/2}, \phi_h^{n+1/2})$$

$$+ \triangle t b_\omega(\phi_h^{n+1/2}, \eta^{n+1/2}, \phi_h^{n+1/2}) + \triangle t b_\omega(w^{n+1/2}, \eta^{n+1/2}, \phi_h^{n+1/2}). \quad (6.1.17)$$

We bound each of the terms on the right hand side of (6.1.17) using the same inequalities and lemmas as above:

$$\triangle t b_\omega(\eta^{n+1/2}, \eta^{n+1/2}, \phi_h^{n+1/2})$$

$$\leq \triangle t\|\nabla \times D_N^h F_h(\frac{3}{2}\eta^n - \frac{1}{2}\eta^{n-1})\|\|\nabla \eta^{n+1/2}\|\|\nabla \phi_h^{n+1/2}\|$$

$$\leq C(N)\triangle t\|\nabla(\frac{3}{2}\eta^n - \frac{1}{2}\eta^{n-1})\|\|\nabla \eta^{n+1/2}\|^2\|\nabla \phi_h^{n+1/2}\|$$

$$\leq \frac{\nu\triangle t}{24}\|\nabla \phi_h^{n+1/2}\|^2 + C(N)\triangle t\nu^{-1}(\|\nabla \eta^n\|^2 + \|\nabla \eta^{n-1}\|^2)\|\nabla \eta^{n+1/2}\|^2, \qquad (6.1.18)$$

$$\triangle t b_\omega(\phi_h^{n+1/2}, \eta^{n+1/2}, \phi_h^{n+1/2}) = \triangle t (\nabla \times D_N^h F_h(\frac{3}{2}\phi_h^n - \frac{1}{2}\phi_h^{n-1}) \times \eta^{n+1/2}, \phi_h^{n+1/2})$$

$$\leq \triangle t |(\phi_h^{n+1/2} \times \eta^{n+1/2}, \nabla \times D_N^h F_h(\frac{3}{2}\phi_h^n - \frac{1}{2}\phi_h^{n-1}))|$$

$$\leq \triangle t |(\phi_h^{n+1/2} \cdot \nabla \eta^{n+1/2}, D_N^h F_h(\frac{3}{2}\phi_h^n - \frac{1}{2}\phi_h^{n-1}))|$$

$$+ \triangle t |(\eta_h^{n+1/2} \cdot \nabla \phi^{n+1/2}, D_N^h F_h(\frac{3}{2}\phi_h^n - \frac{1}{2}\phi_h^{n-1}))|$$

$$\leq C(N)\triangle t \left\|\nabla \eta_h^{n+1/2}\right\| \left\|\nabla \phi^{n+1/2}\right\| \left\|\frac{3}{2}\phi_h^n - \frac{1}{2}\phi_h^{n-1}\right\|^{1/2} \left\|\nabla(\frac{3}{2}\phi_h^n - \frac{1}{2}\phi_h^{n-1}))\right\|^{1/2}$$

$$\leq C(N)h^{-1/2}\triangle t \left\|\nabla \eta_h^{n+1/2}\right\| \left\|\nabla \phi^{n+1/2}\right\| \left\|\frac{3}{2}\phi_h^n - \frac{1}{2}\phi_h^{n-1}\right\|$$

$$\leq \frac{\nu \triangle t}{12}\|\nabla \phi_h^{n+1/2}\|^2 + C(N)\triangle t \,\nu^{-1} h^{-1} (\|\phi_h^n\|^2 + \|\phi_h^{n-1}\|^2)\|\nabla \eta^{n+1/2}\|^2, \qquad (6.1.19)$$

$$\triangle t b_\omega(w^{n+1/2}, \eta^{n+1/2}, \phi_h^{n+1/2})$$

$$\leq \triangle t \|\nabla \times D_N^h F_h(\frac{3}{2}w^n - \frac{1}{2}w^{n-1})\|\|\nabla \eta^{n+1/2}\|\|\nabla \phi_h^{n+1/2}\|$$

$$\leq C(N)\triangle t \|\nabla(\frac{3}{2}w^n - \frac{1}{2}w^{n-1})\|\|\nabla \eta^{n+1/2}\|\|\nabla \phi_h^{n+1/2}\|$$

$$\leq \frac{\nu \triangle t}{24}\|\nabla \phi_h^{n+1/2}\|^2 + C(N)\triangle t \nu^{-1}(\|\nabla w^n\|^2 + \|\nabla w^{n-1}\|^2)\|\nabla \eta^{n+1/2}\|^2$$

$$\leq \frac{\nu \triangle t}{24}\|\nabla \phi_h^{n+1/2}\|^2 + C(N)\triangle t \nu^{-1}\|\nabla \eta^{n+1/2}\|^2. \qquad (6.1.20)$$

Combining (6.1.14)-(6.1.20) and summing from $n = 1$ to $M$ (assuming that $\|\phi_h^0\| = 0$) reduces (6.1.13) to

$$\|\phi_h^M\|^2 + \nu \triangle t \sum_{n=1}^{M-1} \|\nabla \phi_h^{n+1/2}\|^2$$

$$\leq C\triangle t \{ \sum_{n=1}^{M-1} C\nu^{-1}(\|w^{n+1/2}\|_2^2 + h^{-1}\|\nabla \eta^{n+1/2}\|^2)(\|\phi_h^n\|^2 + \|\phi_h^{n-1}\|^2)$$

$$+ \sum_{n=1}^{M-1} \Big( (\nu + \nu^{-1})\|\nabla \eta^{n+1/2}\|^2 + \nu^{-1}(\|\nabla \eta^n\|^2 + \|\nabla \eta^{n-1}\|^2)\|\nabla w^{n+1/2}\|^2$$

$$+ \nu^{-1}(\|\nabla \eta^n\|^2 + \|\nabla \eta^{n-1}\|^2)\|\nabla \eta^{n+1/2}\|^2 \Big) + \sum_{n=1}^{M-1} |Intp(w_n, \phi_{n+1/2}^h)| \}$$

$$\leq C\triangle t \{ \sum_{n=1}^{M-1} C\nu^{-1}(\|w^{n+1/2}\|_2^2 + h^{-2}\|\nabla \eta^{n+1/2}\|^2)\|\phi_h^n\|^2$$

$$+ (\nu + \nu^{-1}) \sum_{n=1}^{M-1} \|\nabla \eta^{n+1/2}\|^2 + \nu^{-1} \sum_{n=0}^{M-1} \|\nabla \eta^n\|^2\|\nabla w^{n+1/2}\|^2$$

$$+ \nu^{-1} \sum_{n=0}^{M} \|\nabla \eta^n\|^4 + \sum_{n=1}^{M-1} |Intp(w_n, \phi_{n+1/2}^h)| \}. \qquad (6.1.21)$$

Now, we continue to bound the terms on the RHS of (6.1.21). We have that

$$C\triangle t(\nu + \nu^{-1}) \sum_{n=1}^{M-1} \|\nabla\eta^{n+1/2}\|^2 \leq C\triangle t(\nu + \nu^{-1}) \sum_{n=0}^{M} \|\nabla\eta^n\|^2$$

$$\leq C\triangle t(\nu + \nu^{-1}) \sum_{n=0}^{M} h^{2k}|w^n|^2_{k+1}$$

$$\leq C(\nu + \nu^{-1})h^{2k}\||w|\|^2_{2,k+1}, \qquad (6.1.22)$$

and similarly,

$$C\triangle t\nu^{-1} \sum_{n=0}^{M} \|\nabla\eta^n\|^4 \leq \triangle t C\nu^{-1} \sum_{n=0}^{M} h^{4k}|w^n|^4_{k+1}$$

$$\leq C\nu^{-1}h^{4k}\||w|\|^4_{4,k+1}. \qquad (6.1.23)$$

For the term

$$C\triangle t\nu^{-1} \sum_{n=0}^{M-1} \|\nabla\eta^n\|^2\|\nabla w^{n+1/2}\|^2 \leq C\triangle t\nu^{-1}h^{2k} \sum_{n=0}^{M} |w^n|^2_{k+1}\|\nabla w^{n+1/2}\|^2$$

$$\leq C\nu^{-1}h^{2k}\left(\||w|\|^4_{4,k+1} + \||\nabla w_{1/2}|\|^4_{4,0}\right). \qquad (6.1.24)$$

We now bound the terms in $Intp(w^n, \phi_h^{n+1/2})$. Using Cauchy-Schwarz and Young's inequalities, and Lemmas 2.0.4, 2.0.10 and 2.0.12 and the regularity assumptions on $w$,

$$\left(\frac{w^{n+1} - w^n}{\Delta t} - w_t(t_{n+1/2}), \phi_h^{n+1/2}\right)$$

$$\leq \frac{1}{2}\|\phi_h^{n+1/2}\|^2 + \frac{1}{2}\|\frac{w^{n+1} - w^n}{\Delta t} - w_t(t_{n+1/2})\|^2$$

$$\leq \frac{1}{2}\|\phi_h^{n+1}\|^2 + \frac{1}{2}\|\phi_h^n\|^2 + \frac{1}{2}\frac{(\Delta t)^3}{1280}\int_{t_n}^{t_{n+1}} \|w_{ttt}\|^2 \, dt, \qquad (6.1.25)$$

$$(f(t_{n+1/2}) - f^{n+1/2}, \phi_h^{n+1/2})$$

$$\leq \frac{1}{2}\|\phi_h^{n+1/2}\|^2 + \frac{1}{2}\|f(t_{n+1/2}) - f^{n+1/2}\|^2$$

$$\leq \frac{1}{2}\|\phi_h^{n+1}\|^2 + \frac{1}{2}\|\phi_h^n\|^2 + \frac{(\Delta t)^3}{48}\int_{t_n}^{t_{n+1}} \|f_{tt}\|^2 \, dt, \qquad (6.1.26)$$

83

$$\nu(\nabla w^{n+1/2} - \nabla w(t_{n+1/2}), \nabla \phi_h^{n+1/2})$$

$$\leq \quad \varepsilon_2 \nu \|\nabla \phi_h^{n+1/2}\|^2 + C\nu \|\nabla w^{n+1/2} - \nabla w(t_{n+1/2})\|^2$$

$$\leq \quad \varepsilon_2 \nu \|\nabla \phi_h^{n+1/2}\|^2 + C\nu \frac{(\Delta t)^3}{48} \int_{t_n}^{t_{n+1/2}} \|\nabla w_{tt}\|^2 \, dt \,, \tag{6.1.27}$$

$$b_\omega(w^{n+1/2}, w^{n+1/2}, \phi_h^{n+1/2}) - b_\omega(w(t_{n+1/2}), w(t_{n+1/2}), \phi_h^{n+1/2})$$

$$= \quad b_\omega(w^{n+1/2} - w(t_{n+1/2}), w^{n+1/2}, \phi_h^{n+1/2}) + b_\omega(w(t_{n+1/2}), w^{n+1/2} - w(t_{n+1/2}), \phi_h^{n+1/2})$$

$$\leq \quad C \|\nabla \times D_N^h F_h(\frac{3}{2}(w^n - w(t_n)) - \frac{1}{2}(w^{n-1} - w(t_{n-1})))\| \, \|\nabla \phi_h^{n+1/2}\| \, \|\nabla w^{n+1/2}\|$$

$$+ C \|\nabla \times D_N^h F_h(\frac{3}{2} w(t_n) - \frac{1}{2} w(t_{n-1}))\| \, \|\nabla \phi_h^{n+1/2}\| \, \|\nabla w^{n+1/2} - \nabla w(t_{n+1/2})\|$$

$$\leq \quad 0 + C(N) \|\nabla(\frac{3}{2} w(t_n) - \frac{1}{2} w(t_{n-1}))\| \, \|\nabla \phi_h^{n+1/2}\| \, \|\nabla w^{n+1/2} - \nabla w(t_{n+1/2})\|$$

$$\leq \quad C(N)\nu^{-1} \left( \|\nabla w(t_n)\|^2 + \|\nabla w(t_{n-1})\|^2 \right) \frac{(\Delta t)^3}{48} \int_{t_n}^{t_{n+1}} \|\nabla w_{tt}\|^2 \, dt + \varepsilon_3 \nu \|\nabla \phi_h^{n+1/2}\|^2$$

$$\leq \quad \varepsilon_3 \nu \|\nabla \phi_h^{n+1/2}\|^2 + C(N)\nu^{-1} \frac{(\Delta t)^3}{48} \int_{t_n}^{t_{n+1}} \|\nabla w_{tt}\|^2 \, dt \,. \tag{6.1.28}$$

Next we will bound the linear extrapolated deconvolved filtering error FE using

$$w(t_{n+1/2}) - (\frac{3}{2} w(t_n) - \frac{1}{2} w(t_{n-1})) = O(\triangle t^2) \tag{6.1.29}$$

and Lemma 2.0.13 as well. Thus,

$$FE \leq \left| (\nabla \times w(t_{n+1/2}) - \nabla \times D_N^h F_h(\frac{3}{2} w(t_n) - \frac{1}{2} w(t_{n-1})) \times w(t_{n+1/2}), \phi_h^{n+1/2}) \right|$$

$$\leq \quad C \|\nabla \times (w(t_{n+1/2}) - D_N^h F_h(\frac{3}{2} w(t_n) - \frac{1}{2} w(t_{n-1}))\| \|\nabla w(t_{n+1/2})\| \|\nabla \phi_h^{n+1/2}\|$$

$$\leq \quad \varepsilon_4 \nu \|\nabla \phi_h^{n+1/2}\|^2 + C\nu^{-1} \|\nabla w(t_{n+1/2})\|^2 \|\nabla \times (w(t_{n+1/2}) - D_N^h F_h(\frac{3}{2} w(t_n) - \frac{1}{2} w(t_{n-1}))\|^2$$

$$\leq \quad \varepsilon_4 \nu \|\nabla \phi_h^{n+1/2}\|^2 + C\nu^{-1} \|\nabla w(t_{n+1/2})\|^2 \left( \|\nabla(I - D_N^h F_h)w(t_{n+1/2})\|^2 \right.$$

$$\left. + \|\nabla D_N^h F_h(w(t_{n+1/2}) - (\frac{3}{2} w(t_n) - \frac{1}{2} w(t_{n-1})))\|^2 \right)$$

$$\leq \quad \varepsilon_4 \nu \|\nabla \phi_h^{n+1/2}\|^2 + C(N)\nu^{-1}(\triangle t^4 + \alpha^{4N+4} + \alpha^2 h^{2k} + h^{2k+2}) \|\nabla w(t_{n+1/2})\|^2. \tag{6.1.30}$$

Combine (6.1.25)-(6.1.30) to obtain

$$\Delta t \sum_{n=1}^{M-1} |Intp(w^n, \phi_h^{n+1/2})|$$

$$\leq \quad \Delta t\, C \sum_{n=0}^{M-1} \|\phi_h^{n+1}\|^2 + (\varepsilon_1 + \varepsilon_2 + \varepsilon_3 + \varepsilon_4)\Delta t\, \nu \sum_{n=1}^{M-1} \|\nabla\phi_h^{n+1/2}\|^2$$

$$+ C(N)(\Delta t)^4 \left( \|w_{ttt}\|_{2,0}^2 + \|f_{tt}\|_{2,0}^2 + (\nu + \nu^{-1})\|\nabla w_{tt}\|_{2,0}^2 \right)$$

$$+ \nu^{-1}(\triangle t^4 + \alpha^{4N+4} + \alpha^2 h^{2k} + h^{2k+2})\|\|\nabla w_{1/2}\|\|_{2,0}^2. \tag{6.1.31}$$

Let $\varepsilon_1 = \varepsilon_2 = \varepsilon_3 = \varepsilon_4 = 1/12$ and with (6.1.22)-(6.1.24), (6.1.31), from (6.1.21) we obtain

$$\|\phi_h^M\|^2 + \nu\triangle t \sum_{n=1}^{M-1} \|\nabla\phi_h^{n+1/2}\|^2$$

$$\leq \quad C\triangle t \sum_{n=1}^{M-1} C\nu^{-1} \left( \|\nabla w^{n+1/2}\|^2 + h^{2k-1}\right)\|\phi_h^n\|^2 + C\Delta t \sum_{n=1}^{M} \|\phi_h^n\|^2$$

$$+ C(\nu + \nu^{-1})h^{2k}\|\|w\|\|_{2,k+1}^2 + C\nu^{-1}h^{4k}\|\|w\|\|_{4,k+1}^4 + C\nu^{-1}h^{2k} \left( \|\|w\|\|_{4,k+1}^4 + \|\|\nabla w_{1/2}\|\|_{4,0}^4 \right)$$

$$+ C(N)(\Delta t)^4 \left( \|w_{ttt}\|_{2,0}^2 + \|f_{tt}\|_{2,0}^2 + (\nu + \nu^{-1})\|\nabla w_{tt}\|_{2,0}^2 \right)$$

$$+ \nu^{-1}(\triangle t^4 + \alpha^{4N+4} + \alpha^2 h^{2k} + h^{2k+2})\|\|\nabla w_{1/2}\|\|_{2,0}^2. \tag{6.1.32}$$

Hence, with $k \geq 1$, from Gronwall's Lemma (see Lemma 2.0.5), we have

$$\|\phi_h^M\|^2 + \nu\triangle t \sum_{n=1}^{M-1} \|\nabla\phi_h^{n+1/2}\|^2$$

$$\leq \quad C^*\{(\nu + \nu^{-1})h^{2k}\|\|w\|\|_{2,k+1}^2 + \nu^{-1}h^{4k}\|\|w\|\|_{4,k+1}^4 + \nu^{-1}h^{2k} \left( \|\|w\|\|_{4,k+1}^4 + \|\|\nabla w_{1/2}\|\|_{4,0}^4 \right)$$

$$+ C(N)(\Delta t)^4 \left( \|w_{ttt}\|_{2,0}^2 + \|f_{tt}\|_{2,0}^2 + (\nu + \nu^{-1})\|\nabla w_{tt}\|_{2,0}^2 \right)$$

$$+ \nu^{-1}(\triangle t^4 + \alpha^{4N+4} + \alpha^2 h^{2k} + h^{2k+2})\|\|\nabla w_{1/2}\|\|_{2,0}^2\}, \tag{6.1.33}$$

where $C^* = C \exp(C\nu^{-1}T)$.

Estimate (6.1.7) then follows from the triangle inequality and (6.1.33).

To obtain (6.1.8), we use (6.1.33) and

$$\|\nabla \left( w(t_{n+1/2}) - (u_{n+1}^h + u_n^h)/2 \right) \|^2$$

$$\leq \quad \|\nabla(w(t_{n+1/2}) - w^{n+1/2})\|^2 + \|\nabla\eta^{n+1/2}\|^2 + \|\nabla\phi_h^{n+1/2}\|^2$$

$$\leq \quad \frac{(\triangle t)^3}{48} \int_{t_n}^{t_{n+1}} \|\nabla w_{tt}\|^2 \, dt + Ch^{2k}|w^{n+1}|_{k+1}^2 + Ch^{2k}|w^n|_{k+1}^2 + \|\nabla\phi_h^{n+1/2}\|^2 .$$

$$\square$$

### 6.1.3 An alternative choice of $\alpha$

It is common in '$\alpha$-models' for the choice of filtering radius parameter to be chosen on the order of the meshwidth, $\alpha = O(h)$. From the preceding error analysis, it can be seen that such a choice of $\alpha$ is the largest it can be without creating suboptimal asymptotic accuracy. Although this provides some guidance on the choice of $\alpha$, finding an optimal $\alpha$ on a particular fixed mesh still may require some tuning. We describe now a connection between NS-$\overline{\omega}$ and the velocity-vorticity-helicity (VVH) formulation of the NSE [60], that suggests an alternative choice of $\alpha$ that may aid in this process.

NS-$\overline{\omega}$ can be considered as a rotational form NSE formulation where the vorticity term is handled by other equations, which for NS-$\overline{\omega}$ is the regularization equations. Such a formulation is quite similar to a velocity-vorticity method, where the vorticity comes directly from solving the vorticity equation. In particular, consider the numerical method devised in [60] for the VVH NSE formulation:

**Algorithm 6.1.2.** ***Step 1.*** *Given $u^n$, $u^{n-1}$, $w^n$ and $u^* = \frac{3}{2}u^n - \frac{1}{2}u^{n-1}$, find $w^{n+1}$ and $hel^{n+1/2}$ from*

$$\frac{w^{n+1} - w^n}{\triangle t} - \nu \triangle w^{n+1/2} + 2D(w^{n+1/2})u^* - \nabla hel^{n+1/2} = \nabla \times f^{n+1/2} \qquad (6.1.34)$$

$$\nabla \cdot w^{n+1} = 0 \qquad (6.1.35)$$

$$w^{n+1} = \nabla \times (2u^n - u^{n-1}) \ on \ \partial\Omega \qquad (6.1.36)$$

***Step 2.*** *Given $u^n$, $w^n$ and $w^{n+1}$, find $u^{n+1}$ and $P^{n+1/2}$*

$$\frac{u^{n+1} - u^n}{\triangle t} - \nu \triangle u^{n+1/2} + w^{n+1/2} \times u^{n+1/2} - \nabla P^{n+1/2} = f^{n+1/2} \qquad (6.1.37)$$

$$\nabla \cdot u^{n+1} = 0 \qquad (6.1.38)$$

$$u^{n+1} = \phi \ on \ \partial\Omega \qquad (6.1.39)$$

*where $\phi$ is the Dirichlet boundary condition function and $D(\cdot)$ denotes the deformation tensor, i.e. $D(v) = \frac{(\nabla v) + (\nabla v)^T}{2}$, $u, w$ denote velocity and vorticity, $P$ is the Bernoulli pressure and hel is helical density.*

If $f$ is irrotational and we remove the nonlinear term from the vorticity equation, this system is analogous the NS-$\overline{\omega}$ scheme herein if we identify helical density with the Lagrange multiplier $\lambda$ corresponding to the incompressibility of the filtered velocity, and $\nu\Delta t$ with $\alpha^2$, i.e. $\alpha = \sqrt{\nu\Delta t}$.

Choosing an optimal filtering radius $\alpha$ is certainly problem dependent, and by no means are we suggesting this choice is always optimal. However, our numerical experiments show it can be a good starting point for choosing $\alpha$ when using NS-$\overline{\omega}$ .  □

## 6.2 Numerical experiments

In this section we present several numerical experiments that demonstrate the effectiveness of the numerical method studied herein. The first two experiments are for benchmark tests of channel flow over a step and around a cylinder, respectively, and both show excellent results. The third and fourth tests are done with SV elements and TH elements, and compare solutions for a problem with known analytical solution and the cylinder problem.

### 6.2.1 Experiment 1: Channel flow over a forward-backward facing step

Our first numerical experiment is for the benchmark 2d problem of channel flow over a forward-backward facing step. The domain $\Omega$ is a 40x10 rectangle with a 1x1 step 5 units into the channel at the bottom. The top and bottom of the channel as well as the step are prescribed with no-slip boundary conditions, and the sides are given the parabolic profile $(y(10-y)/25, 0)^T$. We use the initial condition of $u_0 = (y(10-y)/25, 0)^T$ inside $\Omega$, and run the test to $T = 40$. For a chosen viscosity $\nu = 1/600$, it is known that the correct behavior is for an eddy to form behind the step, grow, detach from the step to move down the channel, and a new eddy forms. For a more detailed description of the problem, see [25, 31]. The eddy formation and separation present in this test problem is part of a complex flow structure, and its capture is critical for an effective fluid flow model. Moreover, a useful fluid model will correctly predict this behavior on a coarser mesh than can a direct numerical simulation of the NSE.

For the following tests, we computed Algorithm 6.1.1 with $(P_2, P_1^{disc})$ SV elements on a barycenter-refined mesh, yielding 14,467 total degrees of freedom, with deconvolution order $N = 1$, and varying $\alpha$. For comparison, we also directly compute the (linearized) NSE ($\alpha = N = 0$). We compute first with timestep $\Delta t = 0.05$, and the solutions at $T = 40$ are shown in Figure 6.1. Several interesting observations can be made. First, we note that the optimal choice of $\alpha$ appears to be near $\alpha = \sqrt{\nu \Delta t}$, as this is the only solution to predict a smooth flow field and eddies forming and detaching behind the step. For the the NSE ($\alpha = 0$), a smooth flow field is predicted; however, the eddies behind the step appear to be stretching instead of detaching. Larger values of $\alpha$, including the common choice of the average element width $\alpha = h$, give increasingly worse solutions. This is

somewhat counterintuitive, as $\alpha$ is a filtering radius that is supposed to regularize and thus smooth oscillations. A closer examination reveals that the oscillations are arising from an inability of the more regularized models to resolve the flow at the top left corner of the step, where the flow near the bottom of the channel is forced up to intersect with the free stream.

To test the scaling of optimal $\alpha$ with $\Delta t$, we compute with the same data, but with timesteps $\Delta t = 0.01$ and $0.025$, with parameter $\alpha = \sqrt{\nu \Delta t}$. The results at $T = 40$ are shown in Figure 6.2, and results are good in both cases. However, for the smaller timestep, we see the eddies stretching instead of detaching. This is not surprising, as one should expect some h-dependence on the choice of $\alpha$.

## 6.2.2   Experiment 2: Channel flow around a cylinder

The benchmark problem of 2d channel flow around a cylinder has been studied in numerous works, e.g. [67, 30, 34, 42], and is well documented in [67]. The domain is the rectangle $[0, 2.2] \times [0, 0.41]$ representing the channel with flow in the positive $x$ direction, with a circle radius $0.05$ centered at $(0.2, 0.2)$ representing the cylinder. No slip boundary conditions are prescribed on the top and bottom of the channel as well as on the cylinder, and the time dependent inflow and outflow velocity profiles are given by

$$u(0, y, t) = u(2.2, y, t) = \left[ \frac{6}{0.41^2} \sin(\pi t/8) y (0.41 - y), \, 0 \right]^T, \quad 0 \leq y \leq 0.41.$$

The forcing function is set to zero, $f = 0$, and the viscosity at $\nu = 0.001$, providing a time dependent Reynolds number, $0 \leq Re(t) \leq 100$. The initial condition is $u = 0$, and we compute to final time $T = 8$ with time-step $\Delta t = 0.005$. An accurate approximation of this flow's velocity field will show a vortex street forming behind the cylinder by $t = 4$, and a fully formed vortex street by $t = 7$.

We test the algorithm with $\alpha = h$ and $\alpha = \sqrt{\nu \Delta t}$, on a barycenter refined mesh that provides 26,656 degrees of freedom for $(P_2, P_1^{disc})$ SV elements, and again find that $\alpha = \sqrt{\nu \Delta t}$ provides a better solution than $\alpha = h$. These results are shown for $t = 7$ in Figure 6.3. The $\alpha = \sqrt{\nu \Delta t}$ solution agrees with documented DNS results [8, 42], but the $\alpha = h$ solution at $t = 7$ is observed to be incorrect, as it does not fully resolve the wake, and its speed contours show it gives a much different (and thus incorrect) solution behind the cylinder.
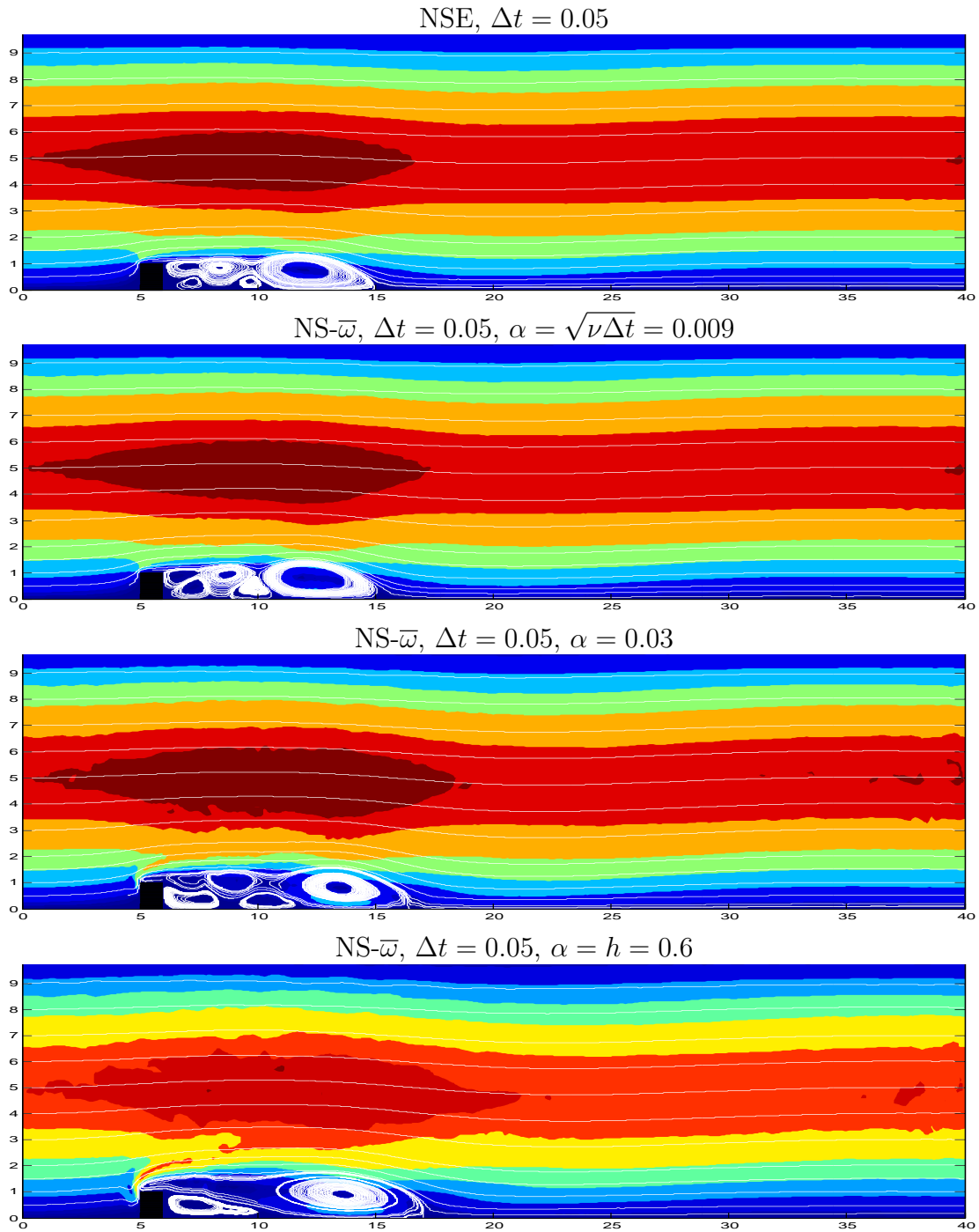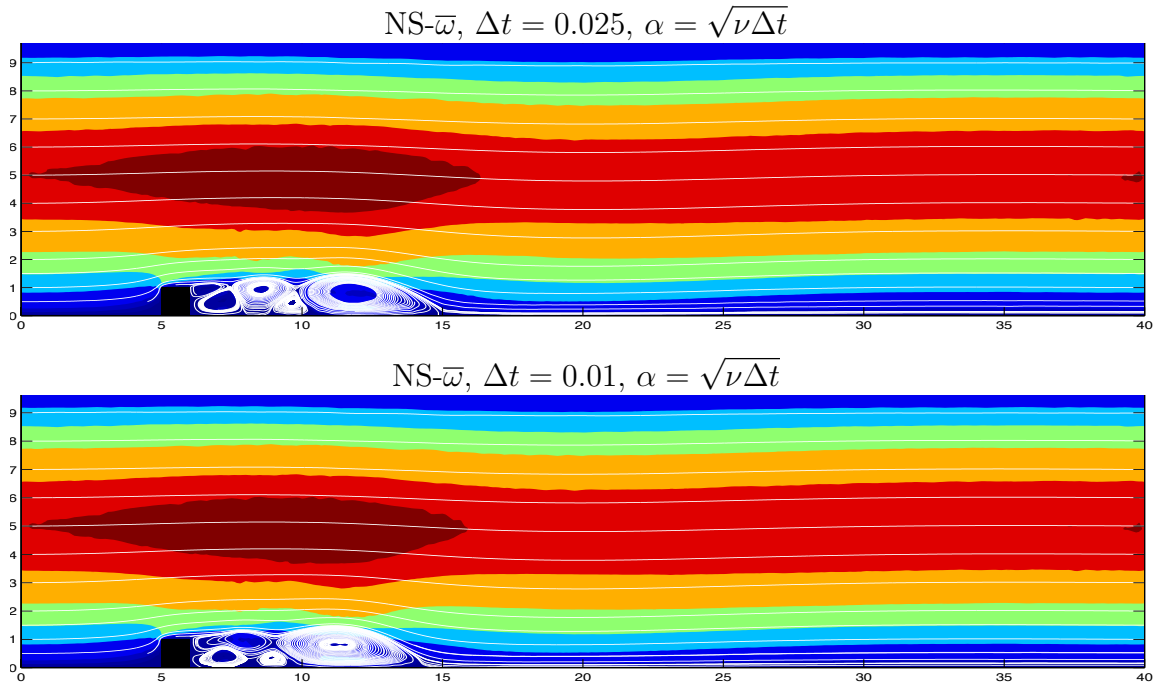
Figure 6.1: Shown above are the $T = 40$ SV solutions as velocity streamlines over speed contours for the step problem from Experiment 1. Shown are the NSE (top) which is somewhat underresolved on this mesh as the eddies are not fully detaching, NS-$\overline{\omega}$ with $\alpha = \sqrt{\nu \Delta t}$ (second from top) which agrees with the known true solution, NS-$\overline{\omega}$ with $\alpha = 0.3$ (third from top) which has oscillations present in the speed contours, and NS-$\overline{\omega}$ with $\alpha = h = 0.6$ (bottom) which is a poor approximation. All of the solutions are pointwise divergence-free.

Figure 6.2: Shown above are the $T = 40$ SV solutions as velocity streamlines over speed contours for the step problem from Experiment 1, with parameter chosen as $\alpha = \sqrt{\nu\Delta t}$, for varying timesteps.
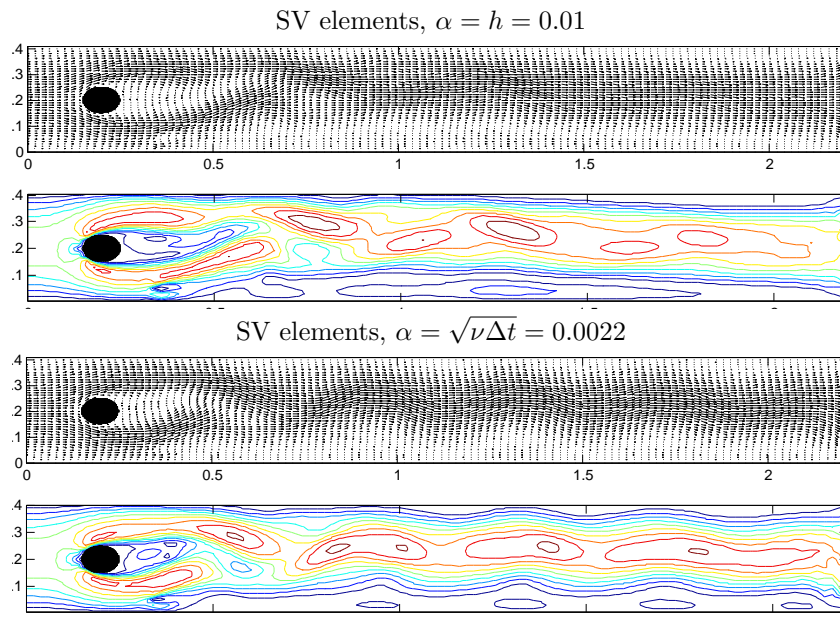


Figure 6.3: The above pictures show the velocity fields and speed contours at $t = 7$ using SV elements with $\alpha = h$ (top) and $\alpha = \sqrt{\nu\Delta t}$ (bottom). The $\alpha = h$ solution is under-resolved, as it loses resolution of the vortex street, and its speed contours are inaccurate. The $\alpha = \sqrt{\nu\Delta t}$ solution captures the entire wake, and its speed contours agree well with the known solution.

#### 6.2.2.1  Comparison to TH element solution

Using the same problem data as Experiment 2 above, we also compute using $(P_2, P_1)$ TH elements, with $\alpha = \sqrt{\nu \Delta t}$ (which gave about the same answer as for $\alpha = h$). Since this element pair is widely used and is closely related to SV elements (they differ only in the pressure space being continuous or not), a comparison is of interest. Since TH uses a continuous pressure space, with the same mesh the total degrees of freedom is 17,306. All of problem data is kept the same, and results are shown in Figures 6.4 and 6.5. In Figure 6.4, we observe that the TH solution is much worse than the SV solution shown in Figure 6.3; the TH solution fails to resolve the important behavior behind the cylinder. Figure 6.5 shows mass conservation versus time for the TH and SV solutions. As expected, the SV solution is divergence-free up to machine precision. The mass conservation offered by the TH solution is very poor.

It is not surprising that the TH solution is much worse than the SV solution. It was shown in [42] that for the rotational form NSE, the Bernoulli pressure error can be large enough to dramatically increase velocity error for this problem. Since NS-$\overline{\omega}$ is also rotational form, this same effect can be expected. However, for the SV solution, as shown herein, the velocity error is independent of the pressure error. Thus even though pressure error may be large, it has no adverse effect on the velocity error, leaving the good solution seen in Figure 6.3.
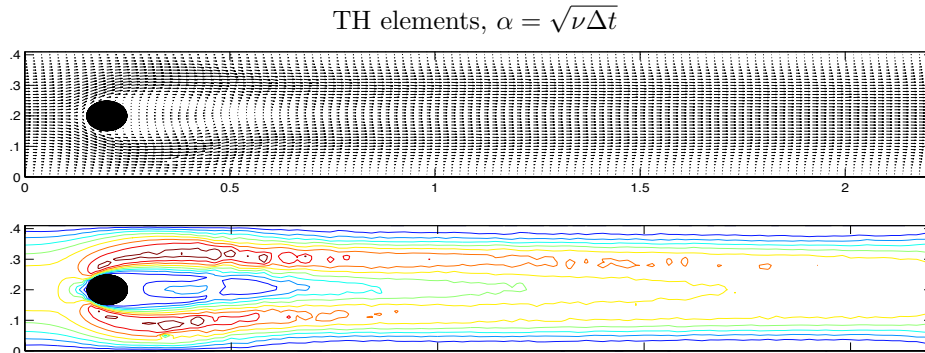


Figure 6.4:  The above picture show the $t = 7$ solution using TH elements, as a velocity vector field and speed contours. This solution is incorrect, as it fails to capture any wake behind the cylinder.

### 6.2.3  Experiment 3: Effect of pressure error on velocity error

In this experiment, we investigate more closely the effect of the pressure error on the velocity error, which caused a dramatic difference between SV and TH solutions in the above experiment of flow around a cylinder. The error analysis in Section 6.1.2 showed that in Algorithm 6.1.1, which uses SV elements, the velocity error is not affected by the pressure error. If TH elements are used, however,
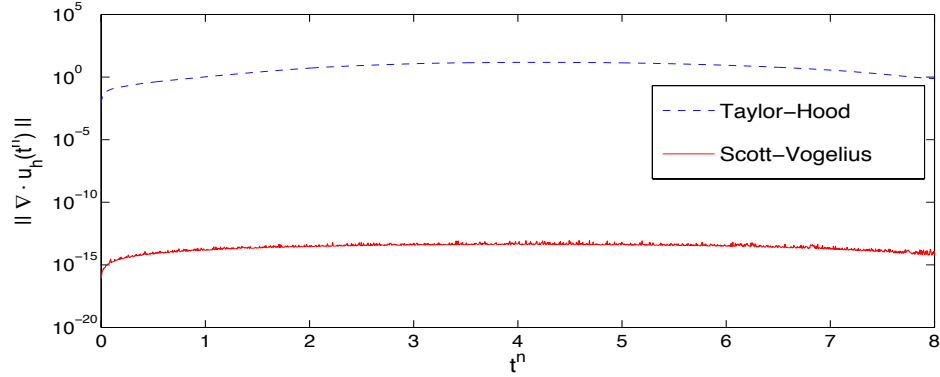
Figure 6.5: Shown above are the plots of the $L^2$ norms of the divergence of the velocity solutions versus time, for the SV and TH solutions, both with $\alpha = \sqrt{\nu \Delta t} = 0.0022$.
As expected, the SV solution is incompressible to near machine precision. The TH solution, however, gives very poor mass conservation.

then the energy error of the velocity can be shown to depend on $C(\nu^{-1})\Delta t \sum_{n=0}^{M-1} \inf_{r_h \in Q_h^{TH}} \|q - r_h\|$, e.g. [44], although the scaling by $C(\nu^{-1})$ of this term can be reduced by using grad-div stabilization [61, 42, 52].

To better demonstrate this effect, we compute Algorithm 6.1.1 with both SV and TH elements, for a series of simple test problems with increasing pressure complexity and the same velocity solution. On the domain, $\Omega = (0,1)^2$ and $0 \le t \le 0.1 = T$, we choose

$$u = (1 + 0.01t) \begin{pmatrix} \cos(y) \\ \sin(x) \end{pmatrix}, \quad p = x + y + \sin(n(x+y)),$$

which will solve the NSE with an appropriate function $f$.

Solutions are approximated to this problem on a quasi-uniform barycenter-refined mesh that provides 12,604 degrees of freedom with $(P_2, P_1^{disc})$ SV elements (7,258 for velocity and 5,364 for pressure) and 8,182 degrees of freedom with $(P_2, P_1)$ TH (7,258 for velocity and 924 for pressure), kinematic viscosity is set to be $\nu = 0.01$, timestep $\Delta t = 0.025$, $\alpha = \sqrt{\nu \Delta t} = 0.0158$, $N = 1$, and the parameter for pressure complexity $n = 0, 1, 2, 3$. The results are shown in Table 6.1, and as expected the error in the SV velocity solution is unaffected by the increase in pressure complexity. However, the TH velocity solution significanty loses accuracy. Also included in the table is the size of the velocity divergence, measured in $L^2(0, T; L^2(\Omega))$. As expected, for the SV solution, near machine epsilon is found for each $n$, but for TH, the quantity is non-negligible and gets significantly worse with increasing pressure complexity.

| $n$ | $\left\|u_{NSE} - u_h^{SV}\right\|_{2,1}$ | $\left\|\nabla \cdot u_h^{SV}\right\|_{2,0}$ | $\left\|u_{NSE} - u_h^{TH}\right\|_{2,1}$ | $\left\|\nabla \cdot u_h^{TH}\right\|_{2,0}$ |
|---|---|---|---|---|
| 0 | 7.332E-5 | 1.106E-14 | 3.075E-3 | 2.775E-3 |
| 1 | 7.332E-5 | 1.167E-14 | 5.315E-3 | 4.763E-3 |
| 2 | 7.332E-5 | 1.102E-14 | 1.716E-2 | 1.533E-2 |
| 3 | 7.330E-5 | 8.724E-15 | 3.584E-2 | 3.235E-2 |

Table 6.1: Errors in velocity and divergence for Experiment 1 for SV and TH elements used with Algorithm 6.1.1.

# Chapter 7

# Leray-deconvolution for MHD

In this chapter we study the Leray-deconvolution model for the MHD. We prove conservation laws for the continuous model, well-posedness, and study limiting behavior as $\alpha \to 0$ and $N \to \infty$. The model is studied in the context of periodic boundary conditions, which are not physically recognized, but restricting to periodic boundary conditions is an important first step in model development. Extensions to homogenous Dirichlet boundary conditions for the velocity (and the regularized velocity) would work in the same way, but such a boundary condition for the regularized velocity is likely not appropriate. To date the correct treatment of other types of boundary conditions for the velocity and the regularized velocity remains an open problem [45].

## 7.0.4   Error, Existence, and Uniqueness of the Continuous Model

The analytical study of the MHD Leray-deconvolution models begins by establishing existence and uniqueness of solutions and an energy balance. We are also interested in the consistency error of the model.

First, we make precise the definition of the MHD Leray-deconvolution model. Let $T > 0$, $f, \nabla \times g \in L^2((0,T); H_p^{-1})$ and $u_0, B_0 \in H_p^0$ be given. Then for $\alpha > 0$ and $0 \leq N < \infty$, the problem is: find $(u, B, p)$ satisfying

$$u, B \quad \in \quad L^2([0,T], H_p^1) \cap L^\infty([0,T]; H_p^0), \tag{7.0.1}$$

$$\frac{\partial u}{\partial t}, \frac{\partial B}{\partial t} \quad \in \quad L^2([0,T]; H_p^{-1}), \tag{7.0.2}$$

$$p \quad \in \quad L^2([0,T]; L_{p,0}^2), \tag{7.0.3}$$

$$\tag{7.0.4}$$

94

and the following relation in a distributional sense

$$\frac{\partial u}{\partial t} + H_N(u) \cdot \nabla u - Re^{-1}\Delta u + \nabla P - sH_N(B) \cdot \nabla B \;=\; f, \tag{7.0.5}$$

$$\frac{\partial B}{\partial t} + H_N(u) \cdot \nabla B - Re_m^{-1}\Delta B - H_N(B) \cdot \nabla u \;=\; \nabla \times g, \tag{7.0.6}$$

$$u(x,0) \;=\; u_0, \tag{7.0.7}$$

$$B(x,0) \;=\; B_0. \tag{7.0.8}$$

Before we study the well-posedness of the model we study the accuracy and show that as $\alpha \to 0$ the asymptotic consistency error is $O(\alpha^{2N+2})$. This is done by rearranging the MHD so that the Leray-$\alpha$ deconvolution model appears on the left, and the residual of the true solution of the MHD in the model on the right. Rearranging gives

$$\frac{\partial u}{\partial t} + H_N(u) \cdot \nabla u - Re^{-1}\Delta u + \nabla P - sH_N(B) \cdot \nabla B - f = \nabla \cdot [H_N(u)u - uu]$$
$$+ s\nabla \cdot [BB - H_N(B)B], \tag{7.0.9}$$

$$\frac{\partial B}{\partial t} + H_N(u) \cdot \nabla B - Re_m^{-1}\Delta B - H_N(B) \cdot \nabla u - \nabla \times g = \nabla \cdot [H_N(u)B - uB]$$
$$+ \nabla \cdot [Bu - H_N(B)u]. \tag{7.0.10}$$

Thus the error tensors in (7.0.9) and (7.0.10), $\tau_1$, and $\tau_2$ respectively are given by

$$\tau_1 \;:=\; H_N(u)u - uu + sBB - H_N(B)B, \tag{7.0.11}$$

$$\tau_2 \;:=\; H_N(u)B - uB + Bu - H_N(B)u. \tag{7.0.12}$$

Adding (7.0.9) and (7.0.10) we see that the MHD Leray-$\alpha$ deconvolution model's consistency error tensor, $\tau$, is

$$\tau := \tau_1 + \tau_2$$

Analysis of modeling error for various models utilizing deconvolution [5, 16, 40, 41], has shown that the error is actually driven by $\tau$ rather than $\nabla \cdot \tau$.

**Theorem 7.0.1.** *The consistency error of the MHD Leray-deconvolution with order $N$ is $O(\alpha^{2N+2})$. That is*

$$\int_\Omega |\tau| dx \leq \alpha^{2N+2} \left( \|\Delta^{N+1}(-\alpha^2\Delta + 1)^{-(N+1)}u\|\|u\| + s\|\Delta^{N+1}(-\alpha^2\Delta + 1)^{-(N+1)}B\|\|B\| \right)$$
$$+ \alpha^{2N+2} \left( \|\Delta^{N+1}(-\alpha^2\Delta + 1)^{-(N+1)}u\|\|B\| + \|\Delta^{N+1}(-\alpha^2\Delta + 1)^{-(N+1)}B\|\|u\| \right).$$

*Proof.* We rewrite (7.0.11) and (7.0.12) to get

$$\tau_1 = (H_N(u) - u)u + s(B - H_N(B))B, \tag{7.0.13}$$

$$\tau_2 = (H_N(u) - u)B + (B - H_N(B))u. \tag{7.0.14}$$

Integrating $|\tau|$ over $\Omega$, using Cauchy-Schwarz, and Lemma 2.0.11 gives

$$\int_\Omega |\tau| dx \leq \alpha^{2N+2} \left( \|\Delta^{N+1} F^{N+1} u\| \|u\| + s\|\Delta^{N+1} F^{N+1} B\| \|B\| \right)$$
$$\alpha^{2N+2} \left( \|\Delta^{N+1} F^{N+1} u\| \|B\| + \|\Delta^{N+1} F^{N+1} B\| \|u\| \right). \tag{7.0.15}$$

Substituting in for the definition of the filter finishes the proof. $\qquad\square$

**Theorem 7.0.2.** *Let $\alpha \geq 0$ and let $N \geq 0$. Assume $u_0, B_0 \in H_p^0$ and $f, \nabla \times g \in L^2([0,T]; H_p^0)$. Then the MHD Leray-deconvolution model admits a unique solution $(u, B, p)$, with $u, B \in L^\infty([0,T]; H_p^1) \cap L^2([0,T]; H_p^2)$. The solution satisfies the integral relation $\forall v, \chi \in V$*

$$\int_0^T (\frac{d}{d\tau} u(\tau), v) d\tau - Re^{-1} \int_0^T (\nabla u(\tau), \nabla v) d\tau + \int_0^T (H_N u(\tau) \cdot \nabla u(\tau), v) d\tau$$
$$-s \int_0^T (H_N B(\tau) \cdot \nabla B(\tau), v) d\tau = \int_0^T (f(\tau), v) d\tau, \tag{7.0.16}$$

$$\int_0^T (\frac{d}{d\tau} B(\tau), \chi) - Re^{-1} \int_0^T (\nabla B(\tau), \nabla \chi) d\tau + \int_0^T (H_N u(\tau) \cdot \nabla B(\tau), \chi) d\tau$$
$$- \int_0^T (H_N B(\tau) \cdot \nabla u(\tau), \chi) d\tau = \int_0^T (\nabla \times g(\tau), \chi) d\tau \tag{7.0.17}$$

*Further, the solution satisfies the regularity*

$$u, B \in L^\infty([0,T]; H_p^1) \cap L^2([0,T]; H_p^2), \tag{7.0.18}$$

*conserves energy*

$$\frac{1}{2} \|u(t)\|^2 + \frac{s}{2} \|B(t)\|^2 + Re^{-1} \int_0^t \int_\Omega \|u\|_1^2 dx d\tau + sRe_m^{-1} \int_0^t \int_\Omega \|B\|_1^2 dx d\tau$$
$$= \frac{1}{2} \|u_0\|^2 + \frac{s}{2} \|B_0\|^2 + \int_0^t \int_\Omega (f, u) dx d\tau + s \int_0^t \int_\Omega (\nabla \times g, B) dx d\tau, \tag{7.0.19}$$

*and conserves cross helicity,*

$$(u(T), B(T)) + \int_0^T (Re^{-1} + Re_m^{-1})(\nabla u, \nabla B) = (u_0, B_0) + \int_0^T (f, B) + \int_0^T (\nabla \times g, u). \tag{7.0.20}$$

96

*Proof.* We prove existence following the Galerkin method, which makes use of the spaces

$$\mathcal{D}(\Omega) \quad := \quad \{u \in C^{\infty}(\Omega) : \text{u is periodic on } \partial\Omega\},$$

$$\mathcal{V} \quad := \quad \{u \in \mathcal{D}(\Omega) : \nabla \cdot u = 0\},$$

$$H \quad := \quad \text{the closure of } \mathcal{V} \text{ in } L^2, \text{ and}$$

$$V \quad := \quad \text{the closure of } \mathcal{V} \text{ in } H^1.$$

The space $V$ is separable and we choose the basis for $V$ to be the eigenfunctions of the Stokes operator, $A$, which we will denote by $\{w_i\}_{i=1}^{\infty}$. We denote the orthogonal projection operator from $H$ onto the space spanned by $w_1, w_2, ..., w_m$ by $P_m$. The Galerkin system of order $m$ corresponding to (7.0.5)-(7.0.8) is thus

$$\frac{d}{dt}u_m + Re^{-1}Au_m + P_m H_N u_m \cdot \nabla u_m - sP_m H_N B_m \cdot \nabla B_m \quad = \quad P_m f_m, \qquad (7.0.21)$$

$$\frac{d}{dt}B_m + Re^{-1}AB_m + P_m H_N u_m \cdot \nabla B_m - P_m H_N B_m \cdot \nabla u_m \quad = \quad P_m \nabla \times g_m, \qquad (7.0.22)$$

$$u_m(0) \quad = \quad P_m u_0, \qquad (7.0.23)$$

$$B_m(0) \quad = \quad P_m B_0. \qquad (7.0.24)$$

Classical results ensure the existence of solutions to the Galerkin system for any finite $m$ on some interval $[0, t_m]$, and that $P_m u_0 \to u_0$ as $m \to \infty$ (see for example [71, 70, 72] ). Our goal is to derive a priori estimates for the Galerkin system that will ensure $t_m = T$, and allow us to pass limits as $m \to \infty$ using the Aubion-Lions Lemma.

We begin deriving the estimates by multiplying (7.0.21) by $u_m$, and multiplying (7.0.22) by $B_m$ to see

$$(\frac{d}{dt}u_m, u_m) + Re^{-1}\|A^{\frac{1}{2}}u_m\|^2 - sP_m(H_N B_m \cdot \nabla B_m, u_m) \quad = \quad (P_m f_m, u_m), \qquad (7.0.25)$$

$$(\frac{d}{dt}B_m, B_m) + Re_m^{-1}\|A^{\frac{1}{2}}B_m\|^2 - P_m(H_N B_m \cdot \nabla u_m, B_m) \quad = \quad (P_m \nabla \times g_m, B_m). \quad (7.0.26)$$

Multiplying (7.0.26) by $s$, adding the result to (7.0.25), and reducing gives

$$(\frac{d}{dt}u_m, u_m) + s(\frac{d}{dt}B_m, B_m) + Re^{-1}\|A^{\frac{1}{2}}u_m\|^2 + sRe_m^{-1}\|A^{\frac{1}{2}}B_m\|^2$$

$$= (P_m f_m, u_m) + s(P_m \nabla \times g_m, B_m). \quad (7.0.27)$$

Integrating (7.0.27) from 0 to $s$, and standard inequalities gives

$$\|u_m(s)\|^2 + \|B_m(s)\|^2$$

$$\leq \|P_m u_0\| + \|P_m B_0\| + 2Re \int_0^s \|f(\tau)\|_{V'}^2 d\tau + 2Re_m \int_0^s \|\nabla \times g(\tau)\|_{V'}^2 d\tau$$

$$\leq \|u_0\| + \|B_0\| + 2Re \int_0^s \|f(\tau)\|_{V'}^2 d\tau + 2Re_m \int_0^s \|\nabla \times g(\tau)\|_{V'}^2 d\tau. \quad (7.0.28)$$

It now follows that

$$\sup_{s \in [0,T]} \|u_m(s)\|^2 \leq \|u_0\| + \|B_0\| + 2Re \int_0^s \|f(\tau)\|_{V'}^2 d\tau + 2Re_m \int_0^s \|\nabla \times g(\tau)\|_{V'}^2 d\tau, \text{ and} \quad (7.0.29)$$

$$\sup_{s \in [0,T]} \|B_m(s)\|^2 \leq \|u_0\| + \|B_0\| + 2Re \int_0^s \|f(\tau)\|_{V'}^2 d\tau + 2Re_m \int_0^s \|\nabla \times g(\tau)\|_{V'}^2 d\tau. \quad (7.0.30)$$

Thus, the sequences $u_m$ and $B_m$ remain in a bounded set of $L^\infty([0,T];H)$. We now integrate (7.0.27) from 0 to $T$ to get

$$Re^{-1} \int_0^T \|A^{\frac{1}{2}} u_m(\tau)\|^2 d\tau + sRe_m^{-1} \int_0^T \|A^{\frac{1}{2}} B_m(\tau)\|^2 d\tau$$

$$\leq \|u_0\|^2 + s\|B_0\| + Re \int_0^T \|f(\tau)\|_{V'}^2 d\tau + sRe_m \int_0^T \|\nabla \times g(\tau)\|_{V'}^2 d\tau. \quad (7.0.31)$$

This estimate shows the sequences $u_m$ and $B_m$ remain in a bounded set of $L^2([0,T];V)$.

To pass the limit as $m \to \infty$ we use the Aubion-Lions Lemma, which requires us to derive bounds for $\frac{d}{dt} u_m$ and $\frac{d}{dt} B_m$. Rearranging (7.0.21) and (7.0.22) gives

$$\frac{d}{dt} u_m = -Re^{-1} A u_m - P_m H_N u_m \cdot \nabla u_m + s P_m H_N B_m \cdot \nabla B_m + P_m f_m, \quad (7.0.32)$$

$$\frac{d}{dt} B_m = -Re^{-1} A B_m - P_m H_N u_m \cdot \nabla B_m + P_m H_N B_m \cdot \nabla u_m - P_m \nabla \times g_m. \quad (7.0.33)$$

We argue that $\frac{d}{dt} u_m$ and $\frac{d}{dt} B_m$ remain in a bounded set in $L^{\frac{4}{3}}([0,T];V')$. It is clear that $P_m f_m$, $P_m \nabla \times g_m$, $A u_m$, and $A B_m$ are in $L^{\frac{4}{3}}([0,T];V')$. So, we argue the nonlinear terms satisfy the desired regularity. We begin by majorizing the first nonlinear term in (7.0.32) as follows

$$s|P_m H_N B_m \cdot \nabla B_m| \leq \|P_m H_N B_m\|^{\frac{1}{2}} \|\nabla B_m\|^{\frac{3}{2}}$$

$$\leq C(N) \|B_m\|^{\frac{1}{2}} \|\nabla B_m\|^{\frac{3}{2}}$$

$$\implies s|P_m H_N B_m \cdot \nabla B_m|^{\frac{4}{3}} \leq C(N) \|B_m\| \|\nabla B_m\|^2 \quad (7.0.34)$$

It now follows from the boundedness of $B_m$ in $L^\infty([0,T];H)$, and integrating (7.0.34) from 0 to $T$

98

that

$$s \int_0^T |P_m H_N B_m(\tau) \cdot \nabla B_m(\tau)|^{\frac{4}{3}} d\tau \leq C(N) \int_0^T \|\nabla B_m(\tau)\|^2 d\tau. \qquad (7.0.35)$$

The remaining nonlinear terms can be shown to satisfy the desired regularity similarly. Thus, we may conclude that $\frac{d}{dt} u_m$ and $\frac{d}{dt} B_m$ remain in a bounded set of $L^{\frac{4}{3}}([0,T]; H')$.

At this point we have argued sufficient regularity to use the Aubion-Lions Lemma and show solutions exist. However, the regularity we have established so far will not allow us to show that solutions are unique. Nor will it allow us to show that the solutions conserve energy and cross-helicity. These properties require more regularity of solutions and so we now establish that $u_m$ and $B_m$ are in $L^\infty([0,T]; V) \cap L^2([0,T]; H_p^2)$. We begin deriving the estimates by multiplying (7.0.21) by $Au_m$, and multiplying (7.0.22) by $AB_m$ to see

$$\frac{d}{dt} \|A^{\frac{1}{2}} u_m\|^2 + Re^{-1} \|Au_m\|^2 - sP_m(H_N B_m \cdot \nabla B_m, Au_m) = (P_m f_m, Au_m), \qquad (7.0.36)$$

$$\frac{d}{dt} \|A^{\frac{1}{2}} B_m\|^2 + Re_m^{-1} \|A^2 B_m\|^2 - P_m(H_N B_m \cdot \nabla u_m, AB_m) = (P_m \nabla \times g_m, AB_m). \qquad (7.0.37)$$

Adding (7.0.36) to (7.0.37) and applying Young's inequality gives

$$\frac{1}{2} \frac{d}{dt} \|A^{\frac{1}{2}} u_m\|^2 + \frac{1}{2} \frac{d}{dt} \|A^{\frac{1}{2}} B_m\|^2 + \frac{5Re^{-1}}{6} \|Au_m\|^2 + \frac{5Re_m^{-1}}{6} \|AB_m\|^2$$
$$\leq CRe\|f\|^2 + CRe_m \|\nabla \times g\|^2 - (H_N u_m \cdot \nabla B_m, AB_m)$$
$$+ (H_N B_m \cdot \nabla u_m, AB_m) - (H_N u_m \cdot \nabla u_m, Au_m) + s(H_N B_m \cdot \nabla B_m, Au_m). \qquad (7.0.38)$$

We now bound the first nonlinear term in (7.0.38) using standard bounds on the nonlinearity and Agmon's inequality as follows:

$$|(H_N u_m \cdot \nabla B_m, AB_m)| \leq \|H_N u_m\|_\infty \|A^{\frac{1}{2}} B_m\| \|AB_m\|$$
$$\leq \|H_N u_m\|_{H^2} \|A^{\frac{1}{2}} B_m\| \|AB_m\|. \qquad (7.0.39)$$

Note that the last inequality in (7.0.39) makes sense because of the regularity of $u$ and Lemma 2.0.14. Applying Young's inequality gives

$$|(H_N u_m \cdot \nabla B_m, AB_m)| \leq CRe\|H_N u_m\|_{H^2}^2 \|A^{\frac{1}{2}} B_m\|^2 + \frac{Re^{-1}}{6} \|AB_m\|^2. \qquad (7.0.40)$$

Similar treatment of the remaining nonlinear terms of (7.0.38) and rearranging gives

$$
\frac{1}{2}\frac{d}{dt}\|A^{\frac{1}{2}}u_m\|^2 + \frac{1}{2}\frac{d}{dt}\|A^{\frac{1}{2}}B_m\|^2 + \frac{Re^{-1}}{2}\|Au_m\|^2 + \frac{Re_m^{-1}}{2}\|AB_m\|^2
$$

$$
\leq CRe\|f\|^2 + CRe_m\|\nabla \times g\|^2 + CRe_m\|H_N u_m\|_{H^2}^2\|A^{\frac{1}{2}}B_m\|^2 + CRe_m\|H_N B_m\|_{H^2}^2\|A^{\frac{1}{2}}u_m\|^2
$$

$$
+ CRe\|H_N u_m\|_{H^2}^2\|A^{\frac{1}{2}}u_m\|^2 + CRe\|H_N B_m\|_{H^2}^2\|A^{\frac{1}{2}}B_m\|^2. \quad (7.0.41)
$$

We now consider two cases,

$$
\text{Case 1:} \quad \|A^{\frac{1}{2}}u_m\|^2 + \|A^{\frac{1}{2}}B_m\|^2 < 1, \text{ and}
$$

$$
\text{Case 2:} \quad \|A^{\frac{1}{2}}u_m\|^2 + \|A^{\frac{1}{2}}B_m\|^2 \geq 1.
$$

If $\|A^{\frac{1}{2}}u_m\|^2 + \|A^{\frac{1}{2}}B_m\|^2 < 1$ then

$$
\frac{1}{2}\frac{d}{dt}\|A^{\frac{1}{2}}u_m\|^2 + \frac{1}{2}\frac{d}{dt}\|A^{\frac{1}{2}}B_m\|^2 \leq CRe\|f\|^2 + CRe_m\|\nabla \times g\|^2
$$

$$
+ CRe_m\|H_N u_m\|_{H^2}^2 + CRe_m\|H_N B_m\|_{H^2}^2 + CRe\|H_N u_m\|_{H^2}^2 + CRe\|H_N B_m\|_{H^2}^2. \quad (7.0.42)
$$

Integrating (7.0.42) from 0 to $t$ gives

$$
\|A^{\frac{1}{2}}u_m(t)\|^2 + \|A^{\frac{1}{2}}B_m(t)\|^2 \leq \int_0^t CRe\|f(\tau)\|^2 d\tau \int_0^t + CRe_m\|\nabla \times g(\tau)\|^2 d\tau
$$

$$
+ CRe_m \int_0^t \|H_N u_m(\tau)\|_{H^2}^2 d\tau + CRe_m \int_0^t \|H_N B_m(\tau)\|_{H^2}^2 d\tau
$$

$$
+ CRe \int_0^t \|H_N u_m(\tau)\|_{H^2}^2 d\tau + CRe \int_0^t \|H_N B_m(\tau)\|_{H^2}^2 d\tau \quad (7.0.43)
$$

Taking a supremum over $t \in [0, T]$ ensures $u, B_m \in L^\infty([0, T]; V)$.

We now consider the case when $\|A^{\frac{1}{2}}u_m\|^2 + \|A^{\frac{1}{2}}B_m\|^2 \geq 1$. Let $\nu^* = \max(Re, Re_m)$. The assumption $\|A^{\frac{1}{2}}u_m\|^2 + \|A^{\frac{1}{2}}B_m\|^2 \geq 1$ implies

$$
\frac{1}{2}\frac{d}{dt}\|A^{\frac{1}{2}}u_m\|^2 + \frac{1}{2}\frac{d}{dt}\|A^{\frac{1}{2}}B_m\|^2 \leq
$$

$$
C\nu^* \max\{(\|f\|^2 + \|\nabla \times g\|^2), (\|H_N u_m\|_{H^2}^2 + \|H_N B_m\|_{H^2}^2)\}(\|A^{\frac{1}{2}}u_m\|^2 + \|A^{\frac{1}{2}}B_m\|^2). \quad (7.0.44)
$$

Integrating from 0 to $t$ and using Gronwalls inequality gives

$$\|A^{\frac{1}{2}}u_m(t)\|^2 + \|A^{\frac{1}{2}}B_m(t)\|^2 \leq$$

$$(\|A^{\frac{1}{2}}u_m(0)\|^2 + \|A^{\frac{1}{2}}B_m(0)\|^2)\exp(\int_0^t C\nu \max\{(\|f\|^2 + \|\nabla \times g\|^2), (\|H_N u_m\|_{H^2}^2 + \|H_N B_m\|_{H^2}^2)\}).$$

$$(7.0.45)$$

Thus, we have shown that $u_m, B_m \in L^\infty([0,T]; V)$. Integrating (7.0.41) from 0 to $T$ and using $u_m, B_m \in L^\infty([0,T]; V)$ implies $u_m, B_m \in L^2([0,T]; H_p^2 \cap V)$. The Aubion-Lions Lemma implies the existence of $u, B \in L^\infty([0,T]; V) \cap L^2([0,T]; H_p^2 \cap V)$ with subsequence $u_{m_j}$ and $B_{m_j}$ so that

$$u_{m_j} \rightarrow u \text{ weakly in } L^2([0,T]; D(A)),$$

$$u_{m_j} \rightarrow u \text{ strongly in } L^2([0,T]; V),$$

$$B_{m_j} \rightarrow B \text{ weakly in } L^2([0,T]; D(A)), \text{ and}$$

$$B_{m_j} \rightarrow B \text{ strongly in } L^2([0,T]; V).$$

$$(7.0.46)$$

We now show the solution is unique. Assume there are two solutions $(u_1, B_1)$ and $(u_2, B_2)$. The solutions satisfy

$$\frac{d}{dt}u_1 - Re^{-1}\Delta u_1 = -H_N u_1 \cdot \nabla u_1 + sH_N B_1 \cdot \nabla B_1 + f, \qquad (7.0.47)$$

$$\frac{d}{dt}B_1 - Re_m^{-1}\Delta B_1 = -H_N u_1 \cdot \nabla B_1 + H_N B_1 \cdot \nabla u_1 + \nabla \times g, \qquad (7.0.48)$$

$$\frac{d}{dt}u_2 - Re^{-1}\Delta u_2 = -H_N u_2 \cdot \nabla u_2 + sH_N B_2 \cdot \nabla B_2 + f, \qquad (7.0.49)$$

$$\frac{d}{dt}B_2 - Re_m^{-1}\Delta B_2 = -H_N u_2 \cdot \nabla B_2 + H_N B_2 \cdot \nabla u_2 + \nabla \times g. \qquad (7.0.50)$$

Let $e_u := u_1 - u_2$ and $e_b := B_1 - B_2$. Subtracting (7.0.50) from (7.0.49), and (7.0.48) from (7.0.47), and rearranging the nonlinear terms gives

$$\frac{d}{dt}e_u - Re^{-1}\Delta e_u = -H_N u_2 \cdot \nabla e_u - H_N e_u \cdot \nabla u_1$$

$$+sH_N B_1 \cdot \nabla e_B + sH_N e_B \cdot \nabla B_2, \qquad (7.0.51)$$

$$\frac{d}{dt}e_B - Re_m^{-1}\Delta e_B = -H_N u_2 \cdot \nabla e_B - H_N e_u \cdot \nabla B_1$$

$$+H_N B_1 \cdot \nabla e_u + H_N e_B \cdot \nabla u_2. \qquad (7.0.52)$$

101

Multiplying (7.0.51) by $e_u$, and (7.0.52) by $e_B$, and reducing gives

$$\frac{1}{2}\frac{d}{dt}\|e_u\|^2 + Re^{-1}\|\nabla u\|^2 = -(H_N e_u \cdot \nabla u_1, e_u) + s(H_N B_1 \cdot \nabla e_B, e_u)$$

$$+ s(H_N e_B \cdot \nabla B_2, e_u) \quad (7.0.53)$$

$$\frac{1}{2}\frac{d}{dt}\|e_B\|^2 + Re_m^{-1}\|\nabla B\|^2 = -(H_N e_u \cdot \nabla B_1, e_B) + (H_N B_1 \cdot \nabla e_u, e_B)$$

$$+ (H_N e_B \cdot \nabla u_2, e_B). \quad (7.0.54)$$

Scaling (7.0.54) by $s$ and adding the result to (7.0.53) and reducing gives

$$\frac{1}{2}\frac{d}{dt}\|e_u\|^2 + \frac{1}{2}\frac{d}{dt}\|e_B\|^2 + Re^{-1}\|\nabla u\|^2 + Re_m^{-1}\|\nabla B\|^2 =$$

$$- (H_N e_u \cdot \nabla u_1, e_u) + (H_N e_B \cdot \nabla B_2, e_u)$$

$$- s(H_N e_u \cdot \nabla B_1, e_B) + s(H_N e_B \cdot \nabla u_2, e_B). \quad (7.0.55)$$

We majorize the first nonlinear term in (7.0.55) using standard inequalities and the regularity of $u_1$ as follows

$$
\begin{aligned}
|(H_N e_u \cdot \nabla u_1, e_u)| &\leq \|H_N e_u\|\|\nabla u_1\|\|e_u\| \\
&\leq C(N, u_1, Re)\|e_u\|^2 + \frac{Re^{-1}}{4}\|\nabla e_u\|^2. \quad (7.0.56)
\end{aligned}
$$

Similar treatment of the remaining nonlinear terms and rearranging gives

$$\frac{d}{dt}\|e_u\|^2 + \frac{d}{dt}\|e_B\|^2 \leq C(N, u_1, u_2, B_1, B_2, Re, Re_m, s)(\|e_u\|^2 + \|e_B\|^2). \quad (7.0.57)$$

Gronwalls inequality finishes the proof of uniqueness. $\qquad\square$

**Remark 7.0.1.** *The energy and cross-helicity balances of the model are a result of the strong convergence of $u_{m_j}$ to $u$ and $B_{m_j}$ to $B$ in $L^2([0, T]; V)$. This allows us to pass limits in the Galerkin system which have energy and cross-helicity balances. If we tried to construct a proof similar to the one above to show energy and cross helicity conservation for the 3d MHD the proof would fail at (7.0.39). Thus, for the MHD Galerkin system we can only show strong convergence in $L^2([0, T]; H)$. Hence we would not be able to pass a limit in terms like $\|\nabla u_{m_j}\|$. Instead we can only argue an inequality using $\|\nabla u\| \leq \liminf_{j \to \infty} \|\nabla u_{m_j}\|$, and other such inequalities.*

### 7.0.5   Limiting behavior

Theorem 7.0.2 states that solutions to the Leray-deconvolution model exist uniquely, provided $\alpha > 0$, and $0 \leq N < \infty$, and that the model conserves energy and cross helicity for ideal MHD. Considering the model as a way to understand the MHD equations, it is natural to study behavior of the model as $\alpha \to 0$ with $N$ fixed. If $N$ is fixed to be 0, then the model is the Leray-$\alpha$ MHD model and Yu and Li [75] proved that as $\alpha \to 0$ there is a subsequence of solutions to the Leray$-\alpha$ model which converges to a weak solution of the MHD.

Computationally, the Leray-deconvolution model is $O(\alpha^{2N+2} + \Delta t^2 + h^k)$ accurate (see Theorem 7.1.2). When computing with the model the filtering radius, $\alpha$, is chosen to be on the order of $h$, the mesh width. Thus, to improve accuracy one may either shrink $\alpha$ or increase $N$. The first approach requires using a finer mesh, which increases the total degrees of freedom and thus increases the runtime. However, increasing $N$ only requires us to solve one more shifted Poisson problem per deconvolution step. This leads one to study the behavior of the model when $N \to \infty$ while $\alpha$ remains constant. This was studied by Layton and Lewandowski for the Leray-Deconvolution model of the NSE [41].

**Theorem 7.0.3.** *Let $\alpha > 0$ be fixed, and assume that $f, g \in L^2((0,T]; H_p^0(\Omega))$ and $u_0, B_0 \in H_p^0(\Omega)$. Let $(u_N, B_N, p)$ denote the solution to (7.0.5)-(7.0.8) for $N > 0$. Then there exist subsequences $\{u_{N_j}\}_{j \in \mathbb{N}}$ of $\{u_N\}_{N \in \mathbb{N}}$ and $\{B_{N_j}\}_{j \in \mathbb{N}}$ of $\{B_N\}_{N \in \mathbb{N}}$ as $N \to \infty$ such that $(u_{N_j}, B_{N_j})$ converge to $(u, B)$, the weak solutions of the MHD equations. The convergence is weak in $L^2((0,T]; H_p^1(\Omega))$ and strong in $L^2((0,T]; H_p^0(\Omega))$.*

*Proof.* This proof requires the use of the Aubion-Lions Lemma and so we must argue regularity of the solutions. It follows immediately from Theorem 7.0.2 that $u_N$ and $B_N$ are bounded in $L^2([0,T]; V) \cap L^\infty([0,T]; H)$, and that $\frac{\partial}{\partial t} u_j, \frac{\partial}{\partial t} B_j \in L^{\frac{4}{3}}([0,T]; H_p^{-1}(\Omega))$. With the established regularity we may use the Aubion-Lions Lemma to extract subsequences, which we continue to denote by $\{u_j\}_{j \in \mathbb{N}}$ and $\{B_j\}_{j \in \mathbb{N}}$, which converge to functions $u$ and $B$ respectively, and that $u, B \in L^2([0,T]; H_p^1(\Omega)) \cap L^\infty([0,T]; H_p^0(\Omega))$ [4, 41, 72]. The convergence is strong in $L^2([0,T]; H_p^0(\Omega))$ and weak in $L^2([0,T]; H_p^1(\Omega))$.

We next verify that $u, B$ satisfy the integral relation $\forall v, \chi \in V$

$$\int_0^T (\frac{d}{d\tau} u(\tau), v) d\tau - Re^{-1} \int_0^T (\nabla u(\tau), \nabla v) d\tau + \int_0^T (u(\tau) \cdot \nabla u(\tau), v) d\tau$$

$$-s \int_0^T (B(\tau) \cdot \nabla B(\tau), v) d\tau = \int_0^T (f(\tau), v) d\tau, \quad (7.0.58)$$

$$\int_0^T (\frac{d}{d\tau} B(\tau), \chi) - Re^{-1} \int_0^T (\nabla B(\tau), \nabla \chi) d\tau + \int_0^T (u(\tau) \cdot \nabla B(\tau), \chi) d\tau$$

$$- \int_0^T (B(\tau) \cdot \nabla u(\tau), \chi) d\tau = \int_0^T (\nabla \times g(\tau), \chi) d\tau. \quad (7.0.59)$$

We now show the solutions satisfy $\forall v, \chi \in V$

$$\int_0^T (\partial_t u_j, v) = \int_0^T Re^{-1} (\nabla u_j(\tau), \nabla v) d\tau - \int_0^T b(H_{N_j} u_j(\tau), u_j(\tau), v) d\tau$$

$$+s \int_0^T (H_{N_j} B_j(\tau) \cdot \nabla B_j(\tau), v) d\tau + \int_0^T (f(\tau), v) d\tau, (7.0.60)$$

$$\int_0^T (\partial_t B_j, \chi) = \int_0^T Re_m^{-1} (\nabla B_j(\tau), \nabla \chi) d\tau - \int_0^T b(H_{N_j} u_j(\tau), B_j(\tau), \chi) d\tau$$

$$+s \int_0^T (H_{N_j} B_j(\tau) \cdot \nabla u_j(\tau), \chi) d\tau + \int_0^T (\nabla \times g(\tau), \chi) d\tau. (7.0.61)$$

It is obvious that we may pass to limits in the linear terms, and so we restrict attention to the nonlinear terms. For the first nonlinear term in (7.0.60) we have

$$\left| \int_0^T b(H_{N_j} u_j, u_j, v) - \int_0^T b(u, u, v) \right| \leq \left| \int_0^T b(H_{N_j} u_j, (u_j - u), v) \right|$$

$$+ \left| \int_0^T b((H_{N_j} u_j - u)u, v) \right| \quad (7.0.62)$$

We majorize (7.0.62) with (2.0.11) and (2.0.13) and then apply Cauchy-Schwarz which gives

$$\left| \int_0^T b(H_{N_j} u_j, u_j, v) - \int_0^T b(u, u, v) \right|$$

$$\leq C \|v\|_2 \{ \int_0^T \|H_{N_j} u_j\|_1 \|(u_j - u)\| + \int_0^T \|(H_{N_j} u_j - u)\| \|u\|_1 \}$$

$$\leq C \|v\|_2 \{ (\int_0^T \|H_{N_j} u_j\|_1^2)^{\frac{1}{2}} \int_0^T (\|u_j - u\|^2)^{\frac{1}{2}}$$

$$+ \int_0^T (\|H_{N_j}(u_j - u)\|^2)^{\frac{1}{2}} (\int_0^T (\|u\|_1^2)^{\frac{1}{2}} + (\int_0^T \|(H_{N_j} u - u)\|^2)^{\frac{1}{2}} \int_0^T (\|u\|_1^2)^{\frac{1}{2}} \}. \quad (7.0.63)$$

It follows from Lemma 2.0.14 and the strong convergence of $u_j$ to $u$ in $L^2([0, T]; H_p^0(\Omega))$ that the RHS of (7.0.63) goes to zero as $j \to \infty$.

The second nonlinear term in (7.0.60) is treated the same way as the first nonlinear term. The behavior of the nonlinear terms in (7.0.61) is less clear because each have a magnetic component and a velocity component, so, we focus on the first nonlinear term in (7.0.61):

$$\left| \int_0^T b(H_{N_j} u_j, B_j, \chi) - \int_0^T (u, B, \chi) \right|$$

$$\leq \left| \int_0^T b(H_{N_j} u_j, (B_j - B), \chi) \right| + \left| \int_0^T b((H_{N_j} u_j - u), B, \chi) \right|$$

$$\leq C\|\chi\|_2 \{ \int_0^T \|H_{N_j} u_j\|_1 \|(B_j - B)\| + \int_0^T \|(H_{N_j} u_j - u)\| \|B\|_1 \} \quad (7.0.64)$$

The nonlinearity is now bounded the same way as before with (2.0.11), (2.0.13) and Cauchy-Schwarz.

$\square$

**Theorem 7.0.4.** *Let $N \geq 0$ be fixed, and assume that $f, g \in L^2([0,T]; H_p^{-1}(\Omega))$ and $u_0, B_0 \in H_p^0(\Omega)$. Let $(u_\alpha, B_\alpha, p)$ denote the solution to (7.0.5)-(7.0.8) for $\alpha > 0$. Then there exist subsequences $\{u_{\alpha_j}\}_{j \in \mathbb{N}}$ of $\{u_\alpha\}_{\alpha \in \mathbb{R}}$ and $\{B_{\alpha_j}\}_{j \in \mathbb{N}}$ of $\{B_\alpha\}_{\alpha \in \mathbb{R}}$ as $\alpha \to 0^+$ such that $(u_{\alpha_j}, B_{\alpha_j})$ converge to $(u, B)$, the weak solutions of the MHD equations. The convergence is weak in $L^2((0,T); H_p^1(\Omega))$ and strong in $L^2((0,T]; H_p^0(\Omega))$.*

*Proof.* The proof of Theorem 7.0.4 follows immediately from the limiting behavior proof for the Leray-$\alpha$ model for the MHD equations done in [75] and Lemma 2.0.11. $\square$

## 7.1 A Numerical Scheme for the Leray-deconvolution model for MHD

In this section we present a numerical scheme for the Leray-deconvolution model of the MHD equations. The numerical scheme is derived with a Galerkin finite element discretization in space and a Crank-Nicolson discretization in time. We show that the method is well-posed, conserves energy and cross helicity, is unconditionally stable with respect to timestep, and is optimally convergent. Additionally, we study the numerical scheme with the Scott-Vogelius (SV) element pair which enforces strong mass and electrical charge conservation.

### 7.1.1 The numerical scheme

We are now ready to introduce the numerical scheme for the model (7.0.5)-(7.0.8). Following [3, 10, 43] we have found it advantageous to linearize the scheme in a manner that maintains stability,

asymptotic accuracy, and conservation laws. This is done by approximating the first term in the nonlinearities with a second order accurate in time extrapolation. Let $\tilde{U}_h^n := \frac{3}{2}u_h^n - \frac{1}{2}u_h^{n-1}$ and $\tilde{B}_h^n := \frac{3}{2}B_h^n - \frac{1}{2}B_h^{n-1}$.

**Algorithm 7.1.1.** *Assume the initial conditions are divergence free, i.e.* $u_h^0$, $B_h^0 \in V_h$. *Then the linearized scheme at each time step is given by,* $\forall(v_h, \chi_h, q_h, r_h) \in (X_h, X_h, Q_h, Q_h)$

$$\frac{1}{\Delta t}(u_h^{n+1} - u_h^n, v_h) + b(D_N^h\overline{\tilde{U}_h^n}^h, u_h^{n+\frac{1}{2}}, v_h) + Re^{-1}(\nabla u_h^{n+\frac{1}{2}}, \nabla v_h)$$
$$-sb(D_N^h\overline{\tilde{B}_h^n}^h, B_h^{n+\frac{1}{2}}, v_h) - (P_h^{n+\frac{1}{2}}, \nabla \cdot v_h) = (f(t^{n+\frac{1}{2}}), v_h), \tag{7.1.1}$$

$$(\nabla \cdot u_h^{n+1}, q_h) = 0, \tag{7.1.2}$$

$$\frac{1}{\Delta t}(B_h^{n+1} - B_h^n, \chi_h) + Re_m^{-1}(\nabla B_h^{n+\frac{1}{2}}, \nabla \chi_h) - b(D_N^h\overline{\tilde{B}_h^n}^h, u_h^{n+\frac{1}{2}}, \chi_h)$$
$$+b(D_N^h\overline{\tilde{U}_h^n}^h, B_h^{n+\frac{1}{2}}, \chi_h) + (\lambda_h^{n+\frac{1}{2}}, \nabla \cdot \chi_h) = (\nabla \times g(t^{n+\frac{1}{2}}), \chi_h), \tag{7.1.3}$$

$$(\nabla \cdot B_h^{n+1}, \chi_h) = 0. \tag{7.1.4}$$

*It is sufficient to maintain all the theoretical results to define* $u_h^{-1} := u_h^0$ *and* $B_h^{-1} := B_h^0$.

Here $P_h^{n+1} := p_h^{n+1} + \frac{s}{2}|B_h^{n+1}|^2$ is a modified pressure derived from the vector identity

$$\Delta B = -\nabla \times (\nabla \times B) + \nabla(\nabla \cdot B),$$

and $\lambda_h^{n+1} := Re_m\nabla \cdot B_h^{n+1}$ is a Lagrange multiplier.

**Remark 7.1.1.** *Extrapolating the nonlinearities in the scheme is computationally attractive as it makes the scheme linear, and decouples the filtering and deconvolution. Thus, the velocity and magnetic fields may be filtered independently of each other. These are fast solves when compared to the full MHD system. Thus, the extra solves required to implement the Leray-α deconvolution model with $N = 1$ do not significantly increase the run time over DNS.*

**Theorem 7.1.1.** *Assuming* $f, \nabla \times g \in L^2((0, T), V'(\Omega))$, *solutions to (7.1.1)-(7.1.4) exist at each timestep. Further, the scheme is unconditionally stable and satisfies the a priori bound:*

$$\left(\|u_h^M\|^2 + s\|B_h^M\|^2\right) + \Delta t \sum_{n=0}^{M-1}(Re^{-1}\|u_h^{n+\frac{1}{2}}\|_1^2 + sRe_m^{-1}\|B_h^{n+\frac{1}{2}}\|_1^2)$$

$$\leq \left(\|u_h^0\|^2 + s\|B_h^0\|^2\right) + \Delta t \sum_{n=0}^{M-1}(Re\|f(t^{n+\frac{1}{2}})\|_{V'} + sRe_m\|g(t^{n+\frac{1}{2}})\|^2) \tag{7.1.5}$$

**Remark 7.1.2.** *Existence of solutions to (7.1.1)-(7.1.4) follows directly from the stability estimate*

and is a straightforward extension of the work done in [10]. The a priori bound can be derived from the following energy conservation lemma by applying standard inequalities.

**Lemma 7.1.1.** *Solutions to* (7.1.1)-(7.1.4) *admit the following conservation laws*

- *Mass conservation*

$$\nabla \cdot u_h^n = 0 \text{ (pointwise)}$$

- *Incompressibility of the magnetic field*

$$\nabla \cdot B_h^n = 0 \text{ (pointwise)}$$

- *Global energy conservation*

$$\left(\frac{1}{2}\|u_h^M\|^2 + \frac{s}{2}\|B_h^M\|^2\right) + \Delta t \sum_{n=0}^{M-1} (Re^{-1}\|u_h^{n+\frac{1}{2}}\|_1^2 + sRe_m^{-1}\|B_h^{n+\frac{1}{2}}\|_1^2)$$

$$= \left(\frac{1}{2}\|u_h^0\|^2 + \frac{s}{2}\|B_h^0\|^2\right) + \Delta t \sum_{n=0}^{M-1} \left((f(t^{n+\frac{1}{2}}), u_h^{n+\frac{1}{2}}) + s(\nabla \times g(t^{n+\frac{1}{2}}), B_h^{n+\frac{1}{2}})\right) \quad (7.1.6)$$

- *Global cross-helicity conservation*

$$(u_h^M, B_h^M) + \Delta t \sum_{n=0}^{M-1} \left((Re^{-1} + Re_m^{-1})(\nabla u_h^{n+\frac{1}{2}}, \nabla B_h^{n+\frac{1}{2}})\right)$$

$$= (u_h^0, B_h^0) + \Delta t \sum_{n=0}^{M-1} \left((\nabla \times g(t^{n+\frac{1}{2}}), u_h^{n+\frac{1}{2}}) + (f(t^{n+\frac{1}{2}}), B_h^{n+\frac{1}{2}})\right) \quad (7.1.7)$$

*Proof.* To prove pointwise mass conservation and incompressibility of the magnetic field, we note that for Scott-Vogelius elements $\nabla \cdot X^h \subseteq Q^h$. Thus, we may choose $q_h$ in (7.1.2) to be $u_h^{n+1}$ and we may choose $r_h$ in (7.1.4) to be $B_h^{n+1}$. The results now follow.

To prove energy conservation we chose $v_h = u_h^{n+\frac{1}{2}}$ in (7.1.1) and $\chi_h = B_h^{n+\frac{1}{2}}$ in (7.1.3). This annihilates the first nonlinear term in (7.1.1) as well as the pressure term. In (7.1.3), this annihilates the second nonlinear terms and the Lagrange multiplier term. This leaves

$$\frac{1}{2\Delta t}(\|u_h^{n+1}\|^2 - \|u_h^n\|^2) + Re^{-1}\|u_h^{n+\frac{1}{2}}\|_1^2 - sb(D_N^h \overline{\tilde{B}_h^n}^h, B_h^{n+\frac{1}{2}}, u_h^{n+\frac{1}{2}})$$
$$= (f(t^{n+\frac{1}{2}}), u_h^{n+\frac{1}{2}}), \quad (7.1.8)$$

$$\frac{1}{2\Delta t}(\|B_h^{n+1}\|^2 - \|B_h^n\|^2) + Re_m^{-1}\|B_h^{n+\frac{1}{2}}\|_1^2 - b(D_N^h \overline{\tilde{B}_h^n}^h, u_h^{n+\frac{1}{2}}, B_h^{n+\frac{1}{2}})$$
$$= (\nabla \times g(t^{n+\frac{1}{2}}), B_h^{n+\frac{1}{2}}). \quad (7.1.9)$$

107

Next, scale (7.1.9) by $s$, add (7.1.8) to (7.1.9), and rewrite the nonlinear term in (7.1.8) using (2.0.11). This gives

$$\frac{1}{2\Delta t}(\|u_h^{n+1}\|^2 - \|u_h^n\|^2) + \frac{s}{2\Delta t}(\|B_h^{n+1}\|^2 - \|B_h^n\|^2) + Re^{-1}\|u_h^{n+\frac{1}{2}}\|_1^2$$
$$+ sRe_m^{-1}\|B_h^{n+\frac{1}{2}}\|_1^2 = (f(t^{n+\frac{1}{2}}), u_h^{n+\frac{1}{2}}) + s(\nabla \times g(t^{n+\frac{1}{2}}), B_h^{n+\frac{1}{2}}).$$

To finish the the proof of (7.1.6) we multiply by $\Delta t$, and sum over timesteps.

To prove cross helicity is conserved, we begin by choosing $v_h = B_h^{n+\frac{1}{2}}$ in (7.1.1) which annihilates the fourth and fifth terms. Next we choose $\chi_h = u_h^{n+\frac{1}{2}}$ in (7.1.3) which annihilates the third and fifth terms. What remains is

$$\frac{1}{\Delta t}(u_h^{n+1} - u_h^n, B_h^{n+\frac{1}{2}}) + b(D_N^h \overline{\tilde{U}_h^n}^h, u_h^{n+\frac{1}{2}}, B_h^{n+\frac{1}{2}}) + Re^{-1}(\nabla u_h^{n+\frac{1}{2}}, \nabla B_h^{n+\frac{1}{2}})$$
$$= (f(t^{n+\frac{1}{2}}), B_h^{n+\frac{1}{2}}), \qquad (7.1.10)$$
$$\frac{1}{\Delta t}(B_h^{n+1} - B_h^n, u_h^{n+\frac{1}{2}}) + Re_m^{-1}(\nabla B_h^{n+\frac{1}{2}}, \nabla u_h^{n+\frac{1}{2}}) + b(D_N^h \overline{\tilde{U}_h^n}^h, B_h^{n+\frac{1}{2}}, u_h^{n+\frac{1}{2}})$$
$$= (\nabla \times g(t^{n+\frac{1}{2}}), u_h^{n+\frac{1}{2}}). \qquad (7.1.11)$$

Adding (7.1.10) to (7.1.11) and using (2.0.11) gives

$$\frac{1}{\Delta t}(u_h^{n+1} - u_h^n, B_h^{n+\frac{1}{2}}) + \frac{1}{\Delta t}(B_h^{n+1} - B_h^n, u_h^{n+\frac{1}{2}})$$
$$= \frac{1}{2\Delta t}\left((u_h^{n+1}, B_h^{n+1}) - (u_h^n, B_h^n)\right) + \frac{1}{2\Delta t}\left((u_h^{n+1}, B_h^n) - (u_h^n, B_h^{n+1})\right)$$
$$+ \frac{1}{2\Delta t}\left((B_h^{n+1}, u_h^{n+1}) - (B_h^n, u_h^n)\right) - \frac{1}{2\Delta t}\left((B_h^{n+1}, u_h^n) - (B_h^n, u_h^{n+1})\right),$$

which reduces to

$$\frac{1}{\Delta t}\left((u_h^{n+1}, B_h^{n+1}) - (u_h^n, B_h^n)\right) + (Re^{-1} + Re_m^{-1})(\nabla u_h^{n+\frac{1}{2}}, \nabla B_h^{n+\frac{1}{2}})$$
$$= (\nabla \times g(t^{n+\frac{1}{2}}), u_h^{n+\frac{1}{2}}) + (f(t^{n+\frac{1}{2}}), B_h^{n+\frac{1}{2}}). \qquad (7.1.12)$$

The proof of (7.1.7) is completed by multiplying (7.1.12) by $\Delta t$, and summing over timesteps. $\quad\square$

**Remark 7.1.3.** *If $f = \nabla \times g = Re^{-1} = Re_m^{-1} = 0$ then energy and cross helicity are exactly conserved.*

**Theorem 7.1.2.** *Suppose $(u, B)$ solve the 3d MHD and that $u$, $B$, $f$, $\nabla \times g$ satisfy the following*

*regularity*

$$u, B \in L^\infty([0,T]; H^{k+1}), \tag{7.1.13}$$

$$u, B \in L^\infty([0,T]; H^{2N+2}), \tag{7.1.14}$$

$$u_t, B_t \in L^\infty([0,T]; H^1), \tag{7.1.15}$$

$$u_{tt}, B_{tt} \in L^4([0,T]; H^1), \tag{7.1.16}$$

$$u_{ttt}, B_{ttt} \in L^2([0,T]; H^{-1}), \text{ and} \tag{7.1.17}$$

$$f_{tt}, \nabla \times g_{tt} \in L^2([0,T]; H^{-1}). \tag{7.1.18}$$

Then the solution $(u_h, B_h, p_h, \lambda_h)$ to (7.1.1)-(7.1.4) converges to the true solution with optimal rate,

$$\|u - u_h\|_{2,1} + \|B - B_h\|_{2,1} = O(\Delta t^2 + h^k + \alpha^{2N+2}).$$

*Proof.* For the analysis we assume the use of SV elements. We begin by adding identically zero terms to the continuous MHD to get

$$\frac{1}{\Delta t}(u^{n+1} - u^n, v_h) + Re^{-1}(\nabla u^{n+\frac{1}{2}}, \nabla v_h) = (f(t^{n+\frac{1}{2}}), v_h)$$

$$- (u_t(t^{n+\frac{1}{2}}), v_h) + \frac{1}{\Delta t}(u^{n+1} - u^n, v_h) + Re^{-1}(\nabla u^{n+\frac{1}{2}}, \nabla v_h) - Re^{-1}(\nabla u(t^{n+\frac{1}{2}}), \nabla v_h)$$

$$+ (D_N^h \overline{(\frac{3}{2}u^n - \frac{1}{2}u^{n-1})}^h \cdot \nabla u^{n+\frac{1}{2}}, v_h) - (u(t^{n+\frac{1}{2}}) \cdot \nabla u(t^{n+\frac{1}{2}}), v_h)$$

$$+ s(B(t^{n+\frac{1}{2}}) \cdot \nabla B(t^{n+\frac{1}{2}}), v_h) - s(D_N^h \overline{(\frac{3}{2}B^n - \frac{1}{2}B^{n-1})}^h \cdot \nabla B^{n+\frac{1}{2}}, v_h)$$

$$- (D_N^h \overline{(\frac{3}{2}u^n - \frac{1}{2}u^{n-1})}^h \cdot \nabla u^{n+\frac{1}{2}}, v_h) + s(D_N^h \overline{(\frac{3}{2}B^n - \frac{1}{2}B^{n-1})}^h \cdot \nabla B^{n+\frac{1}{2}}, v_h), \tag{7.1.19}$$

$$\frac{1}{\Delta t}(B^{n+1} - B^n, \chi_h) + Re_m^{-1}(\nabla B^{n+\frac{1}{2}}, \nabla \chi_h) = (\nabla \times g(t^{n+\frac{1}{2}}), \chi_h)$$

$$- (B_t(t^{n+\frac{1}{2}}), \chi_h) + \frac{1}{\Delta t}(B^{n+1} - B^n, \chi_h) + Re_m^{-1}(\nabla B^{n+\frac{1}{2}}, \nabla \chi_h) - Re_m^{-1}(\nabla B(t^{n+\frac{1}{2}}), \nabla \chi_h)$$

$$+ (B(t^{n+\frac{1}{2}}) \cdot \nabla u(t^{n+\frac{1}{2}}), \chi_h) - (D_N^h \overline{(\frac{3}{2}B^n - B^{n-1})}^h \cdot \nabla u^{n+\frac{1}{2}}, \chi_h)$$

$$- (u(t^{n+\frac{1}{2}}) \cdot \nabla B(t^{n+\frac{1}{2}}), \chi_h) + (D_N^h \overline{(\frac{3}{2}u^n - \frac{1}{2}u^{n-1})}^h \cdot \nabla B^{n+\frac{1}{2}}, \chi_h)$$

$$+ (D_N^h \overline{(\frac{3}{2}B^n - B^{n-1})}^h \cdot \nabla u^{n+\frac{1}{2}}, \chi_h) - (D_N^h \overline{(\frac{3}{2}u^n - \frac{1}{2}u^{n-1})}^h \cdot \nabla B^{n+\frac{1}{2}}, \chi_h). \tag{7.1.20}$$

Subtracting (7.1.19) from (7.1.1) and labeling $e_u^n := u_h^n = u^n$, and $e_B^n := B_h^n - B^n$ gives

$$\frac{1}{\Delta t}(e_u^{n+1} - e_u^n, v_h) + Re^{-1}(\nabla e_u^{n+\frac{1}{2}}, \nabla v_h) =$$

$$(D_N^h \overline{(\frac{3}{2}u^n - \frac{1}{2}u^{n-1})}^h \cdot \nabla u^{n+\frac{1}{2}}, v_h) - (D_N^h \overline{(\frac{3}{2}u_h^n - \frac{1}{2}u_h^{n-1})}^h \cdot \nabla u_h^{n+\frac{1}{2}}, v_h)$$

$$+ s(D_N^h \overline{(\frac{3}{2}B_h^n - \frac{1}{2}B_h^{n-1})}^h \cdot \nabla B_h^{n+\frac{1}{2}}, v_h) - s(D_N^h \overline{(\frac{3}{2}B^n - \frac{1}{2}B^{n-1})}^h \cdot \nabla B^{n+\frac{1}{2}}, v_h)$$

$$+ G_1(u, B, n, v_h), \quad (7.1.21)$$

where

$$G_1(u, B, n, v_h) := (f^{n+\frac{1}{2}} - f(t^{n+\frac{1}{2}}), v_h) - (u_t(t^{n+\frac{1}{2}}), v_h) + \frac{1}{\Delta t}(u^{n+1} - u^n), v_h)$$

$$+ Re^{-1}(\nabla u^{n+\frac{1}{2}}, \nabla v_h) - Re^{-1}(\nabla u(t^{n+\frac{1}{2}}), \nabla v_h)$$

$$+ (D_N^h \overline{(\frac{3}{2}u^n - \frac{1}{2}u^{n-1})}^h \cdot \nabla u^{n+\frac{1}{2}}, v_h) - (u(t^{n+\frac{1}{2}}) \cdot \nabla u(t^{n+\frac{1}{2}}), v_h)$$

$$+ s(B(t^{n+\frac{1}{2}}) \cdot \nabla B(t^{n+\frac{1}{2}}), v_h) - s(D_N^h \overline{(\frac{3}{2}B^n - \frac{1}{2}B^{n-1})}^h \cdot \nabla B^{n+\frac{1}{2}}, v_h). \quad (7.1.22)$$

Next we decompose the velocity and magnetic errors respectively as

$e_u^n = (u(t^n) - P_{V_h}u(t^n)) - (P_{V_h}u(t^n) - u_h^n) =: \eta_u^n - \phi_h^n$, and $e_B^n = (B(t^n) - P_{V_h}B(t^n)) - (P_{V_h}B(t^n) - B_h^n) =: \eta_B^n - \psi_h^n$, where $P_{V_h}u(t^n)$ and $P_{V_h}B(t^n)$ denote the $L^2$ projection of $u(t^n)$ and $B(t^n)$ respectively in $V_h$. Specifying $v_h = \phi_h^{n+\frac{1}{2}}$ in (7.1.21), rearranging, and noting that $(\eta_u^{n+1} - \eta_u^n, \phi_h^{n+\frac{1}{2}}) = 0$ gives

$$\frac{1}{2\Delta t}(\|\phi_h^{n+1}\|^2 - \|\phi_h^n\|^2) + Re^{-1}\|\nabla \phi_h^{n+\frac{1}{2}}\|^2 = Re^{-1}(\nabla \eta_u^{n+\frac{1}{2}}, \nabla \phi_h^{n+\frac{1}{2}})$$

$$+ D_N^h \overline{(\frac{3}{2}u^n - \frac{1}{2}u^{n-1})}^h \cdot \nabla u^{n+\frac{1}{2}}, \phi_h^{n+\frac{1}{2}}) - (D_N^h \overline{(\frac{3}{2}u_h^n - \frac{1}{2}u_h^{n-1})}^h \cdot \nabla u_h^{n+\frac{1}{2}}, \phi_h^{n+\frac{1}{2}})$$

$$+ s(D_N^h \overline{(\frac{3}{2}B_h^n - \frac{1}{2}B_h^{n-1})}^h \cdot \nabla B_h^{n+\frac{1}{2}}, \phi_h^{n+\frac{1}{2}}) - s(D_N^h \overline{(\frac{3}{2}B^n - \frac{1}{2}B^{n-1})}^h \cdot \nabla B^{n+\frac{1}{2}}, \phi_h^{n+\frac{1}{2}})$$

$$+ G_1(u, B, n, \phi_h^{n+\frac{1}{2}}). \quad (7.1.23)$$

110

Rewriting the explicitly written nonlinearities in (7.1.23) and reducing gives

$$
\frac{1}{2\Delta t}(\|\phi_h^{n+1}\|^2 - \|\phi_h^n\|^2) + Re^{-1}\|\nabla\phi_h^{n+\frac{1}{2}}\|^2 = Re^{-1}(\nabla\eta_u^{n+\frac{1}{2}}, \nabla\phi_h^{n+\frac{1}{2}})
$$

$$
+ D_N^h\overline{(\frac{3}{2}u^n - \frac{1}{2}u^{n-1})}^h \cdot \nabla\eta_u^{n+\frac{1}{2}}, \phi_h^{n+\frac{1}{2}}) - (D_N^h\overline{(\frac{3}{2}e_u^n - \frac{1}{2}e_u^{n-1})}^h \cdot \nabla u_h^{n+\frac{1}{2}}, \phi_h^{n+\frac{1}{2}})
$$

$$
- s(D_N^h\overline{(\frac{3}{2}B_h^n - \frac{1}{2}B_h^{n-1})}^h \cdot \nabla e_B^{n+\frac{1}{2}}, \phi_h^{n+\frac{1}{2}}) - s(D_N^h\overline{(\frac{3}{2}e_B^n - \frac{1}{2}e_B^{n-1})}^h \cdot \nabla B^{n+\frac{1}{2}}, \phi_h^{n+\frac{1}{2}})
$$

$$
+ G_1(u, B, n, \phi_h^{n+\frac{1}{2}}). \quad (7.1.24)
$$

Next subtracting (7.1.20) from (7.1.3) gives

$$
\frac{1}{\Delta t}(e_B^{n+1} - e_B^n, \chi_h) + Re_m^{-1}(\nabla e_B^{n+\frac{1}{2}}, \nabla\chi_h) =
$$

$$
(D_N^h\overline{(\frac{3}{2}B_h^n - \frac{1}{2}B_h^{n-1})}^h \cdot \nabla u_h^{n+\frac{1}{2}}, \chi_h) - (D_N^h\overline{(\frac{3}{2}B^n - \frac{1}{2}B^{n-1})}^h \cdot \nabla u^{n+\frac{1}{2}}, \chi_h)
$$

$$
+ (D_N^h\overline{(\frac{3}{2}u^n - \frac{1}{2}u^{n-1})}^h \cdot \nabla B^{n+\frac{1}{2}}, \chi_h) - (D_N^h\overline{(\frac{3}{2}u_h^n - \frac{1}{2}u_h^{n-1})}^h \cdot \nabla B_h^{n+\frac{1}{2}}, \chi_h)
$$

$$
+ G_2(u, B, n, \chi_h), \quad (7.1.25)
$$

where

$$
G_2(u, B, n, \chi_h) := (\nabla\times(g^{n+\frac{1}{2}} - g(t^{n+\frac{1}{2}})), \chi_h) - (B_t(t^{n+\frac{1}{2}}), \chi_h) + \frac{1}{\Delta t}(B^{n+1} - B^n, \chi_h)
$$

$$
+ Re_m^{-1}(\nabla B^{n+\frac{1}{2}}, \nabla\chi_h) - Re_m^{-1}(\nabla B(t^{n+\frac{1}{2}}), \nabla\chi_h)
$$

$$
+ (D_N^h\overline{(\frac{3}{2}B^n - B^{n-1})}^h \cdot \nabla u^{n+\frac{1}{2}}, \chi_h) - (B(t^{n+\frac{1}{2}}) \cdot \nabla u(t^{n+\frac{1}{2}}), \chi_h)
$$

$$
+ (u(t^{n+\frac{1}{2}}) \cdot \nabla B(t^{n+\frac{1}{2}}), \chi_h) - (D_N^h\overline{(\frac{3}{2}u^n - \frac{1}{2}u^{n-1})}^h \cdot \nabla B^{n+\frac{1}{2}}, \chi_h). \quad (7.1.26)
$$

Choosing $\chi_h = \psi_h^{n+\frac{1}{2}}$ in (7.1.25), reducing, and rearranging yields

$$
\frac{1}{2\Delta t}(\|\psi_h^{n+1}\|^2 - \|\psi_h^n\|^2) + Re_m^{-1}\|\nabla\psi_h^{n+\frac{1}{2}}\|^2 = Re_m^{-1}(\nabla\eta_B^{n+\frac{1}{2}}, \nabla\psi_h^{n+\frac{1}{2}})
$$

$$
+ (D_N^h\overline{(\frac{3}{2}B_h^n - \frac{1}{2}B_h^{n-1})}^h \cdot \nabla u_h^{n+\frac{1}{2}}, \psi_h^{n+\frac{1}{2}}) - (D_N^h\overline{(\frac{3}{2}B^n - \frac{1}{2}B^{n-1})}^h \cdot \nabla u^{n+\frac{1}{2}}, \psi_h^{n+\frac{1}{2}})
$$

$$
+ (D_N^h\overline{(\frac{3}{2}u^n - \frac{1}{2}u^{n-1})}^h \cdot \nabla B^{n+\frac{1}{2}}, \psi_h^{n+\frac{1}{2}}) - (D_N^h\overline{(\frac{3}{2}u_h^n - \frac{1}{2}u_h^{n-1})}^h \cdot \nabla B_h^{n+\frac{1}{2}}, \psi_h^{n+\frac{1}{2}})
$$

$$
+ G_2(u, B, n, \psi_h^{n+\frac{1}{2}}). \quad (7.1.27)
$$

111

Rewriting the nonlinear terms in (7.1.27) and reducing gives

$$
\frac{1}{2\Delta t}(\|\psi_h^{n+1}\|^2 - \|\psi_h^n\|^2) + Re_m^{-1}\|\nabla\psi_h^{n+\frac{1}{2}}\|^2 = Re_m^{-1}(\nabla\eta_B^{n+\frac{1}{2}}, \nabla\psi_h^{n+\frac{1}{2}})
$$
$$
- (D_N^h \overline{(\frac{3}{2}B_h^n - \frac{1}{2}B_h^{n-1})}^h \cdot \nabla e_u^{n+\frac{1}{2}}, \psi_h^{n+\frac{1}{2}}) - (D_N^h \overline{(\frac{3}{2}e_B^n - \frac{1}{2}e_B^{n-1})}^h \cdot \nabla u^{n+\frac{1}{2}}, \psi_h^{n+\frac{1}{2}})
$$
$$
+ (D_N^h \overline{(\frac{3}{2}u^n - \frac{1}{2}u^{n-1})}^h \cdot \nabla\eta_B^{n+\frac{1}{2}}, \psi_h^{n+\frac{1}{2}}) + (D_N^h \overline{(\frac{3}{2}e_u^n - \frac{1}{2}e_u^{n-1})}^h \cdot \nabla B_h^{n+\frac{1}{2}}, \psi_h^{n+\frac{1}{2}})
$$
$$
+ G_2(u, B, n, \psi_h^{n+\frac{1}{2}}). \quad (7.1.28)
$$

Multiplying (7.1.28) by $s$, adding (7.1.28) and (7.1.24), and reducing with the identity $(u\cdot\nabla v, w) = -(u\cdot\nabla w, v)$ yields

$$
\frac{1}{2\Delta t}(\|\phi_h^{n+1}\|^2 - \|\phi_h^n\|^2) + \frac{s}{2\Delta t}(\|\psi_h^{n+1}\|^2 - \|\psi_h^n\|^2) + Re^{-1}\|\nabla\phi_h^{n+\frac{1}{2}}\|^2 + sRe_m^{-1}\|\nabla\psi_h^{n+\frac{1}{2}}\|^2
$$
$$
= Re^{-1}(\nabla\eta_u^{n+\frac{1}{2}}, \nabla\phi_h^{n+\frac{1}{2}}) + sRe_m^{-1}(\nabla\eta_B^{n+\frac{1}{2}}, \nabla\psi_h^{n+\frac{1}{2}})
$$
$$
+ D_N^h \overline{(\frac{3}{2}u^n - \frac{1}{2}u^{n-1})}^h \cdot \nabla\eta_u^{n+\frac{1}{2}}, \phi_h^{n+\frac{1}{2}}) - (D_N^h \overline{(\frac{3}{2}\eta_u^n - \frac{1}{2}\eta_u^{n-1})}^h \cdot \nabla u_h^{n+\frac{1}{2}}, \phi_h^{n+\frac{1}{2}})
$$
$$
+ (D_N^h \overline{(\frac{3}{2}\phi_h^n - \frac{1}{2}\phi_h^{n-1})}^h \cdot \nabla u_h^{n+\frac{1}{2}}, \phi_h^{n+\frac{1}{2}}) - s(D_N^h \overline{(\frac{3}{2}B_h^n - \frac{1}{2}B_h^{n-1})}^h \cdot \nabla\eta_B^{n+\frac{1}{2}}, \phi_h^{n+\frac{1}{2}})
$$
$$
- s(D_N^h \overline{(\frac{3}{2}\eta_B^n - \frac{1}{2}\eta_B^{n-1})}^h \cdot \nabla B^{n+\frac{1}{2}}, \phi_h^{n+\frac{1}{2}}) + s(D_N^h \overline{(\frac{3}{2}\phi_h^n - \frac{1}{2}\phi_h^{n-1})}^h \cdot \nabla B^{n+\frac{1}{2}}, \phi_h^{n+\frac{1}{2}})
$$
$$
- s(D_N^h \overline{(\frac{3}{2}B_h^n - \frac{1}{2}B_h^{n-1})}^h \cdot \nabla\eta_u^{n+\frac{1}{2}}, \psi_h^{n+\frac{1}{2}}) - s(D_N^h \overline{(\frac{3}{2}\eta_B^n - \frac{1}{2}\eta_B^{n-1})}^h \cdot \nabla u^{n+\frac{1}{2}}, \psi_h^{n+\frac{1}{2}})
$$
$$
+ s(D_N^h \overline{(\frac{3}{2}\psi_h^n - \frac{1}{2}\psi_h^{n-1})}^h \cdot \nabla u^{n+\frac{1}{2}}, \psi_h^{n+\frac{1}{2}}) + s(D_N^h \overline{(\frac{3}{2}u^n - \frac{1}{2}u^{n-1})}^h \cdot \nabla\eta_B^{n+\frac{1}{2}}, \psi_h^{n+\frac{1}{2}})
$$
$$
+ s(D_N^h \overline{(\frac{3}{2}\eta_u^n - \frac{1}{2}\eta_u^{n-1})}^h \cdot \nabla B_h^{n+\frac{1}{2}}, \psi_h^{n+\frac{1}{2}}) - s(D_N^h \overline{(\frac{3}{2}\phi_h^n - \frac{1}{2}\phi_h^{n-1})}^h \cdot \nabla B_h^{n+\frac{1}{2}}, \psi_h^{n+\frac{1}{2}})
$$
$$
+ G_1(u, B, n, \phi_h^{n+\frac{1}{2}}) + G_2(u, B, n, \psi_h^{n+\frac{1}{2}}). \quad (7.1.29)
$$

We now bound the RHS terms in (7.1.29) individually. For the first two terms we use Cauchy-Schwarz and Young's inequalities

$$
Re^{-1}(\nabla\eta_u^{n+\frac{1}{2}}, \nabla\phi_h^{n+\frac{1}{2}}) \leq \frac{Re^{-1}}{14}\|\nabla\phi_h^{n+\frac{1}{2}}\|^2 + CRe^{-1}\|\nabla\eta_u^{n+\frac{1}{2}}\|^2, \text{ and} \quad (7.1.30)
$$
$$
sRe_m^{-1}(\nabla\eta_B^{n+\frac{1}{2}}, \nabla\psi_h^{n+\frac{1}{2}}) \leq \frac{sRe_m^{-1}}{14}\|\nabla\psi_h^{n+\frac{1}{2}}\|^2 + CRe_m^{-1}\|\nabla\eta_B^{n+\frac{1}{2}}\|^2. \quad (7.1.31)
$$

We bound the first two nonlinear terms in (7.1.29) using Lemma 2.0.3, and standard inequalities

$$|D_N^h(\overline{\tfrac{3}{2}u^n - \tfrac{1}{2}u^{n-1}}^h) \cdot \nabla\eta_u^{n+\frac{1}{2}}, \phi_h^{n+\frac{1}{2}})|$$

$$\leq C\|D_N^h(\overline{\tfrac{3}{2}u^n - \tfrac{1}{2}u^{n-1}}^h)\|^{\frac{1}{2}} \|\nabla D_N^h(\overline{\tfrac{3}{2}u^n - \tfrac{1}{2}u^{n-1}}^h)\|^{\frac{1}{2}} \|\nabla\eta_u^{n+\frac{1}{2}}\| \|\nabla\phi_h^{n+\frac{1}{2}}\|$$

$$\leq \frac{Re^{-1}}{14}\|\nabla\phi_h^{n+\frac{1}{2}}\|^2 + CRe\|\tfrac{3}{2}u^n - \tfrac{1}{2}u^{n-1}\| \|\nabla(\tfrac{3}{2}u^n - \tfrac{1}{2}u^{n-1})\| \|\nabla\eta_u^{n+\frac{1}{2}}\|^2, \qquad (7.1.32)$$

$$|(D_N^h(\overline{\tfrac{3}{2}\eta_u^n - \tfrac{1}{2}\eta_u^{n-1}}^h) \cdot \nabla u_h^{n+\frac{1}{2}}, \phi_h^{n+\frac{1}{2}})|$$

$$\leq C\|\nabla D_N^h(\overline{\tfrac{3}{2}\eta_u^n - \tfrac{1}{2}\eta_u^{n-1}}^h)\| \|\nabla u_h^{n+\frac{1}{2}}\| \|\phi_h^{n+\frac{1}{2}}\|$$

$$\leq \frac{Re^{-1}}{14}\|\nabla\phi_h^{n+\frac{1}{2}}\|^2 + CRe\|\nabla u_h^{n+\frac{1}{2}}\|^2\|\nabla\eta_u^n\|^2 + CRe\|\nabla u_h^{n+\frac{1}{2}}\|^2\|\nabla\eta_u^{n-1}\|^2. \qquad (7.1.33)$$

The third and fourth nonlinear terms in (7.1.29) are bounded as follows:

$$|(D_N^h(\overline{\tfrac{3}{2}\phi_h^n - \tfrac{1}{2}\phi_h^{n-1}}^h) \cdot \nabla u_h^{n+\frac{1}{2}}, \phi_h^{n+\frac{1}{2}})|$$

$$\leq |(D_N^h \overline{\tfrac{3}{2}\phi_h^n}^h \cdot \nabla u_h^{n+\frac{1}{2}}, \phi_h^{n+\frac{1}{2}})| + |(D_N^h \overline{\tfrac{1}{2}\phi_h^{n-1}}^h \cdot \nabla u_h^{n+\frac{1}{2}}, \phi_h^{n+\frac{1}{2}})|$$

$$\leq C\|\phi_h^n\| \|\nabla u_h^{n+\frac{1}{2}}\|_\infty \|\nabla\phi_h^{n+\frac{1}{2}}\| + C\|\phi_h^{n-1}\| \|\nabla u_h^{n+\frac{1}{2}}\|_\infty \|\nabla\phi_h^{n+\frac{1}{2}}\|$$

$$\leq \frac{Re^{-1}}{14}\|\nabla\phi_h^{n+\frac{1}{2}}\|^2 + CRe\|\nabla u_h^{n+\frac{1}{2}}\|_\infty^2(\|\phi_h^n\|^2 + \|\phi_h^{n-1}\|^2), \qquad (7.1.34)$$

$$s|(D_N^h(\overline{\tfrac{3}{2}B_h^n - \tfrac{1}{2}B_h^{n-1}}^h) \cdot \nabla\eta_B^{n+\frac{1}{2}}, \phi_h^{n+\frac{1}{2}})|$$

$$\leq Cs\|\nabla(D_N^h(\overline{\tfrac{3}{2}B_h^n - \tfrac{1}{2}B_h^{n-1}}^h)\| \|\nabla\eta_B^{n+\frac{1}{2}}\| \|\nabla\phi_h^{n+\frac{1}{2}}\|$$

$$\leq \frac{Re^{-1}}{14}\|\nabla\phi_h^{n+\frac{1}{2}}\|^2 + CRe\|\nabla\eta_B^{n+\frac{1}{2}}\|^2(\|\nabla B_h^n\|^2 + \|\nabla B_h^{n-1}\|^2). \qquad (7.1.35)$$

The fifth and sixth nonlinear terms in (7.1.29) are bounded as follows

$$s|(D_N^h(\overline{\tfrac{3}{2}\eta_B^n - \tfrac{1}{2}\eta_B^{n-1}}^h) \cdot \nabla B^{n+\frac{1}{2}}, \phi_h^{n+\frac{1}{2}})|$$

$$\leq \|\nabla(D_N^h(\overline{\tfrac{3}{2}\eta_B^n - \tfrac{1}{2}\eta_B^{n-1}}^h)\| \|\nabla B^{n+\frac{1}{2}}\| \|\nabla\phi_h^{n+\frac{1}{2}}\|$$

$$\leq \frac{Re^{-1}}{14}\|\nabla\phi_h^{n+\frac{1}{2}}\|^2 + CRe\|\nabla B^{n+\frac{1}{2}}\|^2(\|\nabla\eta_B^n\|^2 + \|\nabla\eta_B^{n-1}\|^2), \qquad (7.1.36)$$

$$s|(D_N^h(\overline{\tfrac{3}{2}\phi_h^n - \tfrac{1}{2}\phi_h^{n-1}}^h) \cdot \nabla B^{n+\frac{1}{2}}, \phi_h^{n+\frac{1}{2}})|$$

$$\leq |(D_N^h \overline{\tfrac{3}{2}\phi_h^n}^h \cdot \nabla B^{n+\frac{1}{2}}, \phi_h^{n+\frac{1}{2}})| + |(D_N^h \overline{\tfrac{1}{2}\phi_h^{n-1}}^h \cdot \nabla B^{n+\frac{1}{2}}, \phi_h^{n+\frac{1}{2}})|$$

$$\leq C\|\phi_h^n\| \|\nabla B^{n+\frac{1}{2}}\|_\infty \|\phi_h^{n+\frac{1}{2}}\| + C\|\phi_h^{n-1}\| \|\nabla B^{n+\frac{1}{2}}\|_\infty \|\phi_h^{n+\frac{1}{2}}\|$$

$$\leq \frac{Re^{-1}}{14}\|\nabla\phi_h^{n+\frac{1}{2}}\|^2 + CRe\|\nabla B^{n+\frac{1}{2}}\|_\infty^2(\|\phi_h^n\|^2 + \|\phi_h^{n-1}\|^2). \qquad (7.1.37)$$

The six remaining nonlinear terms are bounded similar to the first six nonlinear terms bounded above. Combining the upper bounds, using regularity of the continuous and discrete solutions, and grouping like terms gives

$$
\frac{1}{2\Delta t}(\|\phi_h^{n+1}\|^2 - \|\phi_h^n\|^2) + \frac{s}{2\Delta t}(\|\psi_h^{n+1}\|^2 - \|\psi_h^n\|^2) + \frac{Re^{-1}}{2}\|\nabla\phi_h^{n+\frac{1}{2}}\|^2 + \frac{sRe_m^{-1}}{2}\|\nabla\psi_h^{n+\frac{1}{2}}\|^2
$$

$$
\leq C(Re + sRe_m)(\|\phi_h^n\|^2 + \|\phi_h^{n-1}\|^2) + sCRe_m(\|\psi_h^n\|^2 + \|\psi_h^{n-1}\|^2)
$$

$$
+ C(Re + Re_m)(\|\nabla\eta_u^n\|^2 + \|\nabla\eta_u^{n-1}\|^2) + CRe(\|\nabla\eta_B^n\|^2 + \|\eta_B^{n-1}\|^2)
$$

$$
+ C(Re^{-1} + Re + sRe_m)\|\nabla\eta_u^{n+\frac{1}{2}}\|^2 + C(Re + Re_m^{-1} + sRe_m)\|\nabla\eta_B^{n+\frac{1}{2}}\|^2
$$

$$
+ |G_1(u, B, n, \phi_h^{n+\frac{1}{2}})| + |G_2(u, B, n, \psi_h^{n+\frac{1}{2}})| \quad (7.1.38)
$$

It remains to bound the terms in $G_1(u, B, n, \phi_h^{n+\frac{1}{2}})$ and $G_1(u, B, n, \psi_h^{n+\frac{1}{2}})$. The bounds for $G_1$ and $G_2$ are derived similarly and so we only write out the details explicitly for $G_1$. The linear terms are bounded with Cauchy-Schwarz and Young's inequality as follows:

$$
(f(t^{n+\frac{1}{2}}) - f^{n+\frac{1}{2}}, \phi_h^{n+\frac{1}{2}}) \leq \frac{1}{2}\|\phi_h^{n+\frac{1}{2}}\|^2 + \frac{1}{2}\|f(t^{n+\frac{1}{2}}) - f^{n+\frac{1}{2}}\|^2
$$

$$
\leq \frac{1}{2}\|\phi_h^n\|^2 + \frac{1}{2}\|\phi_h^{n+1}\|^2 + \frac{(\Delta t)^3}{48}\int_{t^n}^{t^{n+1}}\|f_{tt}\|^2 dt, \quad (7.1.39)
$$

$$
(\frac{u^{n+1} - u^n}{\Delta t} - u_t(t^{n+\frac{1}{2}}), \phi_h^{n+\frac{1}{2}}) \leq \frac{1}{2}\|\phi_h^{n+\frac{1}{2}}\|^2 + \frac{1}{2}\|\frac{u^{n+1} - u^n}{\Delta t} - u_t(t^{n+\frac{1}{2}})\|^2
$$

$$
\leq \frac{1}{2}\|\phi_h^n\|^2 + \frac{1}{2}\|\phi_h^{n+1}\|^2 + \frac{1}{2}\frac{(\Delta t)^3}{1280}\int_{t^n}^{t^{n+1}}\|u_{ttt}\|^2 dt, (7.1.40)
$$

$$
(\nabla u^{n+\frac{1}{2}} - \nabla u(t^{n+\frac{1}{2}}), \nabla\phi_h^{n+\frac{1}{2}}) \leq \varepsilon Re^{-1}\|\nabla\phi_h^{n+\frac{1}{2}}\|^2 + CRe\|\nabla u^{n+\frac{1}{2}} - \nabla u(t^{n+\frac{1}{2}})\|^2
$$

$$
\leq \varepsilon Re^{-1}\|\nabla\phi_h^{n+\frac{1}{2}}\|^2 + CRe\frac{(\Delta t)^3}{48}\int_{t^n}^{t^{n+1}}\|\nabla u_{tt}\|^2 dt. (7.1.41)
$$

To bound the first nonlinear term we add an identically zero term, and rearrange to get

$$
(D_N^h \overline{(\frac{3}{2}u^n - \frac{1}{2}u^{n-1})}^h \cdot \nabla u^{n+\frac{1}{2}}, \phi_h^{n+\frac{1}{2}}) - (u(t^{n+\frac{1}{2}}) \cdot \nabla u(t^{n+\frac{1}{2}}), \phi_h^{n+\frac{1}{2}}) =
$$

$$
(D_N^h \overline{(\frac{3}{2}u^n - \frac{1}{2}u^{n-1})}^h \cdot \nabla u^{n+\frac{1}{2}}, \phi_h^{n+\frac{1}{2}}) - (D_N^h \overline{u(t^{n+\frac{1}{2}})}^h \cdot \nabla u(t^{n+\frac{1}{2}}), \phi_h^{n+\frac{1}{2}})
$$

$$
+ (D_N^h \overline{u(t^{n+\frac{1}{2}})}^h \cdot \nabla u(t^{n+\frac{1}{2}}), \phi_h^{n+\frac{1}{2}}) - (u(t^{n+\frac{1}{2}}) \cdot \nabla u(t^{n+\frac{1}{2}}), \phi_h^{n+\frac{1}{2}})
$$

$$
= (D_N^h \overline{(\frac{3}{2}u^n - \frac{1}{2}u^{n-1})}^h \cdot \nabla(u^{n+\frac{1}{2}} - u(t^{n+\frac{1}{2}})), \phi_h^{n+\frac{1}{2}}) + (D_N^h \overline{(\frac{3}{2}u^n - \frac{1}{2}u^{n-1} - u(t^{n+\frac{1}{2}}))}^h \cdot \nabla u^{n+\frac{1}{2}}, \phi_h^{n+\frac{1}{2}})
$$

$$
+ ((D_N^h \overline{u(t^{n+\frac{1}{2}})}^h - u(t^{n+\frac{1}{2}})) \cdot \nabla u(t^{n+\frac{1}{2}}), \phi_h^{n+\frac{1}{2}}). \quad (7.1.42)
$$

114

Next we bound the terms in (7.1.42) individually:

$$(D_N^h \overline{(\frac{3}{2}u^n - \frac{1}{2}u^{n-1}})^h) \cdot \nabla(u^{n+\frac{1}{2}} - u(t^{n+\frac{1}{2}})), \phi_h^{n+\frac{1}{2}})$$

$$\leq \|\nabla D_N^h \overline{(\frac{3}{2}u^n - \frac{1}{2}u^{n-1}})^h\| \|\nabla(u^{n+\frac{1}{2}} - u(t^{n+\frac{1}{2}}))\| \|\nabla \phi_h^{n+\frac{1}{2}}\|$$

$$\leq \varepsilon Re^{-1}\|\nabla \phi_h^{n+\frac{1}{2}}\|^2 + CRe(\|\nabla u^n\|^2 + \|\nabla u^{n-1}\|^2)\Delta t^3 \int_{t^n}^{t^{n+1}} \|\nabla u_{tt}\|^2 dt$$

$$\leq \varepsilon Re^{-1}\|\nabla \phi_h^{n+\frac{1}{2}}\|^2 + CRe\Delta t^3 \int_{t^n}^{t^{n+1}} (\|\nabla u^n\|^4 + \|\nabla u^{n-1}\|^4 + \|\nabla u_{tt}\|^4) dt$$

$$\leq \varepsilon Re^{-1}\|\nabla \phi_h^{n+\frac{1}{2}}\|^2 + CRe\Delta t^4(\|\nabla u^n\|^4 + \|\nabla u^{n-1}\|^4) + CRe\Delta t^3 \int_{t^n}^{t^{n+1}} \|\nabla u_{tt}\|^4 dt. \quad (7.1.43)$$

$$(D_N^h \overline{(\frac{3}{2}u^n - \frac{1}{2}u^{n-1} - u(t^{n+\frac{1}{2}})})^h) \cdot \nabla u^{n+\frac{1}{2}}, \phi_h^{n+\frac{1}{2}})$$

$$\leq \|\nabla D_N^h \overline{(\frac{3}{2}u^n - \frac{1}{2}u^{n-1} - u(t^{n+\frac{1}{2}})})^h\| \|\nabla u^{n+\frac{1}{2}}\| \|\nabla \phi_h^{n+\frac{1}{2}}\|$$

$$\leq \varepsilon Re^{-1}\|\nabla \phi_h^{n+\frac{1}{2}}\|^2 + CRe\Delta t^2 \|\nabla D_N^h \overline{u_{tt}(t^{n+\frac{1}{2}})}\|^2 \|\nabla u^{n+\frac{1}{2}}\|^2$$

$$\leq \varepsilon Re^{-1}\|\nabla \phi_h^{n+\frac{1}{2}}\|^2 + CRe\Delta t^2 \|\nabla D_N^h \overline{u_{tt}(t^{n+\frac{1}{2}})}\|^2 \|\nabla u^{n+\frac{1}{2}}\|^2$$

$$\leq \varepsilon Re^{-1}\|\nabla \phi_h^{n+\frac{1}{2}}\|^2 + CRe\Delta t^3 \int_{t^n}^{t^{n+1}} \|\nabla u_{tt}\|^4 dt + CRe\Delta t^4 \|\nabla u^{n+\frac{1}{2}}\|^4$$

$$\leq \varepsilon Re^{-1}\|\nabla \phi_h^{n+\frac{1}{2}}\|^2 + CRe\Delta t^3 \int_{t^n}^{t^{n+1}} \|\nabla u_{tt}\|^4 dt + CRe\Delta t^4(\|\nabla u^{n+1}\|^4 + \|\nabla u^n\|^4) \quad (7.1.44)$$

$$((D_N^h \overline{u(t^{n+\frac{1}{2}})}^h - u(t^{n+\frac{1}{2}})) \cdot \nabla u(t^{n+\frac{1}{2}}), \phi_h^{n+\frac{1}{2}})$$

$$\leq C\|D_N^h \overline{u(t^{n+\frac{1}{2}})}^h - u(t^{n+\frac{1}{2}})\| \|\nabla u(t^{n+\frac{1}{2}})\|_\infty \|\nabla \phi_h^{n+\frac{1}{2}}\|$$

$$\leq \varepsilon Re^{-1}\|\nabla \phi_h^{n+\frac{1}{2}}\|^2 + CRe\|D_N^h \overline{u(t^{n+\frac{1}{2}})}^h - u(t^{n+\frac{1}{2}})\|^2$$

$$\leq \varepsilon Re^{-1}\|\nabla \phi_h^{n+\frac{1}{2}}\|^2 + CRe\alpha^{4N+4}\|\Delta^{N+1}A^{-(N+1)}u\|^2$$

$$+ CRe(\alpha^2 h^{2k} + h^{2k+2})(\sum_{n=0}^{N} |A^{-n}u|_{k+1}^2). \quad (7.1.45)$$

The bound on the remaining nonlinear terms in $G_1$ is derived similarly. Specifying $\varepsilon = \frac{1}{28}$, substi-

tuting in the above bounds, and multiplying through by $2\Delta t$ gives

$$(\|\phi_h^{n+1}\|^2 - \|\phi_h^n\|^2) + s(\|\psi_h^{n+1}\|^2 - \|\psi_h^n\|^2) + \frac{\Delta t}{2} Re^{-1}\|\nabla \phi_h^{n+\frac{1}{2}}\|^2 + \frac{s\Delta t}{2} Re_m^{-1}\|\nabla \psi_h^{n+\frac{1}{2}}\|^2$$

$$\leq C(Re, Re_m, s)\Delta t\Big( \|\phi_h^{n+1}\|^2 + \|\phi_h^n\|^2 + \|\phi_h^{n-1}\|^2 + \|\psi_h^{n+1}\|^2 + \|\psi_h^n\|^2 + \|\psi_h^{n-1}\|^2$$

$$+ \|\nabla\eta_u^n\|^2 + \|\nabla\eta_u^{n-1}\|^2 + \|\nabla\eta_B^n\|^2 + \|\eta_B^{n-1}\|^2 + \|\nabla\eta_u^{n+\frac{1}{2}}\|^2 + \|\nabla\eta_B^{n+\frac{1}{2}}\|^2$$

$$+ \Delta t^3 \int_{t^n}^{t^{n+1}} \|f_{tt}\|^2 dt + \Delta t^3 \int_{t^n}^{t^{n+1}} \|\nabla \times g_{tt}\|^2 dt + \Delta t^3 \int_{t^n}^{t^{n+1}} \|u_{ttt}\|^2 dt + \Delta t^3 \int_{t^n}^{t^{n+1}} \|\nabla u_{tt}\|^2 dt$$

$$+ \Delta t^3 \int_{t^n}^{t^{n+1}} \|\nabla u_{tt}\|^4 dt + \Delta t^3 \int_{t^n}^{t^{n+1}} \|B_{ttt}\|^2 dt + \Delta t^3 \int_{t^n}^{t^{n+1}} \|\nabla B_{tt}\|^2 dt + \Delta t^3 \int_{t^n}^{t^{n+1}} \|\nabla B_{tt}\|^4 dt$$

$$+ \Delta t^4 (\|\nabla u^{n+1}\|^4 + \|\nabla u^n\|^4 + \|\nabla u^{n-1}\|^4 + \|\nabla B^{n+1}\|^4 + \|\nabla B^n\|^4 + \|\nabla B^{n-1}\|^4)$$

$$+ \alpha^{4N+4}\|\Delta^{N+1}A^{-(N+1)}u\|^2 + (\alpha^2 h^{2k} + h^{2k+2})(\sum_{n=0}^{N} |A^{-n}u|_{k+1}^2)$$

$$+ \alpha^{4N+4}\|\Delta^{N+1}A^{-(N+1)}B\|^2 + (\alpha^2 h^{2k} + h^{2k+2})(\sum_{n=0}^{N} |A^{-n}B|_{k+1}^2)\Big). \quad (7.1.46)$$

Recall that $\eta_u^n = (u(t^n) - P_{V_h}u(t^n))$ and $\eta_B^n = (B(t^n) - P_{V_h}B(t^n))$ implies

$$\|\eta_\alpha^n\|^2 \leq h^{k+1}|u^n|_{k+1}^2 \text{ for } \alpha = u, B, \quad (7.1.47)$$

$$\|\nabla\eta_\alpha^n\| \leq h^{2k+2}|u^n|_{k+1}^2 \text{ for } \alpha = u, B. \quad (7.1.48)$$

Summing the terms in (7.1.46) and using the bounds above gives

$$\|\phi_h^M\|^2 + s\|\psi_h^M\|^2 + \frac{\Delta t}{2}\sum_{n=0}^{M-1} \Big( Re^{-1}\|\nabla \phi_h^{n+\frac{1}{2}}\|^2 + sRe_m^{-1}\|\nabla\psi_h^{n+\frac{1}{2}}\|^2 \Big)$$

$$\leq C(Re, Re_m, s)\Delta t \sum_{n=0}^{M-1} \Big( \|\phi_h^{n+\frac{1}{2}}\|^2 + \|\psi_h^{n+\frac{1}{2}}\|^2 \Big)$$

$$+ C(Re, Re_m, s)\Big( h^{2k}\||u\||_{4,k+1}^4 + h^{2k}\||u\||_{4,k+1}^2 + h^{2k}\||B\||_{4,k+1}^4 + h^{2k}\||B\||_{4,k+1}^2$$

$$+ \Delta t^4\||f\||_{2,*}^2 + \Delta t^4\||\nabla\times g\||_{2,*}^2 + \Delta t^4\|u_{ttt}\|_{2,0}^2 + \Delta t^4\|\nabla u_{tt}\|_{2,0}^2 + \Delta t^4\|\nabla u_{tt}\|_{4,0}^4$$

$$+ \Delta t^4\|B_{ttt}\|_{2,0}^2 + \Delta t^4\|\nabla B_{tt}\|_{2,0}^2 + \Delta t^4\|\nabla B_{tt}\|_{4,0}^4 + \Delta t^4\||\nabla u\||_{4,0}^4 + \Delta t^4\||\nabla B\||_{4,0}^4$$

$$+ \alpha^{4N+4}\|\Delta^{N+1}A^{-(N+1)}u\|_{2,0}^2 + \alpha^{4N+4}\|\Delta^{N+1}A^{-(N+1)}B\|_{2,0}^2$$

$$+ (\alpha^2 h^{2k} + h^{2k+2})(\sum_{n=0}^{N} \|A^{-n}u\|_{2,k+1}^2) + (\alpha^2 h^{2k} + h^{2k+2})(\sum_{n=0}^{N} \|A^{-n}B\|_{2,k+1}^2)\Big). \quad (7.1.49)$$

The proof is finished with an application of Gronwall's inequality and the triangle inequality.

$\square$

**Remark 7.1.4.** *The algorithm has two important features which the error analysis reveals. The first is that the velocity and magnetic field errors (and convergence rates) are independent of the pressure error. This follows because the SV element is pointwise divergence free. The second important feature is as a result of linearizing the scheme there is no restriction on the timestep, which is analogous to the results in [34, 51].*

**Remark 7.1.5.** *The filtering parameter, $\alpha$, is typically chosen on the order of h. This simplifies the error estimate to $O(\Delta t^2 + h^l)$ where $l = \min(2(N+1), k)$. We note that by choosing $N = 1$ when $k = 3$ we maintain third order convergence. However, if we choose $N = 0$ then we only expect second order convergence.*

## 7.2 Numerical Experiments

In this section we test the numerical scheme on some benchmark problems. All computations are done in 2d on a barycenter refinement of a regular mesh (to ensure stability) with $((P^3)^2, P^2_{disc})$ SV elements, and $\alpha = O(h)$.

### 7.2.1 Convergence Rates

From Theorem 7.1.2, with $k = 3$ we expect the asymptotic error in Algorithm 7.1.1 to converge as

$$\|u - u_h\|_{2,1} + \|B - B_h\|_{2,1} = O(\Delta t^2 + h^3 + \alpha^{2N+2}).$$

Thus, for the Leray-$\alpha$ model (i.e. $N = 0$) we expect the error to be $O(\Delta t^2 + h^2)$ because $\alpha \approx h$. However, if we use the Leray-deconvolution model with $N = 1$ we expect the error to be $O(\Delta t^2 + h^3)$, which is optimal using the SV element $((P^3)^2, P^2_{disc})$, and a reduction in error over the case where N is chosen to be 0.

To verify the convergence rates we compute solutions to a problem with known solutions on a series of refined meshes and timesteps. The test problem is chosen to have solution

$$u = (1 + 0.01t)\begin{pmatrix} \cos(2\pi y) \\ \sin(2\pi x) \end{pmatrix}, \quad B = (1 - 0.01t)\begin{pmatrix} \sin(2\pi y) \\ \cos(2\pi x) \end{pmatrix}, \quad P = x + y.$$

on the unit square with $Re = Re_m = 100$, $s = 1$, endtime $T = 0.1$, and $f$ and $\nabla \times g$ calculated from $u, B, p$ and the MHD equations. The meshwidth and timestep are tied together so that when $h$ is halved, the timestep is divided by $2\sqrt{2}$ (approximately).

Table 7.1 shows that we achieve third order convergence when $N = 1$, while we only achieve second order convergence when $N = 0$. This agrees with our analysis. Further, Table 7.1 shows that on the three finest discretizations the Leray-Deconvolution (N=1) model has an order of magnitude reduction in error compared to the Leray-$\alpha$ (N=0) model with only a modest increase in runtime (approximately 8% on the finest mesh). This confirms our theory, and demonstrates a clear advantage of deconvolution.

| $h$ | $\Delta t$ | $\|u - u_h\|_{2,1} + \|B - B_h\|_{2,1}$ (N=1) | rate | time (sec) | $\|u - u_h\|_{2,1} + \|B - B_h\|_{2,1}$ (N=0) | rate | time (sec) |
|---|---|---|---|---|---|---|---|
| $\frac{1}{2}$ | $T$ | 0.810088 | - | 1.04 | 1.131522 | - | |
| $\frac{1}{4}$ | $\frac{T}{3}$ | 0.167449 | 2.27 | 6.97 | 0.423210 | 1.42 | 0.85 |
| $\frac{1}{8}$ | $\frac{T}{8}$ | 0.022034 | 2.93 | 62.73 | 0.127370 | 1.73 | 6.59 |
| $\frac{1}{16}$ | $\frac{T}{22}$ | 0.002504 | 3.13 | 668.18 | 0.034316 | 1.90 | 649.19 |
| $\frac{1}{32}$ | $\frac{T}{62}$ | 3.0824e-4 | 3.02 | 2250.94 | 0.008680 | 1.98 | 2080.84 |

Table 7.1: Convergence rates for the Leray-deconvolution ($N = 1$) and the Leray -$\alpha$ ($N = 0$) models.

## 7.2.2 Channel Flow over a Step

For our second experiment, we consider a variation of the benchmark problem of flow through a channel over a step found in [14, 23, 57]. The parameters are specified as follows $Re = 500$, $Re_m = 1$, $s = 0.05$, and endtime $T = 50$. The initial conditions are $u_0 = 0$ and $B_0 = 0$. For the velocity we assume constant inflow and constant outflow on the left and right boundaries, and all other boundaries are prescribed no-slip conditions. The magnetic field is set to be 1 in the $y$ direction and 0 in the $x$ direction on all boundaries. Figure 7.1 shows the domain and boundary conditions.
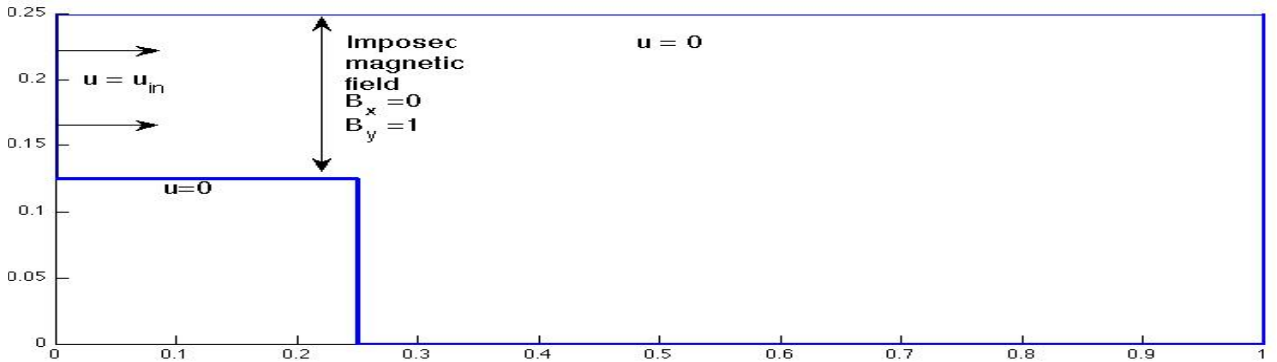


Figure 7.1: The domain and boundary conditions for channel flow problem.

It is known from [14, 23, 57] that the correct physical behavior is for an eddy to form behind the step. To verify this we compute a DNS of MHD flow on a mesh which gave 102,650 degrees of freedom and a timestep $\Delta t = 0.01$. Figure 7.2 shows the correct behavior of the simulation
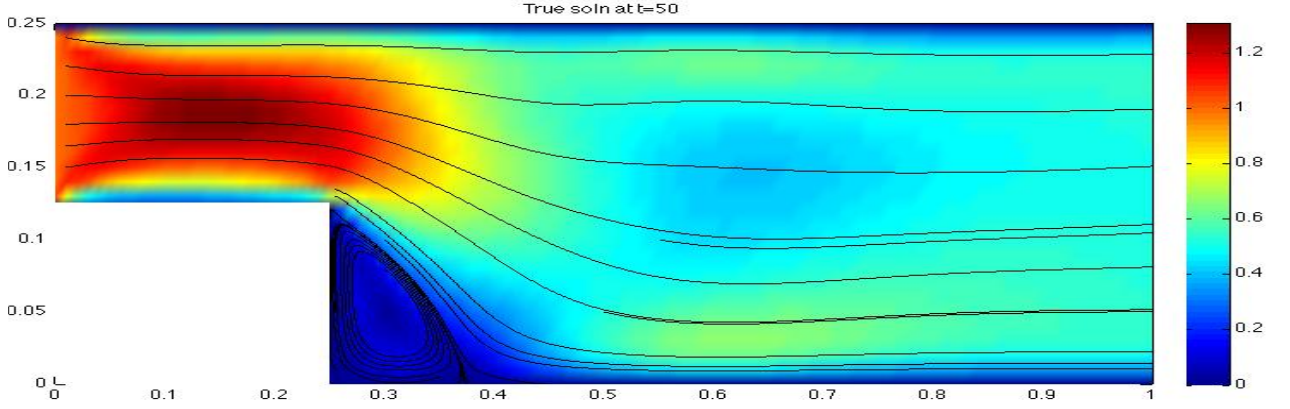


Figure 7.2: The 'true' solution.

The goal of a model is to provide more accurate (at least in an averaging sense) simulations than DNS on coarse spacial and temporal discritizations. Thus, to test our model we now compare the MHD Leray-deconvolution model and DNS of MHD on a mesh which gave 8,666 degrees of freedom and timestep $\Delta t = 0.1$. The model parameters were chosen to be $N = 1$ and $\alpha = 0.08 (\approx h)$. The results are shown in Figure 7.3 as velocity streamlines over speed contours. The coarse-mesh DNS failed to provide a plausible solution due to numerical oscillations. The Leray-deconvolution model does stretch the recirculation region but it has captured the recirculation behind the step and the solution still maintains smooth velocity contours. This demonstrates the effectiveness of the model at capturing (qualitative) long term behavior of MHD flows on coarse discretizations.

### 7.2.3   Orszag-Tang Vortex Problem

We conclude the section by repeating an experiment done by J.-G Liu and W. Wang in [49]. Consider the ideal 2d MHD equations with $Re = Re_m = \infty$, $f = \nabla \times g = 0$, $s = 1$, and compute on the $2\pi$ periodic box with initial conditions

$$
u_0 = \begin{pmatrix} -\sin(y + 2.0) \\ \sin(x + 1.4) \end{pmatrix}, B_0 = \begin{pmatrix} \frac{-1}{3}\sin(y + 6.2) \\ \frac{2}{3}\sin(2x + 2.3) \end{pmatrix}.
$$

The computations were done on a mesh which gives a total of 129,410 degrees of freedom, and parameters were specified as follows: $N = 1$, $\alpha = \frac{1}{90}$, $\Delta t = 0.1$, and $T = 2.7$. The configuration is
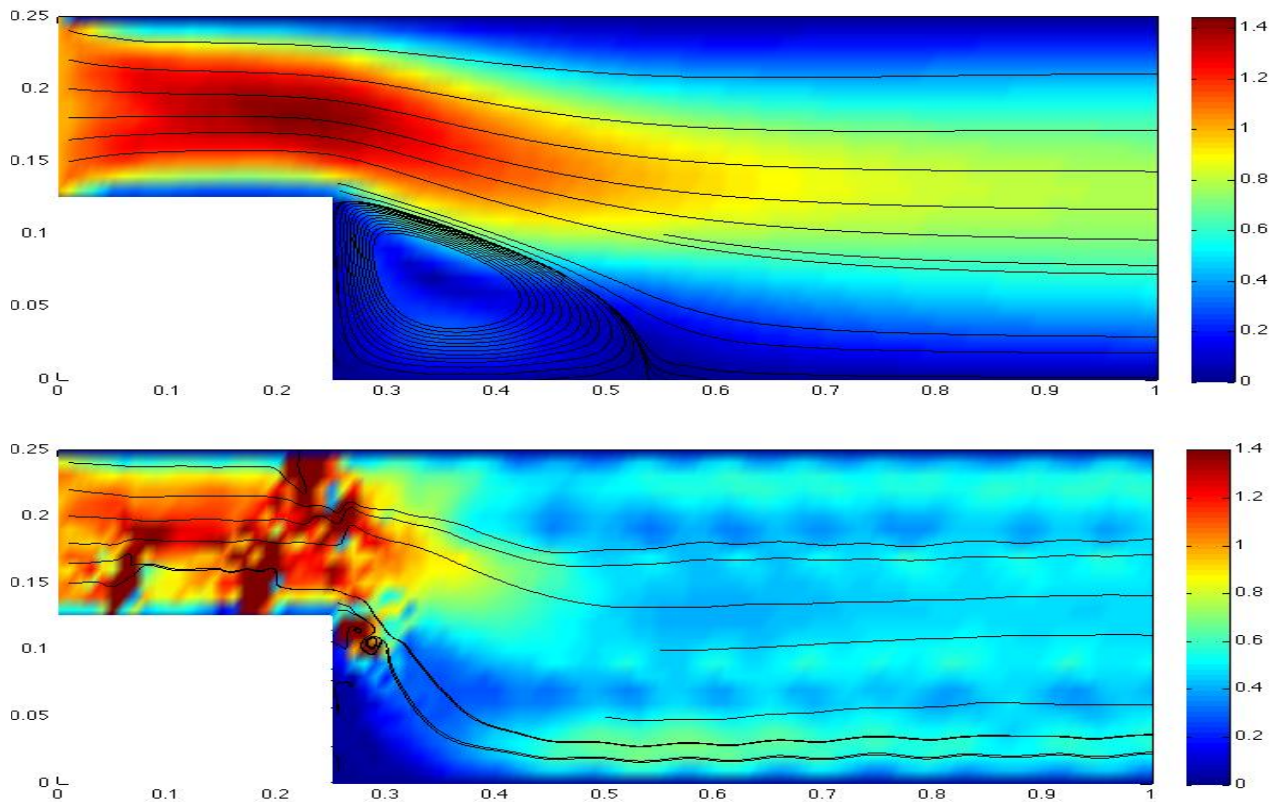
Figure 7.3: Top: MHD Leray-deconvolution, Bottom: DNS of MHD, at $T = 50$ on mesh giving 8,666 dof.

known to develop singularity-like structures known as current sheets. Figure 7.4 shows the current sheets at time $T$ and we observe that, although only marginally resolved, the plot agrees qualitatively with the those in the literature [49, 20, 10]. However, we find our solution with significantly less degrees of freedom and a larger timestep than [49, 20, 10].
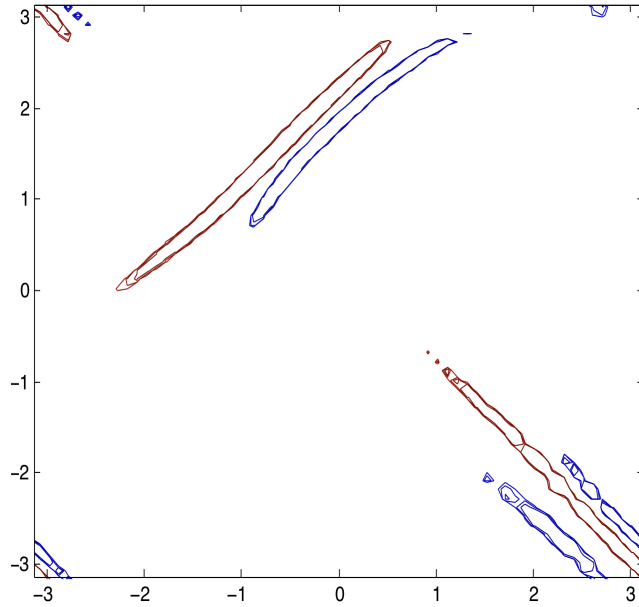


Figure 7.4: Current sheets found with Leray$-\alpha$ deconvolution (N=1) at $t$=2.7.

Since this is an ideal MHD problem, we expect energy and cross helicity to remain constant throughout the simulation, by Remark 7.1.3. Figure 7.5 shows that these physical entities remain constant for the duration of the simulation, verifying the model conserves energy and cross helicity.
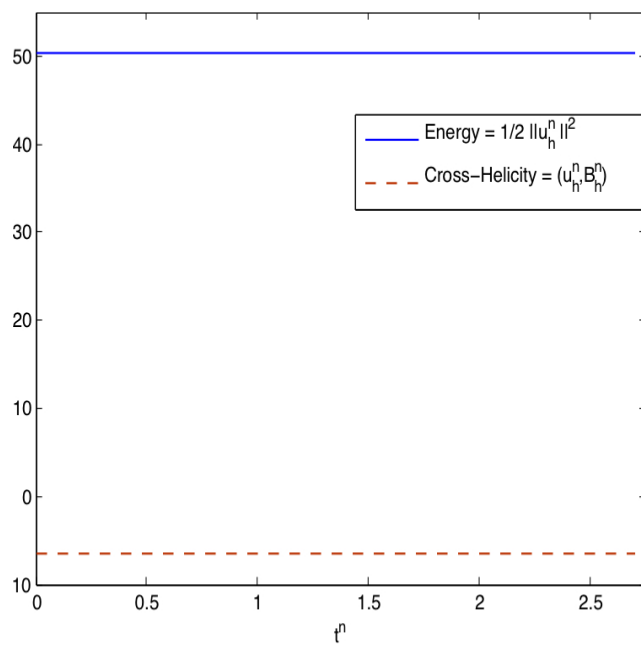
Figure 7.5: Energy and Cross helicity versus time for Orszat-Tang Vortex problem; they are conserved.

# Chapter 8

# Conclusions

Chapter 3 extended the energy and helicity conserving scheme of [64] to include homogenous Dirichlet boundary conditions. The adverse effect of Bernoulli pressure, which can be the dominant source of error in finite element computations, was nullified by the use of grad-div type stabilizations. We proposed and analyzed an altered grad-div stabilization and found that it is more physically accurate than the traditional grad-div stabilization term because the energy balance is not altered. The modified stabilization term also appears to stabilize similarly to the usual grad-div stabilization. Finally, we provided a numerical experiment that showed the advantage of the energy and helicity conserving scheme as well as the altered grad-div stabilization term.

In Chapter 4 we studied a finite element scheme for the 3d NSE which we proved globally conserved energy and helicity. We demonstrated an efficient way to compute solutions by removing the pressure space. We provided numerical experiments which show optimal convergence rates, and correct behavior for the benchmark problem of 3d channel flow over a forward-backward facing step.

Chapter 5 shows that under assumptions A1-A4 grad-div stabilized TH solutions to incompressible Stokes type problems converge to their respective SV solutions with rate $\gamma^{-1}$. This connection demonstrates that TH elements can provide excellent mass conservation when the grad-div stabilization term is large and a setting where the use of a large grad-div stabilization parameter is stable.

In Chapter 6 we studied a finite element method for the NS-$\overline{\omega}$ model, which improved accuracy by using van Cittert approximate deconvolution and the SV element. We performed a complete numerical analysis of the method, and found the SV element improved accuracy by providing pointwise mass conservation as well as completely eliminating the dependence of the velocity error on the Bernoulli pressure error. We also provided numerical experiments that demonstrated the effective-

ness of the scheme. However, as the model is currently understood the literature suggests that the Leray-deconvolution and NS-$\alpha$ models are superior.

Chapter 7 provides an analytic study of the continuous Leray-deconvolution model for the incompressible MHD equations. The model is well-posed and conserves two fundamentally important physical quantities in MHD flows, namely energy and cross helicity. Further, solutions to a specific model converge (modulo a subsequence) to a solution of the MHD when $N \to \infty$ (and $\alpha > 0$ is fixed) and when $\alpha \to 0$ (and $0 \leq N < \infty$ is fixed). These properties make the models excellent candidates for simulating complex fluid flows which are described by the incompressible MHD equations.

A numerical scheme was presented for the MHD Leray-deconvolution model. The scheme was shown to be well-posed, conserve energy as well as cross-helicity, and enforce the constraints $\nabla \cdot u = \nabla \cdot B = 0$ pointwise. Thus, the numerical scheme provides solutions which are physically relevant. Additionally, the numerical scheme is computationally efficient. Since the scheme linearized the velocity and magnetic terms which are filtered and then approximately unfiltered, we were able to filter independently of the full MHD system. Thus, the runtime did not increase significantly by using deconvolution. Three experiments were provided that demonstrated the effectiveness of the scheme.

# Bibliography

[1] A. Arakawa. Computational design for long-term numerical integration of the equations of fluid motion: Two dimensional incompressible flow, Part I. *J. Comput. Phys.*, 1:119–143, 1966.

[2] A. Arakawa and V. Lamb. A potential enstrophy and energy conserving scheme for the shallow water equations. *Monthly Weather Review*, 109:18–36, 1981.

[3] G. Baker. Galerkin approximations for the Navier-Stokes equations. Harvard University, August 1976.

[4] L. Berselli and R. Lewandowski. Convergence of approximate deconvolution models to the filtered Navier-Stokes equations. *Annales de l'Institut henri Poincare (C), Non Linear Analysis*, 29:171–198, 2012.

[5] L.C. Berselli, T. Iliescu, and W. J. Layton. *Mathematics of Large Eddy Simulation of Turbulent Flows*. Scientific Computation. Springer, 2006.

[6] A. Bowers and L. Rebholz. Increasing accuracy and efficiency in FE computations of the Leray-deconvolution model. *Numerical Methods for Partial Differential Equations*, 28(2):720–736, 2012.

[7] E. Burman and A. Linke. Stabilized finite element schemes for incompressible flow using Scott-Vogelius elements. *Applied Numerical Mathematics*, 58(11):1704–1719, 2008.

[8] M. Case, V. Ervin, A. Linke, and L. Rebholz. A connection between Scott-Vogelius elements and grad-div stabilization. *SIAM Journal on Numerical Analysis*, 49(4):1461–1481, 2011.

[9] M. Case, V. Ervin, A. Linke, L. Rebholz, and N. Wilson. Stable computing with an enhanced physics based scheme for the 3d Navier-Stokes equations. *International Journal of Numerical Analysis and Modeling*, 11(1):219–238, 2011.

[10] M. Case, A. Labovsky, L. Rebholz, and N. Wilson. A high physical accuracy method for incompressible magnetohydrodynamics. *International Journal on Numerical Analysis and Modeling, Series B*, 1(2):219–238, 2010.

[11] S. Chen, C. Foias, D. Holm, E. Olson, E. Titi, and S. Wynne. The Camassa-Holm equations as a closure model for turbulent channel and pipe flow. *Phys. Rev. Lett.*, 81:5338–5341, 1998.

[12] S. Chen, D. Holm, L. Margolin, and R. Zhang. Direct numerical simulations of the Navier-Stokes alpha model. *Physica D*, 133:66–83, 1999.

[13] A. Cheskidov, D. Holm, E. Olson, and E. Titi. On a Leray-alpha model of turbulence. *Royal Society London, Proceedings, Series A, Mathematical, Physical and Engineering Sciences*, pages 629–649, 2005.

[14] R. Codina and N.H. Silva. Stabilized finite element approximation to the stationary magneto-hydrodynamics equations. *Computational Mechanics*, 194:334–355, 2006.

[15] P.A. Davidson. *An introduction to magnetohydrodynamics*. Cambridge, 2001.

[16] A. Dunca and Y. Epshteyn. On the Stolz-Adams deconvolution model for the Large-Eddy simulation of turbulent flows. *SIAM J. Math. Anal.*, 37(6):1890–1902, 2005.

[17] V. Ervin, W. Layton, and M. Neda. Numerical analysis of filter based stabilization for evolution equations. *Technical Report, University of Pittsburgh*, 2010.

[18] V.J. Ervin and N. Heuer. Approximation of time-dependent, viscoelastic fluid flow: Crank-Nicolson, finite element approximation. *Numer. Methods Partial Differential Eq.*, 20:248–283, 2003.

[19] C. Ethier and D. Steinman. Exact fully 3d Navier-Stokes solutions for benchmarking. *International Journal for Numerical Methods in Fluids*, 19(5):369–375, 1994.

[20] H. Friedel, R. Grauer, and C. Marliani. Adaptive mesh refinement for singular current sheets in incompressible magnetohydrodynamic flows. *Journal of Computational Physics*, 134:190–198, 1997.

[21] G. Galdi and W. Layton. Approximating the larger eddies in fluid motion II: A model for space filtered flow. *Math. Methods and Models in Appl. Sci.*, 10(3):1–8, 2000.

[22] M. Gavrilov and Z. Janji. Computed rotational energy spectra of two energy and enstrophy conserving schemes on semi-staggered grids. *Meteorology and Atmospheric Physics*, 41(1):1–4, 1989.

[23] J.F. Gerbeau. A stabilized finite element method for the incompressible magnetohydrodynamic equations. *Numerische Mathematik*, 87:83–111, 2000.

[24] M. Germano. Differential filters for the large eddy numerical simulation of turbulent flows. *Physics of Fluids*, 29:1755–1757, 1986.

[25] M. Gunzburger. *Finite Element Methods for Viscous Incompressible Flow: A Guide to Theory, Practice, and Algorithms.* Academic Press, Boston, 1989.

[26] M. Gunzburger and C. Trenchea. Analysis and discretization of an optimal control problem for the time-periodic MHD equations. *J. Math Anal. Appl.*, 308(2):440–466, 2005.

[27] M. Gunzburger and C. Trenchea. Analysis of optimal control problem for three-dimensional coupled modified Navier-Stokes and Maxwell equations. *J. Math Anal. Appl.*, 333:295–310, 2007.

[28] D. Holm and B. Guerts. Leray and LANS-$\alpha$ modelling of turbulent mixing. *J. of Turbulence*, 7(10), 2006.

[29] V. John. *Large Eddy Simulation of Turbulent Incompressible Flows. Analytical and Numerical Results for a Class of LES Models*, volume 34 of *Lecture Notes in Computational Science and Engineering.* Springer-Verlag Berlin, Heidelberg, New York, 2004.

[30] V. John. Reference values for drag and lift of a two dimensional time-dependent flow around a cylinder. *International Journal for Numerical Methods in Fluids*, 44:777–788, 2004.

[31] V. John and W. J. Layton. Analysis of numerical errors in Large Eddy Simulation. *SIAM J. Numer. Anal.*, 40(3):995–1020, 2002.

[32] V. John and A. Liakos. Time dependent flow across a step: The slip with friction boundary condition. *International Journal of Numerical Methods in Fluids*, 50:713 – 731, 2006.

[33] P. Kuberry, A. Larios, L. Rebholz, and N. Wilson. Numerical approximation of the Voigt regularization of incompressible Navier-Stokes and magnetohydrodynamics flows. *Submitted*, 2012.

[34] A. Labovsky, W. Layton, C. Manica, M. Neda, and L. Rebholz. The stabilized extrapolated trapezoidal finite element method for the Navier-Stokes equations. *Comput. Methods Appl. Mech. Engrg.*, 198:958–974, 2009.

[35] A. Labovsky and C. Trenchea. A family of approximate deconvolution models for magnetohydrodynamic turbulence. *Numerical Functional Analysis and Optimization*, 31(12):1362–1385, 2010.

[36] W. Layton. A remark on regularity of an elliptic-elliptic singular perturbation problem. Technical report, University of Pittsburgh, 2007.

[37] W. Layton. *An Introduction to the Numerical Analysis of Viscous Incompressible Flows.* SIAM, 2008.

[38] W. Layton. The existence of smooth attractors for the NS-$\overline{\omega}$ model of turbulence. *Journal of Mathematical Analysis and Applications*, 366:81–89, 2010.

[39] W. Layton, W. Lenferink, and J. Peterson. A two-level Newton, finite element algorithm for approximating electrically conducting, incompressible fluid flows. *Computers and Mathematics with Applications*, 28, 1994.

[40] W. Layton and R. Lewandowski. Residual stress of approximate deconvolution large eddy simulation models of turbulence. *J. of Turbulence*, 7(46):1–21, 2006.

[41] W. Layton and R. Lewandowski. A high accuracy Leray-deconvolution model of turbulence and its limiting behavior. *Analysis and Applications*, 6(1), 2008.

[42] W. Layton, C. Manica, M. Neda, M.A. Olshanskii, and L. Rebholz. On the accuracy of the rotation form in simulations of the Navier-Stokes equations. *J. Comput. Phys.*, 228(5):3433–3447, 2009.

[43] W. Layton, C. Manica, M. Neda, and L. Rebholz. Numerical analysis and computational testing of a high-accuracy Leray-deconvolution model of turbulence. *Numerical Methods for Partial Differential Equations*, 24(2):555–582, 2008.

[44] W. Layton, C. Manica, M. Neda, and L. Rebholz. Numerical analysis and computational comparisons of the NS-omega and NS-alpha regularizations. *Comput. Methods Appl. Mech. Engrg.*, 199:916–931, 2010.

[45] W. Layton and L. Rebholz. *Approximate Deconvolution Models of Turbulence.* Springer, 2012.

[46] W. Layton, I. Stanculescu, and C. Trenchea. Theory of the NS-$\overline{\omega}$ model: A complement to the NS-alpha model. *Communications on Pure and Applied Analysis*, 10(6):1763–1777, 2011.

[47] A. Linke. Collision in a cross-shaped domain — A steady 2d Navier-Stokes example demonstrating the importance of mass conservation in CFD. *Comp. Meth. Appl. Mech. Eng.*, 198(41–44):3278–3286, 2009.

[48] A. Linke, G. Matthies, and L. Tobiska. Non-nested multi-grid solvers for mixed divergence free Scott-Vogelius discretizations. *Computing*, 83(2-3):87–107, 2008.

[49] J. Liu and W. Wang. Energy and helicity preserving schemes for hydro and magnetohydrodynamics flows with symmetry. *J. Comput. Phys.*, 200:8–33, 2004.

[50] E. Lunasin, S. Kurien, M. Taylor, and E.S. Titi. A study of the Navier-Stokes-alpha model for two-dimensional turbulence. *Journal of Turbulence*, 8:751–778, 2007.

[51] C. Manica, M. Neda, M. Olshanskii, L. Rebholz, and N. Wilson. On an efficient finite element method for Navier-Stokes-omega with strong mass conservation. *Computational Methods in Applied Mathematics*, 11(1), 2011.

[52] C. Manica, M. Neda, M.A. Olshanskii, and L. Rebholz. Enabling accuracy of Navier-Stokes-alpha through deconvolution and enhanced stability. *M2AN: Mathematical Modelling and Numerical Analysis*, 45(2):277–308, 2010.

[53] C.C. Manica and S. Kaya Merdan. Convergence analysis of the finite element method for a fundamental model in turbulence. *Mathematical Models and Methods in Applied Sciences*, to appear, 2012.

[54] H. Moffatt and A. Tsoniber. Helicity in laminar and turbulent flow. *Annual Review of Fluid Mechanics*, 24:281–312, 1992.

[55] I.M. Navon. Implementation of a posteriori methods for enforcing conservation of potential enstrophy and mass in discretized shallow water equation models. *Monthly Weather Review*, 109:946–958, 1981.

[56] I.M. Navon. A Numerov-Galerkin technique applied to a finite element shallow water equations model with enforced conservation of integral invariants and selective lumping. *J. Comput. Phys.*, 52:313–339, 1983.

[57] A.I. Nesliturk, S.H. Aydin, and M. Tezer-Sezgin. Two-level finite element with a stabilizing subgrid for the incompressible Navier-Stokes equations. *International Journal for Numerical Methods in Fluids*, 58(5):551–572, 2008.

[58] M.A. Olshanskii. A low order Galerkin finite element method for the Navier-Stokes equations of steady incompressible flow: A stabilization issue and iterative methods. *Comp. Meth. Appl. Mech. Eng.*, 191:5515–5536, 2002.

[59] M.A. Olshanskii, G. Lube, T. Heister, and J. Löwe. Grad-div stabilization and subgrid pressure models for the incompressible Navier-Stokes equations. *Comp. Meth. Appl. Mech. Eng.*, 198:3975–3988, 2009.

[60] M.A. Olshanskii and L. Rebholz. Velocity-vorticity-helicity formulation and a solver for the Navier-Stokes equations. *Journal of Computational Physics*, 229:4291–4303, 2010.

[61] M.A. Olshanskii and A. Reusken. Navier-Stokes equations in rotation form: a robust multigrid solver for the velocity problem. *SIAM J. Sci. Comput.*, 23:1682–1706, 2002.

[62] M.A. Olshanskii and A. Reusken. Grad-Div stabilization for the Stokes equations. *Math. Comp.*, 73:1699–1718, 2004.

[63] J. Qin. *On the convergence of some low order mixed finite elements for incompressible fluids*. PhD thesis, Pennsylvania State University, 1994.

[64] L. Rebholz. An energy and helicity conserving finite element scheme for the Navier-Stokes equations. *SIAM Journal on Numerical Analysis*, 45(4):1622–1638, 2007.

[65] L. Rebholz and M.A. Olshanskii. An application of barycenter refined meshes in linear elasticity and incompressible fluid dynamics. *Electronic Transactions in Numerical Analysis*, 38:258–274, 2011.

[66] L. Rebholz and M. Sussman. On the high accuracy NS-$\alpha$-deconvolution model of turbulence. *Mathematical Models and Methods in Applied Sciences*, 20:611–633, 2010.

[67] M. Schäfer and S. Turek. The benchmark problem 'flow around a cylinder' flow simulation with high performance computers II. *in E.H. Hirschel (Ed.), Notes on Numerical Fluid Mechanics*, 52, Braunschweig, Vieweg:547–566, 1996.

[68] L.R. Scott and M. Vogelius. Conforming finite element methods for incompressible and nearly incompressible continua. In *Large-scale computations in fluid mechanics, Part 2*, volume 22-2 of *Lectures in Applied Mathematics*, pages 221–244. Amer. Math. Soc., 1985.

[69] R. Temam. Sur l'approximation des solutions des equations de Navier-Stokes. *C.R. Acad. Sci. Paris, Series A*, 262:219–221, 1966.

[70] R. Temam. *Navier-Stokes Equations : Theory and Numerical Analysis*. Elsevier North-Holland, 1979.

[71] R. Temam. *Navier-Stokes Equations and Nonlinear Functional Analysis*. SIAM, Philadelphia, 1995.

[72] R. Temam. *Navier-Stokes Equations*. American Mathematical Society, 2001.

[73] M. Vogelius. An analysis of the $p$-version of the finite element method for nearly incompressible materials. Uniformly valid, optimal error estimates. *Numer. Math.*, 41:39–53, 1983.

[74] M. Vogelius. A right-inverse for the divergence operator in spaces of piecewise polynomials. Application to the $p$-version of the finite element method. *Numer. Math.*, 41:19–37, 1983.

[75] Yongjiang Yu and Kaitai Li. Existence of solutions for the MHD-Leray-alpha equations and their relations to the MHD equations. *Journal of Mathematical Analysis and Applications*, 329:298–326, 2006.

[76] S. Zhang. A new family of stable mixed finite elements for the 3d Stokes equations. *Mathematics and Computation*, 74(250):543–554, 2005.

[77] S. Zhang. Divergence-free finite elements on tetrahedral grids for $k \geq 6$. *Mathematics and Computation*, 80:669–695, 2011.

[78] S. Zhang. Quadratic divergence-free finite elements on Powell-Sabin tetrahedral grids. *Calcolo*, 48(3):211–244, 2011.